

UNIVERSITY OF OKLAHOMA
GRADUATE COLLEGE

CONFINED QUANTUM SYSTEMS: BEYOND HARMONIC
ORDER IN DIMENSIONAL PERTURBATION THEORY

A DISSERTATION
SUBMITTED TO THE GRADUATE FACULTY
in partial fulfillment of the requirements for the
Degree of
DOCTOR OF PHILOSOPHY

BY
WILLIAM BLAKE LAING, III

Norman, Oklahoma

2008

CONFINED QUANTUM SYSTEMS: BEYOND HARMONIC
ORDER IN DIMENSIONAL PERTURBATION THEORY

A DISSERTATION APPROVED FOR THE
HOMER L. DODGE DEPARTMENT OF PHYSICS AND ASTRONOMY

BY

Dr. Deborah K. Watson

Dr. Eric R. I. Abraham

Dr. Bruce A. Mason

Dr. Michael A. Morrison

Dr. Gregory A. Parker

Dr. Krishnaiya Thulasiraman

© Copyright by WILLIAM BLAKE LAING, III 2008
All Rights Reserved.

Dedication

To Teresa Ann Laing.

Acknowledgements

Having reached the end of my formal preparation, I have many people to thank who have helped me on my way.

I thank my thesis advisor Professor Deborah Watson for her guidance in my doctoral research, financial support as a research assistant (also for sending me to six professional meetings), and giving advice on my research career. I am grateful for the chance to work closely with Martin Dunn in developing the formalism in this work and am grateful for his friendship. I thank Professor Michael Morrison for teaching me how to write a scientific paper, for extensive comments on this manuscript, for many conversations about practical aspects of the scholarly life, and especially for taking me to coffee and offering his perspective during times when I was making critical career decisions. I thank Professor Greg Parker for comments on the presentation of this work, for classroom instruction, taking a personal interest in my progress, and for giving guidance as needed. I also thank Professor Bruce Mason for allowing me the opportunity to work on the COMPADRE education resource project. I thank Professors Bruce Mason and Eric Abraham for mentorship while I was a teaching assistant. I thank Brett McKinney for guidance on understanding his work (which I have extended in this thesis to next order). I thank fellow and former graduate students for their friendship: Paul, Hans, John Walkup, Chris Stockdale, Larry Maddox, Aïda Nava, Darrin Casebeer, Roland Thomas, Jim Hicks, Juliette Dalhed, Stéphane Valladier, James Dizikes, Jeremy Jernigen, Xuan Li, Dan Brue, Albert Chuang, Wesley Tennyson, Tom Aiken, everyone who grew a beard in November and probably a few more people I can't think of at the moment.

As a freshman physics/pre-med major at Southern Adventist University, I had difficulty adapting to college. I thank Professor Ray “Doc” Hefferlin for providing guidance, inspiration, and a watchful eye even when I had dropped my classes and was facing an uncertain future, and for introducing me to physics research. I also thank Professor Chris Hansen for guidance in my upper-division classes (some in which I

was the only student). Thanks also to Professors Ken Caviness, Henry Kuhlman, Robert Moore, Art Richert, and Helen Pyke for my liberal arts college experience.

I thank my mother Louise for nurturing in me a joy and fascination in nature as perceived through the senses (as well as reading and commenting on Appendix C of the thesis), my father Richard for engaging me in logical and philosophical discussions, my sister Amber for interest in late-night physics discussions. I thank my father-in-law Jerry Wagner for reading through Appendix C and actually finding mathematical errors.

Finally, I thank my wife Teresa. We began our relationship around the time that I choose this career over ten years ago. Although she wonders why I throw myself into hard problems (and on purpose), she has weathered the hard times with me and has been content to wait for the payoff.

Contents

Dedication	iii
Acknowledgements	iv
Abstract	xii
I Prologue	1
1 Introduction to the dissertation	2
1.1 Ultracold atoms exhibit wave-like properties	2
1.1.1 The wave-particle duality of nature	2
1.1.2 Low temperature tilts the odds in favor of coherence	3
1.1.3 Atoms are described by “wavefunctions”	4
1.2 Research questions	4
2 A short history of BEC theory	6
2.1 BEC in an ultracold atomic gas	6
2.2 A mean-field description of a BEC is quite useful	7
2.3 Sometimes one must venture beyond the mean-field description	9
2.3.1 Theory and computation beyond the mean-field	10
2.3.2 Adiabatic hyperspherical harmonic approaches	11
2.3.3 Monte Carlo methods	12
2.4 Does the shape of the interaction matter?	13
2.5 N -body dimensional perturbation theory	15
3 N-body dimensional perturbation theory	16
3.1 Perturbation theory in general	16
3.1.1 Example: solution of a cubic polynomial	17
3.2 Dimensional perturbation theory: an extensible framework	18
3.2.1 A brief history of dimensional scaling and DPT	19
3.2.1.1 Dimensional scaling	19
3.2.1.2 N -body dimensional perturbation theory	20
3.2.2 New N -body DPT work in this dissertation	22
3.2.2.1 Influential preliminary work	22
3.2.2.2 Work that is in this dissertation	22

3.3	N bodies in higher dimensions	24
3.3.1	The D -dimensional Schrödinger equation	24
3.3.2	Confined quantum systems in internal coordinates	24
3.3.3	The Jacobian-weighted Schrödinger equation	25
3.4	There's plenty of room for additional symmetry in larger dimensions .	27
3.4.1	Preparation for the large-dimension limit: dimensional scaling	27
3.4.2	Large-D limit of the Hamiltonian	28
3.4.3	Symmetric minimum of the effective potential	29
3.5	Perturbation about large- D structure	30
3.5.1	Series expansion of the kinetic term, G	32
3.5.2	Series expansion of the effective potential, F	33
3.5.3	Perturbation series expressions	34
3.6	Solution of the harmonic-order equation	35
3.6.1	Normal-mode frequencies, harmonic energy	35
3.6.2	Normal-mode coordinates, harmonic wavefunction	36
3.7	Solution of the first-anharmonic-order equation	37

II Anharmonic-order formalism development 38

4 Fearful symmetry, framed 39

4.1	Hamiltonian indicial structure and group symmetry	40
4.1.1	Indical structure of internal coordinate tensors	40
4.1.1.1	Harmonic order	41
4.1.1.2	Anharmonic order	42
4.1.2	Symmetry creates a patchwork of equivalence classes	42
4.2	Decomposition in the basis of binary invariants	44
4.2.1	Introducing binary invariants	44
4.2.2	Binary invariants are a basis	45
4.2.3	Expansion in the binary invariant basis	46
4.3	Graphical representation of tensor structure	47
4.3.1	Introducing graph theory	48
4.3.2	Mapping tensor structure onto graphs	48
4.3.3	Graphical decomposition of harmonic-order matrices	49
4.3.4	Graphical decomposition of first anharmonic-order matrices	49

5 Transformation of Hamiltonian to normal-coordinate basis 53

5.1	Two-step transformation of the Hamiltonian	53
5.1.1	Transformation of coordinate vectors	54
5.1.2	Transformation of Hamiltonian tensors	55
5.1.3	Intermediate step: transformation to symmetry coordinates	57
5.1.4	Final step: transformation to normal coordinates	60
5.2	Transformation to symmetry coordinates	61

5.2.1	Clebsch-Gordon coefficients of the transformation	62
5.2.2	Symmetry-transformed binary invariants	64
5.3	Transformation to normal coordinates	65
6	Anharmonic Wave Function And Density Profile	67
6.1	Derivation of the first-anharmonic-order ground-state wavefunction	67
6.1.1	Harmonic-order wavefunction	67
6.1.2	Harmonic-order ground-state wavefunction	68
6.1.3	First anharmonic wave function	69
6.1.3.1	Derivatives at first-anharmonic order	70
6.1.3.2	Derivation of the cubic Δ	71
6.2	Derivation of the first-anharmonic order density profile	71
6.2.1	Harmonic order density profile	71
6.2.2	First-anharmonic-order corrections	73
6.3	The view from Plato's cave	75
III	Application	76
7	Application to the (fully-interacting) Hooke's law gas	77
7.1	Application of DPT formalism to the Hooke's-law gas	78
7.1.1	Dimensional scaling of the Hamiltonian	78
7.1.2	Large-D limit	79
7.1.3	Perturbation series	79
7.1.3.1	Harmonic order	79
7.1.3.2	First anharmonic order	80
7.1.4	DPT Wavefunction and density profile	81
7.2	Direct derivation of the exact solution	81
7.2.1	The exact wavefunction through first order	81
7.2.2	The exact density profile through first anharmonic order	82
8	Application to BEC: a preliminary peek	86
8.1	Bose-Einstein condensate Hamiltonian	86
8.1.1	Atoms in a trap	87
8.1.2	A smooth, short-range potential	87
8.1.3	"Soft-sphere" interaction potential	87
8.2	Large-dimension limit of BEC Hamiltonian	89
8.2.1	Dimensional scaling	89
8.2.2	Large-dimension limit of the Hamiltonian	90
8.2.3	Determination of the lowest-order symmetric arrangement	91
8.3	Perturbation series	92
8.4	Optimization	93
8.4.1	Previous work	93

8.5	Preliminary results	94
8.5.1	Intermediate interaction	94
8.5.2	Strong interaction strength	99
8.6	Conclusions we can draw at this stage	102
IV Epilogue		103
9	Looking back... and looking forward	104
9.1	Summary of contributions	104
9.2	Future research	105
Reference List		107
Appendix A		
	Three-body dimensional perturbation theory	112
A.3	3-body dimensional perturbation theory	112
A.3.3	Three bodies in higher dimensions	112
A.3.4	The large-dimension limit	114
A.3.4.1	Perturbation about large- D structure	115
A.3.6	Solution of the harmonic-order equation	118
A.3.7	Solution of the first-anharmonic equation	118
A.4	Decomposition in a structural basis, invariant under S_3	119
A.4.2	Example: harmonic Hamiltonian tensor for $N = 3$	119
A.4.3	Decomposition in the basis of binary invariants	120
A.4.3.1	Introducing binary invariants	120
A.4.4	Graphical representation of tensor structure	121
A.4.4.2	Mapping tensor structure onto graphs	121
A.4.4.3	Graphical decomposition, harmonic-order	121
A.4.4.4	Graphical decomposition, first-anharmonic-order	121
A.5	Transformation of Hamiltonian to normal-coordinate basis	123
A.5.1	Two-step transformation of the Hamiltonian	123
A.5.1.3	Intermediate step: transformation to symmetry coordinates	123
A.5.1.4	Final step: transformation to normal coordinates	124
A.5.2	Transformation to symmetry coordinates	125
A.5.2.1	Clebsch-Gordon coefficients of the transformation	126
A.5.2.2	Symmetry-transformed binary invariants	127
Appendix B		
	A Note on Index Notation	133
Appendix C		
	Binary invariants	136
C.1	Construction of binary invariants	136
C.1.1	The recipe	136

C.1.2	Examples: harmonic-order graphs	137
C.1.2.1	The rr block	137
C.1.2.2	The γr and $r\gamma$ blocks	137
C.1.2.3	The $\gamma\gamma$ block	138
C.2	Results: binary invariants in closed form	139
C.2.1	Harmonic order	139
C.2.2	First anharmonic order	139
C.2.2.1	Rank-one blocks r and γ	139
C.2.2.2	Rank-three Sector rrr	139
C.2.2.3	Rank-three Sector γrr	140
C.2.2.4	Rank-three Sector $\gamma\gamma r$	140
C.2.2.5	Rank-three Sector $\gamma\gamma\gamma$	140
C.3	Extension of previous work	142

Appendix D

	Perturbative expansion of Hamiltonian	144
D.1	Perturbative expansion of the kinetic term	145
D.2	Perturbative expansion of the effective potential	146
D.3	Binary invariant expansion the kinetic series	148
D.4	Binary invariant expansion of the effective potential series	152
D.4.1	Calculation of derivatives	152
D.4.2	Elements of the harmonic-order Hamiltonian	152
D.4.3	Elements of the first anharmonic-order Hamiltonian	153
D.4.3.1	Rank-one Hamiltonian elements	154
D.4.3.2	Rank-three Hamiltonian elements	154

Appendix E

	The S_N Clebsch-Gordon coefficients	156
E.1	Harmonic order	156
E.2	First anharmonic order	156
E.2.1	Rank-one Clebsch-Gordon coefficients	156
E.2.2	Rank-three Clebsch-Gordon coefficients for S_N	157

Appendix F

	Binary invariants transformed to symmetry coordinates	159
F.1	Harmonic order	159
F.2	First anharmonic order	160
F.2.1	Rank one first anharmonic	160
F.2.2	Rank-three first anharmonic order	162

Appendix G

	Derivation of the probability density profile	167
G.1	Harmonic-order density profile	167
G.2	First anharmonic density profile	172

G.2.1	Normal-coordinate integrals	172
G.2.2	Clebsch-Gordon tensor contractions	174
G.2.3	Transformation of the integrals to symmetry coordinates	175
G.2.4	Evaluation of the integrals	176
G.2.5	Result: first-anharmonic-order density profile	177
Appendix H		
	Calculation of the Δ^2 term	179
Appendix I		
	Derivation of the Hooke's law gas wave function and density profile	181
I.1	First-anharmonic-order wavefunction	181
I.1.1	A perturbation series in $1/\sqrt{D}$ for the exact wavefunction	182
I.1.1.1	Dimensional scaling	182
I.1.1.2	The large-dimension limit	183
I.1.1.3	A series expansion about the large- D limit	184
I.1.2	Comparison of direct derivation to DPT	188
I.2	First-anharmonic-order density profile	191
I.2.1	Dimensional scaling	191
I.2.2	Series expansion	192
Appendix J		
	Details of the application to BEC	194
J.1	Hamiltonian Elements for a BEC Potential	194
J.1.1	Elements of the harmonic-order Hamiltonian	195
J.1.1.1	Derivatives with respect to δ : ${}^{(0)}_0F$	195
J.1.1.2	Derivatives with respect to internal coordinates: ${}^{(0)}_2F$	195
J.1.2	Elements of the first anharmonic-order Hamiltonian	196
J.1.2.1	Rank-one Hamiltonian Elements	196
J.1.2.2	Rank-three Hamiltonian Elements	196
J.2	Optimization to benchmark data	198
J.2.1	Fitness function	198
J.2.2	Benchmark data	198

Abstract

We generalize the harmonic-order N -body DPT method for an isotropically confined quantum system of identical interacting bosons to first-anharmonic order and, in principle, higher orders. We introduce a graphical decomposition of the perturbative expansion of the N -body Hamiltonian. We calculate the Clebsch-Gordon coefficient tensors that couple together 3 irreducible representations of S_N analytically, and analytically transformed the graphical basis to collective coordinates. We calculate the N -body wavefunction and density profile in general and have demonstrated agreement with an analytic model. We apply this formalism to the exactly-solvable example of a trapped gas of atoms interacting with a (fully-interacting) harmonic-oscillator “Hooke’s law” interaction and compare with the dimensional expansion of the exact ground-state wavefunction and density profile. We report progress on the example of a cold gas BEC (with zero angular momentum).

Part I

Prologue

Chapter 1

Introduction to the dissertation

1.1 Ultracold atoms exhibit wave-like properties

1.1.1 The wave-particle duality of nature

In 1906, the Nobel prize in physics was awarded to J.J. Thomson for showing that electricity in gases is conducted by a particle which we now call the electron. In 1937, G.P. Thomson, the son of J.J. Thomson, shared the Nobel prize with Clinton J. Davisson for the discovery that the electron is also a wave. Is an electron a particle or is it a wave? In the heady days leading up to modern quantum mechanics, this was a common topic of discussion. Light was shown to have discrete (quantized) properties like particles, and fundamental particles were shown to exhibit interference phenomena as if they were waves.

Louis de Broglie synthesized these paradoxical findings by proposing that *any* moving body (atoms or airplanes) has an associated wave with a wavelength inversely proportional to its momentum

$$\lambda = \frac{h}{p}. \quad (1.1)$$

The de Broglie relation is an example of an intriguing aspect of quantum mechanics: *the wave-particle duality* of nature. Atkins and Friedman (1) suggest that the terms “particle” and “wave” should be regarded as artifacts from a language based on an antiquated understanding of nature. Note that as the momentum of a particle gets smaller, its de Broglie wavelength gets larger and its wave-like properties more apparent. That is significant in this thesis, because we are interested in a gas of atoms near absolute zero temperature, where thermal motion dies down and the wave-like behavior of atoms exhibits stunning phenomena.

If two stones are dropped in a pond, the radiating ripples will eventually coincide. When two waves in a pond collide, two peaks combine to yield a bigger peak, two troughs combine to make a deeper trough, but a peak and a trough can combine to yield—nothing. This behavior of waves is called “interference” and a picture of this scenario would show an interference pattern showing the above wave arithmetic. A similar effect occurs in sound waves. One may enjoy a quieter flight when wearing “noise-canceling headphones” that emit the right kind of sound waves to cancel out the effect of the ambient noise. If atoms truly have wave-like properties, one would expect similar phenomena. Two colliding “matter waves” should also exhibit an interference pattern, where matter plus matter equals more matter in some places—and nothing at all in others. In order to observe such a phenomenon, it is necessary to construct a “matter wave” composed of many atoms in the same quantum state, an improbable situation given the huge number of possible quantum states often available.

1.1.2 Low temperature tilts the odds in favor of coherence

In 1924 Einstein showed that if a gas of non-interacting identical (boson) atoms was cooled below some critical temperature many of the atoms would “condense” in the quantum state with the lowest energy. Notice that this condensation occurs without interactions: it is a purely statistical effect that occupation of the lowest energy state becomes more likely as the temperature of the system falls. This condensed fraction of the gas is called a Bose-Einstein condensate (BEC).

This condensation into a single quantum state only happens if each of the atoms in question has a total number of protons, neutrons and electrons that is an even number. One aspect of quantum mechanics is that these things matter. In the periodic table of elements, each atom has either an even or an odd number of particles. Those with an even number are said to be “bosons” (named after Satyendranath Bose, who introduced Bose statistics (2)). Those with an odd number are said to be fermions, after Enrico Fermi. An even number of fermions form a composite boson, and protons, neutrons, and electrons are all fermions. While any number of bosons can occupy the same quantum state, Fermi-Dirac statistics dictate that no two fermions can occupy the same state.

This distinction becomes relevant in a gas of very cold atoms, because as the temperature decreases, the average energy of each atom decreases and whether or not more than one atom can occupy the state with the lowest energy level becomes important. This quantum state with the lowest energy is called the “ground state.”

Recently, gasses of fermion atoms have been cooled low enough that Fermi-Dirac statistics are important. In this gas, the atoms are “stacked up” in the lowest energy levels such that each atom has a partner with an equal and opposite momentum. Such cold gases of bosons or fermions are said to be “quantum degenerate”, since the degeneracy restrictions become significant in both cases.

People sometimes ask what a BEC is “good for”. The same people may have asked the same question of the academics developing the laser in the 1960s. In the 1970s, lasers were being used to scan barcodes in supermarkets and by the 1990s, lasers had become household devices used in compact-disc players. What makes a laser different from other light sources is that in a laser the photons are *coherent*. That is, they are all in the same quantum state. During the same decade, those lasers (in some case the same lasers developed for playing the compact-disc) were used to create a BEC; i.e. coherent atoms in the same quantum state. A better question to ask is “what is an understanding and control over the quantum behavior of matter good for?”

1.1.3 Atoms are described by “wavefunctions”

Atoms in a BEC have wave-like properties. In the formalism of quantum mechanics, the collection of atoms in the same quantum state are described by a mathematical equation known as “the wavefunction” of the quantum state. This wavefunction is often denoted $\Psi(\mathbf{r}, t)$ and is a function of space and time. Sometimes the time-dependence of the wavefunction is known or can be treated separately. In such a case, one obtains a stationary wavefunction $\Psi(\mathbf{r})$ by solving the Schrödinger equation

$$\hat{H}\Psi(\mathbf{r}) = E\Psi(\mathbf{r}) \tag{1.2}$$

where \hat{H} is the Hamiltonian operator which acts on the wavefunction, the result being a constant E times the wavefunction. The constant E is the energy of the quantum state associated with the wavefunction. The wavefunction $\Psi(\mathbf{r})$ contains *all* information about the physical system. All physical observables can be obtained if the wavefunction is known.

1.2 Research questions

The primary purpose of this thesis is to derive the wavefunction of a potentially large number of identical bosons in the same quantum state and from this wavefunction

calculate two physical observables: the energy and spatial distribution of the macroscopic occupation of the ground state.

In order to do this, we further develop a method which has been used to calculate the ground-state energy, the wave function, and the density profile for a BEC confined by an isotropic (spherical) trap. This method, N -body dimensional perturbation theory (DPT), is in the class of perturbative methods, in which a calculation is refined by including additional “orders”.

In particular, this thesis will address the following questions.

1. Can the harmonic-order DPT method be extended to first anharmonic order and, in principle, higher to address large- N , strongly interacting, and highly correlated systems?
2. What improvement in the DPT-calculated BEC density profile is obtained by adding the first anharmonic order correction?

Chapter 2

A short history of relevant theoretical investigations into the BEC phenomenon

From a certain temperature on, the molecules condense without attractive forces, that is, they accumulate at zero velocity. The theory is pretty, but is there also some truth to it?

Albert Einstein, 1924

2.1 BEC in an ultracold atomic gas

A dilute atomic gas BEC is a clean manifestation of the N -body problem in which the specific form of the interactions is of little importance. This is in contrast to the N -body problem in liquids and solids. Collective coherence phenomena like those observed in quantum liquids and nuclei may be observed in a gas that is so dilute that interactions may be well-approximated by a mean-field theory. Due to the low density, quantum phenomena which are typically infinitesimal, such as the structure of the wavefunction, can be observed by optical means (3).

A Bose-Einstein condensate (BEC) of a cold gas of boson atoms was predicted in 1924 by Einstein (4; 5) based on some work by Bose (2) on the statistics of a gas of photons (which are massless bosons). A BEC in a cold gas was first observed in 1995, nearly 70 years later, for rubidium (6), sodium (7), and lithium (8). To achieve

condensation, these alkali vapors were cooled down toward the absolute zero limit—to a few nanokelvin¹ The achievement of such low temperatures was made possible by laser-based cooling and “trapping” techniques which were developed in the 1980s (for reviews, see (9; 10; 11)). These gases were “trapped” in a confining potential provided by magnetic fields and/or lasers, then cooled by Doppler laser cooling and by “old-fashioned” evaporation.

A BEC is a state of matter where many atoms occupy a single quantum state, forming a coherent matter wave. An early experiment demonstrating the stunning behavior of coherent matter split a BEC into two parts and observed interference fringes between the two matter waves as they expanded—like incident ripples on a pond (12). A BEC can be used to perform precision measurements. A measurement of the Casimir-Polder force between a BEC and a surface has been performed by measuring perturbations in the center-of-mass oscillations (13).

The theory of a BEC goes back to the 1940s. For a tutorial review of fundamental ideas implicit in the theory of a BEC, see Reference (14). A recent article (15) reviews advances in the theoretical description of the homogeneous (not in a trap), weakly interacting Bose gas at zero and finite temperatures. Although a BEC occurs so near absolute zero, the temperature of the condensate is still an important quantity. Much physical insight can still be obtained in the zero temperature approximation, which we focus on in this thesis. A tutorial for the non-specialist on the most common theoretical methods used to describe weakly-interacting BEC at finite temperatures is provided in Reference (16).

2.2 A mean-field description of a BEC is quite useful

In a dilute BEC, the interaction between an atom and the $N - 1$ other atoms can be approximated by the interaction between that atom and a “mean-field”. In this sense, the mean-field description is a single-particle approximation to the full N -body problem. If an atomic BEC is so dilute, a mean-field description is effective in calculating both quantitative and qualitative descriptions of its properties. For

¹The Kelvin scale is a temperature scale similar to Celsius, except that a system at 0 kelvin, “absolute zero”, has no thermal energy at all. A nanokelvin is one billionth of one kelvin. Absolute zero is $-273^{\circ}C$ or $-459^{\circ}F$.

a review of the use of mean-field theory for calculating properties of a BEC, see Reference (17).

Applied to a dilute gas, where the interactions can be taken to be two-body and short-range, the mean-field time-dependent Schrödinger equation is

$$i\hbar\frac{\partial}{\partial t}\Phi(\mathbf{r},t) = \left(-\frac{\hbar^2\nabla^2}{2m} + V_{\text{ext}}(\mathbf{r}) + g|\Phi(\mathbf{r},t)|^2\right)\Phi(\mathbf{r},t) \quad (2.1)$$

Equation (2.1) is called the Gross-Pitaevskii (GP) equation (see Eq. (35) in Reference (17) and references therein). In the above equation, $V_{\text{ext}}(\mathbf{r})$ is the external confining potential. The order parameter $\Phi(\mathbf{r},t)$ depends on the single particle wavefunction $\varphi(\mathbf{r};t)$ (a function of \mathbf{r} parameterized by t) and occupancy of the BEC state $N_0(t)$:

$$\Phi(\mathbf{r},t) = \sqrt{N_0(t)}\varphi(\mathbf{r};t). \quad (2.2)$$

The coupling constant g is proportional to the scattering length a : $g = \frac{4\pi\hbar^2 a}{m}$. The chemical potential μ is adjusted so that the total number of atoms is equal to sum of the occupancies of each state (3).

The ground state can be obtained (Eq. (39) in Reference (17)) by making the substitution $\Phi(\mathbf{r},t) = \phi(\mathbf{r})e^{i\mu t/\hbar}$

$$\left(-\frac{\hbar^2\nabla^2}{2m} + V_{\text{ext}}(\mathbf{r}) + g\phi(\mathbf{r})^2\right)\phi(\mathbf{r}) = \mu\phi(\mathbf{r}), \quad (2.3)$$

where the mean-field term is proportional to the particle density $n(\mathbf{r}) = \phi(\mathbf{r})^2$.

The GP equation is valid in a dilute gas: when the number of atoms in a “scattering volume” $|a|^3$ is much less than one. This condition is expressed using the so-called “gas parameter” $\bar{n}|a|^3$ where \bar{n} is the average density of the gas. Typical values of \bar{n} range from 10^{13} to 10^{15}cm^{-3} (17) and the natural scattering length of ^{87}Rb is 5.77 nm, which corresponds to $\bar{n}|a|^3$ of 1.92×10^{-12} to 1.92×10^{-10} .

When $\bar{n}|a|^3 \ll 1$ the gas is said to be dilute or, confusingly, weakly interacting. This does not mean the effects of interactions are negligible. As discussed in Dalfovo *et al.* (17), the ratio of the (ground-state) energy due to interactions to the kinetic energy is another useful parameter which indicates the importance of interactions,

$$\frac{E_{\text{int}}}{E_{\text{kin}}} \propto \frac{N|a|}{a_{\text{ho}}}, \quad (2.4)$$

where the harmonic oscillator length a_{ho} is a measure of the width of the ground-state trap potential² and provides a useful length-scale.

²The harmonic oscillator length is the classical turning point of the ground state of the non-interacting trap.

For ^{87}Rb , $|a|/a_{\text{ho}}$ is on the order of 10^{-3} , so it does not take many atoms in a dilute gas before the effect of interactions becomes significant, even when the gas parameter indicates a dilute gas.

For a discussion on excitations in a weakly-interacting BEC and a review of experimental investigations of Bogoliubov excitations in a BEC, see Reference (18).

2.3 Sometimes one must venture beyond the mean-field description

The GP equation is valid in the dilute gas limit, when $n|a|^3 \ll 1$. Even in such a dilute regime the accuracy of the GP equation may be estimated by calculating corrections to the mean-field approximation. Recent experiments have produced BECs which are not so dilute, making beyond-mean-field corrections imperative. Experimental advances have demonstrated control over the strength of interactions between atoms in a BEC. A BEC with interactions “tuned” by changing the magnetic field was demonstrated in Reference (19). A gas parameter of $n|a|^3 \sim 10^{-2}$ (19) was reported, a regime where the mean-field does not provide quantitatively correct results (see for example Reference (20)). This approach is limited by the increase in three-body collisions (which is proportional to a^4), but similar results can be obtained using lattice techniques (see for example, Greiner *et al.* (21)). For a recent review of experimental and theoretical investigations of N -body physics in confined (strongly interacting) dilute gases in an optical potential see Bloch *et al.* (22) (both Bose and Fermi gases) or Morsch *et al.* (23).

Obtaining solutions for large systems of interacting particles continues to challenge existing approaches and current numerical resources. As the number of particles N increases, the Hilbert space that holds an exact solution of the problem scales exponentially in N making a direct numerical simulation intractable(24; 25). For general interparticle interactions, this necessitates approximations which effectively truncate the Hilbert space of the solution, usually by choosing a particular ansatz for the many-body wavefunction or by truncating a perturbation series. In this section, we provide a partial listing and brief description of several different approaches.

2.3.1 Theory and computation beyond the mean-field

Braaten and Nieto (26) derived quantum corrections to the GP equation (a classical field equation) for the ground state. The resulting correction is proportional to $1/\sqrt{n(0)a^3}$ (where $n(0)$ is the BEC density at the trap center) and the equation is often called a modified Gross-Pitaevskii equation (MGP)³. In a later paper, Anderson and Braaten extended this analysis to include vortex states. Fu *et al.* (29) introduce a modified GP equation which uses an energy-dependent effective potential and introduces an additional shape-dependent term.

Timmermans *et. al* (30) derived a Thomas-Fermi-Bogoliubov theory, a description of a BEC and quantum fluctuations based on the approximation that the BEC is locally homogeneous. The resulting perturbation series is analytic for a zero-temperature, weakly-interacting BEC. The authors point out that the Thomas-Fermi description really involves more than merely neglecting the kinetic energy in the GP equation, and produce a more rigorous derivation of the Thomas-Fermi equation. In addition to an analytic calculation of the chemical potential, the condensate depletion, pressure and density of states are calculated. The result is valid when the size of the condensate exceeds the “size” of the ground state of the trap a_{ho} .

Just as the Thomas-Fermi equation may be obtained by neglecting the kinetic energy of the GP equation, Gupta *et al.* propose a modified Thomas-Fermi equation by neglecting the kinetic energy of the MGP for the isotropic (31) and anisotropic (32) traps. The authors match the MGP (28) results for a ⁸⁵Rb BEC with 10^4 atoms for both the isotropic and the cylindrical trap. The corresponding excitation frequency for the compressional mode also agrees with numerical results.

Fabrocini and Polls (33) compare a local-density approximation (which adds additional terms beyond the GP) to a correlated-wavefunction approach for both isotropic (33) and a cylindrical (34) traps. The two approaches give similar results, up to $na^3 = 10^{-3}$ for the isotropic case and up to $na^3 = 10^{-2}$ for the cylindrical case.

Esry (35) developed an approach which uses atomic physics to derive equations which are similar to the Bogoliubov approach. Hartree-Fock, random-phase, and configuration interaction approximations are used to solve the N -body Schrödinger equation. This method has the advantages of using a familiar atomic physics perspective, maintaining “number conservation” and multiparticle excitations may be

³Other similar equations which go beyond the GP are sometimes called MGP, such as in Reference (27) referring to an equation derived by Nunes (28) using density functional theory. One can tell which MGP is being discussed by noting the reference.

included. Other authors have used multi-configurational Hartree-Fock approaches to investigate trapped BECs (see for example Reference (36) and references therein). Vanska *et al.* (37) develop a program for a direct configuration interaction (CI) calculation for a BEC. Cederbaum *et al.* (38) developed a coupled-cluster approach for a BEC in a $1 - D$ trap (for a recent review of coupled cluster theory, see (39)).

Mazzanti *et al.* (40) used correlated-basis theory (41) to study a BEC using both a hard-sphere and soft-sphere potential. They found that the energy became shape-dependent when the gas parameter was around 10^{-3} , and that other quantities (such as the density profile) were shape-dependent over the whole range of the gas parameter.

Thogersen *et al.* (42) write the variational wavefunction in a basis of correlated Gaussians. A direct numerical diagonalization of the N -body Hamiltonian (with an attractive interaction potential) is performed for up to 30 atoms (convergence to four digits typically requires 500 Gaussians).

Schneider and Feder (43) used a discrete variable representation (DVR) of the Hamiltonian of a dilute, zero-temperature BEC to determine the ground and excited states. This approach has been shown (44) to parallelize well.

2.3.2 Adiabatic hyperspherical harmonic approaches

Bohn *et al.* (45) applied the adiabatic hyperspherical harmonic expansion (with the K-harmonic approximation(46)), in which certain BEC properties are described by motion in an effective potential of a single collective coordinate (the hyperspherical radius). The interactions are zero-range. Sorensen *et al.* (47; 48; 49) discuss a similar adiabatic hyperspherical approach for a central two-body interaction potential and discuss the BEC phenomena in the context of the surface of the hyperradial effective potential. Sogo *et al.* (50) have derived a semianalytic solution to the hyperspherical effective potential for N bosons with zero-range interactions. Rajabi(51) showed that by making an ansatz for the wavefunction, the adiabatic hyperspherical harmonic approach may be used to solve the N -body Schrödinger equation analytically (within the approximation) for a class of potentials that include the Hooks-law and Coulomb interaction potentials.

Das *et al.* (52) proposed an alternative to an expansion in a hyperspherical harmonic basis: an expansion in a “potential harmonic basis”. Calculations for a small number of particles were shown to be near exact diffusion Monte Carlo (DMC) calculations with a strong scattering length (53), (the same DMC data referenced in

Chapter 8). Calculations for a dilute BEC with a large number of atoms interacting with a van der Waals interaction (54) are shown to agree with experimental results for dilute ${}^7\text{Li}$ (55) and ${}^{85}\text{Rb}$ (56) BEC.

2.3.3 Monte Carlo methods

For an introduction to Monte Carlo methods in physics, see for example References (57; 58).

In an early computational verification of the signature distribution of particles in a BEC, Krauth (59) used essentially exact path-integral Monte Carlo (PIMC) methods to simulate 10,000 atoms in a spherical trap with weak interactions ($a/a_{\text{ho}} = 0.00433$). He calculated the density profile for the Bose gas at small finite temperatures to show that below the critical temperature the condensed part of the gas can be described by the GP wavefunction. Holzmann *et al.* (60) showed that for the same scattering length, the density profiles calculated using Hartree-Fock and PIMC are in good agreement near the critical temperature, but that the HF approximation fails for zero temperature. These calculations are performed in the dilute regime and agree with the mean-field GP results.

In References (53; 61; 62; 63; 20; 64), Monte Carlo methods are employed to study the validity of the GP equation at larger interaction strengths in a BEC. These results exhibit “universal” behavior in the dilute regime that is characterized by the parameter na^3 or $(n-1)a^3$.

Blume *et al.* (53) and Nilsen *et al.* have verified at low- N that a modified GP equation which includes quantum fluctuations in References (26; 65; 33) leads to a greatly improved ground-state energy and density profile. Blume *et al.* (53) show that for a scattering length of $a = 0.433a/a_{\text{ho}}$, the GP underestimates the ground-state energy by 4% and 10% for $N = 3$ and $N = 10$, respectively, but underestimates the height of the condensate peak $n(0)/N$ by 20% and 35% for those numbers. In contrast, the MGP peak coincides with the DMC result for $N = 3$ and $N = 10$.

DuBois and Glyde (62) use an approximate variational Monte Carlo approach (VMC) to show that as the scattering length increases, the bulk of the BEC is actually pushed to the outer edges of the gas. In a later paper (20) the analysis is carried further to show that at $na^3 \geq 10^{-2}$ the mean-field theory fails and that at $na^3 \geq 0.1$ the BEC behaves like a liquid ${}^4\text{He}$ droplet. This reference also reports the appearance of correlations (“wiggles”) in the N -body density profile, which suggest that the

hard-sphere particles become packed in some arrangement as the effective size of the hard-spheres is increased in relation to the trap size.

DuBois, Glyde, and Sakhel (62; 63; 20) find that the shape of the probability density profile for the trapped condensate becomes flat for strong interactions, as opposed to the parabolic shape (due to the parabolic confining potential) predicted by mean-field theory in Reference (17). This shape is believed to be significantly influenced by interactions and depletion.

In Reference (66), Purwanto and Zhang use the ground-state auxiliary-field quantum Monte Carlo (AF QMC) method (67) to calculate the ground-state energy and density profile for a trapped BEC with strong interactions. The AF QMC method uses second-quantization and accounts for particle permutation statistics. This method is not exact (as DMC is) for bosons with repulsive interactions, but it is shown that the systematic errors are very small. The authors point out that the kinetic portion of both the GP and MGP do not include correlation effects, while the Bogoliubov approximation under the local density approximation (Bogoliubov+LDA) does so and demonstrates much closer agreement with AF QMC results. The authors also find that despite this discrepancy, the MGP and Bogoliubov+LDA yield similar total energies.

2.4 Does the shape of the interaction matter?

Most of the above references model the low-temperature interactions between atoms with a short-range potential, such as a “hard sphere” potential with a radius equal to the scattering length a

$$V(\mathbf{r}) = \begin{cases} 0 & \text{if } a < |\mathbf{r}| \\ \infty & \text{if } |\mathbf{r}| \leq a \end{cases}, \quad (2.5)$$

or the Fermi pseudopotential(68)

$$V = \frac{4\pi\hbar^2}{m} a\delta(\mathbf{r}) \frac{\partial}{\partial r} r. \quad (2.6)$$

These simple models of atomic collisions have been shown to be valid only in weak traps where the width of the trap ground state is larger than the scattering length $|a|$. For two or three atoms in strong confinement, several groups have shown(69; 70; 71; 72) that the shape-independence approximation breaks down for strong traps.

Blume and Greene (53) and Giorgini *et al.* (61) employ the diffusion Monte Carlo (DMC) (73; 74) method to show that the ground-state energy depends, to a good approximation, only on the s -wave scattering length for low densities ($n(0)a^3 \leq 2 \times 10^{-3}$) and that a modified GP equation yields a more accurate ground-state energy. This threshold for shape dependence is in agreement with the correlated basis function results of Mazzanti *et al.* (40). In Reference (53), DMC was applied to a trapped BEC at zero temperature with strong interactions. It was shown that for sufficiently low densities three different model potentials with the same s -wave scattering length yield the same ground-state energy, verifying the premise that properties of an ultracold dilute gas depend only on the scattering length to a good approximation. The DMC method can calculate the lowest energy essentially exactly (if there is no guiding function bias and the time step has been extrapolated to zero) for a low number of atoms. Esry and Greene (72) also showed that for three atoms in a trap the shape-independent approximation agrees with exact results only for dilute densities.

In early traps shape dependence was not an issue. More recent work requires consideration of the effect of trap confinement on scattering (71). In both the optical lattice work (see, for example the work of Greiner *et al.* (21)) and the large-gas parameter BEC's obtained by the use of a Feshbach resonance (see for example Cornish *et al.* (19)) the scattering length can exceed the trap width. Blume and Greene (70) and Bolda *et al.* (71) independently showed that the introduction of an *energy-dependent* effective scattering length (of the untrapped atoms) in the Fermi pseudopotential (2.6) yields good agreement with exact results for two atoms in a trap. In Reference (75), Collin *et al.* propose a similar energy-dependent generalization of the Fermi pseudopotential and derive a generalized GP equation that includes an effective-range scattering length.

In Reference (76), Kalas and Blume show that while interactions in a dilute gas could be characterized by a van der Waals interaction (proportional to r^{-6} for neutral atoms), a pseudopotential with an energy-dependent scattering length (70; 71) yields results close to fixed-node DMC (FN-DMC) calculations with a hard-sphere plus a van der Waals tail. Using such a pseudopotential or a hard-sphere contact potential gives rise to correlations due to two-body interactions only.

Thogersen *et al.* (42) point out that due to the use of an attractive interaction potential with a two-body bound state, a large and diverging scattering length results from small changes to the depth of the potential near the two-body threshold. Because an infinitesimal change in the potential leads to a disproportional large change in the

scattering length, the latter ceases to be a physically meaningful length scale when the scattering length diverges.

2.5 N -body dimensional perturbation theory

And now for something completely
different

John Cleese, 1969

In this chapter, we have discussed a few different kinds of theoretical and computational techniques used to understand the behavior of a BEC (a macroscopic quantum object) from a microscopic model that keeps track of each particle. In this thesis, we employ dimensional perturbation theory, a complementary N -body perturbative approach. This N -body dimensional perturbation theory (DPT) is essentially analytic and avoids costly computation. One significant advantage of analytic approaches in general is the physical insight that may be gained. N -body DPT is no exception. The macroscopic behavior of the BEC, such as the energy levels, what it looks like, the vibrational-mode characters and frequencies can be obtained. We will be interested in applying DPT in both the dilute gas limit, as well as in the regime $na^3 > 10^{-3}$ where the mean field GPE is no longer useful. We provide an introduction to the present N -body DPT method as well as background material in the next chapter.

Chapter 3

N-body dimensional perturbation theory

”Ha! Is it come to this?” thundered
the Stranger: ”then meet your Fate:
out of your Plane you go. Once,
twice, thrice! ’Tis done!”

Lord Sphere in Edwin A. Abbot’s
Flatland: a Romance of Many
Dimensions, 1884

In this dissertation, I present a formalism suitable for the study of confined, correlated systems of N bodies. In this chapter, I set the stage by reviewing perturbation theory, previous work by our group and others in dimensional perturbation theory, and how this dissertation extends the framework to higher perturbative orders. Because most of this work was performed in collaboration with group members, in this thesis I will revert to the editorial “we”.

3.1 Perturbation theory in general

The method we develop is based on a dimensional perturbation theory (DPT) approach, where the number of spatial dimensions is generalized to an arbitrary number of dimensions. This may seem odd to one who has studied perturbation theory in the context of an atom “perturbed” by an electric field (the Stark effect) or by a magnetic field (the Zeeman effect). In both of these examples, the perturbation parameter is a physical quantity, in the sense that it is something that can be controlled in the lab. The N -body problem is difficult enough, and one may well ask why the choice to include unphysical dimensions is of any use to those of us bound to three spatial

dimensions. A proper understanding of perturbation theory outside of the context of the typical undergraduate introduction will be helpful.

Perturbation theory is a technique by which a difficult problem is broken down into a series of easier problems using an iterative method of obtaining successive approximations. There are many examples of perturbation theory in atomic and high energy physics. In Ref. (77) it is pointed out that there are generally three steps to a perturbative analysis:

1. Convert the original problem into a perturbation problem by introducing a small parameter ε .
2. Assume an expression for the answer in the form of a perturbation series and compute the coefficients of that series.
3. Obtain the answer to the original problem by summing the perturbation series for the appropriate value of ε .

There are many ways to accomplish step one, so why not introduce a perturbation parameter in such a way that the zeroth-order solution has a closed-form, analytic expression? In general, if a closed-form zeroth-order solution exists, then the higher-order terms introduced in step two may also be soluble in an analytic closed form (77)¹.

3.1.1 Example: solution of a cubic polynomial

Also in Ref. (77), the following elementary example is given which illustrates the above steps without the trappings of a particular physical theory: finding the roots of the cubic polynomial

$$x^3 - 4.001x + 0.002 = 0. \tag{3.1}$$

The first step is to introduce an expedient perturbation parameter, ε , generalizing Eq. (3.1):

$$x^3 - (4 + \varepsilon)x + 2\varepsilon = 0. \tag{3.2}$$

The second step is to assume the roots to have a perturbation series solution of the form

¹The summation of the series in the third step is often complicated in that many non-trivial perturbation series are actually not convergent. See Ref. (78) for an extended discussion of divergent series in perturbation theory.

$$x(\varepsilon) = \sum_{n=0}^{\infty} a_n \varepsilon^n, \quad (3.3)$$

The zeroth-order ($n=0$) coefficient is determined by solving the roots of Eq. (3.2) with $\varepsilon = 0$:

$$x^3 - 4x = 0. \quad (3.4)$$

The above equation has three roots: $x(0) = a_0 = (-2, 0, 2)$. These are said to be the “zeroth-order” solutions. The second-order solution to the root -2 is determined by substituting Eq. (3.3) with $n = 2$ into the cubic polynomial (3.2), obtaining

$$(8a_1 + 4)\varepsilon + (8a_2 - a_1 - 6a_1^2)\varepsilon^2 = O(\varepsilon^3). \quad (3.5)$$

Since ε is a parameter, each coefficient of the above polynomial in ε must be zero. This condition is used to determine the values a_1 and a_2 and therefore the perturbation expansion for the -2 root to second perturbative order:

$$x_1 = -2 - \frac{1}{2}\varepsilon + \frac{1}{8}\varepsilon^2 + \dots \quad (3.6)$$

A similar procedure may be used to calculate the perturbative solution to the other two roots as well. Finally, to obtain the second-order perturbative calculation of the roots, one simply lets $\varepsilon = 0.001$ to recover the original problem. For this example, the convergence is striking: the difference between the second-order perturbative root near -2 and a numerical calculation is 6×10^{-11} .

3.2 Dimensional perturbation theory: an extensible framework

Dimensional perturbation theory (DPT) (79; 80) provides a systematic approach to the study of correlation in confined quantum systems. This method takes advantage of the high degree of symmetry possible among identical particles in higher dimensions to obtain an analytic description of the confined quantum system, without making any assumptions about the number of particles or the strength of interparticle interactions. Because the perturbation parameter is the inverse of the dimensionality of space

$$\delta \equiv \frac{1}{D},$$

DPT is equally applicable to weakly- or strongly-interacting systems. Another important advantage of DPT is that low-order DPT calculations are essentially *analytic*

in nature(81). As a consequence, the number of atoms enters into the calculations as a parameter, and so, in principle, results for any N are obtainable from a single calculation(82). Also, even the lowest-order result includes correlation, and so DPT may also be used to explore the transition between weakly interacting systems and those which are strongly interacting. These results can be systematically improved by going to higher perturbative order. In reference (83), Dunn *et al* relate a general method to calculate much higher-order corrections efficiently and exactly using tensor algebra.

The dimensional perturbation theory approach also follows the above three basic steps: the original $D = 3$ problem is generalized to D dimensions, a $1/D$ perturbation series is assumed, and the $D = 3$ solution is ultimately obtained.

3.2.1 A brief history of dimensional scaling and DPT

3.2.1.1 Dimensional scaling

Contemporary dimensional perturbation theory (DPT) has an interesting background story. In 1980, *Physics Today* carried an article (84) by theoretical physicist Edward Witten entitled “Quarks, atoms, and the $1/N$ expansion” discussing a perturbative quantum chromodynamics solution (in a referenced earlier work) in which three quark colors are generalized to N quark colors, the large- N limit is determined, and a $1/N$ perturbative calculation is performed. This is not the first example of a $1/N$ expansion; previous articles are referenced in (84). The article also showed the utility of a large-dimension limit in the examples of the hydrogen and helium atoms and a $1/N$ (where N is the number of spatial dimensions) perturbative calculation of the ground-state energy. The results discussed (reported from another reference) were not numerically impressive at lowest order.

Chemist Dudley Herschbach read the article and states in Ref. (79)

...since I was teaching a quantum mechanics course and on the lookout for provocative problems, I tried setting up the helium example as a homework exercise. By merely recasting the large- D limit to factor out the hydrogenic portion, I found that a very simple calculation gave 1% accuracy. This encouraged me to try to make use of another unphysical limit, $D \rightarrow 1$, which had a known solution. In order to interpolate, I assumed a geometric series in powers of $1/D$, fixing the parameters by means of the simple, exactly calculable $D \rightarrow \infty$ and $D \rightarrow 1$ limits. Setting

$D = 3$ in the resulting series gave the correct energy within 0.002%. The question of whether this was a portent or a fluke provoked much further work, in collaboration with enterprising students and colleagues, which led us to other intriguing surprises.

Dimensional scaling work flourished in the following decade or so, aided by a few specialty conferences. A 1996 article by Dunn and Watson (85) contains an overview of dimensional scaling studies in physics and physical chemistry with well over 100 related references. Dimensional scaling studies have been applied to a broad range of problems, but have a few general features in common (79):

1. The model for the physical system is generalized to D spatial dimensions.
2. The model is transformed and the coordinates and parameters are dimensionally-scaled to remove the leading-order D -dependence.
3. The model is solved exactly at one or more values of D .
4. The solution for $D = 3$ is calculated in terms of the unphysical D solution(s), by interpolation or perturbation.

3.2.1.2 N -body dimensional perturbation theory

When the $D = 3$ solution is obtained from a perturbation series in $\delta = 1/D$, the dimensional scaling method is called dimensional perturbation theory. In the present formulation, the perturbation series for the energy and wavefunction of a system of N bodies is written in the form

$$\begin{aligned}\bar{E} &= \bar{E}_\infty + \delta \sum_{j=0}^{\infty} \left(\delta^{\frac{1}{2}}\right)^j \bar{E}_j \\ \Phi &= \sum_{j=0}^{\infty} \left(\delta^{\frac{1}{2}}\right)^j \Phi_j.\end{aligned}$$

In practice $\bar{E}_j = 0$ when j is odd². The terms of order $j = 0$ are derived from a Hamiltonian of the form of uncoupled harmonic oscillators (written in a collective coordinate basis) and so we refer to the $j = 0$ perturbative terms as “harmonic order”. The higher-order terms are called “anharmonic.” The present work draws most directly from the N -body DPT application developed by Loeser in Ref. (86) for

²For a non-degenerate perturbation theory

an atom with many electrons. In this paper, Loeser introduced a (harmonic-order) N -body DPT perturbation formalism for the N -electron atom and the ground-state energy was calculated to harmonic order ($j = 0$) in $1/D$. The more specific features of this N -body DPT approach are:

1. The DPT method begins with a fully-interacting Hamiltonian in internal coordinates, generalized to arbitrary dimension.
2. The Hamiltonian is dimensionally-scaled and the Schrödinger equation is similarity transformed to obtain a Hamiltonian of the form of kinetic-energy derivative terms plus an effective potential which remains finite in the large-dimension limit.
3. In the large-dimension limit (a classical limit similar to $\hbar \rightarrow 0$), the wavefunction collapses to a classical symmetric arrangement of particles, which represents a minimum of the (multivariate) effective potential. The large- D energy is simply the minimal value of the effective potential.
4. By considering displacements of the internal coordinates from this large-dimension configuration we obtain a perturbation series of the Hamiltonian, where the perturbation parameter depends only on D .

The group of Deborah Watson began the extension of Loeser’s seminal work to a Bose-Einstein condensate in a spherically-symmetric trap, calculating the harmonic-order energy in References (82; 81). In Reference (87) Dunn *et al* used the theory of group representations to derive the harmonic-order ground-state wavefunction for $L = 0$. A crucial development in Reference (87) is the transformation of the harmonic-order Hamiltonian in internal coordinates to normal coordinates by introducing an intermediate step: the construction of so-called “symmetry coordinates.” An earlier work by Dunn *et al* showed how these results could be systematically improved by going to higher order(83). The harmonic-order DPT formalism in these references is directly applicable to any confined quantum system with a two-body interaction potential, although the focus has been on a BEC. This method is truly general for any isotropic confined quantum system of identical bosons in an isotropic confining potential with two-body interactions.

3.2.2 New N -body DPT work in this dissertation

3.2.2.1 Influential preliminary work

My first assignment was to generalize the above formalism for a BEC in a spherical trap to a cylindrical trap at harmonic order. The results were not as good as we had expected (88). In this work, we followed the example of McKinney *et al* (82) in modeling the atom-atom interaction potential by a step function with adjustable parameters, and “calibrating” the potential: the potential parameters are determined by optimizing the ground-state energies for different numbers of particles to benchmark diffusion Monte Carlo data(89) for $N \leq 100$ and extrapolating to higher N . In addition to determining the form of the large- D interaction potential, such an optimization makes the most of the current order in the perturbation series. We had hoped for results like Ref. (82), where the extrapolated ground-state energy compared favorably with other calculations up to a BEC with many thousands of identical atoms. We found that our extrapolations were not as good.

The harmonic-order cylindrical trap energy results needed improvement, so we sought to add more information to the fit. Reference (53), from which we obtained our benchmark low- N energy data, also contains the ground-state density profile for a cylindrical trap. The density profile is a directly observable manifestation of the quantized behavior of the confined quantum system. In order to add this additional information to our calibration to benchmark data, we generalized the harmonic-order ($L = 0$) wavefunction from a spherical geometry to a cylindrical geometry(88), and derived the harmonic-order density profile for both a spherical trap (90) and for a cylindrical trap (91). Due to the inflexible form of the harmonic-order density profile, we could not fit well to benchmark data and the results still did not meet our expectations. We knew that the density profile could be greatly improved by including the next-order (first anharmonic) term which would give the density profile the flexibility to conform to the benchmark data. We settled for publishing the harmonic-order density profile for a spherical trap (90) and made the decision to generalize the formalism to higher order.

3.2.2.2 Work that is in this dissertation

In Part II we develop the formalism of N -body DPT for first anharmonic order and, in principle, higher orders. To calculate the first-anharmonic-order wavefunction, it

was necessary to extend the structural expression of the harmonic-order Hamiltonian, which was written in Ref (81) as a bilinear form of coordinate vectors contracted with a coefficient matrix. The coefficient matrix in Ref (81) was shown to have a completely symmetric particle-label permutation symmetry and was written in terms of structural matrices which were derived from spectral graph theory. Not finding any corresponding higher-rank structural tensors from spectral graph theory, we constructed our own using a general procedure that can be employed at any order (Appendix C), for any rank Hamiltonian coefficient tensor. We also showed that these structural tensors (which we call “binary invariants”) form a basis for the coefficient tensors (Chapter 4). We calculated the terms of the first-anharmonic-order Hamiltonian, written in the form of coordinate and derivative vectors contracted with a rank-three tensor.

Having decomposed the first-anharmonic-order Hamiltonian coefficient tensors in a basis of binary invariants, we then transformed each binary tensor to normal coordinates (Chapter 5). In Ref. (87) it was shown using the theory of group representations that the transformed harmonic-order Hamiltonian coefficient matrices are proportional to Clebsch-Gordon coefficient matrices. These Clebsch-Gordon matrices are simply identity matrices. In Chapter 5, we use the same transformation matrices to transform the first anharmonic order Hamiltonian coefficient tensors to normal coordinates by transforming the binary invariants, showing that they are proportional to rank-three Clebsch-Gordon tensors, and by deriving both the transformations and the Clebsch-Gordon tensors in closed-form. By this transformation of binary invariants, the N -body Hamiltonian is *analytically* transformed to collective “normal” coordinates.

The reader is referred to Appendix A, which provides a parallel narrative to Chapters 3-5 for the simpler $N = 3$ case. The reader is also referred to Appendix B for an index convention “reference card”.

As discussed in Chapter 6, the first-anharmonic-order wavefunction is calculated using a simple commutation relation in Eq. (3.54). Having derived the first-anharmonic-order wavefunction, we calculate the ground-state probability density profile in Chapter 6.

In Part III, we apply the N -body DPT formalism developed in Part II to two examples. In Chapter 7 we derive the wavefunction and density profile of a trapped gas with interactions modeled by a Hooke’s law (spring-force) potential. While this system is not physical (in a real gas, interactions do not increase with larger distance),

it is exactly soluble. We derive the exact wavefunction and density profile, derive an analogous perturbation series, and demonstrate that the DPT wavefunction and density profile formalism (as well as the coded implementation) are in agreement with the exact results. In Chapter 8, we begin the application of the formalism to a BEC by optimizing the spherical density profile and energy to benchmark data.

3.3 N bodies in higher dimensions

In this section, we perform the first two steps of any dimensional scaling procedure. First, we make a difficult three-dimensional N -body problem seemingly more difficult by generalizing it to arbitrary dimensions. Second, we see that the system has a simple solution (which is exactly soluble in closed form) in the large-dimension limit.

3.3.1 The D -dimensional Schrödinger equation

We consider a system of N identical particles confined by a spherically symmetric potential and interacting via a two-body potential g_{ij} . It is easy enough to generalize the 3-dimensional Schrödinger equation in Cartesian coordinates to D dimensions:

$$H\Psi = \left[\sum_{i=1}^N h_i + \sum_{i=1}^{N-1} \sum_{j=i+1}^N g_{ij} \right] \Psi = E\Psi, \quad (3.7)$$

where

$$h_i = -\frac{\hbar^2}{2m_i} \sum_{\nu=1}^D \frac{\partial^2}{\partial x_{i\nu}^2} + V_{\text{conf}} \left(\sqrt{\sum_{\nu=1}^D x_{i\nu}^2} \right) \quad (3.8)$$

and

$$g_{ij} = V_{\text{int}} \left(\sqrt{\sum_{\nu=1}^D (x_{i\nu} - x_{j\nu})^2} \right) \quad (3.9)$$

are the single-particle Hamiltonian and the two-body interaction potential, respectively. The operator H is the D -dimensional Hamiltonian, and $x_{i\nu}$ is the ν^{th} Cartesian component of the i^{th} particle. V_{conf} is an external confining potential and V_{int} is the two-body interaction potential.

3.3.2 Confined quantum systems in internal coordinates

Internal coordinates provide a convenient description of quantum systems confined by a central potential. For a system of N atoms, we define the following internal

coordinates: r_i measures the distance of particle i from some common origin and $\gamma_{i,j}$ depends on the angle between r_i and r_j .

The definition of internal coordinates is easily extended to D dimensions by defining the D -dimensional radius, r_i

$$r_i = \sqrt{\sum_{\nu=1}^D x_{i\nu}^2} \quad (1 \leq i \leq N), \quad (3.10)$$

and the angle cosines, $\gamma_{i,j}$, as

$$\gamma_{ij} = \cos(\theta_{ij}) = \frac{\left(\sum_{\nu=1}^D x_{i\nu}x_{j\nu}\right)}{r_i r_j} \quad 1 \leq i < j \leq N. \quad (3.11)$$

Each of the coordinates $\gamma_{i,j}$ are defined in the 2-dimensional plane defined by the D -dimensional vectors r_i and r_j .

We transform the Hamiltonian to internal coordinates, following the derivation in Ref. (81) and restricting our attention to $L = 0$:

$$H = \sum_i \left\{ -\frac{\hbar^2}{2m_i} \left(\frac{\partial^2}{\partial r_i^2} + \frac{D-1}{r_i} \frac{\partial}{\partial r_i} + \sum_{j \neq i} \sum_{k \neq i} \frac{\gamma_{jk} - \gamma_{ij}\gamma_{ik}}{r_i^2} \frac{\partial^2}{\partial \gamma_{ij} \partial \gamma_{ik}} - \frac{D-1}{r_i^2} \sum_{j \neq i} \gamma_{ij} \frac{\partial}{\partial \gamma_{ij}} \right) + V_{\text{conf}}(r_i) \right\} + \sum_{i=1}^{N-1} \sum_{j=i+1}^N V_{\text{int}}(r_{ij}) \quad (3.12)$$

3.3.3 The Jacobian-weighted Schrödinger equation

In the internal coordinate Hamiltonian, integrals over internal coordinates must include a weight function of the Jacobian of the transformation from Cartesian to internal coordinates. In what follows, it would be convenient if this weight function was unity. This can be accomplished by performing a similarity transformation on the Schrödinger equation.

Similarity transformations of the wave function Ψ and operators \hat{O} have the following form:

$$\Phi = \chi^{-1}\Psi, \quad \text{and} \quad \tilde{O} = \chi^{-1}\hat{O}\chi. \quad (3.13)$$

There are many ways to perform such a transformation, depending on the choice of the transformation χ . In Ref. (92), Avery *et al.* considered the several choices of the transformation χ , all of which are related to the Jacobian of the transformation from Cartesian coordinates to internal coordinates J , where

$$J = (r_1 r_2 \dots r_N)^{(D-1)} \Gamma^{(D-N-1)/2}. \quad (3.14)$$

The quantity Γ is the Grammian determinant: the determinant of the matrix $[\gamma_{ij}]_{i,j}$ (see Appendix D of Ref. (81)).

We use the transformation that Avery *et al.* called case (i) (Table 3 in Ref. (92)), in which

$$\chi = J^{-\frac{1}{2}}. \quad (3.15)$$

The transformation χ has three useful properties.

- When integrating (such as when we determine the density profile), the weight function of the integral W is equal to unity, i.e.

$$W = J\chi^2 = 1. \quad (3.16)$$

- A first derivative of an internal coordinate is the conjugate momentum to that coordinate.
- The expression for T is explicitly Hermitian (or self-adjoint).

The result is the similarity-transformed (3.13) Schrödinger equation Eq. (3.17)

$$(T + V_{\text{eff}}) \Phi = E \Phi, \quad (3.17)$$

which has an operator T which is the derivative portion of the kinetic energy plus an centrifugal-like “effective potential” V_{eff} . This distinction is analogous to the solution of the Schrödinger equation of the hydrogen atom, where the angular momentum eigenvalue “centrifugal” term is added to the potential energy so that the equation is of the form of two terms: a purely derivative kinetic term plus an “effective potential.”

In the above, the derivative portion of the Jacobian-weighted Hamiltonian T is

$$\begin{aligned} T &= \hbar^2 \sum_{i=1}^N \left[-\frac{1}{2m_i} \frac{\partial^2}{\partial r_i^2} - \frac{1}{2m_i r_i^2} \left(\sum_{j \neq i} \sum_{k \neq i} (\gamma_{jk} - \gamma_{ij} \gamma_{ik}) \frac{\partial^2}{\partial \gamma_{ij} \partial \gamma_{ik}} - N \sum_{j \neq i} \gamma_{ij} \frac{\partial}{\partial \gamma_{ij}} \right) \right. \\ &\quad \left. + \frac{N(N-2) + (D-N-1)^2 \left(\frac{\Gamma^{(i)}}{\Gamma} \right)}{8m_i r_i^2} \right] \\ &= \hbar^2 \sum_{i=1}^N \left[-\frac{1}{2m_i} \frac{\partial^2}{\partial r_i^2} - \frac{1}{2m_i r_i^2} \sum_{j \neq i} \sum_{k \neq i} \frac{\partial}{\partial \gamma_{ij}} (\gamma_{jk} - \gamma_{ij} \gamma_{ik}) \frac{\partial}{\partial \gamma_{ik}} \right. \\ &\quad \left. + \frac{N(N-2) + (D-N-1)^2 \left(\frac{\Gamma^{(i)}}{\Gamma} \right)}{8m_i r_i^2} \right]. \end{aligned} \quad (3.18)$$

In the above equations, $\Gamma^{(i)}$ is the determinant of the Gramian matrix $[\gamma_{ij}]_{i,j}$ with row and column i removed (see Appendix D of Ref. (81)).

3.4 There's plenty of room for additional symmetry in larger dimensions

Generalizing the Schrödinger equation to higher dimensions allows us to introduce additional symmetries that are not present in three dimensions.

3.4.1 Preparation for the large-dimension limit: dimensional scaling

Following Ref. (81), we regularize the large- D limit of the Schrödinger equation by defining the dimensionally-scaled variables

$$\bar{r}_i = r_i/\kappa(D), \quad \bar{E} = \kappa(D) E, \quad \text{and} \quad \bar{H} = \kappa(D) H, \quad (3.19)$$

where $\kappa(D)$ is the dimension-dependent scale factor which regularizes the large- D limit³. The actual choice of $\kappa(D)$ depends on the physical system. In Table 3.4.1, we list choices of the $\kappa(D)$ used in (81; 82; 90).

The kinetic energy T in Equation (3.18) scales in the same way as $1/r^2$, so the dimensionally-scaled Schrödinger equation is

$$\bar{H}\Phi = \left(\frac{1}{\kappa(D)}\bar{T} + \bar{U} + \bar{V} \right) \Phi = \bar{E}\Phi, \quad (3.20a)$$

³In order to be consistent with previous DPT references the terms \hbar and m_i in the Hamiltonian later are included here, but will later be neglected by an implicit change to oscillator units, where \hbar and m are unity.

Physical System	$\kappa(D)$	$\Omega(D)$	Auxiliary variables
N -electron atom	$\Omega(D)/Z$	$(D-1)(D-2N-1)/4$	
quantum dot	$\Omega(D) l_{\text{ho}}$	$(D-1)(D-2N-1)/4$	$l_{\text{ho}} = \sqrt{\frac{\hbar}{m^* \bar{\omega}_{\text{ho}}}}$
BEC	$D^2 \bar{a}_{\text{ho}}$	D^2	$\bar{a}_{\text{ho}} = \sqrt{\frac{\hbar}{m \bar{\omega}_{\text{ho}}}} = a_{\text{ho}} D^{-\frac{3}{2}}$ $\bar{\omega}_{\text{ho}}^2 = \Omega(D)^3 \omega_{\text{ho}}^2$

Table 3.1: Dimensional scaling for three different confined quantum systems.

where

$$\bar{T} = \hbar^2 \sum_{i=1}^N \left(-\frac{1}{2m_i} \frac{\partial^2}{\partial \bar{r}_i^2} - \frac{1}{2m_i \bar{r}_i^2} \sum_{j \neq i} \sum_{k \neq i} \frac{\partial}{\partial \gamma_{ij}} (\gamma_{jk} - \gamma_{ij} \gamma_{ik}) \frac{\partial}{\partial \gamma_{ik}} \right), \quad (3.20b)$$

$$\bar{U} = \hbar^2 \sum_{i=1}^N \frac{1}{\kappa(D)} \left(\frac{N(N-2) + (D-N-1)^2 \left(\frac{\Gamma^{(i)}}{\Gamma} \right)}{8m_i \bar{r}_i^2} \right), \quad (3.20c)$$

$$\bar{V} = \sum_{i=1}^N \bar{V}_{\text{conf}}(\bar{r}_i) + \sum_{i=1}^{N-1} \sum_{j=i+1}^N \bar{V}_{\text{int}}(\bar{r}_{ij}). \quad (3.20d)$$

The centrifugal-like term \bar{U} of Eq. (3.20c) has quadratic D dependence, so the scale factor $\kappa(D)$ must also be quadratic in D , otherwise the $D \rightarrow \infty$ limit of the Hamiltonian would not be finite. The precise form of $\kappa(D)$ depends on the particular system and is chosen so that the result of the scaling is as simple as possible.

3.4.2 Large- D limit of the Hamiltonian

We consider the large-dimension limit of the Schrödinger equation by first rewriting (3.20a) in terms of the inverse dimensionality δ , where

$$\delta \equiv 1/D. \quad (3.21)$$

In the large-dimension limit ($\delta \rightarrow 0$) the factor of $\kappa(D)$ (which is quadratic in D) in the denominator of Eq. (3.20a) suppresses the derivative terms of (\bar{T}), leaving behind only centrifugal-like term,

$$\bar{U}(\bar{r}_i; \delta) \Big|_{\infty} = \hbar^2 \frac{1}{8m_i \bar{r}_i^2} \frac{1}{\delta^2 \kappa(D)} \left(\delta^2 N(N-2) + (1 - (N+1)\delta)^2 \frac{\Gamma^{(i)}}{\Gamma} \right) \Big|_{\infty}. \quad (3.22)$$

as well as the large- D limit of the confining and interacting potential terms.

This centrifugal-like term, together with the confining and interaction potentials form an effective potential, \bar{V}_{eff} :

$$\bar{V}_{\text{eff}}(\bar{r}, \gamma; \delta) = \sum_{i=1}^N (\bar{U}(\bar{r}_i; \delta) + \bar{V}_{\text{conf}}(\bar{r}_i; \delta)) + \sum_{i=1}^{N-1} \sum_{j=i+1}^N \bar{V}_{\text{int}}(\bar{r}_i, \gamma_{ij}; \delta). \quad (3.23)$$

The centrifugal-like term provides a repulsive core, even in the ground state.

3.4.3 Symmetric minimum of the effective potential

Due to the disappearance of the derivative portion of the kinetic energy, the particles in the system become “frozen” in some arrangement which minimizes the (multivariate) large- D effective potential, and the excited states collapse onto the ground state at the minimum of V_{eff} . We assume that this minimal arrangement is totally symmetric under particle interchange. The N particles are arranged on a hypersphere, each particle with a radius \bar{r}_∞ from the center of the confining potential. Furthermore, the angle cosines between each pair of particles takes on the same value, γ_∞ .

Thus in the large- D limit we assume the following values for \bar{r}_i and $\gamma_{i,j}$:

$$\lim_{D \rightarrow \infty} \bar{r}_i = \bar{r}_\infty \quad (1 \leq i \leq N) \quad \text{and} \quad (3.24)$$

$$\lim_{D \rightarrow \infty} \gamma_{ij} = \gamma_\infty \quad (1 \leq i < j \leq N).$$

This symmetric structure in which all N particles are equidistant and equiangular from every other particle can only exist in a higher-dimensional space and is impossible in a three-dimensional space unless $N \leq 3$ ⁴. The defining parameters of this high dimensional structure, \bar{r}_∞ and γ_∞ , are the lowest-order DPT expectation values for \bar{r}_i and γ_{ij} . This would indicate that the expectation values for the radii and interparticle angles for actual $D = 3$ systems should have values corresponding to structures that can only exist in higher ($D > 3$) dimensional spaces. Accurate configuration interaction calculations for atoms in three dimensions do indeed have expectation values for the radii and inter-electron angles which define higher-dimensional structures (93). This symmetric high-dimensional structure is also not unlike the localized structure found in a hyperspherical treatment of the confined two-component normal Fermi gas in the $N \rightarrow \infty$ limit (94).

In dimensionally-scaled units the $D \rightarrow \infty$ approximation for the energy is simply the effective potential minimum, i.e.

$$\bar{E}_\infty = \bar{V}_{\text{eff}}(\bar{r}_\infty, \gamma_\infty; \delta = 0). \quad (3.25)$$

In this $D \rightarrow \infty$ approximation, the centrifugal-like term that appears in \bar{V}_{eff} , which is nonzero even for the ground state.

⁴In a special case, valid for only one interparticle angles, 4 particles can be arranged at the points of a tetrahedron in three dimensions. The interparticle angle is in no way fixed by the number of particles.

Beyond-mean-field effects are already present in this approximation. This may be seen in the value of γ_∞ , the $D \rightarrow \infty$ expectation value for the interparticle angle cosine (see Eqs. (3.24) and (3.26)). In the mean-field approximation, the expectation value for the interparticle angle cosine for the $L = 0$ states considered here is zero. The fact that γ_∞ is *not* zero is an indication that beyond-mean-field effects are included even in the $D \rightarrow \infty$ limit.

The $D \rightarrow \infty$ approximation may also be systematically improved by using it as the starting point for a perturbation expansion (DPT). This highly-symmetric, $D \rightarrow \infty$ structure imparts a point-group structure to the system which is isomorphic to the symmetric group of N identical objects (95), S_N . This symmetry allows for an analytic determination of the higher-order perturbative terms, even though the number of degrees of freedom becomes very large when N is large.

3.5 Perturbation about large- D structure

The method of N -body dimensional perturbation theory used here starts with the large- D , symmetric, static arrangement and forms a perturbation series by considering small displacements about that static arrangement. We consider small, dimensionally-scaled displacements about the minimum of \bar{V}_{eff} :

$$\bar{r}_i = \bar{r}_\infty + \delta^{1/2} \bar{r}'_i \quad (3.26)$$

$$\gamma_{ij} = \gamma_\infty + \delta^{1/2} \gamma'_{ij}. \quad (3.27)$$

We will perform a series expansion of \bar{V}_{eff} about $\delta^{\frac{1}{2}} = 0$ to obtain \bar{V}_{eff} as a power series in $\delta^{\frac{1}{2}}$, but first we find it expedient to express the internal coordinates using the vectors $\bar{\mathbf{y}}$ and $\bar{\mathbf{y}}'$. We define a vector $\bar{\mathbf{y}}$ consisting of all the $\frac{N(N+1)}{2}$ internal coordinates,

$$\bar{\mathbf{y}} = \begin{pmatrix} \bar{\mathbf{r}} \\ \gamma \end{pmatrix}, \quad \text{where} \quad \bar{\mathbf{r}} = \begin{pmatrix} \bar{r}_1 \\ \bar{r}_2 \\ \vdots \\ \bar{r}_N \end{pmatrix} \quad \text{and} \quad \gamma = \begin{pmatrix} \gamma_{12} \\ \gamma_{13} \\ \gamma_{23} \\ \gamma_{14} \\ \gamma_{24} \\ \gamma_{34} \\ \gamma_{15} \\ \gamma_{25} \\ \vdots \\ \gamma_{N-2,N} \\ \gamma_{N-1,N} \end{pmatrix}. \quad (3.28)$$

We make a similar definition for the internal displacement coordinate vector $\bar{\mathbf{y}}'$,

$$\mathbf{y}' = \begin{pmatrix} \bar{\mathbf{r}}' \\ \gamma' \end{pmatrix}, \quad \text{where} \quad \bar{\mathbf{r}}' = \begin{pmatrix} \bar{r}'_1 \\ \bar{r}'_2 \\ \vdots \\ \bar{r}'_N \end{pmatrix} \quad \text{and} \quad \gamma' = \begin{pmatrix} \gamma'_{12} \\ \gamma'_{13} \\ \gamma'_{23} \\ \gamma'_{14} \\ \gamma'_{24} \\ \gamma'_{34} \\ \gamma'_{15} \\ \gamma'_{25} \\ \vdots \\ \gamma'_{N-2,N} \\ \gamma'_{N-1,N} \end{pmatrix}. \quad (3.29)$$

We then make the substitution

$$\bar{\mathbf{y}} = \bar{\mathbf{y}}_\infty + \delta^{1/2} \bar{\mathbf{y}}' \quad (3.30)$$

in the dimensionally-scaled Schrödinger equation (3.20a). As we shall see, writing \bar{T} and \bar{V}_{eff} as functions of the column vector $\bar{\mathbf{y}}'$ will enable us to write the corresponding series expansions in a compact form.

3.5.1 Series expansion of the kinetic term, G

The series expansion about $\delta = 0$ of (3.20b) is calculated in Appendix D. Here are the results:

$$\begin{aligned}
\mathcal{T} = & -\frac{1}{2}\delta \left(\sum_{i=1}^N \frac{\partial^2}{\partial \bar{r}_i'^2} + \sum_{i=1}^N \sum_{j \neq i} \frac{1 - \gamma_\infty^2}{\bar{r}_\infty^2} \frac{\partial^2}{\partial \gamma_{ij}'^2} + \right. \\
& \left. \sum_{i=1}^N \sum_{j \neq i} \sum_{k \neq i} (1 - \delta_{j,k}) \frac{(1 - \gamma_\infty) \gamma_\infty}{\bar{r}_\infty^2} \frac{\partial^2}{\partial \gamma_{ij}' \partial \gamma_{ik}'} \right) \\
& - \frac{1}{2} \delta^{3/2} \left(\sum_{i=1}^N \sum_{j \neq i} \left(-\frac{2(1 - \gamma_\infty^2)}{\bar{r}_\infty^3} \bar{r}_i' - \frac{2\gamma_\infty}{\bar{r}_\infty^2} \gamma_{ij}' \right) \frac{\partial^2}{\partial \gamma_{ij}'^2} \right. \\
& + \sum_{i=1}^N \sum_{j \neq i} \sum_{k \neq i} \left(\frac{(2(\gamma_\infty - 1)\gamma_\infty)}{\bar{r}_\infty^3} \bar{r}_i' - \frac{\gamma_\infty}{\bar{r}_\infty^2} (\gamma_{ij}' + \gamma_{ik}') + \frac{\gamma_{jk}'}{\bar{r}_\infty^2} \right) \frac{\partial^2}{\partial \gamma_{ij}' \gamma_{ik}'} \\
& \left. + \sum_{i=1}^N \sum_{j \neq i} \left(-N \frac{\gamma_\infty}{\bar{r}_\infty^2} \right) \frac{\partial}{\partial \gamma_{ij}'} \right) + O(\delta^2). \tag{3.31}
\end{aligned}$$

Equation (3.31) may be written in the compact form of (as of yet undefined) tensors G contracted with the column vectors \bar{y}'_ν and $\partial_{\bar{y}'_\nu}$ by summing over all $P = N(N+1)/2$ internal coordinates,

$$\begin{aligned}
\mathcal{T} = & -\frac{1}{2}\delta \sum_{\nu_1=1}^P \sum_{\nu_2=1}^P {}^{(0)}G_{\nu_1, \nu_2} \partial_{\bar{y}'_{\nu_1}} \partial_{\bar{y}'_{\nu_2}} - \frac{1}{2}\delta^{3/2} \left(\sum_{\nu_1=1}^P \sum_{\nu_2=1}^P \sum_{\nu_3=1}^P {}^{(1)}G_{\nu_1, \nu_2, \nu_3} \bar{y}'_{\nu_1} \partial_{\bar{y}'_{\nu_2}} \partial_{\bar{y}'_{\nu_3}} \right. \\
& \left. + \sum_{\nu=1}^P {}^{(1)}G_\nu \partial_{\bar{y}'_\nu} \right) + O(\delta^2), \tag{3.32}
\end{aligned}$$

The tensors ${}^{(0)}G_{\nu_1, \nu_2}$, ${}^{(1)}G_{\nu_1, \nu_2, \nu_3}$, and ${}^{(1)}G_\nu$ have an intricate but well-defined structure, which is the subject of the next chapter. The actual values are calculated in Appendix D. A few notes on notation are in order here

- We differentiate between the tensors (e.g. ${}^{(0)}G_{\nu_1, \nu_2}$ and ${}^{(1)}G_{\nu_1, \nu_2, \nu_3}$) with a pre-superscript for perturbative order (0 for harmonic, n for n^{th} anharmonic), and a presubscript for tensor rank.
- We reserve the index label ν or ν_i to label the elements of the internal displacement coordinate \bar{y}'_ν or the normal coordinate vector \bar{q}'_ν . In both cases, the range of ν is from 1 to $P = \frac{N(N+1)}{2}$ for a spherically-symmetric system.

- We will often employ the repeated summation convention, where repeated ν indices in a tensor contraction are assumed to be under a summation from $\nu = 1$ to P

With these conventions, we write the perturbative series of the derivative portion of the kinetic term as a series of G tensor contractions:

$$\mathcal{T} = -\frac{1}{2}\delta \binom{(0)}{2}G_{\nu_1, \nu_2} \partial_{\bar{y}'_{\nu_1}} \partial_{\bar{y}'_{\nu_2}} - \frac{1}{2}\delta^{3/2} \left(\binom{(1)}{3}G_{\nu_1, \nu_2, \nu_3} \bar{y}'_{\nu_1} \partial_{\bar{y}'_{\nu_2}} \partial_{\bar{y}'_{\nu_3}} + \binom{(1)}{1}G_{\nu} \partial_{\bar{y}'_{\nu}} \right) + O(\delta^2). \quad (3.33)$$

In previous papers, in which orders beyond harmonic were not considered, $\binom{(0)}{2}G_{\nu_1, \nu_2}$ was simply labeled \mathbf{G} or G_{ν_1, ν_2} . Also, Eq. (19) in Reference (87) is incorrect: $\partial_{\bar{y}'_{\nu}}$ is a row vector (a covariant Cartesian tensor) and therefore the relevant part should read $\partial_{\bar{y}'_{\nu_1}} G_{\nu_1, \nu_2} \partial_{\bar{y}'_{\nu_2}}^T$. The same mistake is in Eq. (30) of Reference (81). This clarification is necessary in order to correctly transform (3.33) to a normal-mode coordinate basis.

3.5.2 Series expansion of the effective potential, F

In Appendix D we calculate the series expansion of the effective potential $\bar{V}_{\text{eff}}[\bar{\mathbf{y}}'; \delta]$ about $\delta = 0$, obtaining

$$\begin{aligned} \bar{V}_{\text{eff}}[\bar{\mathbf{y}}'; \delta] &= \bar{V}_{\text{eff}}[\bar{\mathbf{y}}_{\infty}; \delta] \Big|_{\infty} + \delta \left(\frac{d}{d\delta} \bar{V}_{\text{eff}}[\bar{\mathbf{y}}; \delta] + \frac{1}{2} \sum_{\nu_1=1}^P \sum_{\nu_2=1}^P \bar{y}'_{\nu_1} \bar{y}'_{\nu_2} \frac{\partial^2 \bar{V}_{\text{eff}}[\bar{\mathbf{y}}; \delta]}{\partial \bar{y}_{\nu_1} \partial \bar{y}_{\nu_2}} \right) \Big|_{\infty} \\ &\delta^{3/2} \left(\sum_{\nu=1}^P \bar{y}'_{\nu} \frac{\partial}{\partial \bar{y}_{\nu}} \frac{d}{d\delta} \bar{V}_{\text{eff}}[\bar{\mathbf{y}}; \delta] \right) \Big|_{\infty} + \frac{1}{3!} \sum_{\nu_1=1}^P \sum_{\nu_2=1}^P \sum_{\nu_3=1}^P \bar{y}'_{\nu_1} \bar{y}'_{\nu_2} \bar{y}'_{\nu_3} \frac{\partial^3 \bar{V}_{\text{eff}}[\bar{\mathbf{y}}; \delta]}{\partial \bar{y}_{\nu_1} \partial \bar{y}_{\nu_2} \partial \bar{y}_{\nu_3}} \Big|_{\infty} \\ &+ O(\delta^2). \end{aligned} \quad (3.34)$$

We may express Eq. (3.34) in a compact tensor form with the following definitions:

$$\bar{E}_{\infty} = \bar{V}_{\text{eff}}[\bar{\mathbf{y}}; \delta] \Big|_{\infty} \quad (3.35a)$$

$$\binom{(0)}{0}F = \frac{d}{d\delta} \bar{V}_{\text{eff}}[\bar{\mathbf{y}}; \delta] \Big|_{\infty} \quad (3.35b)$$

$$\binom{(0)}{2}F_{\nu_1, \nu_2} = \frac{\partial^2}{\partial \bar{y}_{\nu_1} \partial \bar{y}_{\nu_2}} \bar{V}_{\text{eff}}[\bar{\mathbf{y}}; \delta] \Big|_{\infty} \quad (3.35c)$$

$$\binom{(1)}{1}F_{\nu} = \frac{\partial}{\partial \bar{y}_{\nu}} \frac{d}{d\delta} \bar{V}_{\text{eff}}[\bar{\mathbf{y}}; \delta] \Big|_{\infty} \quad (3.35d)$$

$${}^{(1)}_3 F_{\nu_1, \nu_2, \nu_3} = \frac{\partial^3}{\partial \bar{y}_{\nu_1} \partial \bar{y}_{\nu_2} \partial \bar{y}_{\nu_3}} \bar{V}_{\text{eff}}[\bar{\mathbf{y}}; \delta] \Big|_{\infty} \quad (3.35e)$$

With the above definitions for the effective potential F tensors, the perturbative expansion of the effective potential is expressed in the following series of tensor contractions:

$$\begin{aligned} \bar{V}_{\text{eff}}[\bar{\mathbf{y}}'; \delta] = & E_{\infty} + \delta \left({}^{(0)}_0 F + \frac{1}{2} \sum_{\nu_1=1}^P \sum_{\nu_2=1}^P {}^{(1)}_2 F_{\nu_1, \nu_2} \bar{y}'_{\nu_1} \bar{y}'_{\nu_2} \right) \\ & + \delta^{3/2} \left(\sum_{\nu=1}^P {}^{(1)}_1 F_{\nu} \bar{y}'_{\nu} + \frac{1}{3!} \sum_{\nu_1=1}^P \sum_{\nu_2=1}^P \sum_{\nu_3=1}^P {}^{(1)}_3 F_{\nu_1, \nu_2, \nu_3} \bar{y}'_{\nu_1} \bar{y}'_{\nu_2} \bar{y}'_{\nu_3} \right) + O(\delta^2). \end{aligned} \quad (3.36)$$

In previous papers, ${}^{(0)}_0 F$ was labeled ν_0 and ${}^{(0)}_2 F_{\nu_1, \nu_2}$ was labeled F_{ν_1, ν_2} .

3.5.3 Perturbation series expressions

Combining the series expansions for the (derivative portion of the) kinetic term (3.33) and the potential term (3.36), we obtain the Hamiltonian operator as a perturbation series in $\delta^{\frac{1}{2}}$:

$$\bar{H} = E_{\infty} + \delta \bar{H}_0 + \delta^{3/2} \bar{H}_1 + O(\delta^2), \quad (3.37)$$

where

$$\bar{H}_0 = -\frac{1}{2} {}^{(0)}_2 G_{\nu_1, \nu_2} \partial_{\bar{y}'_{\nu_1}} \partial_{\bar{y}'_{\nu_2}} + \frac{1}{2} {}^{(0)}_2 F_{\nu_1, \nu_2} \bar{y}'_{\nu_1} \bar{y}'_{\nu_2} + {}^{(0)}_0 F \quad (3.38)$$

and

$$\bar{H}_1 = -\frac{1}{2} {}^{(1)}_3 G_{\nu_1, \nu_2, \nu_3} \bar{y}'_{\nu_1} \partial_{\bar{y}'_{\nu_2}} \partial_{\bar{y}'_{\nu_3}} + \frac{1}{3!} {}^{(1)}_3 F_{\nu_1, \nu_2, \nu_3} \bar{y}'_{\nu_1} \bar{y}'_{\nu_2} \bar{y}'_{\nu_3} - \frac{1}{2} {}^{(1)}_1 G_{\nu} \partial_{\bar{y}'_{\nu}} + {}^{(1)}_1 F_{\nu} \bar{y}'_{\nu}. \quad (3.39)$$

In the above equations, summation of repeated indices from 1 to $P = N(N+1)/2$ is implied. The tensors F and G in Eqs. (3.38) and (3.39) have an intricate symmetric structure that is difficult to express without the benefit of graph theory, as developed in Section 4.3. We will return to the calculation of the actual elements of F and G in Appendix D.

The N -body wavefunction $\Phi(\bar{r}_i, \gamma_{ij})$ is assumed to have a similar expansion about $\delta = 0$

$$\Phi(\bar{r}_i, \gamma_{ij}) = \sum_{j=0}^{\infty} \left(\delta^{\frac{1}{2}} \right)^j \Phi_j. \quad (3.40)$$

The DPT expansions of the Hamiltonian Eq. (3.37) and of the wavefunction Eq. (3.40) form a series expansion of the Schrödinger equation in which each order in δ must be equal to zero:

$$\delta : (\bar{H}_0 - \bar{E}_0) \Phi_0 = 0 \quad (3.41)$$

$$\delta^{3/2} : (\bar{H}_1 - \bar{E}_1) \Phi_0 + (\bar{H}_0 - \bar{E}_0) \Phi_1 = 0 \quad (3.42)$$

$$\delta^2 : (\bar{H}_2 - \bar{E}_2) \Phi_0 + (\bar{H}_1 - \bar{E}_1) \Phi_1 + (\bar{H}_0 - \bar{E}_0) \Phi_2 = 0 \quad (3.43)$$

$$\vdots : \quad (3.44)$$

The above equations are solved sequentially: the solution to \bar{E}_0 and Φ_0 in Eq. (3.41) are then used in Eq. (3.42) to solve for \bar{E}_1 and Φ_1 , and so on. The resulting perturbative energy series is

$$\bar{E} = \bar{E}_\infty + \delta \sum_{j=0}^{\infty} \left(\delta^{\frac{1}{2}} \right)^j \bar{E}_j. \quad (3.45)$$

3.6 Solution of the harmonic-order equation

3.6.1 Normal-mode frequencies, harmonic energy

To solve the harmonic-order equation (3.41), McKinney *et al* in (82; 81) reasoned that the form of H_0 indicates a solution of the form of P uncoupled harmonic oscillators written in terms of collective “normal mode” coordinates.

In order to determine the frequencies of the normal modes (but not the actual collective coordinates themselves), McKinney *et al* employed the Wilson GF matrix method(96). This method is a way to simultaneously diagonalize both the harmonic order ${}^{(0)}_2G$ and ${}^{(0)}_2F$ coefficient matrices and find the roots of the following characteristic polynomial in λ :

$$\det(\lambda \mathbf{I} - {}^{(0)}_2\mathbf{G} {}^{(0)}_2\mathbf{F}). \quad (3.46)$$

There are $P = N(N + 1)/2$ roots λ , but due to the S_N symmetry of ${}^{(0)}_2\mathbf{G}$ and ${}^{(0)}_2\mathbf{F}$ there are only *five* distinct (though degenerate) roots of λ , labeled $\mathbf{0}\pm$, $\mathbf{1}\pm$, and $\mathbf{2}$.

For each root λ_ν , the normal-mode frequency ω_ν is related to the root value by the equation

$$\lambda_\nu = \omega_\nu^2. \quad (3.47)$$

The energy through first-order in $\delta = 1/D$ is then (81)

$$\bar{E} = \bar{E}_\infty + \delta \left[\sum_{\mu=\{\mathbf{0}^\pm, \mathbf{1}^\pm, \mathbf{2}\}} \sum_{n_\mu=0}^{\infty} (n_\mu + \frac{1}{2}) d_{\mu, n_\mu} \bar{\omega}_\mu + {}_0^{(0)}F \right], \quad (3.48)$$

where the n_μ are the vibrational quantum numbers of the normal modes of the same frequency $\bar{\omega}_\mu$ (n_μ counts the number of nodes in a given normal mode). The quantity d_{μ, n_μ} is the occupancy of the manifold of normal modes with vibrational quantum number n_μ and normal-mode frequency $\bar{\omega}_\mu$, i.e. it is the number of normal modes with the same frequency $\bar{\omega}_\mu$ and the same number of quanta n_μ . The total occupancy of the normal modes with frequency $\bar{\omega}_\mu$ is equal to the multiplicity of the root λ_μ , i.e.

$$d_\mu = \sum_{n_\mu=0}^{\infty} d_{\mu, n_\mu}, \quad (3.49)$$

where d_μ is the multiplicity of the μ^{th} root. The multiplicities of the five roots(81) are

$$\begin{aligned} d_{\mathbf{0}^+} &= 1, \\ d_{\mathbf{0}^-} &= 1, \\ d_{\mathbf{1}^+} &= N - 1, \\ d_{\mathbf{1}^-} &= N - 1, \quad \text{and} \\ d_{\mathbf{2}} &= N(N - 3)/2. \end{aligned} \quad (3.50)$$

The term ${}_0^{(0)}F$ is due to a constant in the Hamiltonian that results from the derivative of the effective potential with respect to δ .

3.6.2 Normal-mode coordinates, harmonic wavefunction

In order to determine the harmonic-order wavefunction, one must also determine the collective normal-mode coordinates. Dunn *et al* explicitly construct the normal-mode coordinates in Ref. (87), as well as the harmonic-order DPT wavefunction

$$\Phi_0(\mathbf{q}') = \prod_{\nu=1}^P \phi_{n_\nu}(\sqrt{\bar{\omega}_\nu} \mathbf{q}'_\nu), \quad (3.51)$$

where $\phi_{n_\nu}(\sqrt{\bar{\omega}_\nu} \mathbf{q}'_\nu)$ is a one-dimensional harmonic-oscillator wave function of frequency $\bar{\omega}_\nu$, and n_ν is the oscillator quantum number, $0 \leq n_\nu < \infty$, which counts the number of quanta in each normal mode.

3.7 Solution of the first-anharmonic-order equation

Having solved the harmonic-order Schrödinger equation, Eq. (3.41), for \bar{E}_0 and Φ_0 , we now proceed to solve the first anharmonic order Schrödinger equation Eq. (3.42). We first assume that the first anharmonic order wavefunction can be obtained from the harmonic wavefunction by some operator $\hat{\Delta}$,

$$\Phi_1(\mathbf{q}') = \hat{\Delta}\Phi_0(\mathbf{q}'), \quad (3.52)$$

so that the wavefunction through first anharmonic order (see Eq. (3.40)) has the form

$$\Phi(\mathbf{q}') = (1 + \delta^{\frac{1}{2}}\hat{\Delta})\Phi_0(\mathbf{q}') + O(\delta) \quad (3.53)$$

We substitute Φ_1 from the above Equation into the first-anharmonic Schrödinger equation, Eq. (3.42), noting that E_1 is zero due to symmetry considerations, and we obtain an expression involving the unknown operator $\hat{\Delta}$ with known quantities:

$$[\hat{\Delta}, \bar{H}_0]\Phi_0 = \bar{H}_1\Phi_0. \quad (3.54)$$

This equation builds upon the above determination of the harmonic order energy and wavefunction. The result will be the calculation of the first-anharmonic-order wavefunction Φ_1 . The key to this solution is to use the normal-mode coordinates determined at harmonic order to transform the first-anharmonic Hamiltonian H_1 to a normal-coordinate basis in order to determine the operator $\hat{\Delta}$ and therefore the wavefunction Φ_1 in normal coordinates.

A brute-force transformation of the F and G tensors in H_1 (which are of dimension $P \times P \times P$, where $P = N(N + 1)/2$ for isotropic confinement) would quickly become computationally prohibitive at large N . In Chapter 4, we show that the Hamiltonian terms in the DPT perturbation series can be resolved in a structural basis, which we call “binary invariants”. In Chapter 5, we show that the transformation of each first anharmonic order binary invariant must be proportional to one of eight group theoretic tensors called “Clebsch-Gordon coefficients” and we calculate the proportionality coefficient. In Chapter 6, we derive the first-anharmonic-order wavefunction as well as the density profile. So far, no physical system has been specified.

This general formalism, particularly the binary invariant basis expansion and the use of Clebsch-Gordon coefficients, can be later used in Eq. (3.43) to calculate the second-anharmonic energy and wavefunction and so on.

Part II

Anharmonic-order formalism development

Chapter 4

Fearful symmetry, framed: decomposition in a structural basis

Tyger! Tyger! burning bright
In the forests of the night,
What immortal hand or eye
Could frame thy fearful symmetry?

William Blake, 1789

We previously alluded to the intricate structure of the coefficient tensors of the DPT Hamiltonian. In this Chapter we capture this structure using graphs and multilinear algebra to define a small basis set which frames the intricate symmetry in the DPT Hamiltonian series. We use this basis set expansion to separate the N -dependence from the details of the physical system. In the following chapter we will transform the basis tensors to normal coordinates, thus analytically determining the DPT Hamiltonian in a basis of normal coordinates and therefore utterly taming the N -body problem at each order.

In previous work (87; 81; 82; 90), the intricate, symmetric structure of the harmonic-order Hamiltonian Eq. (3.38) in matrix form was expressed in terms of the so-called “simple submatrices”, \mathbf{I} , \mathbf{J} , and \mathbf{R} which are used in spectral graph theory. Such matrices actually formed a basis for the harmonic-order matrices. In calculating the transformation of the harmonic (3.38) and first anharmonic (3.39) Hamiltonian to normal mode coordinates, we will need to generalize these basis matrices to basis tensors. In this chapter we introduce such generalized basis tensors, which we call “binary invariants”. Since the F , G , FG , and GF tensors for bosons in a internal coordinate basis must have the same structure (but not necessarily the same elemental values), the decomposition of these matrices in a structural basis allows us

to develop a general theory for quantum confined systems of bosons. In Chapter 5 we show that the transformation of these basis tensors to normal coordinates may be performed analytically, for general N . By decomposing each perturbative order of the DPT Schrödinger equation in the basis of binary invariants, we have opened the door to an analytic DPT solution at orders higher than harmonic for arbitrary number of particles.

The reader is again referred to Section A.4 in the Appendix for a parallel narrative for the simpler $N = 3$ case.

4.1 Hamiltonian indicial structure and group symmetry

The large- D symmetric arrangement specified by $\bar{\mathbf{y}}_\infty$ has the highest degree of symmetry possible, where all particles are equidistant from the center of the trap and equiangular from each other (a configuration that is only possible in higher dimensions). This point group structure is isomorphic to S_N , the group of permutations of N items.

The G and F Hamiltonian tensors in equations (3.38) and (3.39), reproduced below, are written in terms of the Hamiltonian coefficient tensors G and F :

$$\bar{H}_0 = -\frac{1}{2} {}^{(0)}_2 G_{\nu_1, \nu_2} \partial_{\bar{y}'_{\nu_1}} \partial_{\bar{y}'_{\nu_2}} + \frac{1}{2} {}^{(0)}_2 F_{\nu_1, \nu_2} \bar{y}'_{\nu_1} \bar{y}'_{\nu_2} + {}^{(0)}_0 F$$

and

$$\bar{H}_1 = -\frac{1}{2} {}^{(1)}_3 G_{\nu_1, \nu_2, \nu_3} \bar{y}'_{\nu_1} \partial_{\bar{y}'_{\nu_2}} \partial_{\bar{y}'_{\nu_3}} + \frac{1}{3!} {}^{(1)}_3 F_{\nu_1, \nu_2, \nu_3} \bar{y}'_{\nu_1} \bar{y}'_{\nu_2} \bar{y}'_{\nu_3} - \frac{1}{2} {}^{(1)}_1 G_\nu \partial_{\bar{y}'_\nu} + {}^{(1)}_1 F_\nu \bar{y}'_\nu.$$

In the above equations, summation of repeated indices from 1 to $P = N(N+1)/2$ is implied. These tensors represent the coefficients of a Taylor series about the large- D limit, so the elements themselves are evaluated at the large- D limit. We have specified that the system is invariant under the elements of S_N (permutation of particle labels) in the large- D limit. This order-by-order invariance under the permutations of S_N greatly restricts the Hamiltonian tensors so that tensor elements related by a permutation must be equal.

4.1.1 Indicial structure of internal coordinate tensors

The harmonic-order block matrices contain the sets of elements (in Eqs. (4.4)-(4.8)) arranged in an intricate pattern. In Ref. (81) it was shown that, at harmonic order,

this arrangement could be expressed in terms of only seven structural matrices. In this dissertation, we introduce a generalized structural decomposition of the tensors that occur at higher orders.

4.1.1.1 Harmonic order

We refer to the Hamiltonian tensors of a specified order and rank R generically as ${}^{(order)}_R Q$, where Q can represent any Hamiltonian matrix (F , G , GF , or FG). At harmonic order the Hamiltonian involves rank-two ${}^{(0)}_2 Q$ tensors, which are $P \times P$ matrices (where $P = N(N + 1)/2$). In the basis of internal coordinates, these ${}^{(0)}_2 Q$ have the same indicial structure as $\bar{y}_{\nu_1} \bar{y}_{\nu_2}$:

$$\bar{y}_{\nu_1} \bar{y}_{\nu_2} = \begin{pmatrix} \begin{array}{cccc|cccc} \bar{r}_1 \bar{r}_1 & \bar{r}_1 \bar{r}_2 & \cdots & \bar{r}_1 \bar{r}_N & \bar{r}_1 \gamma_{12} & \bar{r}_1 \gamma_{13} & \cdots & \bar{r}_1 \gamma_{N-1N} \\ \bar{r}_2 \bar{r}_1 & \bar{r}_2 \bar{r}_2 & \cdots & \bar{r}_2 \bar{r}_N & \bar{r}_2 \gamma_{12} & \bar{r}_2 \gamma_{13} & \cdots & \bar{r}_2 \gamma_{N-1N} \\ \vdots & \vdots & \ddots & \vdots & \vdots & \vdots & \ddots & \vdots \\ \bar{r}_N \bar{r}_1 & \cdots & & \bar{r}_N \bar{r}_N & \bar{r}_N \gamma_{12} & \cdots & & \bar{r}_N \gamma_{N-1N} \end{array} \\ \hline \begin{array}{cccc|cccc} \gamma_{12} \bar{r}_1 & \gamma_{12} \bar{r}_2 & \cdots & \gamma_{12} \bar{r}_N & \gamma_{12} \gamma_{12} & \gamma_{12} \gamma_{13} & \cdots & \gamma_{12} \gamma_{N-1N} \\ \gamma_{13} \bar{r}_1 & \gamma_{13} \bar{r}_2 & \cdots & \gamma_{13} \bar{r}_N & \gamma_{13} \gamma_{12} & \gamma_{13} \gamma_{13} & \cdots & \gamma_{13} \gamma_{N-1N} \\ \vdots & \vdots & \ddots & \vdots & \vdots & \vdots & \ddots & \vdots \\ \gamma_{N-1N} \bar{r}_1 & \cdots & & \gamma_{N-1N} \bar{r}_N & \gamma_{N-1N} \gamma_{12} & \cdots & & \gamma_{N-1N} \gamma_{N-1N} \end{array} \end{pmatrix},$$

where \bar{y}_ν is defined by Eq. (3.28).

The indicial structure of the ${}^{(0)}_2 Q_{\nu_1, \nu_2}$ matrix reveals a block structure which we write as

$${}^{(0)}_2 Q_{\nu_1, \nu_2} = \begin{pmatrix} {}^{(0)}_2 Q_{i,j}^{rr} & {}^{(0)}_2 Q_{i,(jk)}^{r\gamma} \\ {}^{(0)}_2 Q_{(ij),k}^{\gamma r} & {}^{(0)}_2 Q_{(ij),(kl)}^{\gamma\gamma} \end{pmatrix}. \quad (4.1)$$

- The upper-left block, ${}^{(0)}_2 Q_{i,j}^{rr}$, is an $(N \times N)$ matrix with indices associated with (\bar{r}_i, \bar{r}_j) ; hence, we use the subscript i, j to refer to these indices.
- The upper-right block, ${}^{(0)}_2 Q_{i,(jk)}^{r\gamma}$, is an $(N \times N(N - 1)/2)$ matrix with indices associated with (\bar{r}_i, γ_{jk}) ; hence, we use the subscript $i, (jk)$ to refer to these indices.

- The lower-left block, ${}^{(0)}_2 Q_{(ij),k}^{\gamma r}$, is an $(N(N-1)/2 \times N)$ matrix with indices associated with (γ_{ij}, \bar{r}_k) ; hence, we use the subscript $(ij), k$ to refer to these indices.
- Finally, the lower right block, ${}^{(0)}_2 Q_{(ij),(kl)}^{\gamma\gamma}$, is an $(N(N-1)/2 \times N(N-1)/2)$ matrix with indices associated with $(\gamma_{ij}, \gamma_{kl})$; hence, we use the subscript $(ij), (kl)$ to refer to these indices.

4.1.1.2 Anharmonic order

At first anharmonic order the Hamiltonian has rank-one ${}^{(1)}_1 Q$ (which are column vectors of length P) and rank-three ${}^{(1)}_3 Q$ tensors (which are $P \times P \times P$ tensors). We also write the anharmonic tensors in block form in a similar way. The column vector ${}^{(1)}_1 Q_\nu$ has the same indicial structure as \bar{y}_ν and has a block form

$${}^{(1)}_1 Q_\nu = \begin{pmatrix} {}^{(1)}_1 Q_i^r \\ {}^{(1)}_1 Q_{(ij)}^\gamma \end{pmatrix}. \quad (4.2)$$

The rank-three tensor ${}^{(1)}_3 Q_{\nu_1, \nu_2, \nu_3}$ has the same indicial structure as $\bar{y}_{\nu_1} \bar{y}_{\nu_2} \bar{y}_{\nu_3}$ and has a block form which may be flattened out by nesting column vectors (indexed by ν_3) inside a matrix (indexed by ν_1, ν_2):

$${}^{(1)}_3 Q_{\nu_1, \nu_2, \nu_3} = \begin{pmatrix} \begin{pmatrix} {}^{(1)}_3 Q_{i,j,k}^{rrr} \\ {}^{(1)}_3 Q_{i,(jk),l}^{r\gamma r} \end{pmatrix} & \begin{pmatrix} {}^{(1)}_3 Q_{i,j,(kl)}^{rr\gamma} \\ {}^{(1)}_3 Q_{i,(jk),(lm)}^{r\gamma\gamma} \end{pmatrix} \\ \begin{pmatrix} {}^{(1)}_3 Q_{(ij),k,l}^{\gamma rr} \\ {}^{(1)}_3 Q_{(ij),(kl),m}^{\gamma\gamma r} \end{pmatrix} & \begin{pmatrix} {}^{(1)}_3 Q_{(ij),k,(lm)}^{\gamma r\gamma} \\ {}^{(1)}_3 Q_{(ij),(kl),(mn)}^{\gamma\gamma\gamma} \end{pmatrix} \end{pmatrix}. \quad (4.3)$$

We will refer to the block tensors by their (superscript) block labels.

4.1.2 Symmetry creates a patchwork of equivalence classes

The maximally symmetric point group S_N , together with the invariance of the full Hamiltonian under particle interchange, requires that the F and G tensors be invariant under the elements of S_N . The elements of S_N are permutations which interchange particle labels(95).

Significantly, invariance under permutation requires that Hamiltonian tensor elements related by a label permutation induced by the point group must be equal

(because the perturbation series is an expansion about $D \rightarrow \infty$ so all tensor elements are evaluated in this limit). For example, consider two elements of the rr block matrix ${}^{(0)}_2 Q^{rr} : {}^{(0)}_2 Q^{rr}_{1,1}$ and ${}^{(0)}_2 Q^{rr}_{2,2}$. These are related by the permutation (12) and therefore must be equal. There is no permutation that relates ${}^{(0)}_2 Q^{rr} : {}^{(0)}_2 Q^{rr}_{1,1}$ and ${}^{(0)}_2 Q^{rr}_{1,2}$, so these elements need not be equal.

The requirement that the coefficient tensors in the Hamiltonian series be invariant under the permutations of S_N imparts an intricate structure to the tensors. The set of permutations of S_N effect a partitioning of a Hamiltonian tensor for N particles into disjoint subsets of identical elements. These disjoint sets may be called *equivalence classes*, as the elements of each set are all related by a permutation of S_N and are called *equivalent*. For a more precise definition of equivalence class, see Section 4.2.2. For an explicit example of the partitioning of the Hamiltonian tensors for $N = 3$, see Section A.4.

Consider again the elements of the ${}^{(0)}_2 Q^{rr}$ block. The element ${}^{(0)}_2 Q^{rr}_{1,1}$ belongs to a subset of N elements (of the form ${}^{(0)}_2 Q^{rr}_{i,i}$) which are related by a permutation induced by the point group. This set is the equivalence class of ${}^{(0)}_2 Q^{rr}_{1,1}$. Likewise, the element ${}^{(0)}_2 Q^{rr}_{1,2}$ belongs to a set of $N - 1$ elements related by a permutation induced by the point group and sharing a common value. We see that the ${}^{(0)}_2 Q^{rr}_{i,i}$ is partitioned into two equivalence classes:

$$\{ {}^{(0)}_2 Q^{rr}_{i,i} : 1 \leq i \leq N \} \quad (4.4)$$

$$\{ {}^{(0)}_2 Q^{rr}_{i,j} : 1 \leq i \leq N \ \& \ i \neq j \} \quad (4.5)$$

Proceeding in this fashion, we observe that both the upper-right and the lower-left blocks of the harmonic-order tensors are similarly partitioned into two equivalence classes (where, for compactness, the indices are taken to be integers between 1 and N). We only list the equivalence classes of the upper-right block:

$$\{ {}^{(0)}_2 Q^{r\gamma}_{i,(ik)} : i < k \} \quad (4.6)$$

$$\{ {}^{(0)}_2 Q^{r\gamma}_{i,(jk)} : i \neq j \neq k \ \& \ j < k \} \quad (4.7)$$

Also the lower-right block is partitioned into three equivalence classes:

$$\{ {}^{(0)}_2 Q^{\gamma\gamma}_{(ij),(ij)} : i < j \} \quad (4.8)$$

$$\{ {}^{(0)}_2 Q^{\gamma\gamma}_{(ij),(ik)} : i < j \ \& \ i < k \ \& \ i \neq j \neq k \} \quad (4.9)$$

$$\{ {}^{(0)}_2 Q^{\gamma\gamma}_{(ij),(kl)} : i < j \ \& \ k < l \ \& \ i \neq j \neq k \neq l \}. \quad (4.10)$$

4.2 Decomposition in the basis of binary invariants

The Q -tensors have an intricate arrangement of identical elements over an underlying index structure. We will see that each equivalence class can be represented by a binary tensor which is unchanged by the action of S_N .

4.2.1 Introducing binary invariants

Each tensor block is composed of disjoint sets of identical elements. The elements of each set are related by a permutation. Such a relation is said to be an *equivalence relation*. A set of quantities which are related is called an *equivalence class*; this is a more general group-theoretic definition than the common use in physics. Each block has a finite number of such equivalence classes. We quantify these symmetry properties by introducing a binary tensor, consisting of ones and zeros, for each equivalence class in a block that embodies the structural arrangement of the corresponding elements. For a binary tensor to represent an equivalence class, it must be invariant under particle interchange. This property will later be used to construct the binary invariants.

Definition 1 We define a binary invariant $[B(\mathcal{G})]_{\nu_1, \nu_2, \dots, \nu_R}$ as a rank- R tensor in which elements belonging to the equivalence class \mathcal{G} are one and all other elements are zero.

For example, in Appendix A, Eq. (A.32), it is shown that when $N = 3$ the 3×3 block matrix ${}^{(0)}_2 Q^{rr}$ may be written as

$${}^{(0)}_2 Q^{rr} = {}^{(0)}_2 Q^{rr}_{11} \begin{pmatrix} 1 & 0 & 0 \\ 0 & 1 & 0 \\ 0 & 0 & 1 \end{pmatrix} + {}^{(0)}_2 Q^{rr}_{12} \begin{pmatrix} 0 & 1 & 1 \\ 1 & 0 & 1 \\ 1 & 1 & 0 \end{pmatrix}.$$

The matrices of ones and zeros are the binary invariants for the equivalence classes of ${}^{(0)}_2 Q^{rr}_{11}$ and ${}^{(0)}_2 Q^{rr}_{12}$. A binary invariant $B^{block}(\mathcal{G})$ of a tensor ${}^{(order)}_R Q$ has the same dimensions. It follows from the definitions of binary invariant and equivalent class that a binary invariant is invariant under the permutations of S_N . The above matrices are invariant under the 6 elements of S_3 .

For the DPT Hamiltonian coefficient tensor of a given rank for a given number of particles, it is easy to explicitly construct the set of binary invariants. For each

element of the Hamiltonian tensor, an equivalence class is generated by specifying a tensor with only one non-zero element (in the same location as the chosen Hamiltonian element) and then considering all possible permutations of S_N acting on the binary tensor. Each resulting binary tensor is related to the original binary tensor and the set forms an equivalence class. Summing over the resulting tensors within each equivalence class generated by the permutation, we obtain the binary invariant for that equivalence class in numerical form.

For example, let us construct the binary invariant for the equivalence class of the element ${}^{(0)}_2 Q_{11}^{rr}$ for $N = 3$. First, we write a matrix with only one non-zero element at the position of ${}^{(0)}_2 Q_{11}^{rr}$:

$$\begin{pmatrix} 1 & 0 & 0 \\ 0 & 0 & 0 \\ 0 & 0 & 0 \end{pmatrix}. \quad (4.11)$$

Next we consider the action of the permutation group S_3 ,

$$S_3 = (1)(2)(3), (1)(23), (3)(12), (123), (132), (2)(13) \quad (4.12)$$

on the matrix in Eq. (4.11). There are two permutations which leave the matrix unchanged, and the group S_3 is divided into cosets of two elements which map to the same matrix. We apply one element of S_N from each coset to the matrix and add the result. (Equivalently, we may apply all elements of S_3 and divide by the size of the cosets.) The result is the binary invariant for the equivalence class of ${}^{(0)}_2 Q_{11}^{rr}$,

$$\begin{pmatrix} 1 & 0 & 0 \\ 0 & 1 & 0 \\ 0 & 0 & 1 \end{pmatrix} = \begin{pmatrix} 1 & 0 & 0 \\ 0 & 0 & 0 \\ 0 & 0 & 0 \end{pmatrix} + \begin{pmatrix} 0 & 0 & 0 \\ 0 & 1 & 0 \\ 0 & 0 & 0 \end{pmatrix} + \begin{pmatrix} 0 & 0 & 0 \\ 0 & 0 & 0 \\ 0 & 0 & 1 \end{pmatrix}. \quad (4.13)$$

A similar procedure may be followed to construct the binary invariants in closed form. This construction is established in Appendix C.

4.2.2 Binary invariants are a basis

Here we sketch a short proof that it is always possible to decompose an S_N -symmetric Hamiltonian in the basis of binary invariants. It is not necessary for the invariants to be binary, but it is both sufficient and convenient.

We define an equivalence relation \sim on the set of Hamiltonian tensors in some basis by

$$a \sim b \quad \text{if and only if} \quad \exists p \in S_N \text{ such that } pa = b. \quad (4.14)$$

Definition 2 *The equivalence class of an element a in a set X is the subset of X of all elements that are related to a .*

This definition is true for any relation, in the case considered here the relation is a permutation of particle labels.

Definition 3 *We denote the set of all equivalence classes for a Hamiltonian coefficient tensor block as \mathbb{G} .*

Lemma 1 *The set of binary invariants for all $\mathcal{G} \in \mathbb{G}$ is linearly independent*

Lemma 2 *The set of binary invariants for all $\mathcal{G} \in \mathbb{G}$ spans a unit tensor.*

Theorem 1 *The set of binary invariants $\{B(\mathcal{G}) : \mathcal{G} \in \mathbb{G}\}$ forms a basis for the DPT Hamiltonian coefficient tensors.*

Proof This result follows from the definition of a basis and that the set of binary invariants for all $\mathcal{G} \in \mathbb{G}$ is linearly independent and spans the vector space. \square

In Reference (97) Kelle develops a general proof is given that it is always possible to find such a basis set that is invariant under *any* group. A complex tensor may always be expanded in a basis which is invariant under some group G .

4.2.3 Expansion in the binary invariant basis

The elements of ${}^{(order)}_R Q^{block}$ constitute disjoint sets of identical elements. Because the binary invariants for a block of a DPT Hamiltonian tensor form a basis, it is always possible to decompose such a tensor block as a linear combination of binary invariants, where the coefficient of $B^{block}(\mathcal{G})$ is the value of the set of elements associated with \mathcal{G} .

We decompose the ${}^{(order)}_R Q^{block}$ tensors at any order as a (finite) linear combination of binary invariants:

$${}^{(order)}_R Q^{block}_{\nu_1, \nu_2, \dots, \nu_R} = \sum_{\mathcal{G} \in \mathbb{G}_{block}} Q^{block}(\mathcal{G}) [B^{block}(\mathcal{G})]_{\nu_1, \nu_2, \dots, \nu_R}, \quad (4.15)$$

where \mathbb{G}_{block} represents the set of equivalence classes and the binary invariant $B^{block}(\mathcal{G})$ has the same dimensions as the original Q tensor block. The scalar quantity $Q^{block}(\mathcal{G})$ is the expansion coefficient (a scalar), where the order and the rank R are implied by G . If Q^{block} is symmetric, then we also drop the block label in the above (enough information about the block is implied by \mathcal{G}).

The decomposition of symmetric tensor blocks in the basis of binary invariants in Eq. (4.15) represents a generalization to higher orders of the matrices used at harmonic order in (81). This equation separates the system-specific physical information from the complexity of the general N -body problem. All of the information about the Hamiltonian of the particular system is contained in the scalar quantities $Q^{block}(\mathcal{G})$, while all of the complicated N -dependence is embodied by the binary invariant $B^{block}(\mathcal{G})$.

As the number of particles increases, the size and complexity of the binary invariants also increase rapidly, particularly for the higher-rank tensors. We need to be able to capture the intricate structure of these binary invariants in a closed form for general N if we hope to be able to transform the DPT Hamiltonian tensors analytically. We have determined a closed form expression for the binary invariants in Appendix C.

In Chapter 5 we will show that the transformation to the normal-coordinate basis for each binary invariant in a basis set can be performed analytically, for general N , and that the result is proportional to the generalized Clebsch-Gordan coefficient for the transformation. In fact, we will show that all of the complicated N dependence will be entirely contained within these Clebsch-Gordan coefficients, which are derived from group-theoretic considerations. This analytic transformation avoids large computational cost at large N and need not be repeated for a different value of N or even a different Hamiltonian (for N bosons in an isotropic confining potential).

4.3 Graphical representation of tensor structure

Graph theory is not a new addition to DPT. In previous work (87; 90; 81; 82), graph theory actually played a crucial role in elucidating the structure of the harmonic-order Hamiltonian (3.38). The “simple submatrices” \mathbf{I} , \mathbf{J} , and \mathbf{R} arise from spectral graph theory.

Graph theory provides an elegant correspondence between the indicial structure and the elemental symmetry of the tensors in (3.38) and (3.39). We will label each equivalence class of DPT Hamiltonian coefficient tensor elements by a graph.

4.3.1 Introducing graph theory

Graph theory is a uniquely intuitive and accessible branch of mathematics (98). Simply knowing the definition of a *graph* and adopting the notation of graphs has allowed us to perform feats that would have otherwise been quite difficult.

Definition 4 A graph $\mathcal{G} = (V, E)$ is a set of vertices V and edges E . Each edge has one or two associated vertices, which are called its endpoints.

For example, $\bullet \text{---} \bullet \text{---} \bullet$ is a graph with three vertices and two edges (lines). We allow our graphs to include loops and multiple edges ¹.

4.3.2 Mapping tensor structure onto graphs

Let us introduce a mapping, ϕ , which associates a function of internal coordinates with a graph as follows.

1. For each distinct internal coordinate index, draw a labeled vertex.
2. For each index pair (ij) , draw an edge $(\bullet \text{---} \bullet)$
3. For each distinct single index i , draw a “loop” edge $(\bigcirc \bullet_i)$

The image of this mapping ϕ on each element of a rank- R Hamiltonian tensor in the internal coordinate basis is a graph of R edges. For example, the graph corresponding to the tensor element ${}^{(0)}_2 Q_{i,(jk)}^{r\gamma}$ under this mapping is

$${}^{(0)}_2 Q_{i,(jk)}^{r\gamma} \xrightarrow{\phi} \bigcirc^i \text{---} \bullet^j \text{---} \bullet^k. \quad (4.16)$$

These graphs provide a convenient notation to label the equivalence classes of tensor elements. Under this mapping, each set of identical elements is associated with a set of graphs which are also equivalent under permutation of the index labels—an equivalence class of graphs. Such equivalent graphs are also called *isomorphic*. We represent each equivalence class of isomorphic graphs with a graph with the vertices

¹Strictly speaking, this is a “loop multigraph”: the definition of a graph does not allow for multiple edges between a pair of vertices, nor a “loop” edge with common endpoints.

unlabeled. For instance, the equivalence class of the tensor element ${}^{(0)}_2 Q_{i,(ij)}^{r\gamma}$ will be labeled by the graph $\circ \rightarrow$ and the *value* as ${}^{(0)}_2 Q(\circ \rightarrow)$. The set of graphs representing the equivalence classes of the harmonic-order DPT Hamiltonian tensors are given in Table 4.3.2. The set of graphs representing the equivalence classes of the rank-one and rank-three tensors are given in Tables 4.3.2 and 4.3.2.

The image of this mapping on the set of all internal coordinates for N particles is a graph which is a simplex on N points, with a loop at each vertex. For example, applying this mapping to a tensor representing four particles we obtain Figure 4.1. This simplex can be useful in generating the possible graphs for a given rank. Each graph in the image of the mapping from a rank- R tensor can also be obtained by taking a particular choice of R edges (along with the associated vertices) from the “loopy-simplex” in 4.1. The above graphs can be obtained, for rank- R , by taking R edges of the “loopy simplex” graph at a time, with replacement and with the associated vertices.

4.3.3 Graphical decomposition of harmonic-order matrices

The harmonic-order matrices ${}^{(0)}_2 Q_{\nu_1, \nu_2}^{block}$ may be decomposed using Eq. (4.15),

$${}^{(0)}_2 Q_{\nu_1, \nu_2}^{block} = \sum_{\mathcal{G} \in \mathbb{G}_{block}} Q^{block}(\mathcal{G}) [B^{block}(\mathcal{G})]_{\nu_1, \nu_2}, \quad (4.17)$$

where the equivalence classes \mathbb{G}_{block} are now labeled by graphs

$$\begin{aligned} \mathbb{G}^{rr} &= \{\circ \circ, \circ \circ\} \\ \mathbb{G}^{r\gamma} = \mathbb{G}^{\gamma r} &= \{\circ \rightarrow, \circ \rightarrow\} \\ \mathbb{G}^{\gamma\gamma} &= \{\circ \rightarrow, \rightarrow \circ, \rightarrow \circ\} \end{aligned} \quad (4.18)$$

For example,

$$\left[{}^{(0)}_2 Q^{rr} \right]_{i,j} = Q(\circ \circ) [B(\circ \circ)]_{i,j} + Q(\circ \circ) [B(\circ \circ)]_{i,j}. \quad (4.19)$$

When Q is symmetric (which will be the case for F and G) then the expansions for ${}^{(0)}_2 Q^{\gamma r}$, ${}^{(0)}_2 Q^{r\gamma}$ are the same, so we may drop the block labels on the binary invariant.

4.3.4 Graphical decomposition of first anharmonic-order matrices

The rank-one first-anharmonic tensors ${}^{(1)}_1 Q_{\nu}^{block}$ have a trivial decomposition, since there is only one graph in each block:

Graph	Tensor Elements
	${}^{(0)}_2 Q_{ii}^{rr}$
	${}^{(0)}_2 Q_{ij}^{rr}$
	${}^{(0)}_2 Q_{(ij)i}^{\gamma r} = {}^{(0)}_2 Q_{(ij)j}^{\gamma r},$ ${}^{(0)}_2 Q_{i(ij)}^{r\gamma} = {}^{(0)}_2 Q_{i(ji)}^{r\gamma}$
	${}^{(0)}_2 Q_{(ij)(ij)}^{\gamma\gamma}$
	${}^{(0)}_2 Q_{(ij)(ik)}^{\gamma\gamma} = {}^{(0)}_2 Q_{(ij)(jk)}^{\gamma\gamma} = {}^{(0)}_2 Q_{(ij)(ki)}^{\gamma\gamma} = {}^{(0)}_2 Q_{(ij)(kj)}^{\gamma\gamma}$
	${}^{(0)}_2 Q_{(ij)(kl)}^{\gamma\gamma}$

Table 4.1: Graph labels for the equivalence classes of the rank-two, harmonic-order DPT Hamiltonian coefficient tensors.

Graph	Tensor Elements
	${}^{(1)}_1 Q_i^r$
	${}^{(1)}_1 Q_{(ij)}^\gamma$

Table 4.2: Graphs labeling equivalence classes for the rank-one, first-anharmonic DPT Hamiltonian coefficient tensors.

Graphs	Elements	Graphs	Elements	Graphs	Elements
	${}^{(1)}_3 Q_{i,i,i}^{rrr}$		${}^{(1)}_3 Q_{(ij),(ij),i}^{\gamma\gamma r}$		${}^{(1)}_3 Q_{(ij),(ij),(ij)}^{\gamma\gamma\gamma}$
	${}^{(1)}_3 Q_{i,i,j}^{rrr}$		${}^{(1)}_3 Q_{(ij),(ij),k}^{\gamma\gamma r}$		${}^{(1)}_3 Q_{(ij),(jk),(ik)}^{\gamma\gamma\gamma}$
	${}^{(1)}_3 Q_{i,j,k}^{rrr}$		${}^{(1)}_3 Q_{(ij),(jk),j}^{\gamma\gamma r}$		${}^{(1)}_3 Q_{(ij),(ij),(jk)}^{\gamma\gamma\gamma}$
	${}^{(1)}_3 Q_{(ij),i,i}^{\gamma rr}$		${}^{(1)}_3 Q_{(ij),(jk),i}^{\gamma\gamma r}$		${}^{(1)}_3 Q_{(ij),(jk),(jl)}^{\gamma\gamma\gamma}$
	${}^{(1)}_3 Q_{(ij),i,j}^{\gamma rr}$		${}^{(1)}_3 Q_{(ij),(jk),l}^{\gamma\gamma r}$		${}^{(1)}_3 Q_{(ij),(jk),(kl)}^{\gamma\gamma\gamma}$
	${}^{(1)}_3 Q_{(ij),i,k}^{\gamma rr}$		${}^{(1)}_3 Q_{(ij),(kl),i}^{\gamma\gamma r}$		${}^{(1)}_3 Q_{(ij),(ij),(kl)}^{\gamma\gamma\gamma}$
	${}^{(1)}_3 Q_{(ij),k,k}^{\gamma rr}$		${}^{(1)}_3 Q_{(ij),(kl),m}^{\gamma\gamma r}$		${}^{(1)}_3 Q_{(ij),(jk),(lm)}^{\gamma\gamma\gamma}$
	${}^{(1)}_3 Q_{(ij),k,l}^{\gamma rr}$				${}^{(1)}_3 Q_{(ij),(kl),(mn)}^{\gamma\gamma\gamma}$

Table 4.3: Graphs labeling equivalence classes for the rank-three, first-anharmonic DPT Hamiltonian coefficient tensors.

$$\begin{aligned}
\mathbb{G}^r &= \circlearrowleft \\
\mathbb{G}^\gamma &= \bullet \rightarrow \bullet.
\end{aligned} \tag{4.20}$$

Therefore, Eq. (4.15) becomes

$$\begin{aligned}
{}^{(1)}_1 Q_\nu^r &= {}^{(1)}_1 Q^r (\circlearrowleft) [B(\circlearrowleft)]_\nu \\
{}^{(1)}_1 Q_\nu^\gamma &= {}^{(1)}_1 Q^\gamma (\bullet \rightarrow \bullet) [B(\bullet \rightarrow \bullet)]_\nu.
\end{aligned} \tag{4.21}$$

The rank-three tensors ${}^{(1)}_3 Q_{\nu_1, \nu_2, \nu_3}^{block}$ may also be decomposed using Eq. (4.15),

$${}^{(1)}_3 Q_{\nu_1, \nu_2, \nu_3}^{block} = \sum_{\mathcal{G} \in \mathbb{G}_{block}} Q^{block}(\mathcal{G}) [B^{block}(\mathcal{G})]_{\nu_1, \nu_2, \nu_3}, \tag{4.22}$$

where the equivalence classes \mathbb{G}_{block} are now labeled by graphs

$$\begin{aligned}
\mathbb{G}^{rrr} &= \left\{ \begin{array}{c} \text{two circles connected by a line} \\ \text{circle with a loop} \\ \text{three circles in a line} \end{array} \right\} \\
\mathbb{G}^{\gamma rr} = \mathbb{G}^{r\gamma r} = \mathbb{G}^{rr\gamma} &= \left\{ \begin{array}{c} \text{circle with a line to a circle} \\ \text{circle with a line to a circle with a loop} \\ \text{circle with a line to a circle with a loop} \\ \text{two circles with a line between them} \\ \text{two circles with a line between them} \end{array} \right\} \\
\mathbb{G}^{\gamma\gamma r} = \mathbb{G}^{\gamma r\gamma} = \mathbb{G}^{r\gamma\gamma} &= \left\{ \begin{array}{c} \text{two circles with a line between them} \\ \text{circle with a line to a circle} \\ \text{circle with a line to a circle} \\ \text{circle with a line to a circle} \\ \text{circle with a line to a circle} \\ \text{circle with a line to a circle} \\ \text{circle with a line to a circle} \\ \text{circle with a line to a circle} \end{array} \right\} \\
\mathbb{G}^{\gamma\gamma\gamma} &= \left\{ \begin{array}{c} \text{circle with a line to a circle} \\ \text{triangle} \\ \text{circle with a line to a circle} \\ \text{circle with a line to a circle} \\ \text{circle with a line to a circle} \\ \text{circle with a line to a circle} \\ \text{circle with a line to a circle} \\ \text{circle with a line to a circle} \end{array} \right\}.
\end{aligned} \tag{4.23}$$

For example, tensors in the rrr block may be decomposed as follows:

$$\begin{aligned}
[Q^{rrr}]_{i,j,k} &= Q(\text{two circles connected by a line}) [B(\text{two circles connected by a line})]_{i,j,k} + Q(\text{circle with a loop}) [B(\text{circle with a loop})]_{i,j,k} \\
&\quad + Q(\text{three circles in a line}) [B(\text{three circles in a line})]_{i,j,k}.
\end{aligned} \tag{4.24}$$

The use of graphs has provided an intuitive way to label the sets of identical elements in the Hamiltonian coefficient tensors. The binary invariants are labeled by a graph \mathcal{G} , but the use of graphs is not essential to the definition of a binary invariant.

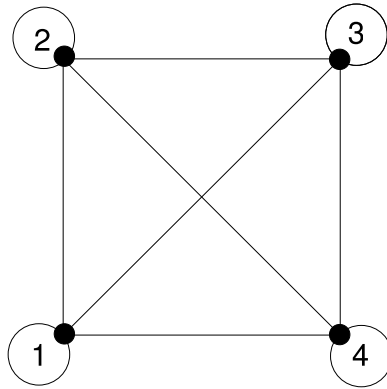


Figure 4.1: The graph one obtains by applying the mapping ϕ to the set of all internal coordinates for $N = 4$. All of the smaller graphs may be obtained from this graph by considering all the possible ways to take a certain number of loops and edges.

Chapter 5

Transformation of Hamiltonian to normal-coordinate basis

Reference (87) laid the foundation for the analytic transformation of the DPT Hamiltonian series to a collective “normal coordinate” basis. This work extends (87) from harmonic order by paving the way for the transformation of higher orders in the DPT series. In section 5.1, we consolidate and slightly revise the notation of the results of (87) with the purpose of application to higher orders. In section 5.2, we show that the tensor coefficients of the DPT Hamiltonian transformed to symmetry coordinates are proportional to the Clebsch-Gordon coefficients of the transformation, and show how the decomposition in the basis of binary invariants is transformed to symmetry coordinates. Finally, we transform the DPT Hamiltonian to collective coordinates in Section 5.3.

The result is that the DPT Hamiltonian has been analytically transformed to a basis of the collective motions of the system. Not only does this analytic result avoid a computationally expensive procedure but it also offers the potential to study the collective motions of a confined quantum system.

The reader is referred to Section A.5 in the Appendix for explicit examples in the simpler $N = 3$ case.

5.1 Two-step transformation of the Hamiltonian

In a previous paper (87), Dunn *et al* derived a transformation V_{ν_1, ν_2} from internal coordinates $\bar{\mathbf{y}}'$ to normal coordinates \mathbf{q}' . One might imagine that analytically determining the eigenvectors of the $\approx N^2 \times N^2$ matrices in the harmonic-order DPT Hamiltonian series for an arbitrarily large number N interacting particles is a daunting task. In Ref. (87) this feat is accomplished by using an intermediate step: a

transformation of the internal coordinate vector $\bar{\mathbf{y}}'$ to the ‘‘symmetry coordinate’’ vector \mathbf{S} ,

$$\mathbf{S} = \mathbf{W}\bar{\mathbf{y}}', \quad (5.1)$$

where W is an $\frac{N(N+1)}{2} \times \frac{N(N+1)}{2}$ matrix (Eq. (45) in (87)).

With a subsequent transformation \mathcal{C} (Eq. (63) in (87)) of the symmetry coordinate vector \mathbf{S} , one obtains the normal-mode coordinate vector

$$\mathbf{q}' = \mathcal{C}\mathbf{S}. \quad (5.2)$$

Note that, in this work, \mathcal{C} replaces $\mathbf{c}^{(b)}$ in Ref. (87).

5.1.1 Transformation of coordinate vectors

Using Equations (63) and (81) in Ref. (87) we transform the internal coordinate vectors q'_ν and internal coordinate derivative vectors $\partial_{q'_\nu}$ to obtain their normal coordinate analogs,

$$q'_{\nu_1} = \sum_{a=1}^P \sum_{\nu_2=1}^P \mathcal{C}_{\nu_1,a} W_{a,\nu_2} \bar{y}'_{\nu_2}$$

$$\frac{\partial}{\partial q'_{\nu_1}} = \sum_{a=1}^P \sum_{\nu_2=1}^P [\mathcal{C}^{-1}]^T_{\nu_1,a} W_{a,\nu_2} \frac{\partial}{\partial \bar{y}'_{\nu_2}},$$

where $P = N(N+1)/2$.

We will use the summation convention for repeated indices. Also we will drop the brackets on $[\mathcal{C}^{-1}]_{a,\nu}$, writing instead $\mathcal{C}^{-1}_{a,\nu}$. With these notation conventions and using the summation convention for repeated indices, we write the normal coordinates q_ν in terms of the internal displacement coordinates \bar{y}_ν :

$$q'_{\nu_1} = \mathcal{C}_{\nu_1,a} W_{a,\nu_2} \bar{y}'_{\nu_2} \quad (5.3)$$

$$\frac{\partial}{\partial q'_{\nu_1}} = [\mathcal{C}^{-1}]^T_{\nu_1,a} W_{a,\nu_2} \frac{\partial}{\partial \bar{y}'_{\nu_2}}. \quad (5.4)$$

We use the following identities (from Equations (47) in (87)),

$$\mathbf{I} = \mathbf{W}^T \mathbf{W}, \quad \mathbf{I} = \mathcal{C}^{-1} \mathcal{C}, \quad (5.5)$$

which we will employ in tensor-contraction form

$$I_{\nu_1, \nu_2} = W_{a, \nu_1} W_{a, \nu_2}, \quad I_{\nu_1, \nu_2} = \mathcal{C}_{\nu_1, a}^{-1} \mathcal{C}_{a, \nu_2}, \quad (5.6)$$

where summation over repeated indices is implied. Using the tensor form of these identities with the transformed internal displacement coordinates and derivatives in Eq. (5.3), we obtain an expression for the internal displacement coordinates in terms of the normal coordinates,

$$\begin{aligned} \bar{y}'_{\nu_2} &= W_{\nu_2, a}^T \mathcal{C}_{a, \nu_1}^{-1} q'_{\nu_1} \\ \frac{\partial}{\partial y'_{\nu_2}} &= W_{\nu_2, a}^T \mathcal{C}_{a, \nu_1}^T \frac{\partial}{\partial q'_{\nu_1}}. \end{aligned} \quad (5.7)$$

We here generalize previous work which involved matrix equations to tensor equations. The transpose operation is only defined for a rank-two tensor and has the effect of transposing the order of the indices.

5.1.2 Transformation of Hamiltonian tensors

We substitute the internal coordinate and internal coordinate derivative vectors from the above Eqs. (5.7) into the Hamiltonian terms in Eq. (3.37) reproduced below:

$$\bar{H}_0 = -\frac{1}{2} {}^{(0)}_2 G_{\nu_1, \nu_2} \partial_{\bar{y}'_{\nu_1}} \partial_{\bar{y}'_{\nu_2}} + \frac{1}{2} {}^{(0)}_2 F_{\nu_1, \nu_2} \bar{y}'_{\nu_1} \bar{y}'_{\nu_2} + {}^{(0)}_0 F$$

and

$$\bar{H}_1 = -\frac{1}{2} {}^{(1)}_3 G_{\nu_1, \nu_2, \nu_3} \bar{y}'_{\nu_1} \partial_{\bar{y}'_{\nu_2}} \partial_{\bar{y}'_{\nu_3}} + \frac{1}{3!} {}^{(1)}_3 F_{\nu_1, \nu_2, \nu_3} \bar{y}'_{\nu_1} \bar{y}'_{\nu_2} \bar{y}'_{\nu_3} - \frac{1}{2} {}^{(1)}_1 G_{\nu} \partial_{\bar{y}'_{\nu}} + {}^{(1)}_1 F_{\nu} \bar{y}'_{\nu},$$

where summation over repeated ν_i indices from 1 to P is implied. The result of this substitution is a Hamiltonian written in the basis of normal coordinates:

$$\begin{aligned} \bar{H}_0 &= -\frac{1}{2} {}^{(0)}_2 G_{\nu'_1 \nu'_2} \left(W_{\nu'_1, a}^T \mathcal{C}_{a, \nu_1}^T \partial_{q'_{\nu_1}} \right) \left(W_{\nu'_2, b}^T \mathcal{C}_{b, \nu_2}^T \partial_{q'_{\nu_2}} \right) \\ &\quad + \frac{1}{2} {}^{(0)}_2 F_{\nu'_1 \nu'_2} \left(W_{\nu'_1, a}^T \mathcal{C}_{a, \nu_1}^{-1} q'_{\nu_1} \right) \left(W_{\nu'_2, b}^T \mathcal{C}_{b, \nu_2}^{-1} q'_{\nu_2} \right) + {}^{(0)}_0 F \end{aligned} \quad (5.8)$$

and

$$\begin{aligned} \bar{H}_1 &= -\frac{1}{2} {}^{(1)}_3 G_{\nu'_1 \nu'_2 \nu'_3} \left(W_{\nu'_1, a}^T \mathcal{C}_{a, \nu_1}^{-1} q'_{\nu_1} \right) \left(W_{\nu'_2, b}^T \mathcal{C}_{b, \nu_2}^T \partial_{q'_{\nu_2}} \right) \left(W_{\nu'_3, c}^T \mathcal{C}_{c, \nu_3}^T \partial_{q'_{\nu_3}} \right) \\ &\quad + \frac{1}{3!} {}^{(1)}_3 F_{\nu'_1 \nu'_2 \nu'_3} \left(W_{\nu'_1, a}^T \mathcal{C}_{a, \nu_1}^{-1} q'_{\nu_1} \right) \left(W_{\nu'_2, b}^T \mathcal{C}_{b, \nu_2}^{-1} q'_{\nu_2} \right) \left(W_{\nu'_3, c}^T \mathcal{C}_{c, \nu_3}^{-1} q'_{\nu_3} \right) \\ &\quad + -\frac{1}{2} {}^{(1)}_1 G_{\nu'} W_{\nu', a}^T \mathcal{C}_{a, \nu}^T \partial_{q'_{\nu}} + {}^{(1)}_1 F_{\nu'} W_{\nu', a}^T \mathcal{C}_{a, \nu}^{-1} q'_{\nu}. \end{aligned} \quad (5.9)$$

Regrouping the summations over non-coordinate tensors, we may write \bar{H}_0 and \bar{H}_1 in the following compact form:

$$\bar{H}_0 = -\frac{1}{2} [{}^{(0)}_2 G_V]_{\nu_1, \nu_2} \partial_{q'_{\nu_1}} \partial_{q'_{\nu_2}} + {}^{(0)}_0 F_V + \frac{1}{2} [{}^{(0)}_2 F_V]_{\nu_1, \nu_2} q'_{\nu_1} q'_{\nu_2} \quad (5.10)$$

and

$$\bar{H}_1 = -\frac{1}{2} [{}^{(1)}_3 G_V]_{\nu_1, \nu_2, \nu_3} q'_{\nu_1} \partial_{q'_{\nu_2}} \partial_{q'_{\nu_3}} + \frac{1}{3!} [{}^{(1)}_3 F]_{\nu_1, \nu_2, \nu_3} q'_{\nu_1} q'_{\nu_2} q'_{\nu_3} \quad (5.11)$$

$$-\frac{1}{2} [{}^{(1)}_1 G_V]_{\nu} \partial_{q'_{\nu}} + [{}^{(1)}_1 F]_{\nu} q'_{\nu}, \quad (5.12)$$

where the subscript V on the F and G tensors denotes transformation by the matrix V to the normal-coordinate basis. Implicit in the above equations is the following definitions for the F and G tensors in the normal-coordinate basis:

$$\begin{aligned} [{}^{(0)}_2 G_V]_{\nu_1, \nu_2} &= \sum_{a=1}^P \sum_{b=1}^P \mathcal{C}_{\nu_1, a} \mathcal{C}_{\nu_2, b} \left(\sum_{\nu'_1=1}^P \sum_{\nu'_2=1}^P W_{a, \nu'_1} W_{b, \nu'_2} {}^{(0)}_2 G_{\nu'_1, \nu'_2} \right) \\ [{}^{(0)}_2 F_V]_{\nu_1, \nu_2} &= \sum_{a=1}^P \sum_{b=1}^P [{}^{\mathcal{C}^{-1}}]_{\nu_1, a}^T [{}^{\mathcal{C}^{-1}}]_{\nu_2, b}^T \left(\sum_{\nu'_1=1}^P \sum_{\nu'_2=1}^P W_{a, \nu'_1} W_{b, \nu'_2} {}^{(0)}_2 F_{\nu'_1, \nu'_2} \right) \\ [{}^{(1)}_1 G_V]_{\nu} &= \sum_{a=1}^P \mathcal{C}_{\nu, a} \left(\sum_{\nu'=1}^P W_{a, \nu'} {}^{(1)}_1 G_{\nu'} \right) \\ [{}^{(1)}_1 F_V]_{\nu} &= \sum_{a=1}^P [{}^{\mathcal{C}^{-1}}]_{\nu, a}^T \left(\sum_{\nu'=1}^P W_{a, \nu'} {}^{(1)}_1 F_{\nu'} \right) \\ [{}^{(1)}_3 G_V]_{\nu_1, \nu_2, \nu_3} &= \sum_{a=1}^P \sum_{b=1}^P \sum_{c=1}^P [{}^{\mathcal{C}^{-1}}]_{\nu_1, a}^T \mathcal{C}_{\nu_2, b} \mathcal{C}_{\nu_3, c} \\ &\quad \times \left(\sum_{\nu'_1=1}^P \sum_{\nu'_2=1}^P \sum_{\nu'_3=1}^P W_{a, \nu'_1} W_{b, \nu'_2} W_{c, \nu'_3} {}^{(1)}_3 G_{\nu'_1, \nu'_2, \nu'_3} \right) \\ [{}^{(1)}_3 F_V]_{\nu_1, \nu_2, \nu_3} &= \sum_{a=1}^P \sum_{b=1}^P \sum_{c=1}^P [{}^{\mathcal{C}^{-1}}]_{\nu_1, a}^T [{}^{\mathcal{C}^{-1}}]_{\nu_2, b}^T [{}^{\mathcal{C}^{-1}}]_{\nu_3, c}^T \\ &\quad \times \left(\sum_{\nu'_1=1}^P \sum_{\nu'_2=1}^P \sum_{\nu'_3=1}^P W_{a, \nu'_1} W_{b, \nu'_2} W_{c, \nu'_3} {}^{(1)}_3 F_{\nu'_1, \nu'_2, \nu'_3} \right). \end{aligned} \quad (5.13)$$

The terms in parenthesis in the above equation are simply the F and G tensors transformed to the symmetry coordinate basis. These can be separately defined, with a subscript W denoting transformation from internal to symmetry coordinates.

$$\begin{aligned}
\left[\begin{smallmatrix} (0) \\ 2 \end{smallmatrix} G_W \right]_{a,b} &= \sum_{\nu'_1=1}^P \sum_{\nu'_2=1}^P W_{a,\nu'_1} W_{b,\nu'_2} \begin{smallmatrix} (0) \\ 2 \end{smallmatrix} G_{\nu'_1,\nu'_2} \\
\left[\begin{smallmatrix} (0) \\ 2 \end{smallmatrix} F_W \right]_{a,b} &= \sum_{\nu'_1=1}^P \sum_{\nu'_2=1}^P W_{a,\nu'_1} W_{b,\nu'_2} \begin{smallmatrix} (0) \\ 2 \end{smallmatrix} F_{\nu'_1,\nu'_2} \\
\left[\begin{smallmatrix} (1) \\ 1 \end{smallmatrix} G_W \right]_a &= \sum_{\nu'=1}^P W_{a,\nu'} \begin{smallmatrix} (1) \\ 1 \end{smallmatrix} G_{\nu'} \\
\left[\begin{smallmatrix} (1) \\ 1 \end{smallmatrix} F_W \right]_a &= \sum_{\nu'=1}^P W_{a,\nu'} \begin{smallmatrix} (1) \\ 1 \end{smallmatrix} F_{\nu'} \\
\left[\begin{smallmatrix} (1) \\ 3 \end{smallmatrix} G_W \right]_{a,b,c} &= \sum_{\nu'_1=1}^P \sum_{\nu'_2=1}^P \sum_{\nu'_3=1}^P W_{a,\nu'_1} W_{b,\nu'_2} W_{c,\nu'_3} \begin{smallmatrix} (1) \\ 3 \end{smallmatrix} G_{\nu'_1,\nu'_2,\nu'_3} \\
\left[\begin{smallmatrix} (1) \\ 3 \end{smallmatrix} F_W \right]_{a,b,c} &= \sum_{\nu'_1=1}^P \sum_{\nu'_2=1}^P \sum_{\nu'_3=1}^P W_{a,\nu'_1} W_{b,\nu'_2} W_{c,\nu'_3} \begin{smallmatrix} (1) \\ 3 \end{smallmatrix} F_{\nu'_1,\nu'_2,\nu'_3}.
\end{aligned} \tag{5.14}$$

5.1.3 Intermediate step: transformation to symmetry coordinates

The above-Equation (5.14) represents a crucial simplification in the transformation to normal-mode coordinates: the transformation of the Hamiltonian to symmetry coordinates as an intermediate step.

The symmetry coordinate vector \mathbf{S} has a block form defined in Ref. (87), Eq. (42):

$$\mathbf{S} = \begin{pmatrix} \mathbf{S}_{r'}^{[N]} \\ \mathbf{S}_{\gamma'}^{[N]} \\ \hline \mathbf{S}_{r'}^{[N-1, 1]} \\ \mathbf{S}_{\gamma'}^{[N-1, 1]} \\ \hline \mathbf{S}_{\gamma'}^{[N-2, 2]} \end{pmatrix}, \tag{5.15}$$

where the column vectors $\mathbf{S}_{X'}^{[N]}$, $\mathbf{S}_{X'}^{[N-1, 1]}$, and $\mathbf{S}_{X'}^{[N-2, 2]}$ (where X' means r' or γ') have length 1, $N - 1$, and $N(N - 3)/2$, respectively. As explained in Ref. (87), the symmetry coordinate transforms under three different irreducible representations (irreps) of S_N , which are labeled by $[N]$, $[N - 1, 1]$, and $[N - 2, 2]$. The symmetry

coordinate may be further subdivided into blocks labeled by r and $gamma$ as well as the irrep labels.

Due to the block structure of \mathbf{S} in Eq. (5.15), it is at this point convenient to introduce an index convention which reflects this structure. For a discussion of index notation convention (as well as a reference card), see Appendix B. In what follows, we may change convention mid-equation to reduce indicial complexity, such as

$$S_\nu = [S_X^\alpha]_\xi . \quad (5.16)$$

In the notation on the left side of the above equation, ν runs from 1 to $P = N(N + 1)/2$. In the notation on the right, the W block is labeled by irrep α and matrix block $X = r, \gamma$, and indexed by ξ (whose range depends on α).

Each block in the symmetry coordinate column vector (5.15) transforms under an irreducible representation of S_N . We list below the matrix representations of these irreps from Ref. (87):

$$(W_r^{[N]})_i = \frac{1}{\sqrt{N}} , \quad (5.17)$$

where $1 \leq i \leq N$. Therefore $(W_r^{[N]})_i$ is a $1 \times N$ matrix.

$$(W_\gamma^{[N]})_{(ij)} = \sqrt{\frac{2}{N(N-1)}} , \quad (5.18)$$

where $1 \leq i < j \leq N$. Therefore $(W_\gamma^{[N]})_{(ij)}$ is a $1 \times N(N-1)/2$ matrix.

$$(W_r^{[N-1,1]})_{i,k} = \frac{1}{\sqrt{i(i+1)}} (\Theta_{i-k+1} - i\delta_{i+1,k}) , \quad (5.19)$$

where $1 \leq i \leq N-1$, $1 \leq k \leq N$. Therefore $(W_r^{[N-1,1]})_{i,k}$ is an $(N-1) \times N$ matrix.

In the above equation, we have defined a step function Θ_x

$$\Theta_x = \begin{cases} 1 & \text{if } 0 < x \\ 0 & \text{if } x = 0 \\ 0 & \text{if } x < 0 \end{cases} .$$

There are several variants on the step function, which differ in their values at the origin. The common Heaviside step function has $\Theta_0^H = \frac{1}{2}$ and the `UnitStep[x]` function of *Mathematica* has $\Theta_0 = 1$. For integer arguments, $\Theta_i = \text{UnitStep}[i-1]$.

$$(W_\gamma^{[N-1,1]})_{i,(kl)} = \frac{1}{\sqrt{i(i+1)(N-2)}} (\Theta_{i-k+1} + \Theta_{i-l+1} - i(\delta_{i+1,k} + \delta_{i+1,l})) \quad (5.20)$$

where $1 \leq i \leq N-1$, and $1 \leq k < l \leq N$. Therefore $(W_\gamma^{[N-1,1]})_{i,(kl)}$ is an $(N-1) \times N(N-1)/2$ matrix.

$$(W_\gamma^{[N-2,2]})_{(ij),(mn)} = \frac{1}{\sqrt{i(i+1)(j-3)(j-2)}} \times ((\Theta_{i-m+1} - i\delta_{i+1,m})(\Theta_{j-n} - (j-3)\delta_{j,n}) + (\Theta_{i-n+1} - i\delta_{i+1,n})(\Theta_{j-m} - (j-3)\delta_{j,m})) \quad (5.21)$$

where $1 \leq i \leq j-2$, $4 \leq j < N$ and $1 \leq m < n \leq N$. Therefore $(W_\gamma^{[N-2,2]})_{(ij),(mn)}$ is an $N(N-3)/2 \times N(N-1)/2$ matrix.

These matrices can be assembled into a W block matrix which transforms the entire internal coordinate vector $\bar{\mathbf{y}}'$ to symmetry coordinates: $\mathbf{S} = \mathbf{W}\bar{\mathbf{y}}'$. The W matrix has a block form defined in Eq. (45) of Ref. (87):

$$\mathbf{W} = \begin{pmatrix} \mathbf{W}_{r'}^{[N]} & \mathbf{0} \\ \mathbf{0} & \mathbf{W}_{\gamma'}^{[N]} \\ \hline \mathbf{W}_{r'}^{[N-1, 1]} & \mathbf{0} \\ \mathbf{0} & \mathbf{W}_{\gamma'}^{[N-1, 1]} \\ \hline \mathbf{0} & \mathbf{W}_{\gamma'}^{[N-2, 2]} \end{pmatrix}. \quad (5.22)$$

Each block in the W transformation (5.22) effects the reduction of a reducible representation of S_N to an irreducible representation of S_N . The total dimensions of the W matrix are $N(N+1)/2 \times N(N+1)/2$ and the dimensions of each block have been given above.

The analytic transformation of arbitrarily high- N DPT Hamiltonian tensors to symmetry coordinates might seem an impossible task. Fortunately, in Eq. (5.13) both F and G transform in the same way to symmetry coordinates. This windfall allows us to calculate the transformation to symmetry coordinates of each binary invariant *once* for both F and G for *any* (isotropic) confined quantum system of identical bosons. Having transformed the DPT Hamiltonian to symmetry coordinates, it is relatively simple to finally perform the final transformation to normal coordinates.

5.1.4 Final step: transformation to normal coordinates

In Ref. (87) Eq. (81), the normal-coordinate vector \mathbf{q}' is shown to have the following block form:

$$\mathbf{q}' = \begin{pmatrix} \mathbf{q}'_+^{[N]} \\ \mathbf{q}'_-^{[N]} \\ \mathbf{q}'_+^{[N-1, 1]} \\ \mathbf{q}'_-^{[N-1, 1]} \\ \mathbf{q}'^{[N-2, 2]} \end{pmatrix}. \quad (5.23)$$

The column vectors $\mathbf{q}'_{\pm}^{[N]}$, $\mathbf{q}'_{\pm}^{[N-1, 1]}$, and $\mathbf{q}'^{[N-2, 2]}$ have length 1, $N-1$ and $N(N-3)/2$, respectively.

In Reference (87), Eq. (80), the transformation from symmetry coordinates to normal coordinates $\mathcal{C}_{\mu_1, \mu_2}$ is defined as

$$\mathcal{C}_{\mu_1, \mu_2} = \left(\begin{array}{cc|cc|c} c_+^{[N]} \cos \theta_+^{[N]} & c_+^{[N]} \sin \theta_+^{[N]} & 0 & 0 & 0 \\ c_-^{[N]} \cos \theta_-^{[N]} & c_-^{[N]} \sin \theta_-^{[N]} & 0 & 0 & 0 \\ \hline 0 & 0 & c_+^{[N-1, 1]} \cos \theta_+^{[N-1, 1]} & c_+^{[N-1, 1]} \sin \theta_+^{[N-1, 1]} & 0 \\ 0 & 0 & c_-^{[N-1, 1]} \cos \theta_-^{[N-1, 1]} & c_-^{[N-1, 1]} \sin \theta_-^{[N-1, 1]} & 0 \\ \hline 0 & 0 & 0 & 0 & c^{[N-2, 2]} \end{array} \right). \quad (5.24)$$

We define the 2×2 matrices $\mathcal{C}^{[N]}$ and $\mathcal{C}^{[N-1, 1]}$, writing $\mathcal{C}_{\mu_1, \mu_2}$ in block matrix form:

$$\mathcal{C}_{\mu_1, \mu_2} = \left(\begin{array}{c|c|c} \mathcal{C}^{[N]} & & \\ \hline & \mathcal{C}^{[N-1, 1]} & \\ \hline & & c^{[N-2, 2]} \end{array} \right). \quad (5.25)$$

The transformation matrix $\mathcal{C}_{\mu_1, \mu_2}$ has indices μ which range from 1 to 5. This is to be distinguished the $\mathcal{C}_{\nu_1, \nu_2}$ matrix in Eqs. (5.13) in which a direct product of each of the blocks in the above matrix is formed with the appropriately-sized identity matrix.

$$\mathcal{C}_{\nu_1, \nu_2} = \left(\begin{array}{c|c|c} \mathcal{C}^{[N]} \otimes \mathbf{I}_{[N]} & \mathbf{0} & \mathbf{0} \\ \hline \mathbf{0} & \mathcal{C}^{[N-1, 1]} \otimes \mathbf{I}_{[N-1, 1]} & \mathbf{0} \\ \hline \mathbf{0} & \mathbf{0} & c^{[N-2, 2]} \times \mathbf{I}_{[N-2, 2]} \end{array} \right). \quad (5.26)$$

The matrices $I_{[N]}$, $I_{[N-1, 1]}$, and $I_{[N-2, 2]}$ are square matrices of dimension 1, $N - 1$, and $N(N - 3)/2$, respectively.

The normal coordinate vectors are constructed in a simple way from the symmetry coordinates: $\mathbf{q}' = \mathcal{C}^T \mathbf{S}$ (Eq. (63) in Ref. (87)) results in a normal-coordinate vector of the form

$$\mathbf{q}' = \begin{pmatrix} c_+^{[N]} \cos \theta_+^{[N]} \mathbf{S}_{r'}^{[N]} + c_+^{[N]} \sin \theta_+^{[N]} \mathbf{S}_{\gamma'}^{[N]} \\ c_-^{[N]} \cos \theta_-^{[N]} \mathbf{S}_{r'}^{[N]} + c_-^{[N]} \sin \theta_-^{[N]} \mathbf{S}_{\gamma'}^{[N]} \\ \hline c_+^{[N-1, 1]} \cos \theta_+^{[N-1, 1]} \mathbf{S}_{r'}^{[N-1, 1]} + c_+^{[N-1, 1]} \sin \theta_+^{[N-1, 1]} \mathbf{S}_{\gamma'}^{[N-1, 1]} \\ c_-^{[N-1, 1]} \cos \theta_-^{[N-1, 1]} \mathbf{S}_{r'}^{[N-1, 1]} + c_-^{[N-1, 1]} \sin \theta_-^{[N-1, 1]} \mathbf{S}_{\gamma'}^{[N-1, 1]} \\ \hline c^{[N-2, 2]} \mathbf{S}_{\gamma'}^{[N-2, 2]} \end{pmatrix}. \quad (5.27)$$

In the above equation, the ‘‘mixing angles’’ θ_{\pm}^{α} , $c^{[N-2, 2]}$, and the normalization c_{\pm}^{α} are defined in terms of the harmonic-order Hamiltonian elements: Eqs. (76), (78), and (79) in Ref. (87).

Having seen the transformation of the internal-coordinate column vector to symmetry coordinates, then to normal coordinates, we now perform the same transformations on the DPT Hamiltonian tensors.

5.2 Transformation to symmetry coordinates

We now transform the first-anharmonic Hamiltonian to the basis of symmetry coordinates, obtaining

$$\bar{H}_0 = -\frac{1}{2} \left[\begin{smallmatrix} (0) \\ 2 \end{smallmatrix} G_W \right]_{\nu_1, \nu_2} \partial_{S_{\nu_1}} \partial_{S_{\nu_2}} + \frac{1}{2} \left[\begin{smallmatrix} (0) \\ 2 \end{smallmatrix} F_W \right]_{\nu_1, \nu_2} S_{\nu_1} S_{\nu_2} + \begin{smallmatrix} (0) \\ 0 \end{smallmatrix} F_W. \quad (5.28)$$

and

$$\begin{aligned} \bar{H}_1 = & -\frac{1}{2} \left[\begin{smallmatrix} (1) \\ 3 \end{smallmatrix} G_W \right]_{\nu_1, \nu_2, \nu_3} S_{\nu_1} \partial_{S_{\nu_2}} \partial_{S_{\nu_3}} - \frac{1}{2} \left[\begin{smallmatrix} (1) \\ 1 \end{smallmatrix} G_W \right]_{\nu} \partial_{S_{\nu}} \\ & + \frac{1}{3!} \left[\begin{smallmatrix} (1) \\ 3 \end{smallmatrix} F_W \right]_{\nu_1, \nu_2, \nu_3} S_{\nu_1} S_{\nu_2} S_{\nu_3} + \left[\begin{smallmatrix} (1) \\ 1 \end{smallmatrix} F_W \right]_{\nu} S_{\nu}, \end{aligned} \quad (5.29)$$

where summation over repeated ν_i indices from 1 to $P = N(N + 1)/2$ is implied.

In Ref. (87) using the results of Ref. (99) it has been shown that the harmonic Hamiltonian matrices in the basis of symmetry coordinates, denoted $\begin{smallmatrix} (0) \\ 2 \end{smallmatrix} G_W$ and $\begin{smallmatrix} (0) \\ 2 \end{smallmatrix} F_W$, have a particular block structure where each block is itself a direct product of matrices:

$${}^{(0)}_2 Q_W = \begin{pmatrix} \sigma_{[N][N]}^Q \otimes \mathbf{I}_{[N]} & \mathbf{0} & \mathbf{0} \\ \mathbf{0} & \sigma_{[N-1, 1][N-1, 1]}^Q \otimes \mathbf{I}_{[N-1, 1]} & \mathbf{0} \\ \mathbf{0} & \mathbf{0} & \sigma_{[N-2, 2][N-2, 2]}^Q \times \mathbf{I}_{[N-2, 2]} \end{pmatrix}. \quad (5.30)$$

The matrices $\sigma_{[N][N]}^Q$ and $\sigma_{[N-1,1][N-1,1]}^Q$ are of dimension 2×2 and $\sigma_{[N-2,2][N-2,2]}^Q$ is a scalar.

The matrices \mathbf{I}_α contain all of the N dependence, and are simply identity matrices. Despite their simple form, these \mathbf{I}_α matrices are actually the ‘‘Clebsch-Gordon’’ coefficients of S_N which couple together two different irreps (α and α) to form a $[N]$ irrep (95; 87; 100). These irreps can be coupled together to form irreps other than $[N]$, but the DPT Hamiltonian (similarity-transformed or not) must be invariant under S_N , so only the $[N]$ irrep in the series contributes. These Clebsch-Gordon coefficients are to be distinguished from their $SO(3)$ cousins from the land of electronic angular momentum theory.

5.2.1 Clebsch-Gordon coefficients of the transformation

Writing the Clebsch-Gordon coefficient which couples together α_1 and α_2 to yield $[N]$ as $C_{\xi_1, \xi_2}^{\alpha_1 \alpha_2}$, the harmonic-order Q_W may be written more generally by denoting the structural Clebsch-Gordon coefficient as $C_{\xi_1, \xi_2}^{\alpha_1 \alpha_2}$:

$$\left[{}^{(0)}_2 Q_W^{\alpha_1 \alpha_2} \right]_{\xi_1, \xi_2}^{X_1 X_2} = \left[{}^{(0)}_2 \sigma_{\alpha_1 \alpha_2}^Q \right]_{X_1, X_2} C_{\xi_1, \xi_2}^{\alpha_1 \alpha_2}, \quad (5.31)$$

where no summation over repeated α_i indices is implied. For each tensor element specified on the right hand side, this equation is simply a multiplication equation. Notice that the Clebsch-Gordon coefficient depends on the irrep labels α_i only, not on the block labels X_i ; see the tables in Appendix B. The elements of the coefficient $\left[{}^{(0)}_2 \sigma_{\alpha_1 \alpha_2}^Q \right]_{X_1, X_2}$ form a 5×5 matrix (with the block structure shown above).

At first anharmonic order, the blocks of the symmetry-transformed Hamiltonian tensors are also proportional to Clebsch-Gordon coefficients. In the case of the rank-one Hamiltonian tensor, there is really no coupling of irreps, so the rank-one Clebsch-Gordon¹ has a simple form:

¹Really this is a generalization of the concept of Clebsch-Gordon coefficient to only one irrep for notational convenience.

$$C_\xi^\alpha = \begin{cases} 1 & \text{if } \alpha = [N] \\ 0 & \text{otherwise} \end{cases}. \quad (5.32)$$

Therefore, we can expect the rank-one Hamiltonian tensors to be proportional to this Clebsch-Gordon coefficient by a proportionality vector we denote $\left[\begin{smallmatrix} (1) \\ 1 \end{smallmatrix} \sigma_{\alpha_1}^Q \right]_\mu$:

$$\left[\begin{smallmatrix} (1) \\ 1 \end{smallmatrix} Q_W^\alpha \right]_\xi^X = \left[\begin{smallmatrix} (1) \\ 1 \end{smallmatrix} \sigma_\alpha^Q \right]_X C_\xi^\alpha. \quad (5.33)$$

The Clebsch-Gordon coefficients which couple three irreps to form an $[N]$ irrep are significantly more complex than the above. Fortunately, there are only eight such coefficients at first anharmonic order. Also, there are two Clebsch-Gordon coefficients which couple together $[N-2, 2][N-2, 2][N-2, 2]$ to form $[N]$, so this block of the DPT Hamiltonian is proportional to a sum of the two Clebsch-Gordon coefficients.

Let us denote the number of $[N]$ irreps in a Clebsch-Gordon series by $t(\alpha_1, \alpha_2, \alpha_3)$. In this thesis, there is only one Clebsch-Gordon series for which $t \geq 1$; and that is $t([N-2, 2], [N-2, 2], [N-2, 2]) = 2$.

Therefore, the block tensors of the rank-three, first-anharmonic-order tensor in the symmetry coordinate basis may be written in terms of the Clebsch-Gordon coefficients:

$$\left[\begin{smallmatrix} (1) \\ 3 \end{smallmatrix} Q_W^{\mu_1 \mu_2 \mu_3} \right]_{\xi_1, \xi_2, \xi_3} = \sum_k^{t(\alpha_1, \alpha_2, \alpha_3)} \left[\begin{smallmatrix} (1) \\ 3 \end{smallmatrix} \sigma_{\alpha_1 \alpha_2 \alpha_3 k}^Q \right]_{X_1, X_2, X_3} C_{\xi_1, \xi_2, \xi_3}^{\alpha_1 \alpha_2, \alpha_3, k}, \quad (5.34)$$

where no summation over the repeated α_i indices is implied. This is a simple equation.

The tensor $\left[\begin{smallmatrix} (1) \\ 3 \end{smallmatrix} \sigma_{\alpha_1 \alpha_2 \alpha_3 k}^Q \right]_{X_1, X_2, X_3}$ has dimensions $5 \times 5 \times 5$.

The proportionality coefficient tensor σ contains all of the information about the system's Hamiltonian. This σ is a small tensor with a size that does not grow with N . All of the complicated N -dependence and indicial structure of each transformed block tensor is now entirely contained within the Clebsch-Gordon coefficient. Since there are only eight such Clebsch-Gordon coefficients, otherwise-prohibitive computational expense may be eliminated provided one can, for arbitrary N ,

1. calculate the Clebsch-Gordon coefficient tensors symbolically, and
2. calculate the proportionality coefficient tensors σ symbolically.

It is one thing to calculate the Clebsch-Gordon coefficients for S_3 , S_4 , and so on (one can find some examples of this in some textbooks(95)). It is quite another to calculate the coefficients in general for S_N .

These Clebsch-Gordon coefficient tensors were calculated in closed-form by analytically transforming binary invariants to the symmetry coordinate basis. This involves arduous algebra, for which we developed rule-based (rather than procedural) symbolic programs in *Mathematica*(101). We created a package which performs summations over the discrete Kronecker delta function and the unit step function (102). For details of the derivation of these coefficients, see Appendix E. The analytic derivation of these eight Clebsch-Gordon coefficients represents the subjugation of the DPT N -body problem, at least to first anharmonic order.

5.2.2 Symmetry-transformed binary invariants

To make use of the Clebsch-Gordon coefficients, one must calculate the proportionality coefficients in Eqs. (5.31), (5.33), and (5.34). The difficulty in doing so lies in resolving how, upon transformation to symmetry coordinates, the intricate structure of the Q tensors is folded into the proportionality tensor σ . This folded structure is entirely embodied in the transformed binary invariants. Therefore we may resolve the physical and structural information in the Hamiltonian, noting that the F and G tensors are symmetric so block labels can be dropped.²

From Eq. (4.15), we decompose each tensor block ${}^{(order)}_R Q^{X_1 \dots}$ of blocks (labeled by X_i) as a linear combination of the binary invariants for the graphs of the block,

$${}^{(order)}_R Q^{X_1 \dots X_R} = \sum_{\mathcal{G} \in \mathbb{G}_{X_1 \dots X_R}} {}^{(order)}_R Q^{X_1 \dots X_R}(\mathcal{G}) [B^{X_1 \dots X_R}(\mathcal{G})]_{\xi_1, \dots, \xi_R},$$

where no summation is ever implied over superscript block labels X .

Now, for any graph \mathcal{G} in a block, the transformation of the tensor $B^{block}(\mathcal{G})$ must be proportional to the Clebsch-Gordon coefficient of that transformation. Let us denote that quantity which multiplies the Clebsch-Gordon coefficient as $\beta(\mathcal{G})$:

$$[W_{X_1}^{\alpha_1} W_{X_2}^{\alpha_2} B(\mathcal{G})]_{\xi_1, \xi_2} = \left[\begin{matrix} (0) \\ 2 \end{matrix} \beta^{\alpha_1 \alpha_2}(\mathcal{G}) \right]_{X_1, X_2} C_{\xi_1, \xi_2}^{\alpha_1 \alpha_2} \quad (5.35)$$

$$[W_{X_1}^{\alpha_1} B(\mathcal{G})]_{\xi_1} = \left[\begin{matrix} (1) \\ 1 \end{matrix} \beta^{\alpha_1}(\mathcal{G}) \right]_{X_1} C_{\xi_1}^{\alpha_1} \quad (5.36)$$

$$[W_{X_1}^{\alpha_1} W_{X_2}^{\alpha_2} W_{X_3}^{\alpha_3} B(\mathcal{G})]_{\xi_1, \xi_2, \xi_3} = \sum_k^{t(\alpha_1, \alpha_2, \alpha_3)} \left[\begin{matrix} (1) \\ 3 \end{matrix} \beta^{\alpha_1 \alpha_2 \alpha_3, k}(\mathcal{G}) \right]_{X_1, X_2, X_3} C_{\xi_1, \xi_2, \xi_3}^{\alpha_1 \alpha_2, \alpha_3, k}. \quad (5.37)$$

Comparing the above equations, we can directly write the proportionality coefficients, σ^Q in Eqs. (5.31), (5.33), and (5.34) as a linear combination of these “ $\beta(\mathcal{G})$ multipliers”:

² FG and GF are not symmetric, and these have been transformed in previous works (81; 87), but need not be transformed here

$$\left[\begin{smallmatrix} (0) \\ 2 \end{smallmatrix} \sigma_{\alpha_1 \alpha_2}^Q \right]_{X_1, X_2} = \sum_{\mathcal{G}} \begin{smallmatrix} (0) \\ 2 \end{smallmatrix} Q(\mathcal{G}) \left[\begin{smallmatrix} (0) \\ 2 \end{smallmatrix} \beta^{\alpha_1 \alpha_2}(\mathcal{G}) \right]_{X_1, X_2} \quad (5.38)$$

$$\left[\begin{smallmatrix} (1) \\ 1 \end{smallmatrix} \sigma_{\alpha_1}^Q \right]_{X_1} = \sum_{\mathcal{G}} \begin{smallmatrix} (1) \\ 1 \end{smallmatrix} Q(\mathcal{G}) \left[\begin{smallmatrix} (1) \\ 1 \end{smallmatrix} \beta^{\alpha_1}(\mathcal{G}) \right]_{X_1} \quad (5.39)$$

$$\sum_k^{t(\alpha_1, \alpha_2, \alpha_3)} \left[\begin{smallmatrix} (1) \\ 3 \end{smallmatrix} \sigma_{\alpha_1 \alpha_2 \alpha_3 k}^Q \right]_{X_1, X_2, X_3} = \sum_{\mathcal{G}} \begin{smallmatrix} (1) \\ 3 \end{smallmatrix} Q(\mathcal{G}) \sum_k \left[\begin{smallmatrix} (1) \\ 3 \end{smallmatrix} \beta^{\alpha_1 \alpha_2 \alpha_3 k}(\mathcal{G}) \right]_{X_1, X_2, X_3} \quad (5.40)$$

Recall that the dimensions of σ and therefore $\beta(\mathcal{G})$ do not depend on N : all of the complicated N -dependent index structure is contained within the Clebsch-Gordon coefficient. Again, there is nothing complicated happening in the above equations, only element-by-element multiplication.

In Appendix F, we derive the elements of these $\beta(\mathcal{G})$ multipliers by analytically transforming binary invariants and comparing to the relevant Clebsch-Gordon coefficient in Eqs. (5.35-5.37). These results are used in Eqs. (5.38-5.40) to construct the coefficient tensor σ by which the particular physical system is transformed to symmetry coordinates in Eqs (5.31), (5.33) and (5.34), which we reproduce below in a more convenient form:

$$\left[\begin{smallmatrix} (0) \\ 2 \end{smallmatrix} Q_W^{\mu_1 \mu_2} \right]_{\xi_1, \xi_2} = \begin{smallmatrix} (0) \\ 2 \end{smallmatrix} \sigma_{\mu_1, \mu_2}^Q C_{\xi_1, \xi_2}^{\alpha_1 \alpha_2} \quad (5.41)$$

$$\left[\begin{smallmatrix} (1) \\ 1 \end{smallmatrix} Q_W^\mu \right]_{\xi} = \begin{smallmatrix} (1) \\ 1 \end{smallmatrix} \sigma_\mu^Q C_\xi^\alpha \quad (5.42)$$

$$\left[\begin{smallmatrix} (1) \\ 3 \end{smallmatrix} Q_W^{\mu_1 \mu_2 \mu_3} \right]_{\xi_1, \xi_2, \xi_3} = \sum_k^{t(\alpha_1, \alpha_2, \alpha_3)} \begin{smallmatrix} (1) \\ 3 \end{smallmatrix} \sigma_{\mu_1, \mu_2, \mu_3}^Q C_{\xi_1, \xi_2, \xi_3}^{\alpha_1 \alpha_2, \alpha_3, k}. \quad (5.43)$$

In the above equations, we adopt a notation (see Appendix B) combining α and X to form a single index μ which ranges from 1 to 5: $\mu \in \{\mathbf{0}r, \mathbf{0}\gamma, \mathbf{1}r, \mathbf{1}\gamma, \mathbf{2}\}$ (where $\mathbf{0}$, $\mathbf{1}$, and $\mathbf{2}$ are shorthand for the $[N]$, $[N-1, 1]$, and $[N-2, 2]$ irreps, respectively).

There is nothing complicated happening in these equations. There are no repeated indices to contract so these equations represent simple multiplication for each tensor element. we have indexed the σ tensors in the above equations in preparation for transforming the above equations to normal coordinates by the transformation $\mathcal{C}_{\mu_1, \mu_2}$.

5.3 Transformation to normal coordinates

The transformation of the DPT Hamiltonian tensors from symmetry coordinates to normal coordinates is relatively simple. One must merely transform the σ coefficient

tensors by $\mathcal{C}_{\mu_1, \mu_2}$ according to Eqs. (5.13). The result is DPT Hamiltonian coefficient tensors transformed to the normal-coordinate basis:

$$\left[\begin{matrix} (0) \\ 2 \end{matrix} Q_V \right]_{\nu_1, \nu_2} = \left[\begin{matrix} (0) \\ 2 \end{matrix} Q_V^{\mu_1 \mu_2} \right]_{\xi_1, \xi_2} = \begin{matrix} (0) \\ 2 \end{matrix} \tau_{\mu_1 \mu_2}^Q C_{\xi_1, \xi_2}^{\alpha_1 \alpha_2} \quad (5.44)$$

$$\left[\begin{matrix} (1) \\ 1 \end{matrix} Q_V \right]_{\nu} = \left[\begin{matrix} (1) \\ 1 \end{matrix} Q_V^{\mu} \right]_{\xi} = \begin{matrix} (1) \\ 1 \end{matrix} \tau_{\nu}^Q C_{\xi}^{\alpha_1} \quad (5.45)$$

$$\left[\begin{matrix} (1) \\ 3 \end{matrix} Q_V \right]_{\nu_1, \nu_2, \nu_3} = \left[\begin{matrix} (1) \\ 3 \end{matrix} Q_V^{\mu_1 \mu_2 \mu_3} \right]_{\xi_1, \xi_2, \xi_3} = \sum_k^{t(\alpha_1, \alpha_2, \alpha_3)} \begin{matrix} (1) \\ 3 \end{matrix} \tau_{\mu_1, \mu_2, \mu_3, k}^Q C_{\xi_1, \xi_2, \xi_3}^{\alpha_1 \alpha_2 \alpha_3, k}. \quad (5.46)$$

In the above equations, we have derived the coefficient tensors in the DPT Hamiltonian in normal coordinates, as expressed in Eqs. (5.10) and (5.11) which we reproduce below:

$$\bar{H}_0 = -\frac{1}{2} \left[\begin{matrix} (0) \\ 2 \end{matrix} G_V \right]_{\nu_1, \nu_2} \partial_{q_{\nu_1}} \partial_{q_{\nu_2}} + \frac{1}{2} \left[\begin{matrix} (0) \\ 2 \end{matrix} F_V \right]_{\nu_1, \nu_2} q_{\nu_1} q_{\nu_2} + \begin{matrix} (0) \\ 0 \end{matrix} F_V.$$

and

$$\begin{aligned} \bar{H}_1 = & -\frac{1}{2} \left[\begin{matrix} (1) \\ 3 \end{matrix} G_V \right]_{\nu_1, \nu_2, \nu_3} q_{\nu_1} \partial_{q_{\nu_2}} \partial_{q_{\nu_3}} - \frac{1}{2} \left[\begin{matrix} (1) \\ 1 \end{matrix} G_V \right]_{\nu} \partial_{q_{\nu}} \\ & + \frac{1}{3!} \left[\begin{matrix} (1) \\ 3 \end{matrix} F_V \right]_{\nu_1, \nu_2, \nu_3} q_{\nu_1} q_{\nu_2} q_{\nu_3} + \left[\begin{matrix} (1) \\ 1 \end{matrix} F_V \right]_{\nu} q_{\nu}, \end{aligned}$$

where summation of repeated ν_i indices from 1 to P is implied. In the index contractions in the above equations, most of the ‘‘action’’ occurs between the Clebsch-Gordan coefficients $C_{\mu \dots}^{\alpha_1 \dots}$ and the normal-mode coordinates and derivatives \mathbf{q}'_{ν} and $\partial_{\mathbf{q}'_{\nu}}$. We emphasize that all of the N -dependent structure resides in the Clebsch-Gordan coefficients.

The analytic transformation of a microscopic N -body Hamiltonian to a basis of collective coordinates opens many doors. For one, the full N -body DPT wavefunction can now be easily derived to first anharmonic order.

Chapter 6

Anharmonic Wave Function And Density Profile

In this chapter, we calculate the first anharmonic order, ground-state DPT wavefunction and density profile for a system of identical bosons in an isotropic confining potential. This calculation builds upon previous isotropic work. The isotropic, harmonic-order DPT ground-state wavefunction was derived in Reference (87). The harmonic-order DPT ground-state density profile was derived in Reference (90). The first-anharmonic-order DPT ground-state wavefunction was derived in Reference (100) and the first-anharmonic density profile was derived in Reference (103). Here we reproduce the derivation of the first-anharmonic wavefunction and density profile.

For increased clarity, all summations in this chapter will be made explicit: there will be no implied summation over repeated indices.

6.1 Derivation of the first-anharmonic-order ground-state wavefunction

6.1.1 Harmonic-order wavefunction

The order- δ Hamiltonian (Eq. (3.38)) is of the form of a multi-dimensional harmonic oscillator (hence the name harmonic order). Since we have determined the normal coordinates of the system, we can write the harmonic-order wavefunction in normal coordinates as a product of $P = N(N + 1)/2$ harmonic-oscillator wave functions. We obtain

$$\Phi_0(\mathbf{q}') = \prod_{\nu=1}^P \phi_{n_\nu}(\sqrt{\bar{\omega}_\nu} q'_\nu) , \quad (6.1)$$

where $\phi_{n_\nu}(\sqrt{\bar{\omega}_\nu}q'_\nu)$ is a one-dimensional harmonic-oscillator wave function of frequency $\bar{\omega}_\nu$ and n_ν is the oscillator quantum number, $0 \leq n_\nu < \infty$, which counts the number of quanta in each normal mode.

In Reference (87) (summarized in Chapter 5) the normal-mode coordinates q'_ν were derived from the maximal point group symmetry of the large-dimensional structure. The normal modes transform under the irreducible representations of S_N labeled by $[N]$, $[N-1, 1]$, and $[N-2, 2]$. We employ a short-hand notation for these irreps: $\mathbf{0} = [N]$, $\mathbf{1} = [N-1, 1]$, and $\mathbf{2} = [N-2, 2]$. There are two $[N]$ irreps (each of dimension one), two $[N-1, 1]$ irreps (each of $N-1$ dimensions), and one $[N-2, 2]$ irrep (of $N(N-3)/2$ dimensions). Thus the normal modes are partitioned by irreps: there are 2 normal coordinates which transform under two $[N]$ irreps, $2(N-1)$ which transform under two $[N-1, 1]$, and $N(N-3)/2$ which transform under an $[N-2, 2]$ irrep. In Eq. (6.1), we have adopted a compact notation where the normal coordinates are simply labeled by q'_ν , but it is sometimes necessary to label the normal coordinates $[q'_\mu]_\xi$ by both the block label $\mu \in \{\mathbf{0}^+, \mathbf{1}^+, \mathbf{2}\}$ and the degeneracy index ξ which has a range from 1 to the degeneracy of μ .

Writing the harmonic-order wavefunction in the latter block form, we obtain

$$\Phi_0(\mathbf{q}') = \prod_{\mu=\{\mathbf{0}^\pm, \mathbf{1}^\pm, \mathbf{2}\}} \prod_{\xi=1}^{d_\mu} \phi_{n(\mu, \xi)}(\sqrt{\bar{\omega}_\mu} [q'_\mu]_\xi), \quad (6.2)$$

where $\phi_{n(\mu, \xi)}(\sqrt{\bar{\omega}_\mu} [q'_\mu]_\xi)$ is a one-dimensional harmonic-oscillator wave function of frequency $\bar{\omega}_\mu$ and $n(\mu, \xi)$ is the oscillator quantum number, $0 \leq n(\mu, \xi) < \infty$, which counts the number of quanta in each normal mode. The index μ labels the manifold of normal modes with the same frequency $\bar{\omega}_\mu$, while the degeneracy of the μ th normal mode is denoted $d_\mu = 1, N-1$ or $N(N-3)/2$ for $\mu = \mathbf{0}^\pm, \mathbf{1}^\pm$ or $\mathbf{2}$, respectively.

6.1.2 Harmonic-order ground-state wavefunction

The harmonic-order DPT wave function for the ground state, ${}_g\Phi_0(\mathbf{q}')$, is given by Eq. (6.2) with all of the n_ν set equal to zero, i.e.

$${}_g\Phi_0(\mathbf{q}') = \prod_{\nu=1}^P \phi_0(\sqrt{\bar{\omega}_\nu} q'_\nu), \quad (6.3)$$

where ϕ_0 is the wavefunction of a single harmonic-oscillator,

$$\phi_0(\sqrt{\bar{\omega}_\nu} q'_\nu) = \left(\frac{\bar{\omega}_\nu}{\pi}\right)^{\frac{1}{4}} \exp\left(-\frac{1}{2}\bar{\omega}_\nu q'^2_\nu\right). \quad (6.4)$$

There are $N(N + 1)/2$ normal modes and up to $N(N + 1)/2$ distinct frequencies; analytically determining these normal modes would be a formidable problem if it weren't for the S_N point group symmetry expressed in the invariance of the \mathbf{F} and \mathbf{G} tensors, and the small, N -independent number of binary invariants spanning the invariant tensor spaces. In References (87), (81) and (82) we have used this S_N point group symmetry to derive both the frequencies and normal modes of the lowest-order, Jacobian-weighted wave function for arbitrary N . This analysis results in only five distinct frequencies. These five frequencies are associated with five distinct collective motions: a center-of-mass mode, a breathing mode, radial and angular singly-excited state modes, and phonon modes. Each of these frequencies is associated with a set of normal modes which transforms under an irreducible representation of the S_N point group.

6.1.3 First anharmonic wave function

Previous applications of DPT went to very high order in the asymptotic $1/D$ expansion. For systems with a large number of degrees of freedom, the calculation of these high-order terms can be computationally prohibitive and subject to numerical difficulties. In Reference (83), Dunn *et. al.* present an algorithm by which these corrections may be derived exactly using tensor algebra. Using this formalism, the wavefunction is derived in Ref. (100) to first anharmonic order

$$\Phi(\mathbf{q}') = (1 + \delta^{\frac{1}{2}} \hat{\Delta}) \Phi_0(\mathbf{q}') + O(\delta), \quad (6.5)$$

where $\hat{\Delta}$ is an operator (note the “hat”). This wavefunction is obtained by solving the following eigenvalue equation:

$$[\hat{\Delta}, \bar{H}_0] \Phi_0 = \bar{H}_1 \Phi_0. \quad (6.6)$$

To solve this equation, we note that since $\Phi_0(\mathbf{q}')$ is a Gaussian function, the derivatives in \bar{H}_1 and \bar{H}_0 written in normal coordinates “bring down” normal coordinates from the exponent, so \bar{H}_1 effectively becomes a 3rd-order polynomial of only odd powers in \mathbf{q}' . Then from Eq. (6.6), $\hat{\Delta}$ is a cubic polynomial and of only odd powers in the normal modes. When $\hat{\Delta}$ is re-expressed in terms of internal displacement coordinates, \mathbf{r}' and $\boldsymbol{\gamma}'$, it is cubic and of only odd powers in these internal displacement coordinates.

6.1.3.1 Evaluation of the derivatives in the first-anharmonic-order Hamiltonian

We evaluate the derivatives in Eq. (6.6) to reduce the operator equation to a polynomial equation in q'_ν ,

$$\partial_{q'_\nu} \Phi_0(\mathbf{q}') = -\bar{\omega}_\nu q'_\nu \Phi_0(\mathbf{q}') \quad (6.7)$$

$$\partial_{q'_\nu}^2 \Phi_0(\mathbf{q}') = (-\bar{\omega}_\nu + \bar{\omega}_\nu^2 (q'_\nu)^2) \Phi_0(\mathbf{q}'). \quad (6.8)$$

Therefore with the substitutions

$$\partial_{q'_\nu} \rightarrow -\bar{\omega}_\nu q'_\nu \quad (6.9)$$

$$\partial_{q'^{\nu_i}} \partial_{q'^{\nu_j}} \rightarrow \bar{\omega}_{\nu_i} \bar{\omega}_{\nu_j} q'^{\nu_i} q'^{\nu_j} - \delta_{ij} \bar{\omega}_{\nu_i}, \quad (6.10)$$

the action of \bar{H}_1 on $\Phi_0(\mathbf{q}')$ becomes equivalent to the action of a 3rd-order polynomial $(\bar{H}_1)_{\text{eff}}$ on $\Phi_0(\mathbf{q}')$:

$$\bar{H}_1 \Phi_0(\mathbf{q}') = (\bar{H}_1)_{\text{eff}} \Phi_0(\mathbf{q}')$$

where

$$\begin{aligned} (\bar{H}_1)_{\text{eff}} = & \sum_{\nu_1, \nu_2, \nu_3} \left(-\frac{1}{2} \left[\begin{matrix} (1) \\ 3 \\ G_V \end{matrix} \right]_{\nu_1, \nu_2, \nu_3} \bar{\omega}_{\nu_2} \bar{\omega}_{\nu_3} + \frac{1}{3!} \left[\begin{matrix} (1) \\ 3 \\ F_V \end{matrix} \right]_{\nu_1, \nu_2, \nu_3} \right) q'^{\nu_1} q'^{\nu_2} q'^{\nu_3} \\ & + \sum_{\nu_1} \left(\frac{1}{2} \sum_{\nu_2} \left[\begin{matrix} (1) \\ 3 \\ G_V \end{matrix} \right]_{\nu_1, \nu_2, \nu_2} \bar{\omega}_{\nu_2} + \frac{1}{2} \left[\begin{matrix} (1) \\ 1 \\ G_V \end{matrix} \right]_{\nu_1} \bar{\omega}_{\nu_1} + \left[\begin{matrix} (1) \\ 1 \\ F_V \end{matrix} \right]_{\nu_1} \right) q'^{\nu_1}. \end{aligned} \quad (6.11)$$

Note that the repeated index summation convention is not used in this chapter: all summations are written explicitly.

Let us define the $(4 \times 4 \times 4)$ tensor $\tau_{\mu_1, \mu_2, \mu_3}^{H_1}$ and the length-4 column vector $\tau_{\mu_1}^{H_1}$ so that the above equation may be written in terms of Clebsch-Gordon tensors:

$$\begin{aligned} \tau_{\mu_1, \mu_2, \mu_3, k}^{H_1} &= -\frac{1}{2} \begin{matrix} (1) \\ 3 \\ \tau_{\mu_1, \mu_2, \mu_3, k}^G \end{matrix} \bar{\omega}_{\mu_2} \bar{\omega}_{\mu_3} + \frac{1}{3!} \begin{matrix} (1) \\ 3 \\ \tau_{\mu_1, \mu_2, \mu_3, k}^F \end{matrix} \\ \tau_{\mu_1}^{H_1} &= \frac{1}{2} \sum_{\mu_2} d_{\mu_2} \begin{matrix} (1) \\ 3 \\ \tau_{\mu_1, \mu_2, \mu_2, i}^G \end{matrix} \bar{\omega}_{\mu_2} + \frac{1}{2} \begin{matrix} (1) \\ 1 \\ \tau_{\mu_1}^G \end{matrix} \bar{\omega}_{\mu_1} + \begin{matrix} (1) \\ 1 \\ \tau_{\mu_1}^F \end{matrix}. \end{aligned} \quad (6.12)$$

Therefore, the polynomial $(\bar{H}_1)_{\text{eff}}$ may be written in the following compact form:

$$\begin{aligned} (\bar{H}_1)_{\text{eff}} = & \sum_{\mu_1, \mu_2, \mu_3, k} \tau_{\mu_1, \mu_2, \mu_3, k}^{H_1} \sum_{\xi_1, \xi_2, \xi_3} C_{\xi_1, \xi_2, \xi_3}^{\mu_1 \mu_2 \mu_3 k} [q'_{\mu_1}]_{\xi_1} [q'_{\mu_2}]_{\xi_2} [q'_{\mu_3}]_{\xi_3} + \\ & + \sum_{\mu=0+}^{\mathbf{0}-} \tau_{\mu}^{H_1} q'_{\mu}. \end{aligned} \quad (6.13)$$

6.1.3.2 Derivation of the cubic Δ

From Eqs. (6.6) and (6.13) above, we obtain the polynomial equation (note the absence of a “hat” on Δ , which is a polynomial)

$$[\Delta, H_0]\Phi_0 = (\bar{H}_1)_{\text{eff}}\Phi_0. \quad (6.14)$$

Solving this equation for the polynomial Δ , we obtain

$$\Delta = \sum_{\mu_1, \mu_2, \mu_3, k} \sum_{\xi_1, \xi_2, \xi_3} \left({}_3^{(1)}\tau_{\mu_1, \mu_2, \mu_3, k}^\Delta C_{\xi_1, \xi_2, \xi_3}^{\mu_1 \mu_2 \mu_3, k} \right) [q'_{\mu_1}]_{\xi_1} [q'_{\mu_2}]_{\xi_2} [q'_{\mu_3}]_{\xi_3} + \sum_{\mu=0+}^{0-} {}_1^{(1)}\tau_\mu^\Delta q'_\mu, \quad (6.15)$$

where the indices μ range over the irrep labels $\{\mathbf{0}+, \mathbf{0}-, \mathbf{1}+, \mathbf{1}-, \mathbf{2}\}$ (except for the last term, where μ is explicitly summed over $\mathbf{0}+$ and $\mathbf{0}-$) and

$${}_3^{(1)}\tau_{\mu_1, \mu_2, \mu_3, k}^\Delta = \frac{- {}_3^{(1)}\tau_{\mu_1, \mu_2, \mu_3, k}^{H_1}}{\bar{\omega}_{\mu_1} + \bar{\omega}_{\mu_2} + \bar{\omega}_{\mu_3}} \quad (6.16)$$

$${}_1^{(1)}\tau_{\mathbf{0}\pm}^\Delta = \frac{1}{\bar{\omega}_{\mathbf{0}\pm}} \left(- {}_1^{(1)}\tau_{\mathbf{0}\pm}^{H_1} \right) \quad (6.17)$$

$$+ \sum_{\mu} d_\mu \left({}_3^{(1)}\tau_{\mathbf{0}\pm\mu\mu}^\Delta + {}_3^{(1)}\tau_{\mu\mathbf{0}\pm\mu}^\Delta + {}_3^{(1)}\tau_{\mu\mu\mathbf{0}\pm}^\Delta \right). \quad (6.18)$$

Therefore, the first anharmonic-order many-body wavefunction is obtained by multiplying the harmonic-order wavefunction by Δ , a polynomial in \mathbf{q}' given by Eqs (6.15) and (6.16):

$$\Phi(\mathbf{q}') = (1 + \delta^{\frac{1}{2}}\Delta)\Phi_0(\mathbf{q}') + O(\delta). \quad (6.19)$$

6.2 Derivation of the first-anharmonic order density profile

6.2.1 Harmonic order density profile

In Ref. (90), we derived the DPT density profile at harmonic order by integrating over many of the degrees of freedom of the wavefunction, and transforming that integral from normal to internal coordinates. The essential idea is to integrate over all of the normal coordinates using a Dirac delta function to “project out” a radial dependence for the radius of a single particle r_i , obtaining the single-particle probability density function $\rho_0(r)$ for the harmonic order ground state, where

$$\rho_0(r) = \frac{1}{S(D)} \sum_{i=1}^N \int_{-\infty}^{\infty} \cdots \int_{-\infty}^{\infty} \delta_f(r - r_i) [{}_g\Phi_0(\bar{\mathbf{y}}')]^2 \prod_{\mu=0^\pm, 1^\pm, 2} \prod_{\xi=1}^{d_\mu} d[q'_\mu]_\xi, \quad (6.20)$$

and $\delta_f(r - r_i)$ is the Dirac delta function (differentiated from the inverse dimension, δ , by the subscript f). The factor $S(D)$ is the D -dimensional solid angle(92),

$$S(D) = \frac{2 \pi^{\frac{D}{2}}}{\Gamma(\frac{D}{2})}, \quad (6.21)$$

where we note that $S(1) = 2$, $S(2) = 2\pi$, $S(3) = 4\pi$, $S(4) = 2\pi^2$.

It is more convenient for us to use a density profile $N_0(r)$ weighted by the D -dimensional Jacobian factor

$$N_0(r) = r^{(D-1)} \rho_0(r). \quad (6.22)$$

The Dirac delta function $\delta_f(r - r_i)$ is a function of r_i , while the integral is over the normal coordinates \mathbf{q}'_{0^+} , \mathbf{q}'_{0^-} , $[\mathbf{q}'_{1^+}]_{N-1}$, and $[\mathbf{q}'_{1^-}]_{N-1}$. Thus we need a change of variables to perform the integral. We first note two crucial facts:

- Since ${}_g\Phi_0(\bar{\mathbf{y}}')$ is invariant under particle interchange, we can choose any radius r_i .
- The choice of r_N only appears in four of these $P = N(N + 1)/2$ integrals (\mathbf{q}'_{0^+} , \mathbf{q}'_{0^-} , $[\mathbf{q}'_{1^+}]_{d_{1^+}}$ and $[\mathbf{q}'_{1^-}]_{d_{1^-}}$, where d_{1^\pm} indicates the last 1^\pm normal coordinate).

Therefore, we write the ground-state, harmonic-order, Jacobian-weighted probability density profile $N_0(r)$ as

$$S(D) N_0(r) = N \int_{-\infty}^{\infty} \cdots \int_{-\infty}^{\infty} \delta_f(r - r_N) [{}_g\Phi_0(\bar{\mathbf{y}}')]^2 \prod_{\mu=0^\pm, 1^\pm, 2} \prod_{\xi=1}^{d_\mu} d[q'_\mu]_\xi. \quad (6.23)$$

Upon substituting the form of the ground-state wavefunction using Eq. (6.3) and Eq. (6.4), we note that most integrals are simple Gaussian integrals not involving the coordinate r_N and are simply unity. Only four integrals remain that cannot be immediately evaluated due to the presence of r_N in the delta function: integrals over the four coordinates \mathbf{q}'_{0^+} , \mathbf{q}'_{0^-} , $[\mathbf{q}'_{1^+}]_{d_{1^+}}$ and $[\mathbf{q}'_{1^-}]_{d_{1^-}}$:

$$S(D) N_0(r) = N \int_{-\infty}^{\infty} \int_{-\infty}^{\infty} \int_{-\infty}^{\infty} \int_{-\infty}^{\infty} \delta_f(r - r_N) \prod_{\mu=0^\pm, 1^\pm} [\phi_0(\sqrt{\bar{\omega}_\mu} [q'_\mu]_{d_\mu})]^2 d[q'_\mu]_{d_\mu} \quad (6.24)$$

$$= \frac{N \sqrt{\bar{\omega}_{0^+} \bar{\omega}_{0^-} \bar{\omega}_{1^+} \bar{\omega}_{1^-}}}{\pi^2} \int_{-\infty}^{\infty} \int_{-\infty}^{\infty} \int_{-\infty}^{\infty} \int_{-\infty}^{\infty} \delta_f(r - r_N) \times \exp \left(- \sum_{\mu_1=0^\pm, 1^\pm} \bar{\omega}_{\mu_1} [q'_{\mu_1}]_{d_{\mu_1}}^2 \right) \prod_{\mu_2=0^\pm, 1^\pm} d[q'_{\mu_2}]_{d_{\mu_2}}. \quad (6.25)$$

In order to evaluate this derivative, we must perform a change of variables. The details of this harmonic-order derivation are necessary to derive the first-anharmonic-order density profile, and are reproduced in first section of Appendix G.

The result is the harmonic-order, ground-state probability density profile

$$S(D) N_0(r) = N \sqrt{\frac{D}{\kappa^2(D)} \frac{R}{\pi}} \exp \left(-R \left(r \frac{\sqrt{D}}{\kappa(D)} - \sqrt{D} \bar{r}_\infty \right)^2 \right), \quad (6.26)$$

where R is defined in Eq. (G.22), and $\kappa(D)$ depends on the choice of dimensional scaling for the particular physical system.

Notice that the harmonic-order DPT density profile is a Gaussian (normalized to N) centered around $r = \kappa(D) \bar{r}_\infty$, the $D \rightarrow \infty$ configuration radius (see Eqs. (3.19) and (3.24)). The form of this Gaussian function is fixed by only two parameters: R and \bar{r}_∞ . The harmonic-order density profile is not very “flexible”—it must be symmetric. The the first-anharmonic-order corrections will add flexibility by allowing asymmetry.

6.2.2 First-anharmonic-order corrections

The derivation of the first-anharmonic density profile is similar to that of the harmonic density profile in that the same transformations are used to perform a change of coordinates. Integrals over the normal coordinates \mathbf{q}'_{0^+} , \mathbf{q}'_{0^-} , $[\mathbf{q}'_{1^+}]_{N-1}$, and $[\mathbf{q}'_{1^-}]_{N-1}$ are transformed to \bar{r}'_N , \bar{r}'_S , $\mathbf{S}'_{\bar{\gamma}}^{[N]}$, and $[\mathbf{S}'_{\bar{\gamma}}^{[N-1, 1]}]_{(N-1)}$.

The first-anharmonic-order density profile is derived from the first-anharmonic-order wavefunction in a similar way to the harmonic order density profile, by simply substituting $(1 + \delta^{1/2} \Delta)^2 [{}_g\Phi_0(\bar{\mathbf{q}}')]^2$ from Eq. (6.19) in Eq. (6.23):

$$N_1(r) = \frac{N}{S(D)} \int_{-\infty}^{\infty} \cdots \int_{-\infty}^{\infty} \prod_{\mu=0^\pm, 1^\pm, 2} \prod_{\xi=1}^{d_\mu} d[q'^\mu]_\xi \times \delta_f(r - r_N) (1 + 2\delta^{1/2} \Delta + \delta \Delta^2) [{}_g\Phi_0(\bar{\mathbf{q}}')]^2. \quad (6.27)$$

We are interested in deriving the density profile to first anharmonic order ($\delta^{1/2}$). The order δ contribution of the Δ^2 term comes in at second-anharmonic order is much more difficult to calculate (due to the presence of a sixth-order polynomial). Dropping the order δ term is expedient, but it introduces a liability: it will be possible for the density profile to become negative. In Appendix H, we set up the derivation of the Δ^2 term. We drop the order δ term for now, obtaining

$$N_1(r) = N_0(r) + \frac{N}{S(D)} 2\delta^{1/2} \int_{-\infty}^{\infty} \cdots \int_{-\infty}^{\infty} \prod_{\mu=0^\pm, 1^\pm, 2} \prod_{\xi=1}^{d_\mu} d[q'_\mu]_\xi \times \delta_f(r - r_N) \Delta [{}_g\Phi_0(\bar{\mathbf{q}}')]^2. \quad (6.28)$$

Substituting Δ from Eq. (6.15), we obtain

$$N_1(r) = N_0(r) + \frac{N}{S(D)} 2\delta^{1/2} \int_{-\infty}^{\infty} \cdots \int_{-\infty}^{\infty} \prod_{\mu=0^\pm, 1^\pm, 2} \prod_{\xi=1}^{d_\mu} d[q'_\mu]_\xi \delta_f(r - r_N) \times \sum_{\mu_1, \mu_2, \mu_3, k} \sum_{\xi_1, \xi_2, \xi_3} \left({}_3^{(1)}\tau_{\mu_1, \mu_2, \mu_3, k}^\Delta C_{\xi_1, \xi_2, \xi_3}^{\mu_1 \mu_2 \mu_3, k} [q'_{\mu_1}]_{\xi_1} [q'_{\mu_2}]_{\xi_2} [q'_{\mu_3}]_{\xi_3} + {}_1^{(1)}\tau_{\mu_1}^\Delta [q'_{\mu_1}]_{\xi_1} \right) \times [{}_g\Phi_0(\bar{\mathbf{q}}')]^2. \quad (6.29)$$

We perform this integration in Appendix G, obtaining the first-anharmonic-order ground-state DPT density profile $N_1(r)$:

$$N_1(r) = \frac{N}{S(D)} \sqrt{\frac{R}{\delta \kappa(D)^2 \pi}} (1 + \delta^{\frac{1}{2}} (A_1 \bar{r}' + A_3 \bar{r}'^3)) \exp(-R \bar{r}'^2), \quad (6.30)$$

where the constants A_1 and A_3 are defined in Eqs. (G.66) and (G.67) and

$$\bar{r}' = \left(\frac{r}{a_{ho}} - \sqrt{D} \bar{r}_\infty \right). \quad (6.31)$$

For the case of a BEC, $\kappa(D) = D^2 \bar{a}_{ho}$, where

$$\bar{a}_{ho} = \frac{1}{D^{3/2}} a_{ho}. \quad (6.32)$$

Therefore

$$\kappa(D) = \sqrt{D} a_{ho}. \quad (6.33)$$

Therefore, in oscillator units

$$r_{osc} = \frac{r}{a_{ho}}, \quad (6.34)$$

we obtain the Jacobian-weighted density per particle

$$N_0(r_{osc}) \times \frac{S(D)}{N} = \sqrt{\frac{R}{\pi}} \exp\left(-R \left(r_{osc} - \sqrt{D} \bar{r}_\infty\right)^2\right) \quad (6.35)$$

$$N_1(r_{osc}) \times \frac{S(D)}{N} = \left(1 + \delta^{\frac{1}{2}} \left(A_1 \left(r_{osc} - \sqrt{D} \bar{r}_\infty\right) + A_3 \left(r_{osc} - \sqrt{D} \bar{r}_\infty\right)^3\right)\right) \quad (6.36)$$

$$\times N_0(r_{osc}) \times \frac{S(D)}{N}. \quad (6.37)$$

In this Section, we have derived the N -body density profile through first-anharmonic-order using DPT. In doing so, we have neglected the Δ^2 term in Eq. (6.27). Both the wavefunction and density profile are written in the basis of normal coordinates. The coefficient Δ in the wavefunction and the coefficients A_1 , A_3 , and R in the density profile represent very complicated expressions. Because the expressions are so large, in practice they are evaluated using a computer algebra system (CAS) (in our case *Mathematica*).

In order to check the validity of these expressions and their implementation in the CAS, in the next chapter we derive an exact solution for the fully-interacting Hookes-law gas and form a perturbation series to compare to the DPT expansion.

6.3 The view from Plato's cave

The N -body wavefunction cannot be observed directly. The probability density profile is only a shadow of the full N -body wavefunction, containing much less information than the wavefunction (as seen here by integrating over all but 4 of the $N(N+1)/2$ collective coordinates). The density profile, however, can be observed in the laboratory quite directly. In the case of a BEC, the extent of the density profile is large enough (on the order of the width of a human hair) that the column density can be measured by simply taking a picture.

We have reached the end of the theoretical development in which we have generalized N -body DPT to go to higher orders. For the next intrepid explorer who has worked through the development in the body of this thesis and in the appendices, I leave this (subterranean) vista. We have derived an (essentially) analytic expression for the full N -body wavefunction. The density profile is only one observable property that can be calculated. What will you do next?

Part III
Application

Chapter 7

Application to the (fully-interacting) Hooke's law gas

Ut tensio, sic vis

Robert Hooke, 1676

The general theory developed in Chapters 3 through 6 (also in References (87; 90; 100; 104; 103)) is extensive. In this chapter, we apply the N -body DPT formalism to an N -body system which actually has an exact analytic solution: a system of N identical particles in a harmonic trap with harmonic (Hooke's law or spring-force) interactions. We write the Hamiltonian in units where the mass and Planck's constant have been scaled out¹:

$$H = \frac{1}{2} \left(\sum_i^N \left[-\frac{\partial^2}{\partial \mathbf{r}_i^2} + \omega_t^2 \mathbf{r}_i^2 \right] + \sum_{i < j}^N m_i \omega_p^2 \mathbf{r}_{ij}^2 \right). \quad (7.1)$$

Due to the similarity of the confining and interaction potentials, the Schrödinger equation for this system can be solved directly for any N . In Appendix I (and in References (104) and (103)) we directly determine the exact N -body wavefunction(104) and density profile(103) and form a perturbation series in $\delta^{1/2}$ in order to compare both quantities with the DPT perturbation series.

¹The coordinates are in units of $\sqrt{\frac{\hbar}{m}}$ and energy is in units of \hbar . This choice is to be consistent with previous publications. One might also choose the conventional harmonic oscillator units, where distance is measured in units of the harmonic oscillator length $\sqrt{\frac{\hbar}{m\omega_t}}$ and energy is measured in units of $\hbar\omega_t$.

7.1 Application of DPT formalism to the Hooke's-law gas

First we apply the N -body DPT developed here, which is applicable to any system of identical bosons with a central potential, to the specific case of the trapped Hooke's-law gas.

7.1.1 Dimensional scaling of the Hamiltonian

In order to apply the general DPT results, we must merely specify the dimensional scaling and a few derivatives. We define the dimensionally-scaled radius $\bar{\mathbf{r}}$,

$$\mathbf{r} = \kappa(D)\bar{\mathbf{r}}, \quad (7.2)$$

where we have chosen the scaling

$$\kappa(D) = D^2\bar{a}_{\text{ho}}. \quad (7.3)$$

In the above equation, the length scale \bar{a}_{ho} is the distance to the classical turning point in the ground-state of the non-interacting harmonic trap:

$$\bar{a}_{\text{ho}} = \sqrt{\frac{\hbar}{m\bar{\omega}_{\text{conf}}}} \quad \text{and} \quad \bar{\omega}_{\text{conf}} = D^3\omega_{\text{conf}}. \quad (7.4)$$

Therefore, we write the Hamiltonian in dimensionally-scaled coordinates (also scaling out an overall $\hbar\omega_{\text{t}}$)

$$\bar{H} = \frac{1}{2} \left(\sum_i^N \left[-\frac{\partial^2}{\partial \bar{r}_i^2} + \bar{r}_i^2 \right] + \sum_{i<j}^N \lambda^2 \bar{r}_{ij}^2 \right), \quad (7.5)$$

where we have defined

$$\lambda = \sqrt{1 + N\omega_{\text{p}}^2/\omega_{\text{t}}^2}. \quad (7.6)$$

Substituting these scaled variables into the similarity-transformed Schrödinger equation gives the following equation:

$$\bar{H}\Phi = (\delta^2\bar{T} + \bar{U} + \bar{V}_{\text{conf}} + \bar{V}_{\text{int}})\Phi = \bar{E}\Phi, \quad (7.7a)$$

where

$$\bar{T} = \sum_{i=1}^N \left(-\frac{1}{2} \frac{\partial^2}{\partial \bar{r}_i^2} - \frac{1}{2\bar{r}_i^2} \sum_{j \neq i} \sum_{k \neq i} \frac{\partial}{\partial \gamma_{ij}} (\gamma_{jk} - \gamma_{ij}\gamma_{ik}) \frac{\partial}{\partial \gamma_{ik}} \right), \quad (7.7b)$$

$$\bar{U} = \sum_{i=1}^N \left(\frac{\delta^2 N(N-2) + (1 - \delta(N+1))^2 \left(\frac{\Gamma^{(i)}}{\Gamma} \right)}{8\bar{r}_i^2} \right), \quad (7.7c)$$

$$\bar{V}_{\text{conf}} = \sum_{i=1}^N \frac{1}{2} \bar{r}_i^2 \quad (7.7d)$$

$$\bar{V}_{\text{int}} = \sum_{i=1}^{N-1} \sum_{j=i+1}^N \frac{1}{2} \lambda \bar{r}_{i,j}^2 \quad (7.7e)$$

$$\bar{V}_{\text{eff}} = \bar{U} + \bar{V}_{\text{conf}} + \bar{V}_{\text{int}}.$$

7.1.2 Large-D limit

We determine the minimum of the effective potential \bar{V}_{eff} by invoking the symmetric condition, obtaining an analytic expression for the large- D radius \bar{r}_∞ and the angle cosine γ_∞ ,

$$\bar{r}_\infty^2 = \frac{1}{2(1 + (N-1)\gamma_\infty)} = \frac{N + (\lambda - 1)}{2\lambda N} \quad (7.8)$$

$$\gamma_\infty = \frac{(\lambda - 1)}{(N + (\lambda - 1))}. \quad (7.9)$$

7.1.3 Perturbation series

The DPT perturbation series coefficient tensors G and F have been derived in general in Appendix D. In order to calculate the G and F tensors for this particular system, we must merely specify a constant and a few derivatives. For the G tensors, we must only note that, due to the choice of scaling we have made, $\zeta(0) = 1$. For the F tensors, we specify the (potentially non-zero) derivatives of the confining and effective potential.

7.1.3.1 Harmonic order

The elements of the harmonic-order coefficient matrix ${}^{(0)}_2 F$ are composed of second-order derivatives of the effective potential. Most of these derivatives depend only on $\zeta(0)$ and are calculated in Appendix D. The remaining derivatives particular to the system in question are

$$\left(\frac{\partial^2 \bar{V}_{\text{conf}}}{\partial \bar{r}_i^2} \right) \Bigg|_{\infty} = 1 \quad (7.10a)$$

$$\left(\frac{\partial^2 \bar{V}_{\text{int}}}{\partial \bar{r}_i^2} \right) \Bigg|_{\infty} = 1 + (N-1)\lambda^2 \quad (7.10b)$$

$$\left. \left(\frac{\partial^2 \bar{V}_{\text{int}}}{\partial \bar{r}_i \partial \bar{r}_j} \right) \right|_{\infty} = -\lambda^2 \gamma_{\infty} \quad (7.10c)$$

$$\left. \left(\frac{\partial^2 \bar{V}_{\text{int}}}{\partial \bar{r}_i \partial \gamma_{ij}} \right) \right|_{\infty} = -\lambda^2 \bar{r}_{\infty} \quad (7.10d)$$

$$\left. \left(\frac{\partial^2 \bar{V}_{\text{int}}}{\partial \gamma_{ij}^2} \right) \right|_{\infty} = 0 \quad (7.10e)$$

7.1.3.2 First anharmonic order

The rank-one first-anharmonic-order Hamiltonian coefficients result from a derivative with respect to δ and with respect to an internal coordinate. The confining and interaction potentials do not have any explicit dimensional dependence, so the derivative with respect to δ is zero:

$$\frac{\partial \bar{V}_{\text{conf}}}{\partial \delta} = \frac{\partial \bar{V}_{\text{int}}}{\partial \delta} = 0. \quad (7.11)$$

Therefore the derivatives relevant to the linear first-anharmonic term ${}^{(1)}_1 F$ are

$$\left. \left(\frac{\partial}{\partial \bar{r}_i} \frac{\partial \bar{V}_{\text{int}}}{\partial \delta} \right) \right|_{\infty} = 0 \quad (7.12a)$$

$$\left. \left(\frac{\partial}{\partial \gamma_{ij}} \frac{\partial \bar{V}_{\text{int}}}{\partial \delta} \right) \right|_{\infty} = 0. \quad (7.12b)$$

The rank-three first anharmonic tensor ${}^{(1)}_3 F$ is composed of third-order derivatives of the effective potential. Of the derivatives specific to this physical system, only the following may be non-zero:

$$\left. \left(\frac{\partial^3 \bar{V}_{\text{int}}}{\partial \bar{r}_i^3} \right) \right|_{\infty} = 0 \quad (7.13a)$$

$$\left. \left(\frac{\partial^3 \bar{V}_{\text{int}}}{\partial \bar{r}_i^2 \partial \bar{r}_j} \right) \right|_{\infty} = 0 \quad (7.13b)$$

$$\left. \left(\frac{\partial^3 \bar{V}_{\text{int}}}{\partial \gamma_{ij} \partial^2 \bar{r}_i} \right) \right|_{\infty} = 0 \quad (7.13c)$$

$$\left. \left(\frac{\partial^3 \bar{V}_{\text{int}}}{\partial \gamma_{ij} \partial \bar{r}_i \partial \bar{r}_j} \right) \right|_{\infty} = -\lambda^2 \quad (7.13d)$$

$$\left. \left(\frac{\partial^3 \bar{V}_{\text{int}}}{\partial \gamma_{ij}^2 \partial \bar{r}_i} \right) \right|_{\infty} = 0 \quad (7.13e)$$

$$\left. \left(\frac{\partial^3 \bar{V}_{\text{int}}}{\partial \gamma_{ij}^3} \right) \right|_{\infty} = 0. \quad (7.13f)$$

7.1.4 DPT Wavefunction and density profile

From this scaling and potential, we calculate the wavefunction polynomial coefficient Δ (Eq. (6.15)) and obtain the DPT wavefunction from Eq. (6.19) in the basis of normal coordinates.

$$\Phi(\mathbf{q}') = (1 + \delta^{\frac{1}{2}} \Delta) \Phi_0(\mathbf{q}') + O(\delta),$$

where Δ is a polynomial in the normal coordinates

$$\Delta = \sum_{\mu_1, \mu_2, \mu_3, k} \sum_{\xi_1, \xi_2, \xi_3} \left({}_3^{(1)} \tau_{\mu_1, \mu_2, \mu_3, k}^{\Delta} C_{\xi_1, \xi_2, \xi_3}^{\mu_1 \mu_2 \mu_3, k} \right) [q'_{\mu_1}]_{\xi_1} [q'_{\mu_2}]_{\xi_2} [q'_{\mu_3}]_{\xi_3} + \sum_{\mu''=\mathbf{0}+}^{\mathbf{0}-} {}_1^{(1)} \tau_{\mu''}^{\Delta} q'_{\mu''}.$$

The Jacobian-weighted density profile is then

$$\begin{aligned} N_0(\bar{r}') \times \frac{S(D)}{N} &= \sqrt{\frac{R}{\pi}} \exp(-R \bar{r}'^2) \\ N_1(\bar{r}') \times \frac{S(D)}{N} &= \left(1 + \delta^{\frac{1}{2}} (A_1 \bar{r}' + A_3 \bar{r}'^3) \right) N_0(\bar{r}') \times \frac{S(D)}{N} \end{aligned}$$

where

$$\bar{r}' = \left(\frac{r}{a_{ho}} - \sqrt{D} \bar{r}_{\infty} \right).$$

We have applied the DPT formalism developed in this thesis to the Hooke's-law gas to derive a perturbation series to first anharmonic order for the N -body wavefunction and density profile. In order to check this derivation and its implementation in the *Mathematica* code, we now obtain a corresponding perturbation series for the exact solution to this system.

7.2 Direct derivation of the exact solution

7.2.1 The exact wavefunction through first order

In Appendix I we solve the harmonically confined, harmonically interacting system of N particles exactly for the ground-state wave function (see Eq. (I.6)), and from this derive an analytic perturbation series for the N -body wavefunction (weighted by a Jacobian) through first order:

$$\Psi_J = \left(\frac{1}{\sqrt[4]{\pi}} \right)^{\frac{N(N+1)}{2}} \left(1 + \frac{1}{2} \delta^{\frac{1}{2}} \Delta_{\bar{\mathbf{y}}'} + O(\delta) \right) \exp(-[\bar{\mathbf{y}}']^T \bar{\Omega}_{\bar{\mathbf{y}}'} \bar{\mathbf{y}}'), \quad (7.14)$$

where we have defined $\bar{\Omega}_{\bar{\mathbf{y}}'}$ as $\bar{\Omega}$ (the matrix whose diagonal elements are frequencies) from the normal-coordinate basis, transformed to the internal-coordinate basis,

$$\bar{\Omega}_{\bar{\mathbf{y}}'} = \mathbf{V}^T \bar{\Omega} \mathbf{V} \quad (7.15)$$

$$\bar{\Omega}_{\nu_1, \nu_2} = \delta_{\nu_1, \nu_2} \bar{\omega}_{\nu_1} \quad (7.16)$$

and similarly, have transformed the polynomial Δ from a normal-coordinate basis to a internal-coordinate basis

$$\begin{aligned} \Delta_{\bar{\mathbf{y}}'} = & \Delta(\odot) [B(\odot)]_i \bar{r}'_i + \Delta(\rightarrow) [B(\rightarrow)]_{(ij)} \bar{\gamma}'_{(ij)} + \Delta(\bigcirc) [B(\bigcirc)]_{i,j,k} \bar{r}'_i \bar{r}'_j \bar{r}'_k \\ & + \Delta(\circ \rightarrow \circ) [B(\circ \rightarrow \circ)]_{(ij),k,l} \bar{\gamma}'_{(ij)} \bar{r}'_k \bar{r}'_l + \left(\Delta(\ominus) [B(\ominus)]_{(ij),(kl),(mn)} + \right. \\ & + \Delta(\triangle) [B(\triangle)]_{(ij),(kl),(mn)} + \Delta(\circ \rightarrow) [B(\circ \rightarrow)]_{(ij),(kl),(mn)} + \\ & + \Delta(\underline{\bullet}) [B(\underline{\bullet})]_{(ij),(kl),(mn)} + \Delta(\underline{\bullet}) [B(\underline{\bullet})]_{(ij),(kl),(mn)} \\ & + \Delta(\underline{\circ}) [B(\underline{\circ})]_{(ij),(kl),(mn)} + \Delta(\underline{\circ}) [B(\underline{\circ})]_{(ij),(kl),(mn)} + \\ & \left. + \Delta(\underline{\equiv}) [B(\underline{\equiv})]_{(ij),(kl),(mn)} \right) \bar{\gamma}'_{(ij)} \bar{\gamma}'_{(kl)} \bar{\gamma}'_{(mn)} \end{aligned} \quad (7.17)$$

$$\begin{aligned} \bar{\Omega}_{\bar{\mathbf{y}}'} = & \left(\Delta(\bigcirc) [B(\bigcirc)]_{i,j} + \Delta(\odot \odot) [B(\odot \odot)]_{i,j} \right) \bar{r}'_i \bar{r}'_j + \\ & + \Delta(\circ \rightarrow) [B(\circ \rightarrow)]_{(ij),k} \bar{\gamma}'_{(ij)} \bar{r}'_k + \left(\Delta(\circ) [B(\circ)]_{(ij),(kl)} + \right. \\ & \left. + \Delta(\underline{\bullet}) [B(\underline{\bullet})]_{(ij),(kl)} + \Delta(\underline{\circ}) [B(\underline{\circ})]_{(ij),(kl)} \right) \bar{\gamma}'_{(ij)} \bar{\gamma}'_{(kl)}. \end{aligned} \quad (7.18)$$

The scalar coefficients, $\Delta(\mathcal{G})$ are derived in Appendix I.

This direct calculation of the N -body wave function should yield the same expansion to each order of the wavefunction in the basis of binary invariants. To verify this we compare the coefficients $\Delta(\mathcal{G})$ from the direct calculation to the coefficients in the N -body DPT code. In Tables I.1–I.4 we compare the binary invariant coefficients, $\Delta(\mathcal{G})$, from the general formalism with the above results derived from the full analytical solution above for $N = 10,000$ particles and two different interparticle interaction strengths, λ . One value of λ features strongly-attractive, harmonic interparticle interactions, while the other is for a barely-bound system with repulsive interparticle interactions (negative λ) just below the dissociation threshold at $\lambda = -1/\sqrt{N}$.

In both cases, to within round-off-error determined by the machine precision, exact agreement is found, confirming the correctness of the general formalism and the *Mathematica* code(102).

7.2.2 The exact density profile through first anharmonic order

The exact analytic density profile for this system is derived in Reference (103) and expanded through first order in $\delta^{1/2}$ (See Appendix I) to yield the exact density profile through first order:

$$\mathcal{N}(\bar{r}'_{\text{eff}}) = \left(1 + \delta^{\frac{1}{2}} \sqrt{2} \left(\frac{2 \bar{r}'_{\text{eff}}{}^3}{3} - \bar{r}'_{\text{eff}} \right) + O(\delta) \right) \left(\frac{2}{\pi} \right)^{\frac{1}{2}} \exp(-2 \bar{r}'_{\text{eff}}{}^2). \quad (7.19)$$

This analysis shows that the density profile for any N or interaction strength follows a universal curve when a simple scaling is applied to the radial variable. This is not true of the wavefunction and it is not true in general for the density profile of other systems. This scaled density profile is plotted in Fig. 7.1. One readily sees the improvement obtained at first order in DPT, confirming the efficacy of DPT as an approach to the general confined N -body problem, which may be systematically improved by going to higher orders.

The general theory developed in this thesis for the density profile involves no such harmonic-interaction specific scaling since it's applicable to any interparticle potential, not just harmonic interparticle potentials. Consequently in Figs. 7.2 and 7.3, we plot the density profile without this harmonic-interaction specific scaling for two very different interparticle interaction strengths. Both are for $N = 10,000$ particles, but Fig. 7.2 features strongly attractive interactions, while Fig. 7.3 is for a repulsive interaction just below the dissociation limit. In the former case the system is tightly bound and very compact. In the latter case the confining potential is barely able to hold the system together against the combined effect of the repulsive interactions, and the system is very extended.

The density profile derived from the general N -body DPT formalism developed in this paper, and implemented in *Mathematica* code(102), is indistinguishable from the density profiles derived from the exact solution of the harmonically-interacting system. The agreement between the DPT and the direct density profiles confirms the correctness of the general formalism developed in this thesis, and its implementation in *Mathematica* code.

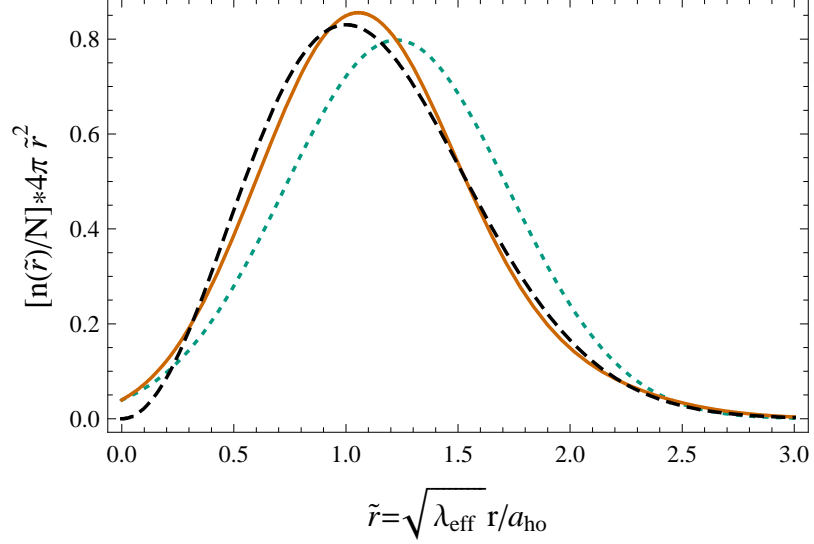


Figure 7.1: Scaled density profile for N harmonically interacting particles under harmonic confinement in oscillator units of the confining potential. The short-dash curve is the lowest-order DPT density profile, while the solid curve is the DPT density profile through first order. The long-dash curve is the exact result. The scaling factor, $\sqrt{\lambda_{\text{eff}}}$ is explained in Appendix I.

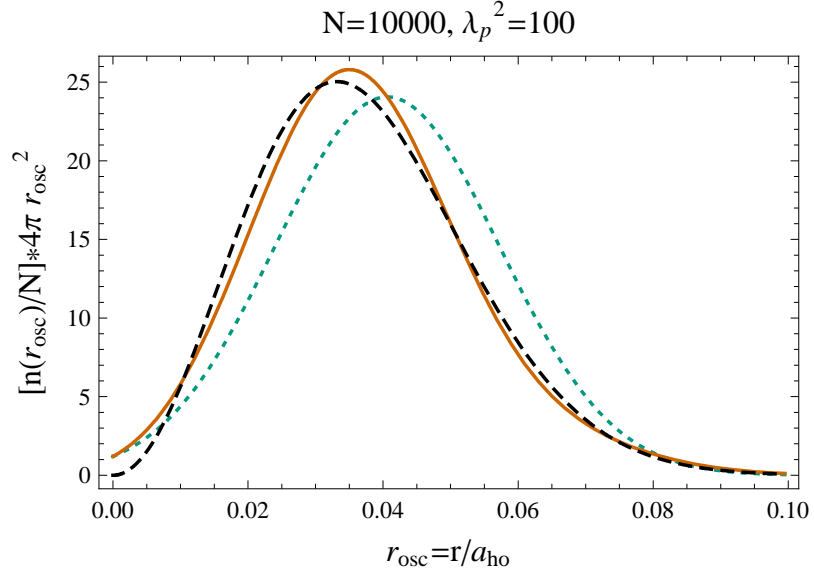


Figure 7.2: Unscaled density profile for $N = 10,000$ particles under harmonic confinement with strong attractive harmonic interactions ($\lambda_p^2 = 100$) in oscillator units of the confining potential. The short-dash curve is the lowest-order DPT density profile, while the solid curve is the DPT density profile through first order. The long-dash curve is the exact result. The parameter λ_p^2 , as explained in Appendix I, is the interaction frequency squared in oscillator units of the confining potential.

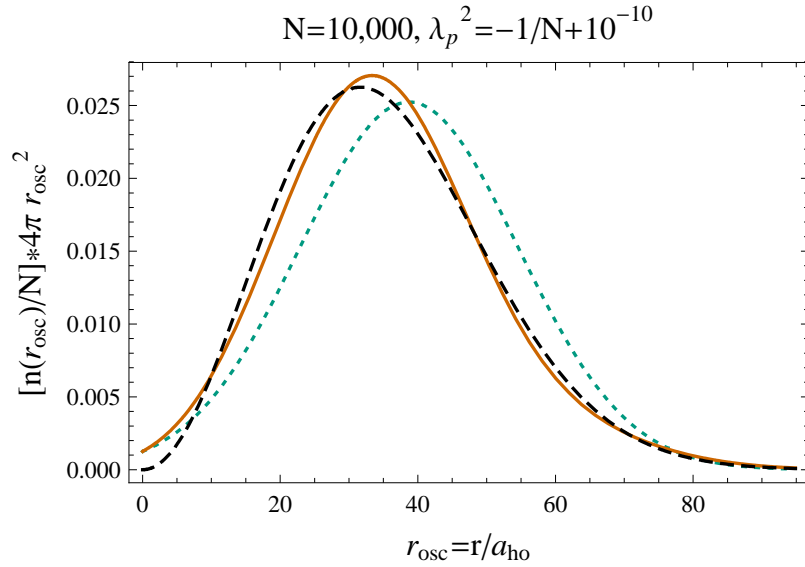


Figure 7.3: Unscaled density profile for $N = 10,000$ particles under harmonic confinement with repulsive harmonic interactions ($\lambda_p^2 = -1/10,000 + 10^{-10}$) in oscillator units of the confining potential. The system is just below the dissociation threshold and very extended. The short-dash curve is the lowest-order DPT density profile, while the solid curve is the DPT density profile through first order. The long-dash curve is the exact result. The parameter λ_p^2 , as explained in Appendix I, is the interaction frequency squared in oscillator units of the confining potential.

Chapter 8

Application to BEC: a preliminary peek

In Part II of this thesis, we presented a general N -body DPT formalism for any isotropic confined quantum system with pairwise interactions. In Chapter 7, we applied the formalism to the case of the fully-interacting Hooke's law gas, verifying the N -body DPT calculation by comparing to the direct solution to the wavefunction and density profile. We noted substantial qualitative improvement due to the first-anharmonic correction to the density profile. In this chapter, we perform preliminary calculations using the verified formalism for a Bose-Einstein condensate (BEC) of ^{87}Rb atoms in an isotropic (spherically-symmetric) trap.

We calculate the ground-state energy through harmonic order, as well as the wavefunction and density profile through first anharmonic order. This is still preliminary work, because the first-anharmonic results indicate that it will be necessary to calculate the extra Δ^2 term in Eq. (6.27). This is a modest extension and all the necessary theoretical work is contained within this thesis. This result indicates a clear next step and the calculation of the Δ^2 term is currently underway (see Appendix H).

8.1 Bose-Einstein condensate Hamiltonian

The similarity-transformed, D -dimensional DPT Hamiltonian for a confined quantum system is written in the form

$$(\mathcal{T} + \bar{U} + \bar{V}_{\text{conf}} + \bar{V}_{\text{int}}) \Phi = \bar{E} \Phi. \quad (8.1)$$

In order to apply this formalism to a particular physical system one must specify the confining potential and the interaction potential.

8.1.1 Atoms in a trap

Many BECs are “trapped” with a confining potential that is approximately proportional to the square of the radius from the center of a trap. Such a potential has the same form as a harmonic oscillator and is called a harmonic trap. This designation of “harmonic” is to be distinguished from the labels of the orders of DPT. We assume a condensate of N identical bosonic atoms with equal masses m confined by an isotropic (spherically-symmetric) harmonic trap with frequency ω_{ho} .

$$V_{\text{trap}} = \sum_{i=1}^N \frac{1}{2} m \omega_{\text{ho}}^2 r_i^2 \quad (8.2)$$

In Reference (53), three different model potentials are used to calculate the ground-state energy of a BEC. It is shown that for sufficiently dilute condensates, the ground-state energy does not depend on the shape of the potential used, but depends only on the scattering length. In order to compare to these exact calculations, we have used two of the potentials in this reference.

8.1.2 A smooth, short-range potential

For some methods, a “hard-sphere” potential such as potential A in Ref. (53) may be convenient. The presence of a discontinuity at $r = a$ makes the derivatives undefined at that point, and DPT requires a differentiable potential. We tried using potential B in Ref. (53), which is a smooth function of a hyperbolic trigonometric function:

$$V(r) = d \cosh^{-2}(r/r_0) , \quad (8.3)$$

where the height is fixed by d and the width by r_0 . This potential decreases exponentially for large- r and is short-range. Due to the DPT expansion about a symmetric arrangement, this short-range potential has no effect and the ideal-gas result is obtained. This result reminds us that DPT requires a long-range potential in the large- D limit. The potential in Eq. (8.3) could be dimensionally continued in a way that produces a long-range potential.

8.1.3 “Soft-sphere” interaction potential

We model the pair-wise interactions (at $D = 3$) in an N -body system by a “hard-sphere” potential similar to potential A in Reference (53), where the interaction is

much like the interaction between two billiard balls on a collision course: the interaction is zero as the distance decreases and then (discontinuously) large when they collide. Similarly, the hard-sphere interaction potential is zero unless the interparticle distance $r_{i,j}$ is equal to some contact distance which we take to be a , the s-wave scattering length:

$$V(r_{i,j}) = \begin{cases} 0 & \text{if } a < r_{i,j} \\ \infty & \text{if } r_{i,j} \leq a \end{cases} .$$

This hard-sphere potential has a discontinuity, and therefore the derivative is not defined everywhere. Because DPT requires well-defined derivatives at large D (but not necessarily $D = 3$), McKinney *et. al.* proposed a “soft-sphere” pairwise interaction potential (82; 81) that becomes a discontinuous hard-sphere potential when $D = 3$. This allows for a DPT analysis as well as a direct comparison at $D = 3$ with other methods which use a discontinuous contact potential. In these references, the interaction potential \bar{V}_{int} was defined (in dimensionally-scaled oscillator units, later defined in Eq. (8.8)) as

$$\bar{V}_{\text{int}} = \frac{\bar{V}_o}{1 - 3\delta} \sum_{i=1}^{N-1} \sum_{j=i+1}^N (1 - \tanh \Theta_{i,j}) , \quad (8.4)$$

where $\delta = 1/D$ is the perturbation parameter. The argument $\Theta_{i,j}$ is defined as

$$\Theta_{i,j} = \frac{\bar{c}_0}{1 - 3\delta} \left(\frac{\bar{r}_{ij}}{\sqrt{2}} - \bar{\alpha} - 3\delta (\bar{a} - \bar{\alpha}) \right) \left(1 + (1 - 3\delta) \frac{\bar{c}_1 \bar{r}_{ij}^2}{2} \right) , \quad (8.5)$$

where $\bar{r}_{i,j}$ is the interatomic separation,

$$\bar{r}_{ij} = \sqrt{\bar{r}_i^2 + \bar{r}_j^2 - 2\bar{r}_i \bar{r}_j \gamma_{ij}} , \quad (8.6)$$

and \bar{a} is the s-wave scattering length in dimensionally-scaled oscillator units. In the large-dimension limit, the argument $\Theta_{i,j}$ (with 4 parameters) becomes

$$\Theta_{\infty} = \Theta_{ij} \Big|_{\infty} = \bar{c}_0 \left(\sqrt{1 - \gamma_{\infty}} \bar{r}_{\infty} - \bar{\alpha} \right) \left(1 + (1 - \gamma_{\infty}) \bar{c}_1 \bar{r}_{\infty}^2 \right) , \quad (8.7)$$

and the potential retains this soft-sphere shape. In the physical $D = 3$ limit, no matter the values of the constants, this potential becomes that of a hard-sphere with radius \bar{a} .

In Figure 8.1, the general form of the soft-sphere interaction potential is shown. The other constants ($\bar{V}_0, \bar{\alpha}, \bar{c}_n$) determine the shape of the potential, and are “calibrated” by comparing to exact calculations¹. In the simplest case, the potential may be specified by only the height \bar{V}_0 and the slope \bar{c}_0 (with $\bar{\alpha} = 0$). The constant $\bar{\alpha}$ introduces an offset in the potential. The constant \bar{c}_1 further refines the shape of the potential.

8.2 Large-dimension limit of BEC Hamiltonian

8.2.1 Dimensional scaling

We regularize the large- D limit of the Schrödinger equation by using the following dimensionally-scaled variables:

$$\begin{aligned}\bar{r}_i &= \frac{r_i}{D^2 \bar{a}_{\text{ho}}}, & \bar{E} &= \frac{D^2}{\hbar \bar{\omega}_{\text{ho}}} E, & \bar{H} &= \frac{D^2}{\hbar \bar{\omega}_{\text{ho}}} H, & \bar{a} &= \frac{a}{\sqrt{2} D^2 \bar{a}_{\text{ho}}} \\ \bar{V}_o &= \frac{D^2}{\hbar \bar{\omega}_{\text{ho}}} V_o, & \bar{\alpha} &= \frac{\alpha}{\sqrt{2} D^2 \bar{a}_{\text{ho}}}, & \bar{c}_o &= \sqrt{2} D^2 \bar{a}_{\text{ho}} c_o,\end{aligned}\quad (8.8)$$

where

$$\bar{a}_{\text{ho}} = \sqrt{\frac{\hbar}{m \bar{\omega}_{\text{ho}}}} \quad \text{and} \quad \bar{\omega}_{\text{ho}} = D^3 \omega_{\text{ho}} \quad (8.9)$$

are the dimensionally-scaled harmonic-oscillator length scale and dimensionally-scaled trap frequency, respectively. Substituting these scaled variables into the similarity-transformed Schrödinger equation, Eq. (8.10a), gives the following equation:

$$\bar{H} \Phi = (\delta^2 \bar{T} + \bar{U} + \bar{V}_{\text{conf}} + \bar{V}_{\text{int}}) \Phi = \bar{E} \Phi. \quad (8.10a)$$

where

$$\bar{T} = \sum_{i=1}^N \hbar^2 \left(-\frac{1}{2} \frac{\partial^2}{\partial m_i \bar{r}_i^2} - \frac{1}{2m_i \bar{r}_i^2} \sum_{j \neq i} \sum_{k \neq i} \frac{\partial}{\partial \gamma_{ij}} (\gamma_{jk} - \gamma_{ij} \gamma_{ik}) \frac{\partial}{\partial \gamma_{ik}} \right), \quad (8.10b)$$

$$\bar{U} = \hbar^2 \sum_{i=1}^N \left(\frac{\delta^2 N(N-2) + (1 - \delta(N+1))^2 \left(\frac{\Gamma^{(i)}}{\Gamma} \right)}{8m_i \bar{r}_i^2} \right), \quad (8.10c)$$

$$\bar{V}_{\text{conf}} = \sum_{i=1}^N \frac{1}{2} \bar{r}_i^2 \quad (8.10d)$$

$$\bar{V}_{\text{int}} = \frac{\bar{V}_0}{1 - 3\delta} \sum_{i=1}^{N-1} \sum_{j=i+1}^N (1 - \tanh[\Theta_{i,j}]). \quad (8.10e)$$

¹“Exact” means accurate to within statistical uncertainty, as opposed to an approximate calculation.

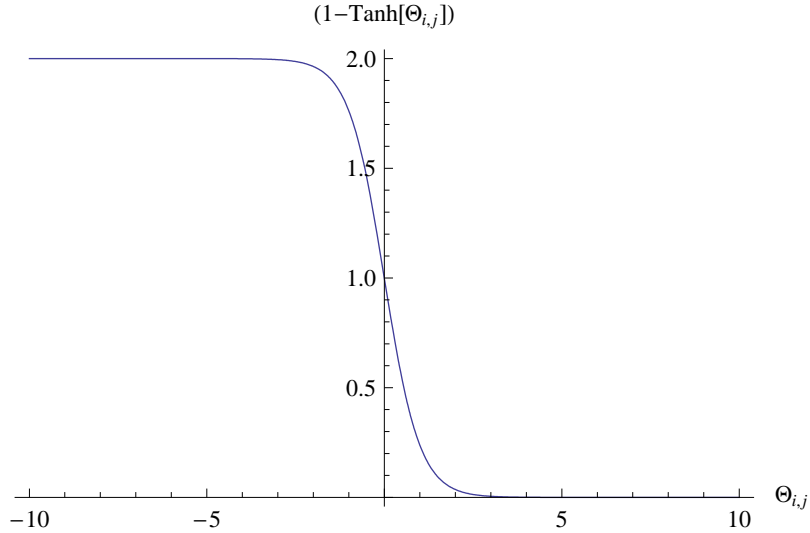


Figure 8.1: The form of the pair-wise interaction potential for $D \rightarrow \infty$ with 3 parameters. The height is given by $2\bar{V}_0$, the slope by $\bar{c}_0/\sqrt{2}$, and the potential is offset by $\sqrt{2}\bar{\alpha}$.

To be consistent with the References (for instance (82; 81; 90)), we have expressed the above dimensionally scaled Hamiltonian with \hbar and m_i . In what follows, as in the references, we will let all of the masses be equal and implicitly use oscillator units where $\hbar = m = 1$.

8.2.2 Large-dimension limit of the Hamiltonian

In the large-dimension limit ($\delta \rightarrow 0$) the factor of δ^2 suppresses the derivative portion of the kinetic energy \bar{T} , but the part of the centrifugal-like term,

$$\bar{U}(\bar{r}_i; \delta) \Big|_{\infty} = \frac{1}{8\bar{r}_i^2} \frac{\Gamma^{(i)}}{\Gamma} \Big|_{\infty}, \quad (8.11)$$

remains. This centrifugal-like term, together with the confining and interaction potentials form an effective potential, \bar{V}_{eff} :

$$\bar{V}_{\text{eff}}(\bar{r}, \gamma; \delta) = \sum_{i=1}^N (\bar{U}(\bar{r}_i; \delta) + \bar{V}_{\text{conf}}(\bar{r}_i; \delta)) + \sum_{i=1}^{N-1} \sum_{j=i+1}^N \bar{V}_{\text{int}}(\bar{r}_i, \gamma_{ij}; \delta). \quad (8.12)$$

The centrifugal-like term provides a repulsive core, even in the ground state. As $D \rightarrow \infty$, it is as if the mass of the particles in \bar{T} is becoming infinite, and the particles slow down and become localized at the bottom of the effective potential. The large- D energy is simply the value of the effective potential at this minimum.

8.2.3 Determination of the lowest-order symmetric arrangement

The static arrangement of the atoms in the large- D limit corresponds to the minimum of the effective potential. We postulate that this minimum is symmetric under interchange and therefore can be characterized by two parameters: \bar{r}_∞ and γ_∞ . The values of these parameters are determined by invoking the following two minimum conditions:

$$\left. \left(\frac{\partial \bar{V}_{\text{eff}}}{\partial \bar{r}_i} \right) \right|_\infty = 0 \quad (8.13)$$

$$\left. \left(\frac{\partial \bar{V}_{\text{eff}}}{\partial \gamma_{i,j}} \right) \right|_\infty = 0. \quad (8.14)$$

Substituting the above definitions of \bar{V}_{eff} into these conditions, we obtain two equations in \bar{r}_∞ and γ_∞ :

$$0 = r_\infty + \frac{(N-2)\gamma_\infty + 1}{4\bar{r}_\infty^3 (\gamma_\infty - 1) ((N-1)\gamma_\infty + 1)} - \frac{1}{\sqrt{2}}(N-1)\sqrt{1-\gamma_\infty}\bar{V}_0\Theta'_\infty \text{sech}^2(\Theta_\infty) \quad (8.15)$$

$$0 = \frac{\gamma_\infty ((N-2)\gamma_\infty + 2)}{4\bar{r}_\infty^2 (1-\gamma_\infty)^2 (1+(N-1)\gamma_\infty)^2} + \frac{\bar{r}_\infty \bar{V}_0 \Theta'_\infty \text{sech}^2(\Theta_\infty)}{\sqrt{2-2\gamma_\infty}}, \quad (8.16)$$

where, Θ'_∞ is defined in Eq. (J.5). One can eliminate the interaction potential from both equations, solving for the radius \bar{r}_∞ :

$$\bar{r}_\infty = \frac{1}{\sqrt{2}\sqrt{1+(N-1)\gamma_\infty}}. \quad (8.17)$$

Substituting \bar{r}_∞ into Eq. 8.16 we solve the following equation for the angle cosine γ_∞

$$\frac{\gamma_\infty (2 + (N-2)\gamma_\infty)}{(1-\gamma_\infty)^{3/2}\sqrt{1+(N-1)\gamma_\infty}} + \bar{V}_0 \text{sech}^2(\Theta_\infty) \Theta'_\infty = 0. \quad (8.18)$$

Because of the presence of $\text{sech}(\Theta_\infty)$, this equation is a transcendental equation, which must be solved for γ_∞ numerically using a root-finding algorithm. This equation has poles and potentially multiple roots, so a numerical solution requires careful analysis.

In previous work (82; 90), an algorithm that starts with an initial guess was used, and the proper root was selected by making an educated guess. This approach works well unless one wishes to perform a large-scale search of the space formed by the

interaction potential parameters. In such a case, a more robust root-finding algorithm which guarantees a solution within some interval would be useful.

This equation has properties that guarantee that a root is always bracketed within the interval $(-1/(N-1), 1)$. First, the transcendental term is finite. It is also positive definite if \bar{c}_1 and higher parameters are zero. Second, the term on the left has two poles: one at $\gamma_\infty = -1/(N-1)$ and one at $\gamma_\infty = 1$. Because the function changes sign between these two poles, we are guaranteed that a root exists in the range $-1/(N-1) < \gamma < 1$ and the root is said to be “bracketed”. Therefore a root-bracketing algorithm, such as Brent’s method, is guaranteed to succeed anywhere in parameter space.

In practice, we actually solve a related, but more convenient, equation in which the poles at either end of the bracket are removed. This related equation, which has the same roots within the bracketed interval, is simply Eq. (8.18) multiplied by the denominator in the left term:

$$\gamma_\infty (2 + (N-2)\gamma_\infty) + \bar{V}_0 \operatorname{sech}^2(\Theta_\infty) \Theta'_\infty (1 - \gamma_\infty)^{3/2} \sqrt{1 + (N-1)\gamma_\infty} = 0. \quad (8.19)$$

The lowest-order energy in the large- D limit is simply the effective potential evaluated at the symmetric minimum specified by \bar{r}_∞ and γ_∞ .

8.3 Perturbation series

Having numerically determined the large- D arrangement parameters \bar{r}_∞ and γ_∞ , we now apply the developed formalism to obtain a perturbation series for the DPT Hamiltonian of the BEC, as discussed for the general case in Section 3.5.

The perturbative expansion of the Hamiltonian in a binary invariant expansion is performed in general for any isotropic confined quantum system in Appendix D. In order to apply this result to a BEC, one must merely specify a scaling factor $\zeta(0)$ and a few derivatives. This is done in Section J.1. The result is a perturbative series of the DPT Hamiltonian to first anharmonic order in which the elements of the Hamiltonian coefficient tensors are resolved in the basis of binary invariant tensors.

As noted in Section 3.6, there are five distinct normal modes $\mathbf{0}+$ (with multiplicity 1), $\mathbf{0}-$ (with multiplicity 1), $\mathbf{1}+$ (with multiplicity $N-1$), $\mathbf{1}-$ (with multiplicity $N-1$), and $\mathbf{2}$ (with multiplicity $N(N-3)/2$). The frequencies for these normal modes for the case of a BEC are given in Eqs. (121)-(123) of Ref. (81). Having obtained the values of the DPT Hamiltonian elements for a BEC, and having calculated

the normal-mode frequencies, no further BEC-specific work must be performed. In order to calculate the ground-state energy, wavefunction, and density profile to first anharmonic order, one must simply use the results derived in general in the chapters of Part II.

8.4 Optimization

As is common with perturbative approaches, calculating each additional order becomes increasingly more complex. We make the most of the terms we have calculated by optimizing a fit to exact calculations which are available for low N ;

This optimization procedure is not an empirical fit to exact data. Even at the lowest order, the DPT perturbation expansion contains contributions from each term in the Hamiltonian, including pairwise interactions. Having “calibrated” the interaction potential in this way, one may increase the number of particles by orders of magnitude beyond the region where exact results are available and still obtain meaningful results.

8.4.1 Previous work

In Reference (53), Blume *et. al.* calculate the exact ground-state energy for an ^{87}Rb BEC with three different scattering lengths: the natural scattering length $a_0 = 0.00433a_{ho}$, an intermediate scattering length $a_0 = 0.0433a_{ho}$, and a strong scattering length $a_0 = 0.433a_{ho}$. Due to computational cost, results have been obtained for only a low number of atoms (in this case 100 atoms or less). A physical BEC can have millions of atoms. In References (82), McKinney *et. al.* calculated the ground-state energy for a BEC by optimizing the analytic DPT harmonic energy to the DMC calculation for low N , and then extrapolating N to many thousands. The results compared favorably with the Gross-Pitaevskii and modified Gross-Pitaevskii results.

Reference (53) also calculates the ground-state BEC density profile for $N = 3, 10$ for both the intermediate $a_0 = 0.0433a_{ho}$ case and for the strong $a_0 = 0.433a_{ho}$ case. The DMC benchmark data and the fitness function are discussed in Section J.2. The Thomas-Fermi estimate of the gas parameter for the three scattering lengths considered is given in Table 8.4.1. The gas parameter indicates that a BEC with $a_0 = 0.0433a_{ho}$ is in the $n(0)|a|^3 \leq 10^{-3}$ regime for up to around 1000 atoms, but $a_0 = 0.433a_{ho}$ has a gas parameter $n(0)|a|^3 \geq 10^{-2}$. Therefore we expect the mean-field results to be wholly inadequate for $a_0 = 0.433a_{ho}$.

In reference (90), Laing *et. al.* derive the harmonic-order DPT density profile and apply it to a BEC by optimizing to DMC energy and density profile for the intermediate $a_0 = 0.0433a_{ho}$ case.

8.5 Preliminary results

We apply the DPT formalism to calculate the ground-state energy and density profile for ^{87}Rb atoms in a BEC held in an isotropic (spherical) trap with trap frequency $\omega_{ho} = 2\pi \times 77.87$ Hz. The natural scattering length of ^{87}Rb , in harmonic oscillator units, is $a_0 = 0.00433 a_{ho}$ (where $a_{ho} = \sqrt{\hbar/(m\omega_{ho})}$). Such a ^{87}Rb BEC is described well by a mean-field approximation to the interparticle interactions. We are interested in the regime of intermediate ($a_0 = 0.0433 a_{ho}$) and strong ($a_0 = 0.433 a_{ho}$) interactions where the gas parameter $n(0)|a|$ is in the region of 10^{-3} or larger, where the mean-field approximation breaks down.

Since we are extending the harmonic-order work of McKinney *et. al.*, we revisit the results of Reference (82) here, examining the behavior of the recently calculated DPT harmonic and first-anharmonic-order density profiles using parameters previously obtained by optimizing only the DPT harmonic order energy to DMC data.

8.5.1 Intermediate interaction

An optimization of the harmonic-order DPT energy to the DMC data for energies up to $N = 100$ yields $\{\bar{V}_0, \alpha, \bar{c}_0, \bar{c}_1\} = \{0.6484, -0.8392, 1.387, 0.0888\}$, with a reduced $\chi^2 = 0.0024^2$. This set of parameters was obtained by performing an optimization in *Mathematica* over the intervals $[\cdot 02, 2]$, $[-2, 1]$, $[0.3, 3]$, $[-.1, .1]$ for $\bar{V}_0, \bar{\alpha}, \bar{c}_0, \bar{c}_1$, respectively. Both the simulated annealing and differential evolution algorithms were used, obtaining the same result³.

This is close to the result related in Reference (82). The additional energy per atom due to interaction (that is, the energy minus the ideal gas energy $3/2N$) is plotted in Figure 8.2. The GP and MGP energies in this and all other figures in

²One expects a reduced χ^2 value near one: a very small reduced χ^2 indicates overfitting. This result suggests that either the uncertainty information in the DMC results has been overestimated or the interparticle potential should be written in terms of fewer parameters.

³Random search takes much longer and since the other two methods converged to the same point it was not attempted.

N	$a = 0.00433a_{\text{ho}}$	$a = 0.0433a_{\text{ho}}$	$a = 0.433a_{\text{ho}}$
3	$4. \times 10^{-7}$	$1. \times 10^{-4}$	$2. \times 10^{-2}$
10	$6. \times 10^{-7}$	$2. \times 10^{-4}$	$4. \times 10^{-2}$
25	$9. \times 10^{-7}$	$2. \times 10^{-4}$	$6. \times 10^{-2}$
50	$1. \times 10^{-6}$	$3. \times 10^{-4}$	$8. \times 10^{-2}$
100	$2. \times 10^{-6}$	$4. \times 10^{-4}$	$1. \times 10^{-1}$
1000	$4. \times 10^{-6}$	$1. \times 10^{-3}$	$2. \times 10^{-1}$
10000	$1. \times 10^{-5}$	$2. \times 10^{-3}$	$6. \times 10^{-1}$

Table 8.1: The Thomas-Fermi estimate of the gas parameter $n(0)|a|^3$ for three scattering lengths. The scattering length $a = 0.433a_{\text{ho}}$ has a gas parameter that is beyond the dilute limit.

this section are from Ref. (82). The GP ground-state energy is known to underestimate the ground-state energy, and the MGP ground-state energy is known to over-estimate. As first observed in Ref. (82), the DPT ground-state energy for the case of intermediate-strength interactions remains between the GP and MGP energies up to around $N = 500$ –5 times higher in N than the benchmark data used to optimize the energy.

Although these parameters were obtained without the benefit of also optimizing the DPT density profile to the DMC data, it is interesting to observe whether the density profiles corresponding to these parameters are reasonable. In Figure 8.3 the harmonic-order density profiles for $N = 3$ and $N = 10$ are close to the DMC profile—and the first-anharmonic-order profiles are even closer. Is this a coincidence?

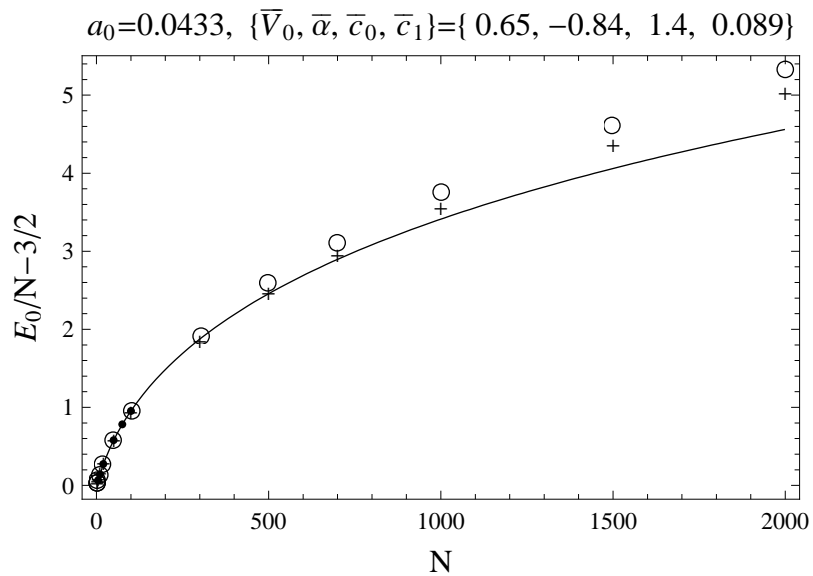


Figure 8.2: The ground-state energy/atom for a BEC of ^{87}Rb atoms with $a_0 = 0.0433 a_{\text{ho}}$. The plus signs represent GP energies and the circles represent MGP energies. The parameters $\{\bar{V}_0, \alpha, \bar{c}_0, \bar{c}_1\}$ were obtained by optimizing the harmonic-order DPT energy to DMC data for $N \leq 100$.

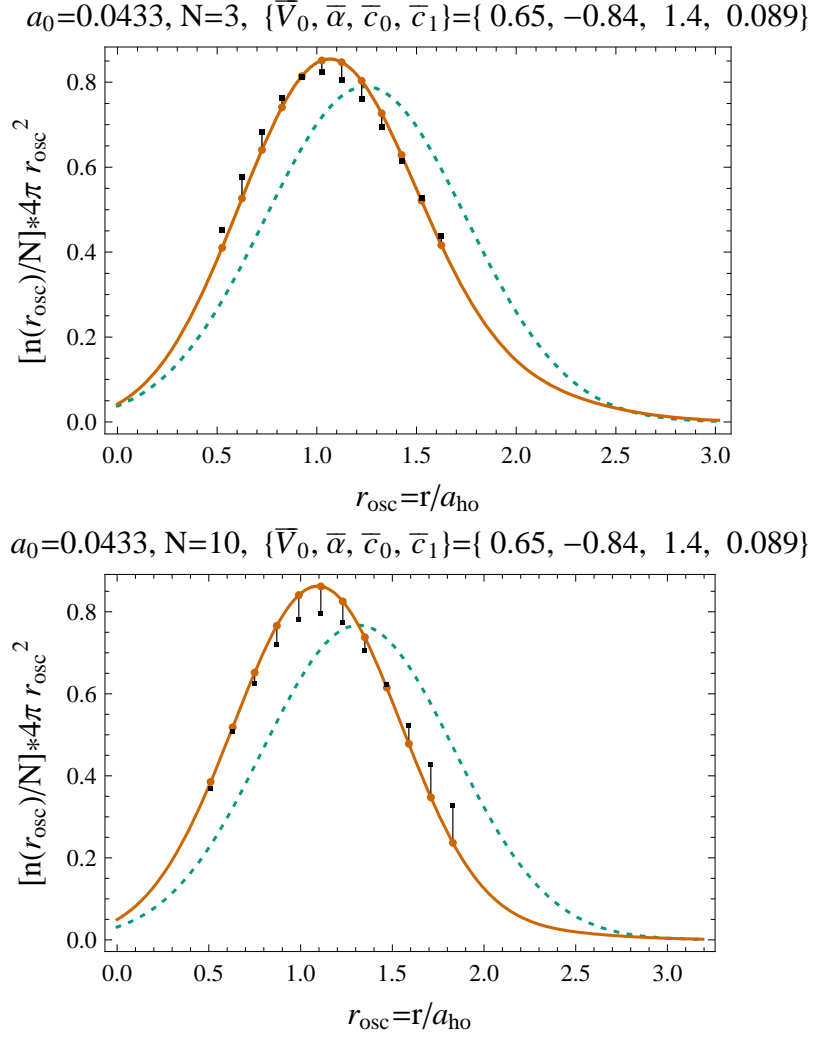


Figure 8.3: Jacobian-weighted probability density profile for a BEC of three (above) and ten (below) ^{87}Rb atoms ($a_0 = 0.0433 a_{\text{ho}}$) in the ground state. The harmonic-order profile is dashed, the first-anharmonic-order profile is solid, and the DMC data are solid circles. Vertical bars denote the difference between the first-anharmonic DPT profile and the DMC data. The parameters were obtained by optimizing to the harmonic energy only. Note the qualitative improvement in the anharmonic density profile compared to the harmonic.

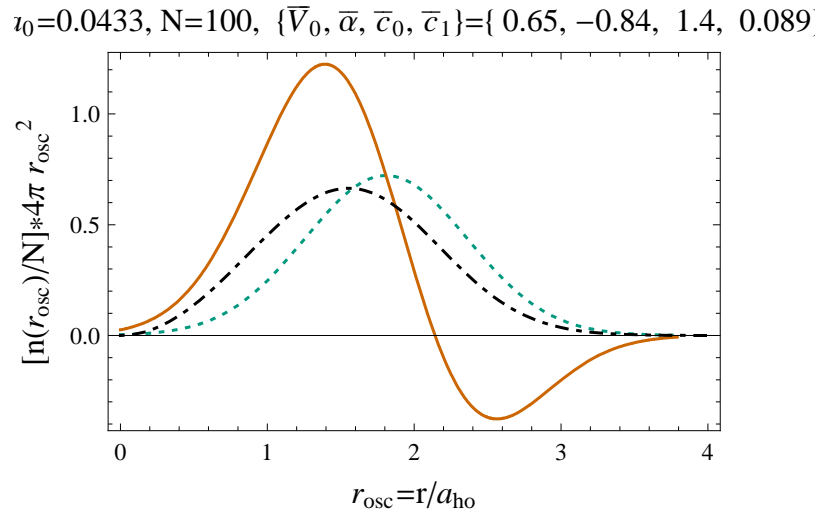


Figure 8.4: Jacobian-weighted probability density profile for a BEC of 100 ^{87}Rb atoms ($a_0 = 0.0433 a_{\text{ho}}$) in the ground state. The harmonic-order profile is a dashed line, the first-anharmonic-order density profile is a solid line. The black dash-dot line corresponds to the MGP density profiles. The parameters were obtained by optimizing the harmonic-order DPT energy only.

8.5.2 Strong interaction strength

An optimization of the harmonic-order DPT energy to the DMC data yields $\{\bar{V}_0, \bar{\alpha}, \bar{c}_0, \bar{c}_1\} = \{4.617 * 10^7, -4.212, 1.555, 0.005\}$, with a reduced $\chi^2 = 0.12$. This result is obtained in *Mathematica* by scanning $\bar{V}_0, \bar{\alpha}, \bar{c}_0, \bar{c}_1$ over an interval tightly centered around the result reported in (82). An expanded search over $[\cdot 02, 2], [-2, 1], [0.3, 3]$, and $[-.1, .1]$ for the parameters $\bar{V}_0, \bar{\alpha}, \bar{c}_0, \bar{c}_1$, respectively, yields a minimum at $\{\bar{V}_0, \bar{\alpha}, \bar{c}_0, \bar{c}_1\} = \{92.08, -0.2209, 1.63, 0.01679\}$ with a reduced χ^2 value of 1.3. It is the latter results that we discuss here. This point in parameter space has a value of \bar{V}_0 that is far outside the original search space. That \bar{V}_0 tends to be so large and $\bar{\alpha}$ tends to be negative causes the center of the tanh function to be shifted out of the physical, positive \bar{r}_{ij} region and suggests that a different way to parametrize the interaction potential might be warranted.

The ground-state energy for these parameters extrapolates well to very large N (40 times larger than the largest N benchmark data), as seen in Figure 8.5.

In contrast to the case of intermediate interactions, where parameters determined from an energy optimization only also yield a qualitatively correct density profile, the density profile for these parameters in Figure 8.6 is not as close to the DMC data. Notice, however, that the first-anharmonic correction is moving in the right direction. It remains to be seen if including the neglected Δ^2 term in the density profile (Eq. (6.27)) will yield a significant improvement.

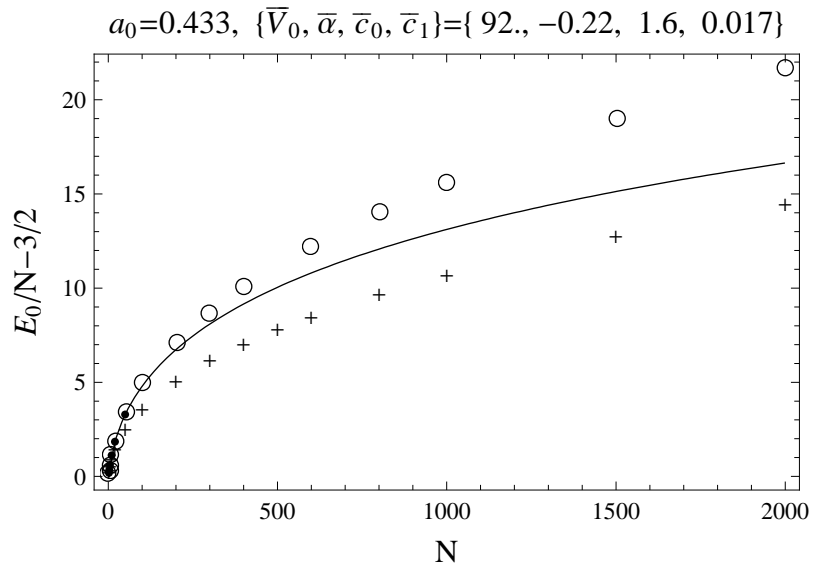


Figure 8.5: The ground-state energy/atom for a BEC of ^{87}Rb atoms with $a_0 = 0.433 a_{\text{ho}}$. The plus signs represent GP energies and the circles represent MGP energies. The parameters were obtained by optimizing the harmonic-order DPT energy only.

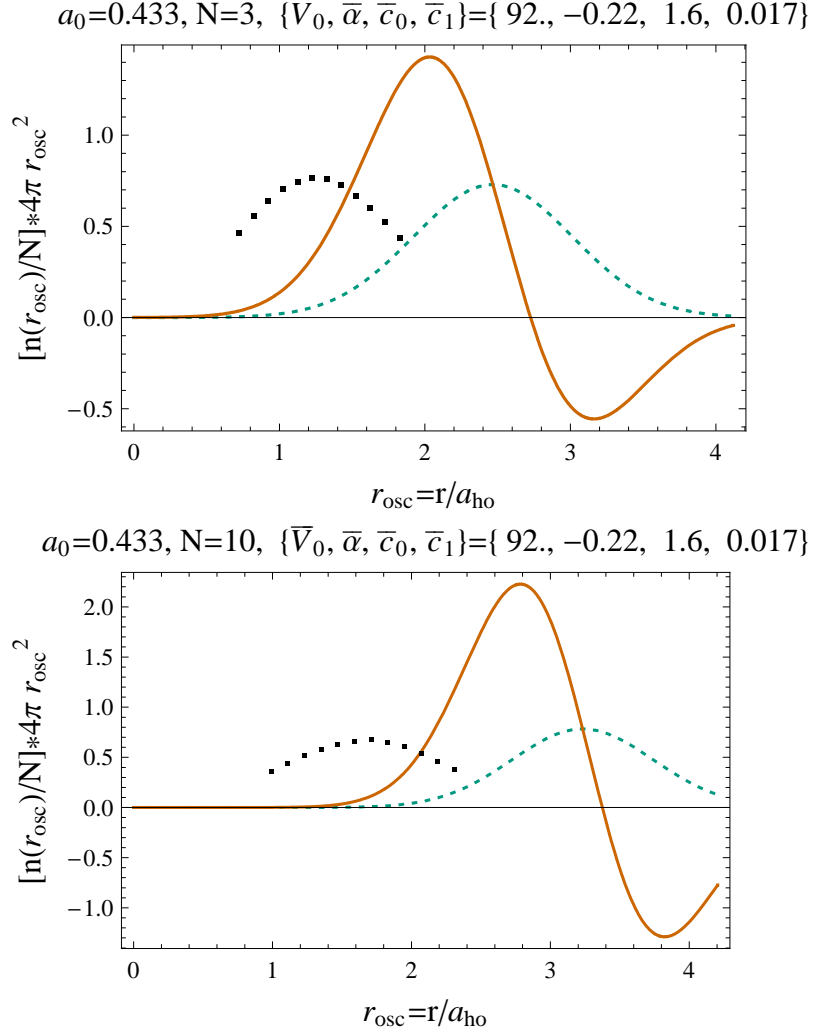


Figure 8.6: Jacobian-weighted probability density profile for a BEC of three (above) and ten (below) ^{87}Rb atoms ($a_0 = 0.433 a_{\text{ho}}$) in the ground state. The harmonic-order profile is a dashed line, the first-anharmonic-order density profile is a solid line, and the DMC data are solid circles. Vertical bars denote the difference between the first-anharmonic DPT density profile and the DMC data. The parameters were obtained by optimizing the harmonic-order DPT energy only.

8.6 Conclusions we can draw at this stage

These results indicate that the next step for this project is to calculate the Δ^2 term contribution to the density profile in Eq. (6.27). The necessary machinery is contained within this thesis and this work is already in progress (see Appendix H).

These results indicate that it is not possible to optimize the first-anharmonic-order density profile as long as the Δ^2 term is neglected in Eq. (6.27). This alone is a result which indicates what our group should do next. Including this extra term will guarantee that the DPT density profile will be positive definite, and should improve the comparison with exact DMC calculations. The N -body density profile contains information about the quantum system and adding this term to the first-anharmonic-order density profile and optimizing to both the exact ground-state energy and density profile will change the optimized potential parameters and therefore the extrapolations in N for the ground-state energy and density profile.

In References (62; 20), it was shown that for a sufficiently large value of the gas parameter $n(0)|a|^3$, the trapped BEC density profile develops “wiggles”, which represent correlations. A physical picture is that the atoms are modeled as hard-spheres, and as the hard-sphere radius approaches the scale of the width of the trap, the spheres become packed in a structure. The density profile with the Δ term is of the form of a sixth-order polynomial multiplied by a Gaussian function. Such a function has the flexibility to reproduce such “wiggles”.

The *tanh* potential used here exhibits correlations in the parameters, indicating that the parameters are not entirely “orthogonal”. Also, an examination of the optimal parameters obtained reveals that in most cases the physical part of the potential (positive interparticle spacing) contains only the tail of the *tanh* function. These results suggest that an alternative way to parameterize the hard-sphere potential or a different kind of interparticle potential is warranted.

Part IV

Epilogue

Chapter 9

Looking back... and looking forward

9.1 Summary of contributions

In this thesis, we have calculated the harmonic-order density profile (105; 90), and the first-anharmonic-order N -body wavefunction (100; 104) and density profile (103). We have generalized the harmonic-order N -body DPT method for an isotropically confined quantum system of identical interacting bosons to first anharmonic order and, in principle, higher orders. We have introduced a graphical decomposition of the perturbative expansion of the N -body Hamiltonian. We have derived the Clebsch-Gordan coefficient tensors that couple together three irreducible representations of S_N analytically, and analytically transformed the graphical basis to collective coordinates. We have calculated the N -body wavefunction and density profile in general and have demonstrated agreement with an analytic model, the fully-interacting Hooke's-law gas. We have begun the application of this formalism to the example of a cold gas BEC (with zero angular momentum), calculating the ground-state energy, wavefunction, and density profile. The next step is to derive the higher-order contribution to the first-anharmonic-order density profile.

This thesis addressed two questions:

1. Can the harmonic-order DPT method be extended to first anharmonic order and, in principle, higher to address large- N , strongly interacting, and highly correlated systems?
2. What improvement in the DPT-calculated BEC density profile is obtained by adding the first anharmonic order correction?

The first question has been answered definitively, as evidenced by the formalism developed in this paper in which the N -body wavefunction and density profile are

derived analytically and the ground-state energy calculated. The method developed here has a straightforward application to higher orders, and the difficulty of calculating the Clebsch-Gordon coefficients will be the most significant challenge.

As seen in the comparison to the exactly soluble “Hookes law” model, the first-anharmonic-order density profile shows qualitative improvement over the harmonic order density profile.

9.2 Future research

This dissertation project has opened the door to several lines of inquiry, most of which would be an excellent introductory project for a new graduate student.

The immediate next step is to derive the Δ^2 term in the density profile to obtain a density profile that is positive definite. The major challenges in this derivation will involve combinatorics of the indices of up to rank-six tensors, as well as contractions of the S_N Clebsch-Gordon coefficients (some of which have a unwieldy closed-form expression). This task is feasible within the existing framework and by using a computer algebra system such as *Mathematica* with the discrete summation package by Laing *et al.* (106). It is expected that with the inclusion of the Δ^2 term, the density profile can be better optimized to the benchmark data and will yield improved extrapolations that will provide new physical insight into a BEC in an isotropic trap in the large-gas parameter regime. This derivation is both narrowly defined and requires the development of necessary tensor algebra and symbolic calculation skills.

Upon successful application to the BEC in an isotropic trap, it would be a modest extension to generalize this work to a system in a cylindrical trap. Most BEC experiments are performed in a cylindrical trap. This has already been done at harmonic order by Laing *et al.* (88; 91). This generalization would only involve introducing distinguishable graph edges to distinguish between loop graphs \circlearrowleft for a radial and for an axial coordinate, as well as the calculation of the derivatives of the effective potential in the F tensors. It turns out that only one binary invariant $B(\circlearrowleft \circlearrowleft)$ will require refinement using distinguishable edges.

Another possibility is to change the interparticle potential we have used for the case of a BEC. One could simply formulate an alternative to the tanh “soft-sphere” potential or use an interparticle potential that has an energy-dependent scattering length (70; 71) or has a shape (76) (perhaps even bound-states) when $D = 3$.

We have focused on the ground-state of the BEC with zero angular momentum, but excited states could also be considered, as well as higher angular momentum states. Dunn *et al.* (85) have applied DPT to systems with very high angular momentum. A BEC with non-zero angular momentum manifests quantized vortex states.

We can also calculate the frequencies of the collective motions that result from our method. It is not yet clear what the correspondence is between these collective motions and the experimentally-observed frequencies.

This dissertation has generalized a harmonic-order N -body DPT approach in References (82; 81; 87; 90) to first anharmonic order and, in principle, higher orders. The focus has been on formalism development and verification. In the next phase of research, there are many applications possible at first anharmonic order. These should be explored before going to higher anharmonic orders.

Bibliography

- [1] P. Atkins and R. Friedman, New York (1983).
- [2] S. Bose, Z. Phys. **26**, 178 (1924).
- [3] C. Pethick and H. Smith, (2002).
- [4] A. Einstein, Sitz. Ber. Preussischen Akad. Wiss. Phys. Math. Kl. , 261 (1924).
- [5] A. Einstein, Sitz. Ber. Preussischen Akad. Wiss. Phys. Math. Kl. , 263 (1924).
- [6] M. H. Anderson, J. R. Ensher, M. R. Matthews, C. E. Wieman, and E. A. Cornell, Science **269**, 198 (1995).
- [7] C. C. Bradley, C. A. Sackett, J. J. Tollett, and R. G. Hulet, Phys. Rev. Lett. **75**, 1687 (1995).
- [8] K. B. Davis et al., Phys. Rev. Lett. **75**, 3969 (1995).
- [9] S. Chu, Rev. Mod. Phys. **70**, 685 (1998).
- [10] C. N. Cohen-Tannoudji, Rev. Mod. Phys. **70**, 707 (1998).
- [11] W. D. Phillips, Rev. Mod. Phys. **70**, 721 (1998).
- [12] M. R. Andrews et al., Science **275**, 637 (1997).
- [13] D. M. Harber, J. M. Obrecht, J. M. McGuirk, and E. A. Cornell, Phys. Rev. A **72**, 033610 (2005).
- [14] A. J. Leggett, Rev. Mod. Phys. **73**, 307 (2001).
- [15] J. O. Andersen, Rev. Mod. Phys. **76**, 599 (2004).
- [16] N. P. Proukakis and B. Jackson, J. Phys. B: At., Mol. Opt. Phys. **41**, 203002 (66pp) (2008).
- [17] F. Dalfovo, S. Giorgini, L. P. Pitaevskii, and S. Stringari, Rev. Mod. Phys. **71**, 463 (1999).
- [18] R. Ozeri, N. Katz, J. Steinhauer, and N. Davidson, Reviews of Modern Physics **77**, 187 (2005).

- [19] S. L. Cornish, N. R. Claussen, J. L. Roberts, E. A. Cornell, and C. E. Wieman, *Phys. Rev. Lett.* **85**, 1795 (2000).
- [20] J. L. DuBois and H. R. Glyde, *Phys. Rev. A* **68**, 033602 (2003).
- [21] M. Greiner, O. Mandel, T. Esslinger, T. Hänsch, and I. Bloch, *Nature* **415**, 39 (2002).
- [22] I. Bloch, J. Dalibard, and W. Zwerger, *Reviews of Modern Physics* **80**, 885 (2008).
- [23] O. Morsch and M. Oberthaler, *Reviews of Modern Physics* **78**, 179 (2006).
- [24] Y. Liu, M. Christandl, and F. Verstraete, *Phys. Rev. Lett.* **98**, 110503 (2007).
- [25] A. Montana, *Phys. Rev. A* **77**, 22104 (2008).
- [26] E. Braaten and A. Nieto, *Phys. Rev. B* **56**, 14745 (1997).
- [27] A. Banerjee and M. P. Singh, *Phys. Rev. A* **64**, 063604 (2001).
- [28] G. S. Nunes, *J. Phys. B: At., Mol. Opt. Phys.* **32**, 4293 (1999).
- [29] H. Fu, Y. Wang, and B. Gao, *Phys. Rev. A* **67**, 053612 (2003).
- [30] E. Timmermans, P. Tommasini, and K. Huang, *Phys. Rev. A* **55**, 3645 (1997).
- [31] M. Gupta and K. R. Dastidar, *Journal of Physics: Conference Series* **80**, 012038 (14pp) (2007).
- [32] M. Gupta and K. R. Dastidar, *J. Phys. B: At., Mol. Opt. Phys.* **41**, 195302 (8pp) (2008).
- [33] A. Fabrocini and A. Polls, *Phys. Rev. A* **60**, 2319 (1999).
- [34] A. Fabrocini and A. Polls, *Phys. Rev. A* **64**, 063610 (2001).
- [35] B. D. Esry, *Phys. Rev. A* **55**, 1147 (1997).
- [36] D. Masiello, S. McKagan, and W. Reinhardt, *Phys. Rev. A* **72**, 63624 (2005).
- [37] T. Vanska, D. Sundholm, and M. Lindberg, *Phys. Rev. A* **75**, 023621 (2007).
- [38] L. S. Cederbaum, O. E. Alon, and A. I. Streltsov, *Phys. Rev. A* **73**, 043609 (2006).
- [39] R. J. Bartlett and M. Musial, *Reviews of Modern Physics* **79**, 291 (2007).
- [40] F. Mazzanti, A. Polls, and A. Fabrocini, *Phys. Rev. A* **67**, 063615 (2003).
- [41] S. Fantoni and A. Fabrocini, page 119, Springer-Verlag, 1998.
- [42] M. Thogersen, D. V. Fedorov, and A. S. Jensen, *EPL (Europhysics Letters)* **79**, 40002 (6pp) (2007).

- [43] B. I. Schneider and D. L. Feder, *Phys. Rev. A* **59**, 2232 (1999).
- [44] B. I. Schneider, L. A. Collins, and S. X. Hu, *Phys. Rev. E* **73**, 036708 (2006).
- [45] J. L. Bohn, B. D. Esry, and C. H. Greene, *Phys. Rev. A* **58**, 584 (1998).
- [46] Y. Smirnov and K. Shitikova, *Sov. J. Particles Nucl.(Engl. Transl* **8** (1977).
- [47] O. Sørensen, D. V. Fedorov, and A. S. Jensen, *Phys. Rev. A* **66**, 032507 (2002).
- [48] O. Sørensen, D. V. Fedorov, and A. S. Jensen, *Phys. Rev. Lett.* **89**, 173002 (2002).
- [49] O. Sorensen, D. V. Fedorov, and A. S. Jensen, *J. Phys. B: At., Mol. Opt. Phys.* **37**, 93 (2004).
- [50] T. Sogo, O. Sorensen, A. S. Jensen, and D. V. Fedorov, *EPL (Europhysics Letters)* **69**, 732 (2005).
- [51] A. Rajabi, *Few-Body Systems* **37**, 197 (2005).
- [52] T. K. Das and B. Chakrabarti, *Phys. Rev. A* **70**, 063601 (2004).
- [53] D. Blume and C. H. Greene, *Phys. Rev. A* **63**, 63061 (2001).
- [54] A. Kundu, B. Chakrabarti, T. K. Das, and S. Canuto, *J. Phys. B: At., Mol. Opt. Phys.* **40**, 2225 (2007).
- [55] C. C. Bradley, C. A. Sackett, and R. G. Hulet, *Phys. Rev. Lett.* **78**, 985 (1997).
- [56] J. L. Roberts et al., *Phys. Rev. Lett.* **86**, 4211 (2001).
- [57] D. Landau and K. Binder, *A Guide to Monte-Carlo Simulations in Statistical Physics*, Cambridge University Press, Cambridge, 2001.
- [58] B. Hammond, W. Lester, and P. Reynolds, (1994).
- [59] W. Krauth, *Phys. Rev. Lett.* **77**, 3695 (1996).
- [60] M. Holzmann and Y. Castin, *The European Physical Journal D - Atomic, Molecular, Optical and Plasma Physics* **7**, 425 (1999).
- [61] S. Giorgini, J. Boronat, and J. Casulleras, *Phys. Rev. A* **60**, 5129 (1999).
- [62] J. L. DuBois and H. R. Glyde, *Phys. Rev. A* **63**, 023602 (2001).
- [63] A. R. Sakhel, J. L. DuBois, and H. R. Glyde, *Phys. Rev. A* **66**, 063610 (2002).
- [64] J. K. Nilsen, J. Mur-Petit, M. Guilleumas, M. Hjorth-Jensen, and A. Polls, *Phys. Rev. A* **71**, 053610 (2005).
- [65] J. O. Andersen and E. Braaten, *Phys. Rev. A* **60**, 2330 (1999).

- [66] W. Purwanto and S. Zhang, Phys. Rev. A **72**, 053610 (2005).
- [67] W. Purwanto and S. Zhang, Phys. Rev. E **70**, 056702 (2004).
- [68] T. D. Lee, K. Huang, and C. N. Yang, Phys. Rev. **106**, 1135 (1957).
- [69] E. Tiesinga, C. J. Williams, F. H. Mies, and P. S. Julienne, Phys. Rev. A **61**, 063416 (2000).
- [70] D. Blume and C. H. Greene, Phys. Rev. A **65**, 043613 (2002).
- [71] E. L. Bolda, E. Tiesinga, and P. S. Julienne, Phys. Rev. A **66**, 013403 (2002).
- [72] B. D. Esry and C. H. Greene, Phys. Rev. A **60**, 1451 (1999).
- [73] D. M. Ceperley and B. J. Alder, Phys. Rev. Lett. **45**, 566 (1980).
- [74] P. J. Reynolds, D. M. Ceperley, B. J. Alder, and W. A. Lester, The Journal of Chemical Physics **77**, 5593 (1982).
- [75] A. Collin, P. Massignan, and C. J. Pethick, Phys. Rev. A **75**, 013615 (2007).
- [76] R. M. Kalas and D. Blume, Phys. Rev. A **77**, 032703 (2008).
- [77] C. Bender and S. Orszag, *Advanced Mathematical Methods for Scientists and Engineers I*, Springer Verlag, 1999.
- [78] G. Dunne, Arxiv preprint hep-th/0207046 .
- [79] D. Herschbach, J. Avery, and O. Goscinski, editors, *Dimensional Scaling in Chemical Physics*, Dordrecht, 1992, Kluwer.
- [80] A. Chatterjee, Physics Reports **186** (1990).
- [81] B. McKinney, M. Dunn, D. Watson, and J. Loeser, Annals of Physics **310**, 56 (2003).
- [82] B. McKinney, M. Dunn, and D. Watson, Phys. Rev. A **69**, 053611 (2004).
- [83] M. Dunn et al., J. Chem. Phys. **101**, 5987 (1994).
- [84] E. Witten, Physics Today **33**, 38 (1980).
- [85] M. Dunn and D. Watson, Annals of Physics **251**, 266 (1996).
- [86] J. G. Loeser, The Journal of Chemical Physics **86**, 5635 (1987).
- [87] M. Dunn, D. Watson, and J. Loeser, Annals of Physics **321**, 1939 (2006).
- [88] W. Laing, M. Dunn, and D. Watson, Derivation of the ground-state energy of a bec in an anisotropic trap.
- [89] D. Blume, private communication (2004).

- [90] W. B. Laing, M. Dunn, and D. K. Watson, *Phys. Rev. A* **74**, 063605 (2006).
- [91] W. Laing, M. Dunn, and D. Watson, Derivation of the ground-state density profile of a bec in an anisotropic trap.
- [92] J. Avery, D. Z. Goodson, and D. R. Herschbach, *Theor. Chim. Acta* **77**, 1 (1991).
- [93] Z. Zhen and J. Loeser, Dimensional scaling in chemical physics, page 90, Dordrecht, 1992, Kluwer.
- [94] S. T. Rittenhouse, M. J. Cavagnero, J. von Stecher, and C. H. Greene, *Phys. Rev. A* **74**, 053624 (2006).
- [95] M. Hamermesh, *Group Theory and its Application to Physical Problems*, Addison-Wesley.
- [96] E. Wilson, J. Decius, and P. Cross, *Molecular Vibrations: The Theory of Infrared and Raman Vibrational Spectra*, Courier Dover Publications, 1980.
- [97] D. Kelle, Binary invariants are a basis, 2008.
- [98] J. L. Gross and J. Yellen, editors, *Handbook of Graph Theory*, CRC Press, Boca Raton, 2004.
- [99] E. Wilson, J. Decius, and P. Cross, *Molecular Vibrations: The Theory of Infrared and Raman Vibrational Spectra*, chapter Appendix XII, In (96), 1980.
- [100] W. Laing, M. Dunn, and D. Watson, *J. Math. Phys.* , submitted.
- [101] Wolfram Research, MATHEMATICA edition: Version 6.0, 2007.
- [102] W. Laing, M. Dunn, and D. Watson, The MATHEMATICA package for the Clebsch-Gordon coefficients is generated from the notebook SNClebschGordon.nb, available at <http://www.nhn.ou.edu/~watson/nbodydpt>.
- [103] W. B. Laing, M. Dunn, and D. K. Watson, (in preparation) .
- [104] W. B. Laing, D. W. Kelle, M. Dunn, and D. K. Watson, (2008).
- [105] W. B. Laing, M. Dunn, J. G. Loeser, and D. K. Watson, Arxiv preprint physics/0510177 (2005).
- [106] W. Laing, M. Dunn, and D. Watson, The MATHEMATICA package for the evaluating summations of Kronecker delta and step functions is generated from the notebook SumDeltaStep.nb, available at <http://www.nhn.ou.edu/~watson/nbodydpt>.
- [107] D. Toth, A *Mathematica* package for evaluating internal coordinate derivatives, 2006.
- [108] P. R. Bevington and D. K. Robinson, *Data reduction and error analysis for the physical sciences*, McGraw-Hill, 1992.

Appendix A

Three-body dimensional perturbation theory

The amount, structure, and detail of the tensor formalism developed in this thesis can be challenging. In this appendix, we provide an explicit development for the N -dependent portion of DPT for the $N = 3$ case through the transformation to symmetry coordinates. Once this transformation is made using binary invariants and Clebsch-Gordon coefficients, the N -dependence of the problem has been tamed.

This appendix is intended to be a “pull-out” guide to aid the reader through the chapters in the thesis, providing both specific examples which could have been littered throughout the thesis but, being in one place, also provide a panoramic view. To this end, the section/subsection numbers in this appendix will be altered (without apology) to match the chapter/section numbers of the corresponding general case in the thesis. Rather than repeat explanatory remarks the reader is referred to the main body for a more detailed discussion.

A.3 3-body dimensional perturbation theory

A.3.3 Three bodies in higher dimensions

In this section, we perform the first two steps of any dimensional scaling procedure for 3 particles. We consider a system of 3 identical particles confined by a spherically-symmetric potential and interacting via a two-body potential g_{ij} . The D -dimensional Schrödinger equation in Cartesian coordinates is

$$\bar{H}\Psi = [h_1 + h_2 + h_3 + g_{12} + g_{13} + g_{23}] \Psi = E\Psi, \quad (\text{A.1})$$

where

$$h_i = -\frac{\hbar^2}{2m_i} \sum_{\nu=1}^D \frac{\partial^2}{\partial x_{i\nu}^2} + V_{\text{conf}} \left(\sqrt{\sum_{\nu=1}^D x_{i\nu}^2} \right) \quad (\text{A.2})$$

and

$$g_{ij} = V_{\text{int}} \left(\sqrt{\sum_{\nu=1}^D (x_{i\nu} - x_{j\nu})^2} \right) \quad (\text{A.3})$$

are the single-particle Hamiltonian and the two-body interaction potential, respectively. The operator \bar{H} is the D -dimensional Hamiltonian, and $x_{i\nu}$ is the ν^{th} Cartesian

component of the i^{th} particle. V_{conf} is an external confining potential and V_{int} is the two-body interaction potential.

For $N = 3$, there are only six internal coordinates: $\{r_1, r_2, r_3, \gamma_{12}, \gamma_{13}, \gamma_{23}\}$. The three particles define a (two-dimensional) plane in some higher-dimensional space.

We transform the Hamiltonian to internal coordinates, following the derivation in Ref. (81) and restricting our attention to $L = 0$:

$$H \Phi = E \Phi \quad (\text{A.4})$$

where

$$H = \sum_{i=1}^3 \left\{ -\frac{\hbar^2}{2m_i} \left(\frac{\partial^2}{\partial r_i^2} + \frac{D-1}{r_i} \frac{\partial}{\partial r_i} + \sum_{j \neq i} \sum_{k \neq i} \frac{\gamma_{jk} - \gamma_{ij}\gamma_{ik}}{r_i^2} \frac{\partial^2}{\partial \gamma_{ij} \partial \gamma_{ik}} - \frac{D-1}{r_i^2} \sum_{j \neq i} \gamma_{ij} \frac{\partial}{\partial \gamma_{ij}} \right) + V_{\text{conf}}(r_i) \right\} + \sum_{i=1}^2 \sum_{j=i+1}^3 V_{\text{int}}(r_{ij}) \quad (\text{A.5})$$

We perform a similarity transformation on the above Schrödinger equation (A.4) so that integrals will have a weight function of unity. The result is a kinetic operator of the form of a second-order derivative kinetic term plus an centrifugal-like repulsive term.

We use the transformation that Avery *et al.* (92) called case (i), in which a first derivative of an internal coordinate is the conjugate momentum to that coordinate,

$$\chi = J^{-\frac{1}{2}}, \quad (\text{A.6})$$

where (for $N = 3$)

$$J = (r_1 r_2 r_3)^{(D-1)} \Gamma^{(D-4)/2}. \quad (\text{A.7})$$

and by which the similarity-transformed Schrödinger equation Eq. (A.8)

$$(T + V) \Phi = E \Phi \quad (\text{A.8})$$

is

$$\begin{aligned} T &= \hbar^2 \sum_{i=1}^3 \left[-\frac{1}{2m_i} \frac{\partial^2}{\partial r_i^2} - \frac{1}{2m_i r_i^2} \left(\sum_{j \neq i} \sum_{k \neq i} (\gamma_{jk} - \gamma_{ij}\gamma_{ik}) \frac{\partial^2}{\partial \gamma_{ij} \partial \gamma_{ik}} - 3 \sum_{j \neq i} \gamma_{ij} \frac{\partial}{\partial \gamma_{ij}} \right) \right. \\ &\quad \left. + \frac{3 + (D-4)^2 \left(\frac{\Gamma^{(i)}}{\Gamma} \right)}{8m_i r_i^2} \right] \\ &= \hbar^2 \sum_{i=1}^3 \left[-\frac{1}{2m_i} \frac{\partial^2}{\partial r_i^2} - \frac{1}{2m_i r_i^2} \sum_{j \neq i} \sum_{k \neq i} \frac{\partial}{\partial \gamma_{ij}} (\gamma_{jk} - \gamma_{ij}\gamma_{ik}) \frac{\partial}{\partial \gamma_{ik}} \right. \\ &\quad \left. + \frac{3 + (D-4)^2 \left(\frac{\Gamma^{(i)}}{\Gamma} \right)}{8m_i r_i^2} \right]. \end{aligned} \quad (\text{A.9})$$

In the above equation, Γ is the Grammian determinant (see Appendix D in Reference (81)),

$$\begin{aligned}
\Gamma &= \begin{vmatrix} 1 & \gamma_{12} & \gamma_{13} \\ \gamma_{12} & 1 & \gamma_{23} \\ \gamma_{13} & \gamma_{23} & 1 \end{vmatrix} \\
&= 1 - \gamma_{12}^2 - \gamma_{13}^2 - \gamma_{23}^2 + 2\gamma_{12}\gamma_{13}\gamma_{23},
\end{aligned} \tag{A.10}$$

and $\Gamma^{(i)}$ is the determinant with row and column i removed,

$$\begin{aligned}
\Gamma^{(1)} &= \begin{vmatrix} 1 & \gamma_{23} \\ \gamma_{23} & 1 \end{vmatrix} = 1 - \gamma_{23}^2 \\
\Gamma^{(2)} &= \begin{vmatrix} 1 & \gamma_{13} \\ \gamma_{13} & 1 \end{vmatrix} = 1 - \gamma_{13}^2 \\
\Gamma^{(3)} &= \begin{vmatrix} 1 & \gamma_{12} \\ \gamma_{12} & 1 \end{vmatrix} = 1 - \gamma_{12}^2.
\end{aligned} \tag{A.11}$$

A.3.4 The large-dimension limit

Following Ref. (81), we regularize the large- D limit of the Schrödinger equation by defining the dimensionally scaled variables

$$\bar{r}_i = r_i/\kappa(D), \quad \bar{E} = \kappa(D) E, \quad \text{and} \quad \bar{H} = \kappa(D) H, \tag{A.12}$$

where $\kappa(D)$ is the dimension-dependent scale factor which regularizes the large- D limit. The actual choice of $\kappa(D)$ depends on the physical system.

The kinetic energy T in Equation (A.9) scales in the same way as $1/r^2$, so the dimensionally-scaled Schrödinger equation is

$$\bar{H}\Phi = \left(\frac{1}{\kappa(D)}\bar{T} + \bar{U} + \bar{V} \right) \Phi = \bar{E}\Phi, \tag{A.13a}$$

where

$$\bar{T} = \hbar^2 \sum_{i=1}^3 \left(-\frac{1}{2m_i} \frac{\partial^2}{\partial \bar{r}_i^2} - \frac{1}{2m_i \bar{r}_i^2} \sum_{j \neq i} \sum_{k \neq i} \frac{\partial}{\partial \gamma_{ij}} (\gamma_{jk} - \gamma_{ij}\gamma_{ik}) \frac{\partial}{\partial \gamma_{ik}} \right), \tag{A.13b}$$

$$\bar{U} = \hbar^2 \sum_{i=1}^3 \frac{1}{\kappa(D)} \left(\frac{3 + (D-4)^2 \left(\frac{\Gamma^{(i)}}{\Gamma} \right)}{8m_i \bar{r}_i^2} \right), \tag{A.13c}$$

$$\bar{V} = \sum_{i=1}^3 \bar{V}_{\text{conf}}(\bar{r}_i) + \sum_{i=1}^2 \sum_{j=i+1}^3 \bar{V}_{\text{int}}(\bar{r}_{ij}). \tag{A.13d}$$

The centrifugal-like term \bar{U} of Eq. (A.13c) is quadratic in D . The precise form of $\kappa(D)$ depends on the particular system and is chosen so that the result of the scaling is as simple as possible.

We consider the large-dimension limit of the Schrödinger equation by first rewriting (A.13a) in terms of the inverse dimensionality δ , where

$$\delta \equiv 1/D. \quad (\text{A.14})$$

In the large-dimension limit ($\delta \rightarrow 0$) the factor of $\kappa(D)$ (which is quadratic in D) in the denominator of Eq. (A.13a) suppresses the derivative terms of (\bar{T}) , leaving behind only centrifugal-like term,

$$\bar{U}(\bar{r}_i; \delta) \Big|_{\infty} = \frac{\hbar^2}{8m_i \bar{r}_i^2} \frac{1}{\delta^2 \kappa(D)} \left(3\delta^2 + (1 - 4\delta)^2 \frac{\Gamma^{(i)}}{\Gamma} \right) \Big|_{\infty} \quad (\text{A.15})$$

as well as the large- D limit of the confining and interacting potential terms.

This centrifugal-like term, together with the confining and interaction potentials form an effective potential, \bar{V}_{eff} :

$$\bar{V}_{\text{eff}}(\bar{r}, \gamma; \delta) = \sum_{i=1}^3 (\bar{U}(\bar{r}_i; \delta) + \bar{V}_{\text{conf}}(\bar{r}_i; \delta)) + \sum_{i=1}^2 \sum_{j=i+1}^3 \bar{V}_{\text{int}}(\bar{r}_i, \gamma_{ij}; \delta). \quad (\text{A.16})$$

The centrifugal-like term provides a repulsive core, even in the ground state.

Due to the disappearance of the derivative portion of the kinetic energy, the particles in the system become localized in some arrangement which minimizes the (multivariate) large- D effective potential, and the excited states collapse onto the ground state at the minimum of V_{eff} . We assume that this minimal arrangement is totally symmetric under particle interchange.

For three particles, this arrangement is easily visualized in three dimensions in Figure A.1. In the large- D limit, the 3 particles in Figure A.1 are arranged on a sphere, each particle with a radius, \bar{r}_{∞} , from the center of the confining potential. Furthermore, the angle cosines between each pair of particles takes on the same value, γ_{∞} .

In scaled units the $D \rightarrow \infty$ approximation for the energy is simply the effective potential minimum, i.e.

$$\bar{E}_{\infty} = \bar{V}_{\text{eff}}(\bar{r}_{\infty}, \gamma_{\infty}; \delta = 0). \quad (\text{A.17})$$

A.3.4.1 Perturbation about large- D structure

We now consider small displacements about the static, symmetric arrangement of three particles shown in Figure A.1:

$$\bar{r}_i = \bar{r}_{\infty} + \delta^{1/2} \bar{r}'_i \quad (\text{A.18})$$

$$\gamma_{ij} = \gamma_{\infty} + \delta^{1/2} \gamma'_{ij}. \quad (\text{A.19})$$

We will perform a Maclaurin expansion of \bar{V}_{eff} about $\delta^{1/2} = 0$ to obtain \bar{V}_{eff} as a power series in $\delta^{1/2}$, but first we find it expedient to express the internal coordinates using the vectors $\bar{\mathbf{y}}$ and $\bar{\mathbf{y}}'$. We define a vector $\bar{\mathbf{y}}$ consisting of all the 6 internal coordinates,

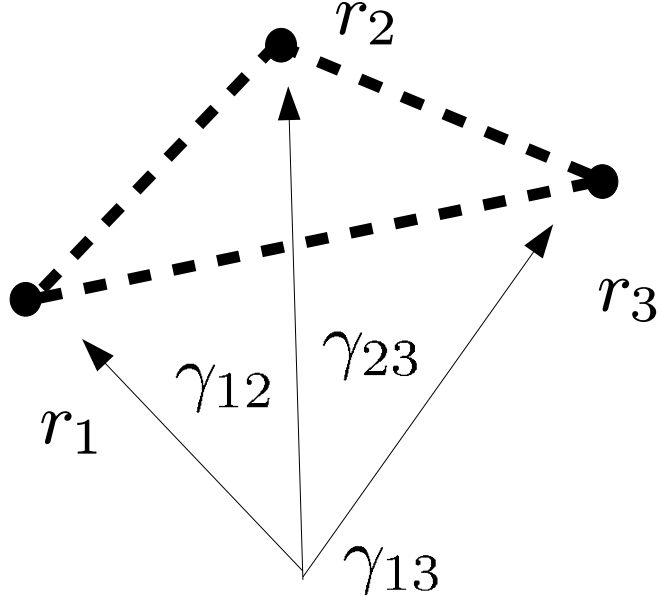


Figure A.1: Three particles in internal coordinates with an origin at the center of a confining potential. In a symmetric arrangement of particles, the particles form the points of an equilateral triangle. Due to the higher-number of dimensions, the particles may be displaced from the trap center in some orthogonal dimension.

$$\bar{\mathbf{y}} = \begin{pmatrix} \bar{\mathbf{r}} \\ \gamma \end{pmatrix}, \quad \text{where} \quad \bar{\mathbf{r}} = \begin{pmatrix} \bar{r}_1 \\ \bar{r}_2 \\ \bar{r}_3 \end{pmatrix} \quad \text{and} \quad \gamma = \begin{pmatrix} \gamma_{12} \\ \gamma_{13} \\ \gamma_{23} \end{pmatrix}. \quad (\text{A.20})$$

We make a similar definition for the internal displacement coordinate vector $\bar{\mathbf{y}}'$. We then make the substitution

$$\bar{\mathbf{y}} = \begin{pmatrix} \bar{r}_\infty \\ \bar{r}_\infty \\ \bar{r}_\infty \\ \gamma_\infty \\ \gamma_\infty \\ \gamma_\infty \end{pmatrix} + \delta^{1/2} \begin{pmatrix} \bar{r}'_1 \\ \bar{r}'_2 \\ \bar{r}'_3 \\ \gamma'_{12} \\ \gamma'_{13} \\ \gamma'_{23} \end{pmatrix} \quad (\text{A.21})$$

in the dimensionally-scaled Schrödinger equation (A.13a). As we shall see, writing \bar{T} and \bar{V}_{eff} as functions of the column vector $\bar{\mathbf{y}}'$ will enable us to write the corresponding series expansions in a compact form.

In Appendix D we calculate the series expansion of the effective potential $\bar{V}_{\text{eff}}[\bar{\mathbf{y}}'; \delta]$ about $\delta = 0$, obtaining

$$\begin{aligned} \bar{V}_{\text{eff}}[\bar{\mathbf{y}}'; \delta] &= E_\infty + \delta \left({}^{(0)}F + \frac{1}{2} \sum_{\nu_1=1}^6 \sum_{\nu_2=1}^6 {}^{(1)}F_{\nu_1, \nu_2} \bar{y}'_{\nu_1} \bar{y}'_{\nu_2} \right) \\ &+ \delta^{3/2} \left(\sum_{\nu=1}^6 {}^{(1)}F_\nu \bar{y}'_\nu + \frac{1}{3!} \sum_{\nu_1=1}^6 \sum_{\nu_2=1}^6 \sum_{\nu_3=1}^6 {}^{(1)}F_{\nu_1, \nu_2, \nu_3} \bar{y}'_{\nu_1} \bar{y}'_{\nu_2} \bar{y}'_{\nu_3} \right) + O(\delta^2). \end{aligned} \quad (\text{A.22})$$

For $N = 3$, these F tensors are

$${}^{(0)}F = \left. \frac{d}{d\delta} \bar{V}_{\text{eff}}[\bar{\mathbf{y}}; \delta] \right|_\infty \quad (\text{A.23a})$$

$$\begin{aligned} {}^{(0)}F_{\nu_1, \nu_2} &= \left. \frac{\partial^2}{\partial \bar{y}_{\nu_1} \partial \bar{y}_{\nu_2}} \bar{V}_{\text{eff}}[\bar{\mathbf{y}}; \delta] \right|_\infty \\ &= \left(\begin{array}{ccc|ccc} \frac{\partial^2}{\partial \bar{r}_1 \partial \bar{r}_1} & \frac{\partial^2}{\partial \bar{r}_1 \partial \bar{r}_2} & \frac{\partial^2}{\partial \bar{r}_1 \partial \bar{r}_3} & \frac{\partial^2}{\partial \bar{r}_1 \partial \gamma_{12}} & \frac{\partial^2}{\partial \bar{r}_1 \partial \gamma_{13}} & \frac{\partial^2}{\partial \bar{r}_1 \partial \gamma_{23}} \\ \frac{\partial^2}{\partial \bar{r}_2 \partial \bar{r}_1} & \frac{\partial^2}{\partial \bar{r}_2 \partial \bar{r}_2} & \frac{\partial^2}{\partial \bar{r}_2 \partial \bar{r}_3} & \frac{\partial^2}{\partial \bar{r}_2 \partial \gamma_{12}} & \frac{\partial^2}{\partial \bar{r}_2 \partial \gamma_{13}} & \frac{\partial^2}{\partial \bar{r}_2 \partial \gamma_{23}} \\ \frac{\partial^2}{\partial \bar{r}_3 \partial \bar{r}_1} & \frac{\partial^2}{\partial \bar{r}_3 \partial \bar{r}_2} & \frac{\partial^2}{\partial \bar{r}_3 \partial \bar{r}_3} & \frac{\partial^2}{\partial \bar{r}_3 \partial \gamma_{12}} & \frac{\partial^2}{\partial \bar{r}_3 \partial \gamma_{13}} & \frac{\partial^2}{\partial \bar{r}_3 \partial \gamma_{23}} \\ \hline \frac{\partial^2}{\partial \gamma_{12} \partial \bar{r}_1} & \frac{\partial^2}{\partial \gamma_{12} \partial \bar{r}_2} & \frac{\partial^2}{\partial \gamma_{12} \partial \bar{r}_3} & \frac{\partial^2}{\partial \gamma_{12} \partial \gamma_{12}} & \frac{\partial^2}{\partial \gamma_{12} \partial \gamma_{13}} & \frac{\partial^2}{\partial \gamma_{12} \partial \gamma_{23}} \\ \frac{\partial^2}{\partial \gamma_{13} \partial \bar{r}_1} & \frac{\partial^2}{\partial \gamma_{13} \partial \bar{r}_2} & \frac{\partial^2}{\partial \gamma_{13} \partial \bar{r}_3} & \frac{\partial^2}{\partial \gamma_{13} \partial \gamma_{12}} & \frac{\partial^2}{\partial \gamma_{13} \partial \gamma_{13}} & \frac{\partial^2}{\partial \gamma_{13} \partial \gamma_{23}} \\ \frac{\partial^2}{\partial \gamma_{23} \partial \bar{r}_1} & \frac{\partial^2}{\partial \gamma_{23} \partial \bar{r}_2} & \frac{\partial^2}{\partial \gamma_{23} \partial \bar{r}_3} & \frac{\partial^2}{\partial \gamma_{23} \partial \gamma_{12}} & \frac{\partial^2}{\partial \gamma_{23} \partial \gamma_{13}} & \frac{\partial^2}{\partial \gamma_{23} \partial \gamma_{23}} \end{array} \right) \\ &\times \bar{V}_{\text{eff}}[\bar{\mathbf{y}}; \delta] \Big|_\infty. \end{aligned} \quad (\text{A.23b})$$

$$\begin{aligned} {}^{(1)}F_\nu &= \left. \frac{\partial}{\partial \bar{y}_\nu} \frac{d}{d\delta} \bar{V}_{\text{eff}}[\bar{\mathbf{y}}; \delta] \right|_\infty \\ &= \left(\begin{array}{c} \frac{\partial}{\partial \bar{r}_1} \frac{d}{d\delta} \bar{V}_{\text{eff}}[\bar{\mathbf{y}}; \delta] \\ \frac{\partial}{\partial \bar{r}_2} \frac{d}{d\delta} \bar{V}_{\text{eff}}[\bar{\mathbf{y}}; \delta] \\ \frac{\partial}{\partial \bar{r}_3} \frac{d}{d\delta} \bar{V}_{\text{eff}}[\bar{\mathbf{y}}; \delta] \\ \hline \frac{\partial}{\partial \gamma_{12}} \frac{d}{d\delta} \bar{V}_{\text{eff}}[\bar{\mathbf{y}}; \delta] \\ \frac{\partial}{\partial \gamma_{13}} \frac{d}{d\delta} \bar{V}_{\text{eff}}[\bar{\mathbf{y}}; \delta] \\ \frac{\partial}{\partial \gamma_{23}} \frac{d}{d\delta} \bar{V}_{\text{eff}}[\bar{\mathbf{y}}; \delta] \end{array} \right) \Big|_\infty \end{aligned} \quad (\text{A.23c})$$

$${}^{(1)}F_{\nu_1, \nu_2, \nu_3} = \left. \frac{\partial^3}{\partial \bar{y}_{\nu_1} \partial \bar{y}_{\nu_2} \partial \bar{y}_{\nu_3}} \bar{V}_{\text{eff}}[\bar{\mathbf{y}}; \delta] \right|_\infty \quad (\text{A.23d})$$

The tensor ${}^{(1)}_3 F_{\nu_1, \nu_2, \nu_3}$ is a $6 \times 6 \times 6$ tensor, which is too large to express in the present print format.

Combining the series expansions for the (derivative portion of the) kinetic term (3.33) (calculated in Section D.3) and the potential term (3.36), we obtain the Hamiltonian operator as a perturbation series in $\delta^{\frac{1}{2}}$:

$$\bar{H} = E_\infty + \delta \bar{H}_0 + \delta^{3/2} \bar{H}_1 + O(\delta^2), \quad (\text{A.24})$$

where

$$\bar{H}_0 = -\frac{1}{2} {}^{(0)}_2 G_{\nu_1, \nu_2} \partial_{\bar{y}'_{\nu_1}} \partial_{\bar{y}'_{\nu_2}} + \frac{1}{2} {}^{(1)}_2 F_{\nu_1, \nu_2} \bar{y}'_{\nu_1} \bar{y}'_{\nu_2} + {}^{(0)}_0 F \quad (\text{A.25})$$

and

$$\bar{H}_1 = -\frac{1}{2} {}^{(1)}_3 G_{\nu_1, \nu_2, \nu_3} \bar{y}'_{\nu_1} \partial_{\bar{y}'_{\nu_2}} \partial_{\bar{y}'_{\nu_3}} + \frac{1}{3!} {}^{(1)}_3 F_{\nu_1, \nu_2, \nu_3} \bar{y}'_{\nu_1} \bar{y}'_{\nu_2} \bar{y}'_{\nu_3} - \frac{1}{2} {}^{(1)}_1 G_\nu \partial_{\bar{y}'_\nu} + {}^{(1)}_1 F_\nu \bar{y}'_\nu. \quad (\text{A.26})$$

In the above tensor contractions, summation over repeated ν_i indices from 1 to 6 is implied. The tensors F and G in the above Eqs. have an intricate symmetric structure that is expressed using graph theory in Section 4.3. We will return to the calculation of the actual elements of F and G in Appendix D.

A.3.6 Solution of the harmonic-order equation

We apply the Wilson GF matrix method(96) to simultaneously diagonalize both the harmonic order ${}^{(0)}_2 F$ and ${}^{(0)}_2 G$. There are $P = 6$ eigenvalues of the matrix ${}^{(0)}_2 G {}^{(0)}_2 F$, corresponding to the squared frequencies of the six collective motions of the three-particle system. Due to the the S_3 symmetry of ${}^{(0)}_2 \mathbf{G}$ and ${}^{(0)}_2 \mathbf{F}$ there are only *four* distinct (though degenerate) eigenvalues $\{\omega_{\mathbf{0}+}, \omega_{\mathbf{0}-}, \omega_{\mathbf{1}+}, \omega_{\mathbf{1}-}\}$. Each eigenvalue ν also has a corresponding eigenvector (called a “normal mode” q_ν).

In order to determine the harmonic-order wavefunction, one must also determine the collective normal-mode coordinates. Dunn *et al* explicitly construct the normal mode coordinates in Ref. (87), as well as the harmonic-order DPT wavefunction

$$\Phi_0(\mathbf{q}') = \prod_{\nu=1}^6 \phi_{n_\nu}(\sqrt{\bar{\omega}_\nu} \mathbf{q}'_\nu), \quad (\text{A.27})$$

where $\phi_{n_\nu}(\sqrt{\bar{\omega}_\nu} \mathbf{q}'_\nu)$ is a one-dimensional harmonic-oscillator wave function of frequency $\bar{\omega}_\nu$, and n_ν is the oscillator quantum number, $0 \leq n_\nu < \infty$, which counts the number of quanta in each normal mode.

A.3.7 Solution of the first-anharmonic equation

Having solved the harmonic-order Schrödinger equation, Eq. (3.41), for E_0 and Φ_0 , we now proceed to solve the first anharmonic order Schrödinger equation. We first assume that the first-anharmonic wavefunction can be obtained from the harmonic wavefunction by some operator of the form

$$\Phi_1(\mathbf{q}') = (1 + \delta^{\frac{1}{2}} \hat{\Delta}) \Phi_0(\mathbf{q}') \quad (\text{A.28})$$

We substitute Φ_1 in the above Eq. (A.28) into the first-anharmonic Schrödinger equation, noting that E_1 is zero due to symmetry considerations, and we obtain an expression involving the unknown operator $\hat{\Delta}$ with known quantities:

$$[\hat{\Delta}, \bar{H}_0]\Phi_0 = \bar{H}_1\Phi_0. \quad (\text{A.29})$$

In the next section A.4, we show that the Hamiltonian terms in the DPT perturbation series can be resolved in a structural basis, which I call “binary invariants”. In the section following A.5, we show that the transformation of each first-anharmonic-order binary invariant must be proportional to one of a few group theoretic tensors called “Clebsch-Gordon coefficients”.

A.4 Decomposition in a structural basis, invariant under S_3

A.4.2 Example: harmonic Hamiltonian tensor for $N = 3$

As an example of how S_3 symmetry affects a partitioning of the DPT Hamiltonian tensors, let us decompose the $N = 3$ harmonic-order ${}^{(0)}_2Q$ tensor blocks for $N = 3$ into equivalence classes. The tensor ${}^{(0)}_2Q$ has the following indicial structure for $N = 3$:

$${}^{(0)}_2\mathbf{Q}: \left(\begin{array}{ccc|ccc} \bar{r}_1\bar{r}_1 & \bar{r}_1\bar{r}_2 & \bar{r}_1\bar{r}_3 & \bar{r}_1\gamma_{12} & \bar{r}_1\gamma_{13} & \bar{r}_1\gamma_{23} \\ \bar{r}_2\bar{r}_1 & \bar{r}_2\bar{r}_2 & \bar{r}_2\bar{r}_3 & \bar{r}_2\gamma_{12} & \bar{r}_2\gamma_{13} & \bar{r}_2\gamma_{23} \\ \bar{r}_3\bar{r}_1 & \bar{r}_3\bar{r}_2 & \bar{r}_3\bar{r}_3 & \bar{r}_3\gamma_{12} & \bar{r}_3\gamma_{13} & \bar{r}_3\gamma_{23} \\ \hline \gamma_{12}\bar{r}_1 & \gamma_{12}\bar{r}_2 & \gamma_{12}\bar{r}_3 & \gamma_{12}\gamma_{12} & \gamma_{12}\gamma_{13} & \gamma_{12}\gamma_{23} \\ \gamma_{13}\bar{r}_1 & \gamma_{13}\bar{r}_2 & \gamma_{13}\bar{r}_3 & \gamma_{13}\gamma_{12} & \gamma_{13}\gamma_{13} & \gamma_{13}\gamma_{23} \\ \gamma_{23}\bar{r}_1 & \gamma_{23}\bar{r}_2 & \gamma_{23}\bar{r}_3 & \gamma_{23}\gamma_{12} & \gamma_{23}\gamma_{13} & \gamma_{23}\gamma_{23} \end{array} \right). \quad (\text{A.30})$$

Consider the elements of the S_3 group,

$$S_3 = \{(1)(2)(3), (1)(23), (3)(12), (123), (132), (2)(13)\} \quad (\text{A.31})$$

acting on the elements of the above matrix, each of which results in a permutation of the particle labels. Note that elements related by a permutation of S_3 must be equal. Matrix elements that are related by a permutation are said to be *equivalent* and the set of objects equivalent under some relation is called an *equivalence class*. Each element of the above matrix belongs to an equivalence class composed of some other elements at other positions in the matrix. We represent each equivalence class as a binary matrix with ones in the places which are related by a permutation of S_3 and zeros elsewhere. Such matrices are binary and are also unchanged by the action of S_3 . Each block may be decomposed as a sum over equivalence classes using a set of binary matrices as follows:

$${}^{(0)}_2\mathbf{Q}^{rr} = {}^{(0)}_2Q_{11}^{rr} \begin{pmatrix} 1 & 0 & 0 \\ 0 & 1 & 0 \\ 0 & 0 & 1 \end{pmatrix} + {}^{(0)}_2Q_{12}^{rr} \begin{pmatrix} 0 & 1 & 1 \\ 1 & 0 & 1 \\ 1 & 1 & 0 \end{pmatrix} \quad (\text{A.32})$$

$${}^{(0)}_2 \mathbf{Q}^{r\gamma} = {}^{(0)}_2 Q_{1(12)}^{r\gamma} \begin{pmatrix} 1 & 1 & 0 \\ 1 & 0 & 1 \\ 0 & 1 & 1 \end{pmatrix} + {}^{(0)}_2 Q_{1(23)}^{r\gamma} \begin{pmatrix} 0 & 0 & 1 \\ 0 & 1 & 0 \\ 1 & 0 & 0 \end{pmatrix} \quad (\text{A.33})$$

$${}^{(0)}_2 \mathbf{Q}^{\gamma r} = {}^{(0)}_2 Q_{(12)1}^{\gamma r} \begin{pmatrix} 1 & 1 & 0 \\ 1 & 0 & 1 \\ 0 & 1 & 1 \end{pmatrix} + {}^{(0)}_2 Q_{(23)1}^{\gamma r} \begin{pmatrix} 0 & 0 & 1 \\ 0 & 1 & 0 \\ 1 & 0 & 0 \end{pmatrix} \quad (\text{A.34})$$

$${}^{(0)}_2 \mathbf{Q}^{\gamma\gamma} = {}^{(0)}_2 Q_{(12)(12)}^{\gamma\gamma} \begin{pmatrix} 1 & 0 & 0 \\ 0 & 1 & 0 \\ 0 & 0 & 1 \end{pmatrix} + {}^{(0)}_2 Q_{(12)(23)}^{\gamma\gamma} \begin{pmatrix} 0 & 1 & 1 \\ 1 & 0 & 1 \\ 1 & 1 & 0 \end{pmatrix}. \quad (\text{A.35})$$

Notice that the matrix structure of each equivalence class is represented by a binary matrix. (For $N \geq 4$ there is a third structural entity in the decomposition of ${}^{(0)}_2 Q^{\gamma\gamma}$ corresponding to elements of the form ${}^{(0)}_2 Q_{(12)(34)}^{\gamma\gamma}$.)

A.4.3 Decomposition in the basis of binary invariants

We term the matrices and tensors by which we perform such an above decomposition *binary invariants*.

A.4.3.1 Introducing binary invariants

For example, let us construct the binary invariant for the equivalence class of the element ${}^{(0)}_2 Q_{11}^{rr}$ for $N = 3$. First, we write a matrix with only one non-zero element at the position of ${}^{(0)}_2 Q_{11}^{rr}$.

$$\begin{pmatrix} 1 & 0 & 0 \\ 0 & 0 & 0 \\ 0 & 0 & 0 \end{pmatrix}. \quad (\text{A.36})$$

Next we consider the action of the permutation group S_3 ,

$$S_3 = \{(1)(2)(3), (1)(23), (3)(12), (123), (132), (2)(13)\} \quad (\text{A.37})$$

on the matrix in Eq. (4.11). There are two permutations which leave the matrix unchanged, and the group S_3 is divided into cosets of two elements which map to the same matrix. We apply one element of S_3 from each coset to the matrix and add the result. (Equivalently, we may apply all elements of S_3 and divide by the size of the cosets.) The result is the binary invariant for the equivalence class of ${}^{(0)}_2 Q_{11}^{rr}$,

$$\begin{pmatrix} 1 & 0 & 0 \\ 0 & 1 & 0 \\ 0 & 0 & 1 \end{pmatrix} = \begin{pmatrix} 1 & 0 & 0 \\ 0 & 0 & 0 \\ 0 & 0 & 0 \end{pmatrix} + \begin{pmatrix} 0 & 0 & 0 \\ 0 & 1 & 0 \\ 0 & 0 & 0 \end{pmatrix} + \begin{pmatrix} 0 & 0 & 0 \\ 0 & 0 & 0 \\ 0 & 0 & 1 \end{pmatrix}. \quad (\text{A.38})$$

A similar procedure may be followed to construct the binary invariants in closed form. This construction is established in Appendix (C).

A.4.4 Graphical representation of tensor structure

A.4.4.2 Mapping tensor structure onto graphs

The set of graphs representing the equivalence classes of the $N = 3$ harmonic-order DPT Hamiltonian tensors are given in Table A.4.4.2. The set of graphs representing the equivalence classes of the rank-one and rank-three tensors are given in Tables A.4.4.2 and A.4.4.2.

A.4.4.3 Graphical decomposition of harmonic-order matrices

The harmonic-order matrices ${}^{(0)}_2 Q_{\nu_1, \nu_2}^{block}$ may be decomposed using Eq. (4.15),

$${}^{(0)}_2 Q_{\nu_1, \nu_2}^{block} = \sum_{\mathcal{G} \in \mathbb{G}_{block}} Q^{block}(\mathcal{G}) [B^{block}(\mathcal{G})]_{\nu_1, \nu_2}. \quad (\text{A.39})$$

where the equivalence classes \mathbb{G}_{block} for $N = 3$ are now labeled by graphs

$$\begin{aligned} \mathbb{G}^{rr} &= \{\text{⊙⊙}, \text{⊙} \text{⊙}\} \\ \mathbb{G}^{r\gamma} = \mathbb{G}^{\gamma r} &= \{\text{⊙} \text{---}, \text{⊙} \text{---}\} \\ \mathbb{G}^{\gamma\gamma} &= \{\text{⊙} \text{---}, \text{---} \text{⊙}\} \end{aligned} \quad (\text{A.40})$$

For example, the rr block can be decomposed as

$$\left[{}^{(0)}_2 Q^{rr} \right]_{i,j} = Q(\text{⊙⊙}) [B(\text{⊙⊙})]_{i,j} + Q(\text{⊙} \text{⊙}) [B(\text{⊙} \text{⊙})]_{i,j}. \quad (\text{A.41})$$

When Q is symmetric (which will be the case for F and G) then the expansions for ${}^{(0)}_2 Q^{rr}$, ${}^{(0)}_2 Q^{r\gamma}$ are the same, so we may drop the block labels on the binary invariant.

A.4.4.4 Graphical decomposition of first-anharmonic-order tensors

The rank-one first-anharmonic tensors ${}^{(1)}_1 Q_{\nu}^{block}$ have a trivial decomposition, since there is only one graph in each block:

$$\begin{aligned} \mathbb{G}^r &= \text{⊙} \\ \mathbb{G}^{\gamma} &= \text{---} \end{aligned} \quad (\text{A.42})$$

Therefore, Eq. (4.15) becomes

$$\begin{aligned} {}^{(1)}_1 Q_{\nu}^r &= {}^{(1)}_1 Q^r (\text{⊙}) [B(\text{⊙})]_{\nu} \\ {}^{(1)}_1 Q_{\nu}^{\gamma} &= {}^{(1)}_1 Q^{\gamma} (\text{---}) [B(\text{---})]_{\nu}. \end{aligned} \quad (\text{A.43})$$

The rank-three tensors ${}^{(1)}_3 Q_{\nu_1, \nu_2, \nu_3}^{block}$ may also be decomposed using Eq. (4.15),

$${}^{(1)}_3 Q_{\nu_1, \nu_2, \nu_3}^{block} = \sum_{\mathcal{G} \in \mathbb{G}_{block}} Q^{block}(\mathcal{G}) [B^{block}(\mathcal{G})]_{\nu_1, \nu_2, \nu_3}, \quad (\text{A.44})$$

where the equivalence classes \mathbb{G}_{block} are now labeled by graphs

Graph	Tensor Elements
	${}^{(0)}_2 Q_{ii}^{rr}$
	${}^{(0)}_2 Q_{ij}^{rr}$
	${}^{(0)}_2 Q_{(ij)i}^{\gamma r} = {}^{(0)}_2 Q_{(ij)j}^{\gamma r}$
	${}^{(0)}_2 Q_{i(ij)}^{r\gamma} = {}^{(0)}_2 Q_{i(ji)}^{r\gamma}$
	${}^{(0)}_2 Q_{(ij)(ij)}^{\gamma\gamma}$
	${}^{(0)}_2 Q_{(ij)(ik)}^{\gamma\gamma} = {}^{(0)}_2 Q_{(ij)(jk)}^{\gamma\gamma} = {}^{(0)}_2 Q_{(ij)(ki)}^{\gamma\gamma} = {}^{(0)}_2 Q_{(ij)(kj)}^{\gamma\gamma}$

Table A.1: Graph labels for the equivalence classes of the rank-two, harmonic-order DPT Hamiltonian coefficient tensors. For $N = 3$, there is one graph from the general case that has more than three vertices and is not shown here.

Graph	Tensor Elements
	${}^{(1)}_1 Q_i^r$
	${}^{(1)}_1 Q_{(ij)}^\gamma$

Table A.2: Graphs labeling equivalence classes for the rank-one, first-anharmonic DPT Hamiltonian coefficient tensors.

Graphs	Elements	Graphs	Elements	Graphs	Elements
	${}^{(1)}_3 Q_{i,i,i}^{rrr}$		${}^{(1)}_3 Q_{(ij),(ij),i}^{\gamma\gamma r}$		${}^{(1)}_3 Q_{(ij),(ij),(ij)}^{\gamma\gamma\gamma}$
	${}^{(1)}_3 Q_{i,i,j}^{rrr}$		${}^{(1)}_3 Q_{(ij),(ij),k}^{\gamma\gamma r}$		${}^{(1)}_3 Q_{(ij),(jk),(ik)}^{\gamma\gamma\gamma}$
	${}^{(1)}_3 Q_{i,j,k}^{rrr}$		${}^{(1)}_3 Q_{(ij),(jk),j}^{\gamma\gamma r}$		${}^{(1)}_3 Q_{(ij),(ij),(jk)}^{\gamma\gamma\gamma}$
	${}^{(1)}_3 Q_{(ij),i,i}^{\gamma rr}$		${}^{(1)}_3 Q_{(ij),(jk),i}^{\gamma\gamma r}$		
	${}^{(1)}_3 Q_{(ij),i,j}^{\gamma rr}$				
	${}^{(1)}_3 Q_{(ij),i,k}^{\gamma rr}$				
	${}^{(1)}_3 Q_{(ij),k,k}^{\gamma rr}$				

Table A.3: Graphs labeling equivalence classes for the rank-three, first-anharmonic DPT Hamiltonian coefficient tensors. Graphs from the general case in Table 4.3.2 with more than three vertices are not shown here.

$$\begin{aligned}
\mathbb{G}^{rrr} &= \{ \text{diagram 1}, \text{diagram 2}, \text{diagram 3} \} \\
\mathbb{G}^{\gamma rr} = \mathbb{G}^{r\gamma r} = \mathbb{G}^{rr\gamma} &= \{ \text{diagram 4}, \text{diagram 5}, \text{diagram 6}, \text{diagram 7} \} \\
\mathbb{G}^{\gamma\gamma r} = \mathbb{G}^{r\gamma\gamma} = \mathbb{G}^{rr\gamma\gamma} &= \{ \text{diagram 8}, \text{diagram 9}, \text{diagram 10}, \text{diagram 11} \} \\
\mathbb{G}^{\gamma\gamma\gamma} &= \{ \text{diagram 12}, \text{diagram 13}, \text{diagram 14} \}.
\end{aligned} \tag{A.45}$$

For example, the rrr block tensors may be decomposed as follows:

$$\begin{aligned}
[Q^{rrr}]_{i,j,k} &= Q(\text{diagram 1}) [B(\text{diagram 1})]_{i,j,k} + Q(\text{diagram 2}) [B(\text{diagram 2})]_{i,j,k} \\
&\quad + Q(\text{diagram 3}) [B(\text{diagram 3})]_{i,j,k}.
\end{aligned} \tag{A.46}$$

A.5 Transformation of Hamiltonian to normal-coordinate basis

Now we transform the binary invariant basis tensors to symmetry coordinates.

A.5.1 Two-step transformation of the Hamiltonian

A.5.1.3 Intermediate step: transformation to symmetry coordinates

The transformation to symmetry coordinates in Eq. (5.14) represents a crucial simplification in the transformation to normal-mode coordinates: the transformation of the Hamiltonian to symmetry coordinates as an intermediate step.

The transformation W has a block form defined in Eq. (45) of Ref. (87) for $N = 3$ is:

$$W = \left(\begin{array}{cc|cc} W_{r'}^0 & \mathbf{0} & & \\ \mathbf{0} & W_{\gamma'}^0 & & \\ \hline W_{r'}^1 & \mathbf{0} & & \\ \mathbf{0} & W_{\gamma'}^1 & & \end{array} \right). \tag{A.47}$$

The block matrices $W_{r'}^0$ and $W_{\gamma'}^0$ have dimensions 1×3 , and the block matrices $W_{r'}^1$ and $W_{\gamma'}^1$ have dimensions 2×3 . One difference between Eq. A.47 and the transformation for general N in Eq. 5.22 is the absence of the $\mathbf{2}$ sector.

Each block in the W transformation (A.47) effects the reduction of a reducible representation of S_3 to an irreducible representation of S_3 :

$$W \bar{\mathbf{y}}' = \left(\begin{array}{ccc|ccc} \frac{1}{\sqrt{3}} & \frac{1}{\sqrt{3}} & \frac{1}{\sqrt{3}} & 0 & 0 & 0 \\ 0 & 0 & 0 & \frac{1}{\sqrt{3}} & \frac{1}{\sqrt{3}} & \frac{1}{\sqrt{3}} \\ \hline \frac{1}{\sqrt{2}} & -\frac{1}{\sqrt{2}} & 0 & 0 & 0 & 0 \\ \frac{1}{\sqrt{6}} & \frac{1}{\sqrt{6}} & -\sqrt{\frac{2}{3}} & 0 & 0 & 0 \\ 0 & 0 & 0 & 0 & \frac{1}{\sqrt{2}} & -\frac{1}{\sqrt{2}} \\ 0 & 0 & 0 & \sqrt{\frac{2}{3}} & -\frac{1}{\sqrt{6}} & -\frac{1}{\sqrt{6}} \end{array} \right) \begin{pmatrix} \bar{r}'_1 \\ \bar{r}'_1 \\ \hline \bar{r}'_1 \\ \gamma'_{12} \\ \gamma'_{13} \\ \gamma'_{23} \end{pmatrix}$$

$$= \begin{pmatrix} \frac{\bar{r}'_1 + \bar{r}'_2 + \bar{r}'_3}{\sqrt{3}} \\ \frac{\gamma'_{12} + \gamma'_{13} + \gamma'_{23}}{\sqrt{3}} \\ \frac{\bar{r}'_1 - \bar{r}'_2}{\sqrt{2}} \\ \frac{\bar{r}'_1 + \bar{r}'_2 - 2\bar{r}'_3}{\sqrt{6}} \\ \frac{\gamma'_{13} - \gamma'_{23}}{\sqrt{2}} \\ \frac{2\gamma'_{12} - \gamma'_{13} - \gamma'_{23}}{\sqrt{6}} \end{pmatrix}. \quad (\text{A.48})$$

Thus the symmetry coordinates in Reference (87) for $N = 3$ are obtained in terms of the internal displacement coordinates. There are two symmetry coordinates which transform under a scalar irrep $[N]$ of S_N :

$$\mathbf{S}_{\bar{r}'}^0 = \frac{1}{\sqrt{3}} (\bar{r}'_1 + \bar{r}'_2 + \bar{r}'_3), \quad (\text{A.49})$$

and

$$\mathbf{S}_{\bar{\gamma}'}^0 = \frac{1}{\sqrt{3}} (\gamma_{12} + \gamma_{13} + \gamma_{23}). \quad (\text{A.50})$$

There are four symmetry coordinates which transform under a $[N - 1, 1]$ irrep of S_N (two constructed from radii and two from angle cosines):

$$\mathbf{S}_{\bar{r}'}^1 = \begin{pmatrix} \frac{1}{\sqrt{2}}(\bar{r}'_1 - \bar{r}'_2) \\ \frac{1}{\sqrt{6}}(\bar{r}'_1 + \bar{r}'_2 - 2\bar{r}'_3) \end{pmatrix}, \quad (\text{A.51})$$

and

$$\mathbf{S}_{\bar{\gamma}'}^1 = \begin{pmatrix} \frac{\gamma'_{13} - \gamma'_{23}}{\sqrt{2}} \\ \frac{2\gamma'_{12} - \gamma'_{13} - \gamma'_{23}}{\sqrt{6}} \end{pmatrix}. \quad (\text{A.52})$$

A.5.1.4 Final step: transformation to normal coordinates

For $N = 3$, the normal-coordinate vector \mathbf{q}' has following block form:

$$\mathbf{q}' = \begin{pmatrix} \mathbf{q}'_+{}^0 \\ \mathbf{q}'_-{}^0 \\ \mathbf{q}'_+{}^1 \\ \mathbf{q}'_-{}^1 \end{pmatrix}. \quad (\text{A.53})$$

In Reference (87) Eq. (80), the transformation from symmetry coordinates to normal coordinates $\mathcal{C}_{\mu_1, \mu_2}$ is defined as (a 4×4 matrix for $N = 3$):

$$\mathcal{C}_{\mu_1, \mu_2} = \left(\begin{array}{cc|cc} c_+^0 \cos \theta_+^0 & c_+^0 \sin \theta_+^0 & 0 & 0 \\ c_-^0 \cos \theta_-^0 & c_-^0 \sin \theta_-^0 & 0 & 0 \\ \hline 0 & 0 & c_+^1 \cos \theta_+^1 & c_+^1 \sin \theta_+^1 \\ 0 & 0 & c_-^1 \cos \theta_-^1 & c_-^1 \sin \theta_-^1 \end{array} \right). \quad (\text{A.54})$$

The normal coordinate vectors are constructed by transforming the symmetry coordinates: $\mathbf{q}' = \mathcal{C}^T \mathbf{S}$ (Eq. (63) in Ref. (87)). The result is a normal-coordinate vector of the form

$$\mathbf{q}' = \left(\begin{array}{c} c_+^0 \cos \theta_+^0 \mathbf{S}_{r'}^0 + c_+^0 \sin \theta_+^0 \mathbf{S}_{\gamma'}^0 \\ c_-^0 \cos \theta_-^0 \mathbf{S}_{r'}^0 + c_-^0 \sin \theta_-^0 \mathbf{S}_{\gamma'}^0 \\ \hline c_+^1 \cos \theta_+^1 \mathbf{S}_{r'}^1 + c_+^1 \sin \theta_+^1 \mathbf{S}_{\gamma'}^1 \\ c_-^1 \cos \theta_-^1 \mathbf{S}_{r'}^1 + c_-^1 \sin \theta_-^1 \mathbf{S}_{\gamma'}^1 \end{array} \right). \quad (\text{A.55})$$

In the above equation, the ‘‘mixing angles’’ θ_{\pm}^{α} , and the normalization c_{\pm}^{α} are defined in terms of the harmonic-order Hamiltonian elements: Eqs. (76), (78), and (79) in Reference (87).

Having seen the transformation of the internal coordinate column vector to symmetry coordinates, then to normal coordinates, we now perform the same transformations on the DPT Hamiltonian tensors.

A.5.2 Transformation to symmetry coordinates

We now transform the first-anharmonic Hamiltonian to the basis of symmetry coordinates, obtaining

$$\bar{H}_0 = -\frac{1}{2} \left[\begin{array}{c} (0) \\ 2 \end{array} G_W \right]_{\nu_1, \nu_2} \partial_{S_{\nu_1}} \partial_{S_{\nu_2}} + \frac{1}{2} \left[\begin{array}{c} (0) \\ 2 \end{array} F_W \right]_{\nu_1, \nu_2} S_{\nu_1} S_{\nu_2} + \begin{array}{c} (0) \\ 0 \end{array} F_W ., \quad (\text{A.56})$$

and

$$\begin{aligned} \bar{H}_1 = & -\frac{1}{2} \left[\begin{array}{c} (1) \\ 3 \end{array} G_W \right]_{\nu_1, \nu_2, \nu_3} S_{\nu_1} \partial_{S_{\nu_2}} \partial_{S_{\nu_3}} - \frac{1}{2} \left[\begin{array}{c} (1) \\ 1 \end{array} G_W \right]_{\nu} \partial_{S_{\nu}} \\ & + \frac{1}{3!} \left[\begin{array}{c} (1) \\ 3 \end{array} F_W \right]_{\nu_1, \nu_2, \nu_3} S_{\nu_1} S_{\nu_2} S_{\nu_3} + \left[\begin{array}{c} (1) \\ 1 \end{array} F_W \right]_{\nu} S_{\nu}. \end{aligned} \quad (\text{A.57})$$

In the above equations, summation is implied over $\nu_i = 1$ to 6.

In Ref. (87) using the results of Ref. (99) it has been shown that the harmonic Hamiltonian matrices $\begin{array}{c} (0) \\ 2 \end{array} G_W$ and $\begin{array}{c} (0) \\ 2 \end{array} F_W$ have a particular block structure where each block is itself a direct product of matrices:

$$\begin{array}{c} (0) \\ 2 \end{array} Q_W = \left(\begin{array}{cc} \sigma_{00}^Q \otimes \mathbf{I}_0 & \mathbf{0} \\ \mathbf{0} & \sigma_{11}^Q \otimes \mathbf{I}_1 \end{array} \right). \quad (\text{A.58})$$

The matrices σ_{00}^Q and σ_{11}^Q are of dimension 2×2 . The matrix \mathbf{I}_0 is actually only a scalar 1 (or, if you prefer, a 1×1 matrix). The matrix \mathbf{I}_1 is the 2×2 identity matrix. These are actually the two Clebsch-Gordon coefficients: C^{00} couples together two $\mathbf{0}$ representations to yield another $\mathbf{0}$ representation, and C^{11} couples together two $\mathbf{1}$ representations to yield another $\mathbf{0}$ representation.

A.5.2.1 Clebsch-Gordon coefficients of the transformation

Writing the Clebsch-Gordon coefficient which couples together α_1 and α_2 to yield $\mathbf{0}$ as $C_{\xi_1, \xi_2}^{\alpha_1 \alpha_2}$, the harmonic-order Q_W may be written more generally as

$$\left[\begin{matrix} (0) \\ 2 \end{matrix} Q_W^{\alpha_1 \alpha_2} \right]_{\xi_1, \xi_2}^{X_1, X_2} = \left[\begin{matrix} (0) \\ 2 \end{matrix} \sigma_{\alpha_1 \alpha_2}^Q \right]_{X_1, X_2} C_{\xi_1, \xi_2}^{\alpha_1 \alpha_2}. \quad (\text{A.59})$$

For $N = 3$, there are only two harmonic-order Clebsch-Gordon coefficients:

$$C^{\mathbf{00}} = 1 \quad (\text{A.60})$$

$$C_{\xi_1, \xi_2}^{\mathbf{11}} = \begin{pmatrix} 1 & 0 \\ 0 & 1 \end{pmatrix}. \quad (\text{A.61})$$

Notice that the Clebsch-Gordon coefficient depends on the irrep labels α_i only, not on the block labels X_i . The factor $\left[\begin{matrix} (0) \\ 2 \end{matrix} \sigma_{\alpha_1 \alpha_2}^Q \right]_{X_1, X_2}$ is a 4×4 matrix (with the block structure shown above)

At first-anharmonic order, the blocks of the symmetry-transformed Hamiltonian tensors are also proportional to Clebsch-Gordon coefficients. In the case of the rank-one Hamiltonian tensor, there is really no coupling of irreps so the rank-one Clebsch-Gordon has a simple form:

$$C_{\xi}^{\alpha} = \begin{cases} 1 & \text{if } \alpha = \mathbf{0} \\ 0 & \text{otherwise} \end{cases}. \quad (\text{A.62})$$

Therefore, we can expect the rank-one Hamiltonian tensors to be proportional to this Clebsch-Gordon coefficient by a proportionality vector we denote $\left[\begin{matrix} (1) \\ 1 \end{matrix} \sigma_{\alpha_1}^Q \right]_{\mu}$:

$$\begin{aligned} \left[\begin{matrix} (1) \\ 1 \end{matrix} Q_W^{\mathbf{0}} \right]_{\mu}^X &= \left[\begin{matrix} (1) \\ 1 \end{matrix} \sigma_{\mathbf{0}}^Q \right]_X \times 1 \\ \left[\begin{matrix} (1) \\ 1 \end{matrix} Q_W^{\mathbf{1}} \right]_{\xi}^X &= 0 \\ \left[\begin{matrix} (1) \\ 1 \end{matrix} Q_W^{\mathbf{2}} \right]_{\xi}^X &= 0. \end{aligned} \quad (\text{A.63})$$

The Clebsch-Gordon coefficient tensors which couple three irreps to form an $\mathbf{0}$ irrep for $N = 3$ are much simpler than the general N case. There are only three non-zero Clebsch-Gordon coefficients for $N = 3$ (From Eqs. E.11-E.13),

$$C^{\mathbf{000}} = 1 \quad (\text{A.64})$$

$$C^{\mathbf{110}} = \begin{pmatrix} \begin{pmatrix} C_{111}^{110} \\ C_{211}^{110} \end{pmatrix} & \begin{pmatrix} C_{121}^{110} \\ C_{221}^{110} \end{pmatrix} \end{pmatrix} = \begin{pmatrix} \begin{pmatrix} 1 \\ 0 \end{pmatrix} & \begin{pmatrix} 0 \\ 1 \end{pmatrix} \end{pmatrix} \quad (\text{A.65})$$

$$C^{\mathbf{111}} = \begin{pmatrix} \begin{pmatrix} C_{111}^{111} \\ C_{112}^{111} \\ C_{211}^{111} \\ C_{212}^{111} \end{pmatrix} & \begin{pmatrix} C_{121}^{111} \\ C_{122}^{111} \\ C_{221}^{111} \\ C_{222}^{111} \end{pmatrix} \end{pmatrix} = \begin{pmatrix} \begin{pmatrix} 0 \\ \frac{1}{\sqrt{6}} \\ \frac{1}{\sqrt{6}} \\ 0 \end{pmatrix} & \begin{pmatrix} \frac{1}{\sqrt{6}} \\ 0 \\ 0 \\ -\frac{1}{\sqrt{6}} \end{pmatrix} \end{pmatrix}. \quad (\text{A.66})$$

In Eq. A.65 the order of the indices and sector labels may be permuted. We know from group representation theory that the transformation of each Hamiltonian tensor must be proportional to one of the above Clebsch-Gordon coefficients for that transformation:

$$\left[\begin{matrix} (1) \\ 3 \end{matrix} Q_W^{\alpha_1 \alpha_2 \alpha_3} \right]_{\xi_1, \xi_2, \xi_3}^{X_1 X_2 X_3} = \left[\begin{matrix} (1) \\ 3 \end{matrix} \sigma_{\alpha_1 \alpha_2 \alpha_3 k}^Q \right]_{X_1, X_2, X_3} C_{\xi_1, \xi_2, \xi_3}^{\alpha_1 \alpha_2, \alpha_3, k}. \quad (\text{A.67})$$

To calculate the actual proportionality coefficients σ , we employ a resolution in a basis of binary invariants.

A.5.2.2 Symmetry-transformed binary invariants

To make use of the Clebsch-Gordon coefficients, one must calculate the proportionality coefficients in Eqs. (A.59), (A.63), and (A.67) by performing the relevant transformations on the each binary invariant. This is easy to do numerically for $N = 3$.

One may actually calculate the Clebsch-Gordon coefficients (to within a constant) by performing each of the transformations below on only one binary invariant. The same transformation on all the others must be proportional to that result.

Now, for any graph \mathcal{G} in a block, the transformation of the tensor $B^{\text{block}}(\mathcal{G})$ must be proportional to the Clebsch-Gordon coefficient of that transformation. At harmonic order the binary invariants are matrices and we can perform a matrix transformation of the binary invariant matrices to obtain something that is proportional to the Clebsch-Gordon coefficient matrix for that transformation.

$$\mathbf{W}_{X_1}^{\alpha_1} \mathbf{B}(\mathcal{G}) [\mathbf{W}_{X_2}^{\alpha_2}]^T = \left[\begin{matrix} (0) \\ 2 \end{matrix} \beta^{\alpha_1 \alpha_2}(\mathcal{G}) \right]_{X_1, X_2} \mathbf{C}_{\xi_1, \xi_2}^{\alpha_1 \alpha_2}. \quad (\text{A.68})$$

As an example, we perform the (non-zero) transformations on the rr sector of the harmonic-order binary invariants $B(\circ\circ)$ and $B(\circ\circ)$:

$$\begin{aligned} \mathbf{W}_{\bar{r}}^0 \mathbf{B}(\circ\circ) [\mathbf{W}_{\bar{r}}^0]^T &= \begin{pmatrix} \frac{1}{\sqrt{3}} & \frac{1}{\sqrt{3}} & \frac{1}{\sqrt{3}} \end{pmatrix} \begin{pmatrix} 1 & 0 & 0 \\ 0 & 1 & 0 \\ 0 & 0 & 1 \end{pmatrix} \begin{pmatrix} \frac{1}{\sqrt{3}} \\ \frac{1}{\sqrt{3}} \\ \frac{1}{\sqrt{3}} \end{pmatrix} \\ &= 1 \end{aligned} \quad (\text{A.69})$$

and

$$\begin{aligned} \mathbf{W}_{\bar{r}}^1 \mathbf{B}(\circ\circ) [\mathbf{W}_{\bar{r}}^1]^T &= \begin{pmatrix} \frac{1}{\sqrt{3}} & \frac{1}{\sqrt{3}} & \frac{1}{\sqrt{3}} \end{pmatrix} \begin{pmatrix} 0 & 1 & 1 \\ 1 & 0 & 1 \\ 1 & 1 & 0 \end{pmatrix} \begin{pmatrix} \frac{1}{\sqrt{3}} \\ \frac{1}{\sqrt{3}} \\ \frac{1}{\sqrt{3}} \end{pmatrix} \\ &= 2. \end{aligned} \quad (\text{A.70})$$

Comparing the above transformations to the $\mathbf{00}$ Clebsch-Gordon coefficient matrix (which is simply 1), we can deduce the value of the proportionality coefficients $\left[\begin{matrix} (0) \\ 2 \end{matrix} \beta^{\mathbf{00}}(\circ\circ) \right]_{\bar{r}, \bar{r}}$ and $\left[\begin{matrix} (0) \\ 2 \end{matrix} \beta^{\mathbf{00}}(\circ\circ) \right]_{\bar{r}, \bar{r}}$:

$$\left[\begin{matrix} (0) \\ 2 \end{matrix} \beta^{00} (\infty\infty) \right]_{\bar{r},\bar{r}} = 1 \quad (\text{A.71})$$

$$\left[\begin{matrix} (0) \\ 2 \end{matrix} \beta^{00} (\ominus\ominus) \right]_{\bar{r},\bar{r}} = 2 \quad (\text{A.72})$$

These results are listed in the first column of the top (rr block) table in Table A.4, which is the $N = 3$ case of the more general Table A.4.

Next, we perform the transformation of the rr block binary invariants to the **11** sector

$$\begin{aligned} \mathbf{W}_{\bar{r}}^1 \mathbf{B}(\infty\infty) [\mathbf{W}_{\bar{r}}^1]^T &= \\ & \begin{pmatrix} \frac{1}{\sqrt{2}} & -\frac{1}{\sqrt{2}} & 0 \\ \frac{1}{\sqrt{6}} & \frac{1}{\sqrt{6}} & -\sqrt{\frac{2}{3}} \end{pmatrix} \begin{pmatrix} 1 & 0 & 0 \\ 0 & 1 & 0 \\ 0 & 0 & 1 \end{pmatrix} \begin{pmatrix} \frac{1}{\sqrt{2}} & \frac{1}{\sqrt{6}} \\ -\frac{1}{\sqrt{2}} & \frac{1}{\sqrt{6}} \\ 0 & -\sqrt{\frac{2}{3}} \end{pmatrix} \\ &= \begin{pmatrix} 1 & 0 \\ 0 & 1 \end{pmatrix} \\ &= 1 \times \mathbf{C}^{11} \end{aligned} \quad (\text{A.73})$$

$$\begin{aligned} \mathbf{W}_{\bar{r}}^1 \mathbf{B}(\ominus\ominus) [\mathbf{W}_{\bar{r}}^1]^T &= \\ & \begin{pmatrix} \frac{1}{\sqrt{2}} & -\frac{1}{\sqrt{2}} & 0 \\ \frac{1}{\sqrt{6}} & \frac{1}{\sqrt{6}} & -\sqrt{\frac{2}{3}} \end{pmatrix} \begin{pmatrix} 0 & 1 & 1 \\ 1 & 0 & 1 \\ 1 & 1 & 0 \end{pmatrix} \begin{pmatrix} \frac{1}{\sqrt{2}} & \frac{1}{\sqrt{6}} \\ -\frac{1}{\sqrt{2}} & \frac{1}{\sqrt{6}} \\ 0 & -\sqrt{\frac{2}{3}} \end{pmatrix} \\ &= \begin{pmatrix} -1 & 0 \\ 0 & -1 \end{pmatrix} \\ &= -1 \times \mathbf{C}^{11} \end{aligned} \quad (\text{A.74})$$

Therefore we deduce that the value of the proportionality coefficients $\left[\begin{matrix} (0) \\ 2 \end{matrix} \beta^{11} (\infty\infty) \right]_{\bar{r},\bar{r}}$ and $\left[\begin{matrix} (0) \\ 2 \end{matrix} \beta^{11} (\ominus\ominus) \right]_{\bar{r},\bar{r}}$ are:

$$\left[\begin{matrix} (0) \\ 2 \end{matrix} \beta^{11} (\infty\infty) \right]_{\bar{r},\bar{r}} = 1 \quad (\text{A.75})$$



$$\left[\begin{matrix} (0) \\ 2 \end{matrix} \beta^{11} (\ominus\ominus) \right]_{\bar{r},\bar{r}} = -1. \quad (\text{A.76})$$



These results are listed in the second column of the top (rr block) table in Table A.4.

We proceed in a similar fashion, performing transformations of $r\gamma$, γr , and $\gamma\gamma$ blocks. The results of these transformations are collected in Table A.4.

For the first-anharmonic-order transformations, only the linear term can be expressed as a matrix equation. Only the **0** sector Clebsch-Gordon is nonzero (it is equal to one). Therefore, there are only two transformations to consider:

$$\mathbf{W}_{\bar{r}}^0 \mathbf{B}(\ominus) = \left[\begin{matrix} (1) \\ 1 \end{matrix} \beta^{\alpha 1} (\ominus) \right]_{\bar{r}}$$

$\left[\begin{smallmatrix} (0) \\ 2 \end{smallmatrix} \beta^{\alpha\alpha}(\mathcal{G}) \right]_{rr}$	00 11
	1 1
	2 -1

$\left[\begin{smallmatrix} (0) \\ 2 \end{smallmatrix} \beta^{\alpha\alpha}(\mathcal{G}) \right]_{\gamma r}$	00 11
	2 1
	1 -1



$\left[\begin{smallmatrix} (0) \\ 2 \end{smallmatrix} \beta^{\alpha\alpha}(\mathcal{G}) \right]_{\gamma\gamma}$	00 11
	1 1
	2 -1

Table A.4: Multipliers of the Clebsch-Gordon coefficients of the harmonic-order transformed binary invariants for $N = 3$

$$\left(\begin{array}{ccc} \frac{1}{\sqrt{3}} & \frac{1}{\sqrt{3}} & \frac{1}{\sqrt{3}} \end{array} \right) \begin{pmatrix} 1 \\ 1 \\ 1 \end{pmatrix} = \sqrt{3} \quad (\text{A.77})$$

and

$$\mathbf{W}_\gamma^0 \mathbf{B}(\bullet \rightarrow) = \left[\begin{smallmatrix} (1) \\ 1 \end{smallmatrix} \beta^{\alpha 1}(\bullet \rightarrow) \right]_\gamma$$

$$\left(\begin{array}{ccc} \frac{1}{\sqrt{2}} & -\frac{1}{\sqrt{2}} & 0 \\ \frac{1}{\sqrt{6}} & \frac{1}{\sqrt{6}} & -\sqrt{\frac{2}{3}} \end{array} \right) \begin{pmatrix} 1 \\ 1 \\ 1 \end{pmatrix} = \sqrt{3}. \quad (\text{A.78})$$

Therefore we deduce that

$$\left[\begin{smallmatrix} (1) \\ 1 \end{smallmatrix} \beta^{\mathbf{0}}(\odot) \right]_{\bar{r}} = \sqrt{3} \quad (\text{A.79})$$

$$\left[\begin{smallmatrix} (1) \\ 1 \end{smallmatrix} \beta^{\mathbf{0}}(\odot) \right]_\gamma = \sqrt{3}. \quad (\text{A.80})$$

For the cubic terms, we lose the ability to express the tensor transformations as a matrix equation.

$$\left[W_{X_1}^{\alpha_1} W_{X_2}^{\alpha_2} W_{X_3}^{\alpha_3} B(\mathcal{G}) \right]_{\xi_1, \xi_2, \xi_3} = \left[\begin{smallmatrix} (1) \\ 3 \end{smallmatrix} \beta^{\alpha_1 \alpha_2 \alpha_3}(\mathcal{G}) \right]_{X_1, X_2, X_3} C_{\xi_1, \xi_2, \xi_3}^{\alpha_1 \alpha_2, \alpha_3}. \quad (\text{A.81})$$

We perform a tensor transformation of the three graphs of the rrr block to the **000**, **110**, and **111** sectors as an example of how the cubic anharmonic order beta multipliers are determined.

First we transform the three binary invariants to the **000** sector. The result must be proportional to the $C^{\mathbf{000}}$ Clebsch-Gordon coefficient (which is simply unity):

$$W_{\bar{r}}^0 W_{\bar{r}}^0 W_{\bar{r}}^0 B(\text{graph}) = \frac{1}{\sqrt{3}} \quad (\text{A.82})$$

$$W_{\bar{r}}^0 W_{\bar{r}}^0 W_{\bar{r}}^0 B(\text{graph}) = 2\sqrt{3} \quad (\text{A.83})$$

$$W_{\bar{r}}^0 W_{\bar{r}}^0 W_{\bar{r}}^0 B(\text{graph}) = \frac{2}{\sqrt{3}} \quad (\text{A.84})$$

We have calculated the beta multipliers for the graphs graph , graph , and graph , which are in the first column of Table A.5. The other columns are determined in a similar manner. This table of multipliers is the $N = 3$ case of the table of multipliers for the general case in Table F.3.




$\left[\begin{smallmatrix} (1) \\ 3 \end{smallmatrix} \beta^{\alpha_1 \alpha_2 \alpha_3, \mathcal{R}}(\mathcal{G}) \right]_{r,r,r}$	000	110, 101, 011	111
	$\frac{1}{\sqrt{3}}$	$\frac{1}{\sqrt{3}}$	1
	$2\sqrt{3}$	0	-3
	$\frac{2}{\sqrt{3}}$	$-\frac{1}{\sqrt{3}}$	2

Table A.5: Multipliers of the $N = 3$ Clebsch-Gordon coefficients of the first-anharmonic-order transformed binary invariants: $\left[\begin{smallmatrix} (1) \\ 3 \end{smallmatrix} \beta^{\alpha_1 \alpha_2 \alpha_3}(\mathcal{G}) \right]_{r,r,r}$.

Below we perform the transformations of these binary invariants to the **110** sector and note the proportionality to the Clebsch-Gordon coefficient. The result is in the second column of Table A.5.

$$\begin{aligned} [W_{\bar{r}}^1 W_{\bar{r}}^1 W_{\bar{r}}^0 B(\text{graph})]_{\xi_1, \xi_2} &= \begin{pmatrix} \begin{pmatrix} \frac{1}{\sqrt{3}} \\ 0 \end{pmatrix} & \begin{pmatrix} 0 \\ \frac{1}{\sqrt{3}} \end{pmatrix} \end{pmatrix}_{\xi_1, \xi_2} \\ &= \frac{1}{\sqrt{3}} C_{\xi_1, \xi_2}^{\mathbf{110}} \end{aligned} \quad (\text{A.85})$$

$$\begin{aligned} [W_{\bar{r}}^1 W_{\bar{r}}^1 W_{\bar{r}}^0 B(\text{graph})]_{\xi_1, \xi_2} &= \begin{pmatrix} \begin{pmatrix} 0 \\ 0 \end{pmatrix} & \begin{pmatrix} 0 \\ 0 \end{pmatrix} \end{pmatrix}_{\xi_1, \xi_2} \\ &= 0 \times C_{\xi_1, \xi_2}^{\mathbf{110}} \end{aligned} \quad (\text{A.86})$$

$$[W_{\bar{r}}^1 W_{\bar{r}}^1 W_{\bar{r}}^0 B(\text{graph})]_{\xi_1, \xi_2} = \begin{pmatrix} \begin{pmatrix} -\frac{1}{\sqrt{3}} \\ 0 \end{pmatrix} & \begin{pmatrix} 0 \\ -\frac{1}{\sqrt{3}} \end{pmatrix} \end{pmatrix}_{\xi_1, \xi_2}$$

$$= -\frac{1}{\sqrt{3}} \times C_{\xi_1, \xi_2}^{\mathbf{110}} \quad (\text{A.87})$$

Below we perform the transformations of these binary invariants to the $\mathbf{111}$ sector, note the proportionality to the Clebsch-Gordon coefficient, obtaining the values in the third column of Table A.5.

$$\begin{aligned} [W_{\bar{r}}^1 W_{\bar{r}}^1 W_{\bar{r}}^1 B(\text{⊗})]_{\xi_1, \xi_2} &= \left(\begin{array}{c} \left(\begin{array}{c} 0 \\ \frac{1}{\sqrt{6}} \\ \frac{1}{\sqrt{6}} \\ 0 \end{array} \right) \\ \left(\begin{array}{c} \frac{1}{\sqrt{6}} \\ 0 \\ 0 \\ -\frac{1}{\sqrt{6}} \end{array} \right) \end{array} \right)_{\xi_1, \xi_2, \xi_3} \\ &= 1 \times C_{\xi_1, \xi_2, \xi_3}^{\mathbf{111}} \end{aligned} \quad (\text{A.88})$$

$$\begin{aligned} [W_{\bar{r}}^1 W_{\bar{r}}^1 W_{\bar{r}}^1 B(\text{⊗} \text{⊙})]_{\xi_1, \xi_2} &= \left(\begin{array}{c} \left(\begin{array}{c} 0 \\ -\sqrt{\frac{3}{2}} \\ -\sqrt{\frac{3}{2}} \\ 0 \end{array} \right) \\ \left(\begin{array}{c} -\sqrt{\frac{3}{2}} \\ 0 \\ 0 \\ \sqrt{\frac{3}{2}} \end{array} \right) \end{array} \right)_{\xi_1, \xi_2, \xi_3} \\ &= -3 \times C_{\xi_1, \xi_2, \xi_3}^{\mathbf{111}} \end{aligned} \quad (\text{A.89})$$

$$\begin{aligned} [W_{\bar{r}}^1 W_{\bar{r}}^1 W_{\bar{r}}^1 B(\text{⊙} \text{⊙} \text{⊙})]_{\xi_1, \xi_2} &= \left(\begin{array}{c} \left(\begin{array}{c} 0 \\ \sqrt{\frac{2}{3}} \\ \sqrt{\frac{2}{3}} \\ 0 \end{array} \right) \\ \left(\begin{array}{c} \sqrt{\frac{2}{3}} \\ 0 \\ 0 \\ -\sqrt{\frac{2}{3}} \end{array} \right) \end{array} \right)_{\xi_1, \xi_2, \xi_3} \\ &= 2 \times C_{\xi_1, \xi_2, \xi_3}^{\mathbf{111}} \end{aligned} \quad (\text{A.90})$$

We could also perform the above transformations on the binary invariants from the γrr , $\gamma \gamma r$, and $\gamma \gamma \gamma$ sectors, obtaining the $N = 3$ case of Tables F.4-F.6.

By transforming the binary-invariant basis to symmetry coordinates, we have effectively performed the transformation of the Hamiltonian coefficient matrices in general (for $N = 3$) to symmetry coordinates (Eq. 5.14) Because all of the complicated N -dependence is entirely contained in the binary invariants and the Clebsch-Gordon coefficients, the transformation to symmetry coordinates brings the N body problem under control.

Comparing the above equations, we can directly write the proportionality coefficients, σ^Q in Eqs. (A.59), (A.63), and (A.67) as a linear combination of these “ $\beta(\mathcal{G})$ multipliers”:

$$\left[\begin{array}{c} (0) \\ 2 \end{array} \sigma_{\alpha_1 \alpha_2}^Q \right]_{X_1, X_2} = \sum_{\mathcal{G}} \begin{array}{c} (0) \\ 2 \end{array} Q(\mathcal{G}) \left[\begin{array}{c} (0) \\ 2 \end{array} \beta^{\alpha_1 \alpha_2}(\mathcal{G}) \right]_{X_1, X_2} \quad (\text{A.91})$$

$$\left[\begin{array}{c} (1) \\ 1 \end{array} \sigma_{\alpha_1}^Q \right]_{X_1} = \sum_{\mathcal{G}} \begin{array}{c} (1) \\ 1 \end{array} Q(\mathcal{G}) \left[\begin{array}{c} (1) \\ 1 \end{array} \beta^{\alpha_1}(\mathcal{G}) \right]_{X_1} \quad (\text{A.92})$$

$$\left[\begin{array}{c} (1) \\ 3 \end{array} \sigma_{\alpha_1 \alpha_2 \alpha_3}^Q \right]_{X_1, X_2, X_3} = \sum_{\mathcal{G}} \begin{array}{c} (1) \\ 3 \end{array} Q(\mathcal{G}) \left[\begin{array}{c} (1) \\ 3 \end{array} \beta^{\alpha_1 \alpha_2 \alpha_3}(\mathcal{G}) \right]_{X_1, X_2, X_3} \quad (\text{A.93})$$

Again we note that, despite the many block labels, these are simple equations with no tensor contraction, only element-by-element multiplication. Recall that the dimensions of σ and therefore $\beta(\mathcal{G})$ do not depend on N : all of the complicated N -dependent index structure is contained within the Clebsch-Gordon coefficient.

In order to code these equations, it is helpful to define an index $\mu_i \in \{\mathbf{0}r, \mathbf{0}\gamma, \mathbf{1}g, \mathbf{1}\gamma\}$ and, with the understanding that the Clebsch Gordon tensor does not depend on the \pm label, write

$$\left[\begin{matrix} (0) \\ 2 \end{matrix} Q_W^{\mu_1 \mu_2} \right]_{\xi_1, \xi_2} = \begin{matrix} (0) \\ 2 \end{matrix} \sigma_{\mu_1, \mu_2}^Q C_{\xi_1, \xi_2}^{\mu_1 \mu_2} \quad (\text{A.94})$$

$$\left[\begin{matrix} (1) \\ 1 \end{matrix} Q_W^\mu \right]_\xi = \begin{matrix} (1) \\ 1 \end{matrix} \sigma_\mu^Q \quad (\text{A.95})$$

$$\left[\begin{matrix} (1) \\ 3 \end{matrix} Q_W^{\mu_1 \mu_2 \mu_3} \right]_{\xi_1, \xi_2, \xi_3} = \begin{matrix} (1) \\ 3 \end{matrix} \sigma_{\mu_1, \mu_2, \mu_3}^Q C_{\xi_1, \xi_2, \xi_3}^{\mu_1 \mu_2, \mu_3, k}. \quad (\text{A.96})$$

In the above equations, μ_i runs from 1 to 4 for $N = 3$, and from 1 to 5 in the general case. Therefore, all the physical information is contained within the σ tensors, the largest of which is $\begin{matrix} (1) \\ 3 \end{matrix} \sigma_{\mu_1, \mu_2, \mu_3}^Q$, a $4 \times 4 \times 4$ tensor.

It still remains to complete the transformation to normal coordinates (Eq. 5.13), but this does not depend on N . The transformation \mathcal{C} (Eq. A.54) from symmetry coordinates to normal coordinates for $N = 3$ (Eq. A.54) is only different from the general case in that it is a 4×4 matrix, rather than a 5×5 matrix in the general case. Performing the transformation to normal coordinates, we finally obtain the DPT perturbation expansion of the N -body Hamiltonian to first harmonic order:

$$\bar{H}_0 = -\frac{1}{2} \left[\begin{matrix} (0) \\ 2 \end{matrix} G_V \right]_{\nu_1, \nu_2} \partial_{q'_{\nu_1}} \partial_{q'_{\nu_2}} + \begin{matrix} (0) \\ 0 \end{matrix} F_V + \frac{1}{2} \left[\begin{matrix} (0) \\ 2 \end{matrix} F_V \right]_{\nu_1, \nu_2} q'_{\nu_1} q'_{\nu_2} \quad (\text{A.97})$$

and

$$\bar{H}_1 = -\frac{1}{2} \left[\begin{matrix} (1) \\ 3 \end{matrix} G_V \right]_{\nu_1, \nu_2, \nu_3} q'_{\nu_1} \partial_{q'_{\nu_2}} \partial_{q'_{\nu_3}} + \frac{1}{3!} \left[\begin{matrix} (1) \\ 3 \end{matrix} F \right]_{\nu_1, \nu_2, \nu_3} q'_{\nu_1} q'_{\nu_2} q'_{\nu_3} \quad (\text{A.98})$$

$$-\frac{1}{2} \left[\begin{matrix} (1) \\ 1 \end{matrix} G_V \right]_\nu \partial_{q'_\nu} + \left[\begin{matrix} (1) \\ 1 \end{matrix} F \right]_\nu q'_\nu. \quad (\text{A.99})$$

Having analytically transformed the Hamiltonian to normal coordinates, the calculation of the wavefunction is relatively simple and does not implicitly depend on N . The wavefunction is derived in Appendix G.

Appendix B

A Note on Index Notation

In this work, I attempt to keep indicial “clutter” to a minimum by use of an index symbol convention. We reserve the index symbols ν, η for use where the range is that of the internal coordinate y'_ν vector, that is $1 \leq \nu \leq N(N+1)/2$. All of the column vectors ($\bar{\mathbf{y}}'$, \mathbf{S} , and \mathbf{q}') and tensors (F , G , and FG in each coordinate basis), may be expressed using these indices. Because these column vectors and tensors have a block form, it is often convenient to adopt a notation whereby ν or η is replaced by more than one index.

Note that the column vectors and tensors in the symmetry coordinate basis can be represented by block labels that are a combination of the irreducible representation labels $\alpha = [N], [N-1, 1], [N-2, 2]$ and coordinate block labels $X = r, \gamma$. For instance, the symmetry coordinate \mathbf{S} has this block structure:

$$\mathbf{S} = \begin{pmatrix} \mathbf{S}_r^{[N]} \\ \mathbf{S}_\gamma^{[N]} \\ \hline \mathbf{S}_r^{[N-1, 1]} \\ \mathbf{S}_\gamma^{[N-1, 1]} \\ \hline \mathbf{S}_\gamma^{[N-2, 2]} \end{pmatrix}.$$

Each block is a column vector with an index for which we reserve the symbol ξ . With this convention, we write

$$S_\nu = [S_X^\alpha]_\xi,$$

where it is understood that there is a (bijective) mapping between ν and $\{\alpha, X, \xi\}$ which we express in Table B.1.

This notation is convenient for addressing individual blocks, but for contracting over all elements of \mathbf{S} , it is convenient to introduce yet another convention: combining the block labels α and X to form a single block index μ which ranges from 1 to 5:

$$\mu \in \{\mathbf{0}r, \mathbf{0}\gamma, \mathbf{1}r, \mathbf{1}\gamma, \mathbf{2}\}$$

(where $\mathbf{0}$, $\mathbf{1}$, and $\mathbf{2}$ are shorthand for the $[N]$, $[N-1, 1]$, and $[N-2, 2]$ irreps, respectively). Thus the following ways to express the block structure of a coordinate (such as S_ν) will be understood to be equivalent:

$$S_\nu = [S_X^\alpha]_\xi = [S_\mu]_\xi. \quad (\text{B.1})$$

ν, η	α	X	ξ	μ
1	0	r	1	0r
2	0	γ	1	0γ
3	1	r	1	1r
4	1	r	2	1r
\vdots			\vdots	
$N + 1$	1	r	$N - 1$	1r
$N + 2$	1	γ	1	1γ
$N + 3$	1	γ	2	1γ
\vdots			\vdots	
$2N$	1	γ	$N - 1$	1γ
$2N + 1$	2	γ	1	2
\vdots			\vdots	
$N(N + 1)/2$	2	γ	$N(N - 3)/2$	2

Table B.1: Mapping between ν , η , (α , X , and ξ), and μ labels for quantities in the symmetry coordinate basis.

In the normal-coordinate basis, the vectors and tensors have a slightly different block form which we label by α and $Y = \pm$, the mappings for which we present in Table B.2.

Again, it is sometimes convenient to adopt a compact notation and represent the both block labels $\{\alpha, Y\}$ by a single block index, for which we also reserve the index μ :

$$\mu \in \{\mathbf{0}^+, \mathbf{0}^-, \mathbf{1}^+, \mathbf{1}^-, \mathbf{2}\}.$$

Whether the index μ represents elements of $\{\mathbf{0}r, \mathbf{0}\gamma, \mathbf{1}r, \mathbf{1}\gamma, \mathbf{2}\}$ or $\{\mathbf{0}^+, \mathbf{0}^-, \mathbf{1}^+, \mathbf{1}^-, \mathbf{2}\}$ will be clear by whether the quantity is in the basis of symmetry coordinates or normal coordinates.

These symbols have been used to label the normal-mode frequencies in References (81; 82; 87; 90), and to label the normal-mode vectors in References (87; 90). The indices ν , η , α , X , Y , ξ , and μ will be reserved for these conventions alone and will be employed with this understanding.

ν, η	α	Y	ξ	μ
1	0	+	1	0+
2	0	-	1	0-
3	1	+	1	1+
4	1	+	2	1+
\vdots			\vdots	
$N+1$	1	+	$N-1$	1+
$N+2$	1	-	1	1-
$N+3$	1	-	2	1-
\vdots			\vdots	
$2N$	1	-	$N-1$	1-
$2N+1$	2		1	2
\vdots			\vdots	
$N(N+1)/2$	2		$N(N-3)/2$	2

Table B.2: Mapping between ν , η , (α , Y , and ξ), and μ labels for quantities in the normal-coordinate basis.

Appendix C

Binary invariants

In section C.1, I introduce a method by which a closed-form expression for the binary invariants is constructed. In section C.2, I report the closed-form expressions for the binary invariants. In section C.3, I provide a correspondence between binary invariants and previous work.

C.1 Construction of binary invariants

To calculate an actual expression for the binary invariants of a particular graph requires careful thought about the various combinations of indices which correspond to that graph. I introduce a symbolic construction procedure, analogous to the numerical tensor construction previously introduced, which can generate symbolic closed form binary invariants. I generate binary invariants in terms of the Kronecker delta function, but first I must define two types of graphs.

Definition 5 *A vertex-labeled graph is a graph for which each vertex is associated with a label (as opposed to an edge-labeled graph).*

For example, $\bigcirc^k \downarrow_j^i$ is a vertex-labeled graph.

Definition 6 *The complement to a graph G is a graph G' with the same set of vertices as G but whose edge set is the complement to the edge set of G*

For example, $\begin{array}{c} \nearrow^i \\ \searrow_j \end{array}$ is the complement to $\bigcirc^k \downarrow_j^i$.

C.1.1 The recipe

Here I provide a recipe for the construction of the binary invariants for a particular set of graphs with the same number of edges. These sets were labeled by elements of the list \mathbb{G}_{block} in Eqs. (4.18), (4.20), and (4.23). Recall that each block of a rank- R DPT Hamiltonian coefficient matrix is decomposed into a basis of binary invariants, labeled by graphs which have R edges.

I construct the set of binary invariants for the set of graphs \mathbb{G}_{block} as follows:

1. Draw the completely disconnected graph in \mathbb{G}_{block} , and label the vertices i, j, \dots . Equivalently, draw vertex-labeled graphs for each coordinate in the block (a one vertex loop for r_i and an edge for $\gamma_{i,j}$).
2. Construct all possible vertex-labeled graphs by combining one or more vertices in the above graph
3. Construct vertex-labeled graph complements for each of the above
4. Form “primitive binary invariants” by associating a product of the following with each graph/graph complement pair:
 - $\delta_{i,k}$ for each pair of “combined” vertices;
 - $(1 - \delta_{j,l})$ for each edge $\{j,l\}$ in the graph or in the graph complement.
5. The binary invariant for the equivalence class (represented by an unlabeled graph) is given by the sum over label permutations of primitive binary invariants of the isomorphic vertex-labeled graphs.

C.1.2 Examples: harmonic-order graphs

As an example of the above recipe, I compute the binary invariants for each block of the harmonic-order graphs for each block (rr , $r\gamma$, γr , and $\gamma\gamma$), showing each step.

C.1.2.1 The rr block

In the first step, I write the vertex-labeled graph elements $\circlearrowleft i$ and $\circlearrowright j$. In steps 2-4, I construct the graphs, graph complements, and primitive binary invariants in the table below.

Graph	Complement	Primitive binary invariant
$\circlearrowleft i = j$	$\overset{i=j}{\bullet}$	$\delta_{i,j}$
$\circlearrowright i \circlearrowright j$	$\overset{i \quad j}{\bullet \text{---} \bullet}$	$1 - \delta_{i,j}$

Finally, in the fifth step, I form the binary invariant by summing over the primitive binary invariants for each set of isomorphic graphs. In this case, each set has only one element, so we obtain the binary invariants for the rr block:

$$[B(\circlearrowleft \circlearrowleft)]_{i,j} = \delta_{i,j} \tag{C.1}$$

$$[B(\circlearrowright \circlearrowright)]_{i,j} = 1 - \delta_{i,j}. \tag{C.2}$$

C.1.2.2 The γr and $r\gamma$ blocks

I start with the vertex-labeled graph elements $\overset{i \quad j}{\bullet \text{---} \bullet}$ and $\circlearrowright k$. Next I perform steps 2-4 in the table below.

Graph	Complement	Primitive binary invariant
		$(1 - \delta_{i,j})\delta_{i,k}$
		$(1 - \delta_{i,j})\delta_{j,k}$
		$(1 - \delta_{i,j})(1 - \delta_{i,k})(1 - \delta_{j,k})$

Summing over permutations of the primitive binary invariants, I obtain

$$[B(\text{circle with dot})]_{(ij),k} = (1 - \delta_{i,j})(\delta_{i,k} + \delta_{j,k}) \quad (\text{C.3})$$

$$[B(\text{circle with two dots})]_{(ij),k} = (1 - \delta_{i,j})(1 - \delta_{i,k})(1 - \delta_{j,k}). \quad (\text{C.4})$$

C.1.2.3 The $\gamma\gamma$ block

I start with the elements and . Next I perform steps 2-4 in the table below.

Graph	Complement	Primitive binary invariant
		$(1 - \delta_{i,j})(1 - \delta_{k,l})\delta_{i,k}\delta_{j,l}$
		$(1 - \delta_{i,j})(1 - \delta_{k,l})\delta_{i,l}\delta_{j,k}$
		$(1 - \delta_{i,j})(1 - \delta_{k,l})\delta_{j,k}(1 - \delta_{i,l})$
		$(1 - \delta_{i,j})(1 - \delta_{k,l})\delta_{j,l}(1 - \delta_{i,k})$
		$(1 - \delta_{i,j})(1 - \delta_{k,l})\delta_{i,k}(1 - \delta_{j,l})$
		$(1 - \delta_{i,j})(1 - \delta_{k,l})\delta_{i,l}(1 - \delta_{j,k})$
		$(1 - \delta_{i,j})(1 - \delta_{k,l})(1 - \delta_{i,l})(1 - \delta_{i,k})(1 - \delta_{j,l})(1 - \delta_{j,k})$

Summing over permutations of the primitive binary invariants, I obtain

$$[B(\text{circle with two dots})]_{(ij),(kl)} = (1 - \delta_{i,j})(1 - \delta_{k,l})(\delta_{i,k}\delta_{j,l} + \delta_{i,l}\delta_{j,k}) \quad (\text{C.5})$$

$$[B(\text{two dots})]_{(ij),(kl)} = (1 - \delta_{i,j})(1 - \delta_{k,l})(\delta_{j,k}(1 - \delta_{i,l}) + \delta_{j,l}(1 - \delta_{i,k}) + \delta_{i,k}(1 - \delta_{j,l}) + \delta_{i,l}(1 - \delta_{j,k})) \quad (\text{C.6})$$

$$[B(\text{two dots with lines})]_{(ij),(kl)} = (1 - \delta_{i,j})(1 - \delta_{k,l})(1 - \delta_{i,l})(1 - \delta_{i,k})(1 - \delta_{j,l})(1 - \delta_{j,k}). \quad (\text{C.7})$$

C.2 Results: binary invariants in closed form

C.2.1 Harmonic order

Here I summarize the harmonic-order binary invariants calculated previously.

$$[B(\textcircled{\circ}\textcircled{\circ})]_{i,j} = \delta_{i,j} \quad (\text{C.8})$$

$$[B(\textcircled{\circ}\textcircled{\circ})]_{i,j} = 1 - \delta_{i,j}. \quad (\text{C.9})$$

$$[B(\textcircled{\circ}\textcircled{\rightarrow})]_{(ij),k} = (1 - \delta_{i,j})(\delta_{i,k} + \delta_{j,k}) \quad (\text{C.10})$$

$$[B(\textcircled{\circ}\textcircled{\rightarrow})]_{(ij),k} = (1 - \delta_{i,j})(1 - \delta_{i,k})(1 - \delta_{j,k}) \quad (\text{C.11})$$

$$[B(\textcircled{\circ}\textcircled{\rightarrow})]_{(ij),(kl)} = (1 - \delta_{i,j})(1 - \delta_{k,l})(\delta_{i,k}\delta_{j,l} + \delta_{i,l}\delta_{j,k}) \quad (\text{C.12})$$

$$[B(\textcircled{\circ}\textcircled{\rightarrow})]_{(ij),(kl)} = (1 - \delta_{i,j})(1 - \delta_{k,l})(\delta_{i,l}(1 - \delta_{j,k}) + (1 - \delta_{i,l})\delta_{j,k} + \delta_{i,k}(1 - \delta_{j,l}) + (1 - \delta_{i,k})\delta_{j,l}) \quad (\text{C.13})$$

$$[B(\textcircled{\circ}\textcircled{\rightarrow})]_{(ij),(kl)} = (1 - \delta_{i,j})(1 - \delta_{k,l})(1 - \delta_{i,l})(1 - \delta_{i,k})(1 - \delta_{j,l})(1 - \delta_{j,k}) \quad (\text{C.14})$$

C.2.2 First anharmonic order

I follow the same procedure to obtain the binary invariants for graphs occurring at first anharmonic order.

C.2.2.1 Rank-one blocks r and γ

The rank-one binary invariants $B(\textcircled{\circ})$ and $B(\textcircled{\rightarrow})$ are simply row vectors of ones with length N and $N(N - 1)/2$, respectively:

$$[B(\textcircled{\circ})]_i = 1$$

$$B(\textcircled{\circ}) = (1, 1, \dots, 1) \quad (\text{C.15})$$

$$[B(\textcircled{\rightarrow})]_{(ij)} = (1 - \delta_{i,j}) \quad (\text{where } i < j)$$

$$B(\textcircled{\rightarrow}) = (1, 1, \dots, 1). \quad (\text{C.16})$$

C.2.2.2 Rank-three Sector rrr

For operations on three graph vertices, I have three representative graphs and their associated invariants.

$$[B(\textcircled{\circ}\textcircled{\circ})]_{i,j,k} = \delta_{i,j,k} \quad (\text{C.17})$$

$$[B(\textcircled{\circ}\textcircled{\circ})]_{i,j,k} = \delta_{i,j}(1 - \delta_{i,k}) + (1 - \delta_{i,j})\delta_{i,k} + (1 - \delta_{j,i})\delta_{j,k} \quad (\text{C.18})$$

$$[B(\textcircled{\circ}\textcircled{\circ})]_{i,j,k} = (1 - \delta_{i,j})(1 - \delta_{i,k})(1 - \delta_{j,k}) \quad (\text{C.19})$$

C.2.2.3 Rank-three Sector γrr

For operations on one graph edge and two graph vertices, I have five representative graphs and associated invariants.

$$[B(\text{Diagram 1})]_{(ij),k,l} = (1 - \delta_{i,j}) \delta_{i,k} \delta_{i,l} + (1 - \delta_{i,j}) \delta_{j,k} \delta_{j,l} \quad (\text{C.20})$$

$$[B(\text{Diagram 2})]_{(ij),k,l} = (1 - \delta_{i,j}) \delta_{i,l} \delta_{j,k} + (1 - \delta_{i,j}) \delta_{i,k} \delta_{j,l} \quad (\text{C.21})$$

$$[B(\text{Diagram 3})]_{(ij),k,l} = (1 - \delta_{i,j}) ((1 - \delta_{i,l}) (\delta_{i,k} + \delta_{j,k}) (1 - \delta_{j,l}) + (1 - \delta_{i,k}) (1 - \delta_{j,k}) (\delta_{i,l} + \delta_{j,l})) \quad (\text{C.22})$$

$$[B(\text{Diagram 4})]_{(ij),k,l} = (1 - \delta_{i,j}) (1 - \delta_{i,k}) (1 - \delta_{j,k}) \delta_{k,l} \quad (\text{C.23})$$

$$[B(\text{Diagram 5})]_{(ij),k,l} = (1 - \delta_{i,j}) (1 - \delta_{i,k}) (1 - \delta_{i,l}) (1 - \delta_{j,k}) (1 - \delta_{j,l}) \times (1 - \delta_{k,l}) \quad (\text{C.24})$$

C.2.2.4 Rank-three Sector $\gamma\gamma r$

For operations on two graph edges and one graph vertex, I have seven representative graphs and their associated invariants.

$$[B(\text{Diagram 1})]_{(ij),(kl),m} = (1 - \delta_{i,j})(1 - \delta_{k,l})(\delta_{i,l}\delta_{j,k} + \delta_{i,k}\delta_{j,l})(\delta_{i,m} + \delta_{j,m}) \quad (\text{C.25})$$

$$[B(\text{Diagram 2})]_{(ij),(kl),m} = (1 - \delta_{i,j})(1 - \delta_{k,l})(1 - \delta_{m,i})(1 - \delta_{m,j}) \times \quad (\text{C.26})$$

$$(\delta_{i,l}\delta_{j,k} + \delta_{i,k}\delta_{j,l}) \quad (\text{C.27})$$

$$[B(\text{Diagram 3})]_{(ij),(kl),m} = (1 - \delta_{i,j})(1 - \delta_{k,l}) (\delta_{i,l}(1 - \delta_{j,k})\delta_{m,i} + \delta_{i,k}(1 - \delta_{j,l})\delta_{m,i} + (1 - \delta_{i,l})\delta_{j,k}\delta_{m,j} + (1 - \delta_{i,k})\delta_{j,l}\delta_{m,j}) \quad (\text{C.28})$$

$$[B(\text{Diagram 4})]_{(ij),(kl),m} = (1 - \delta_{i,j})(1 - \delta_{k,l}) ((1 - \delta_{i,k})\delta_{j,l}(\delta_{i,m} + \delta_{k,m}) + \delta_{i,l}(1 - \delta_{j,k})(\delta_{j,m} + \delta_{k,m}) + (1 - \delta_{i,l})\delta_{j,k}(\delta_{i,m} + \delta_{l,m}) + \delta_{i,k}(1 - \delta_{j,l})(\delta_{j,m} + \delta_{l,m})) \quad (\text{C.29})$$

$$[B(\text{Diagram 5})]_{(ij),(kl),m} = (1 - \delta_{i,j})(1 - \delta_{m,j})(1 - \delta_{m,k})(1 - \delta_{m,l})(1 - \delta_{k,l}) \times ((1 - \delta_{m,i})\delta_{i,l}(1 - \delta_{j,k}) + \delta_{j,k}(1 - \delta_{i,l}) + \delta_{i,k}(1 - \delta_{j,l}) + (1 - \delta_{i,k})\delta_{j,l}) \quad (\text{C.30})$$

$$[B(\text{Diagram 6})]_{(ij),(kl),m} = (1 - \delta_{i,j})(1 - \delta_{i,k})(1 - \delta_{i,l})(1 - \delta_{j,k})(1 - \delta_{j,l})(1 - \delta_{k,l}) (\delta_{m,i} + \delta_{m,j} + \delta_{m,k} + \delta_{m,l}) \quad (\text{C.31})$$

$$[B(\text{Diagram 7})]_{(ij),(kl),m} = (1 - \delta_{i,j})(1 - \delta_{i,k})(1 - \delta_{i,l})(1 - \delta_{j,k})(1 - \delta_{j,l}) (1 - \delta_{k,l})(1 - \delta_{m,i})(1 - \delta_{m,j})(1 - \delta_{m,k})(1 - \delta_{m,l}) \quad (\text{C.32})$$

C.2.2.5 Rank-three Sector $\gamma\gamma\gamma$

$$[B(\text{Diagram 1})]_{(ij),(kl),(mn)} = (1 - \delta_{i,j})(1 - \delta_{k,l}) \times (1 - \delta_{m,n})(\delta_{i,l}\delta_{j,k} + \delta_{i,k}\delta_{j,l})(\delta_{i,n}\delta_{j,m} + \delta_{i,m}\delta_{j,n}) \quad (\text{C.33})$$

$$[B(\text{Diagram 2})]_{(ij),(kl),(mn)} = (1 - \delta_{i,j})(1 - \delta_{k,l}) \times (1 - \delta_{m,n})(\delta_{j,l}\delta_{k,n}\delta_{m,i} + \delta_{j,k}\delta_{l,n}\delta_{m,i} + \delta_{i,l}\delta_{k,n}\delta_{m,j} + \delta_{i,k}\delta_{l,n}\delta_{m,j} + \delta_{j,l}\delta_{k,m}\delta_{n,i} + \delta_{j,k}\delta_{l,m}\delta_{n,i} + \delta_{i,l}\delta_{k,m}\delta_{n,j} + \delta_{i,k}\delta_{l,m}\delta_{n,j}) \quad (\text{C.34})$$

$$[B(\text{Diagram 3})]_{(ij),(kl),(mn)} = (1 - \delta_{i,j})(1 - \delta_{k,l})(1 - \delta_{m,n}) \times \quad (\text{C.35})$$

$$\begin{aligned}
& \times ((\delta_{i,m}\delta_{j,n} + \delta_{i,n}\delta_{j,m})(\delta_{i,k}(1 - \delta_{j,l}) + \delta_{i,l}(1 - \delta_{j,k}) + \delta_{j,k}(1 - \delta_{i,l}) + \delta_{j,l}(1 - \delta_{i,k})) \\
& + (\delta_{i,k}\delta_{j,l} + \delta_{i,l}\delta_{j,k})(\delta_{i,m}(1 - \delta_{j,n}) + \delta_{i,n}(1 - \delta_{j,m}) + \delta_{j,m}(1 - \delta_{i,n}) + \delta_{j,n}(1 - \delta_{i,m})) \\
& + (\delta_{k,m}\delta_{l,n} + \delta_{k,n}\delta_{l,m})(\delta_{k,i}(1 - \delta_{l,j}) + \delta_{k,j}(1 - \delta_{l,i}) + \delta_{l,i}(1 - \delta_{k,j}) + \delta_{l,j}(1 - \delta_{k,i}))
\end{aligned}$$

$$\begin{aligned}
[B(\text{---}\blacksquare)]_{(ij),(kl),(mn)} &= (1 - \delta_{i,j})(1 - \delta_{k,l})(1 - \delta_{m,n}) \times \\
& (\delta_{j,l}\delta_{j,n}(1 - \delta_{i,k})(1 - \delta_{k,m})(1 - \delta_{m,i}) \\
& + \delta_{j,k}\delta_{j,n}(1 - \delta_{i,l})(1 - \delta_{l,m})(1 - \delta_{m,i}) + \delta_{i,l}\delta_{i,n}(1 - \delta_{j,k})(1 - \delta_{k,m})(1 - \delta_{m,j}) \\
& + \delta_{i,k}\delta_{i,n}(1 - \delta_{j,l})(1 - \delta_{l,m})(1 - \delta_{m,j}) + \delta_{j,l}\delta_{j,m}(1 - \delta_{i,k})(1 - \delta_{k,n})(1 - \delta_{n,i}) \\
& + \delta_{j,k}\delta_{j,m}(1 - \delta_{i,l})(1 - \delta_{l,n})(1 - \delta_{n,i}) + \delta_{i,l}\delta_{i,m}(1 - \delta_{j,k})(1 - \delta_{k,n})(1 - \delta_{n,j}) \\
& + \delta_{i,k}\delta_{i,m}(1 - \delta_{j,l})(1 - \delta_{l,n})(1 - \delta_{n,j}))
\end{aligned} \tag{C.36}$$

$$\begin{aligned}
[B(\blacksquare)]_{(ij),(kl),(mn)} &= \\
& (1 - \delta_{i,j})(1 - \delta_{k,l})(1 - \delta_{m,n})(\delta_{i,n}\delta_{m,l}(1 - \delta_{j,m})(1 - \delta_{j,k})(1 - \delta_{i,k}) \\
& + \delta_{i,m}\delta_{n,l}(1 - \delta_{j,n})(1 - \delta_{j,k})(1 - \delta_{i,k}) + \delta_{i,n}\delta_{m,k}(1 - \delta_{j,m})(1 - \delta_{j,l})(1 - \delta_{i,l}) \\
& + \delta_{i,m}\delta_{n,k}(1 - \delta_{j,n})(1 - \delta_{j,l})(1 - \delta_{i,l}) + \delta_{i,l}\delta_{k,n}(1 - \delta_{j,k})(1 - \delta_{j,m})(1 - \delta_{i,m}) \\
& + \delta_{i,k}\delta_{l,n}(1 - \delta_{j,l})(1 - \delta_{j,m})(1 - \delta_{i,m}) + \delta_{i,l}\delta_{k,m}(1 - \delta_{j,k})(1 - \delta_{j,n})(1 - \delta_{i,n}) \\
& + \delta_{i,k}\delta_{l,m}(1 - \delta_{j,l})(1 - \delta_{j,n})(1 - \delta_{i,n}) + \delta_{j,n}\delta_{m,l}(1 - \delta_{i,m})(1 - \delta_{i,k})(1 - \delta_{j,k}) \\
& + \delta_{j,m}\delta_{n,l}(1 - \delta_{i,n})(1 - \delta_{i,k})(1 - \delta_{j,k}) + \delta_{j,n}\delta_{m,k}(1 - \delta_{i,m})(1 - \delta_{i,l})(1 - \delta_{j,l}) \\
& + \delta_{j,m}\delta_{n,k}(1 - \delta_{i,n})(1 - \delta_{i,l})(1 - \delta_{j,l}) + \delta_{j,l}\delta_{k,n}(1 - \delta_{i,k})(1 - \delta_{i,m})(1 - \delta_{j,m}) \\
& + \delta_{j,k}\delta_{l,n}(1 - \delta_{i,l})(1 - \delta_{i,m})(1 - \delta_{j,m}) + \delta_{j,l}\delta_{k,m}(1 - \delta_{i,k})(1 - \delta_{i,n})(1 - \delta_{j,n}) \\
& + \delta_{j,k}\delta_{l,m}(1 - \delta_{i,l})(1 - \delta_{i,n})(1 - \delta_{j,n}) + \delta_{k,j}\delta_{i,n}(1 - \delta_{l,i})(1 - \delta_{l,m})(1 - \delta_{k,m}) \\
& + \delta_{k,i}\delta_{j,n}(1 - \delta_{l,j})(1 - \delta_{l,m})(1 - \delta_{k,m}) + \delta_{k,j}\delta_{i,m}(1 - \delta_{l,i})(1 - \delta_{l,n})(1 - \delta_{k,n}) \\
& + \delta_{k,i}\delta_{j,m}(1 - \delta_{l,j})(1 - \delta_{l,n})(1 - \delta_{k,n}) + \delta_{l,j}\delta_{i,n}(1 - \delta_{k,i})(1 - \delta_{k,m})(1 - \delta_{l,m}) \\
& + \delta_{l,i}\delta_{j,n}(1 - \delta_{k,j})(1 - \delta_{k,m})(1 - \delta_{l,m}) + \delta_{l,j}\delta_{i,m}(1 - \delta_{k,i})(1 - \delta_{k,n})(1 - \delta_{l,n}) \\
& + \delta_{l,i}\delta_{j,m}(1 - \delta_{k,j})(1 - \delta_{k,n})(1 - \delta_{l,n}))
\end{aligned} \tag{C.37}$$

$$\begin{aligned}
[B(\text{---}\circ)]_{(ij),(kl),(mn)} &= (1 - \delta_{i,j})(1 - \delta_{k,l})(1 - \delta_{m,n}) \times \\
& (\delta_{k,n}\delta_{l,m}(1 - \delta_{i,k})(1 - \delta_{i,l})(1 - \delta_{j,k})(1 - \delta_{j,l}) \\
& + \delta_{k,m}\delta_{l,n}(1 - \delta_{i,k})(1 - \delta_{i,l})(1 - \delta_{j,k})(1 - \delta_{j,l}) \\
& + \delta_{m,j}\delta_{n,i}(1 - \delta_{k,m})(1 - \delta_{k,n})(1 - \delta_{l,m})(1 - \delta_{l,n}) \\
& + \delta_{m,i}\delta_{n,j}(1 - \delta_{k,m})(1 - \delta_{k,n})(1 - \delta_{l,m})(1 - \delta_{l,n}) \\
& + \delta_{i,l}\delta_{j,k}(1 - \delta_{m,i})(1 - \delta_{m,j})(1 - \delta_{n,i})(1 - \delta_{n,j}) \\
& + \delta_{i,k}\delta_{j,l}(1 - \delta_{m,i})(1 - \delta_{m,j})(1 - \delta_{n,i})(1 - \delta_{n,j}))
\end{aligned} \tag{C.38}$$

$$\begin{aligned}
[B(\text{---}\blacksquare)]_{(ij),(kl),(mn)} &= (1 - \delta_{i,j})(1 - \delta_{k,l})(1 - \delta_{m,n}) \times \\
& (\delta_{l,m}(1 - \delta_{k,n})(1 - \delta_{k,i})(1 - \delta_{k,j})(1 - \delta_{n,i})(1 - \delta_{n,j})(1 - \delta_{i,l})(1 - \delta_{j,m}) \\
& + \delta_{k,m}(1 - \delta_{l,n})(1 - \delta_{l,i})(1 - \delta_{l,j})(1 - \delta_{n,i})(1 - \delta_{n,j})(1 - \delta_{i,k})(1 - \delta_{j,m}) \\
& + \delta_{l,n}(1 - \delta_{k,m})(1 - \delta_{k,i})(1 - \delta_{k,j})(1 - \delta_{m,i})(1 - \delta_{m,j})(1 - \delta_{i,l})(1 - \delta_{j,n}) \\
& + \delta_{k,n}(1 - \delta_{l,m})(1 - \delta_{l,i})(1 - \delta_{l,j})(1 - \delta_{m,i})(1 - \delta_{m,j})(1 - \delta_{i,k})(1 - \delta_{j,n}) \\
& + \delta_{n,i}(1 - \delta_{m,j})(1 - \delta_{m,k})(1 - \delta_{m,l})(1 - \delta_{j,k})(1 - \delta_{j,l})(1 - \delta_{k,n})(1 - \delta_{l,i}) \\
& + \delta_{m,i}(1 - \delta_{n,j})(1 - \delta_{n,k})(1 - \delta_{n,l})(1 - \delta_{j,k})(1 - \delta_{j,l})(1 - \delta_{k,m})(1 - \delta_{l,i}) \\
& + \delta_{n,j}(1 - \delta_{m,i})(1 - \delta_{m,k})(1 - \delta_{m,l})(1 - \delta_{i,k})(1 - \delta_{i,l})(1 - \delta_{k,n})(1 - \delta_{l,j}) \\
& + \delta_{m,j}(1 - \delta_{n,i})(1 - \delta_{n,k})(1 - \delta_{n,l})(1 - \delta_{i,k})(1 - \delta_{i,l})(1 - \delta_{k,m})(1 - \delta_{l,j}) \\
& + \delta_{j,k}(1 - \delta_{i,l})(1 - \delta_{i,m})(1 - \delta_{i,n})(1 - \delta_{l,m})(1 - \delta_{l,n})(1 - \delta_{m,j})(1 - \delta_{n,k})
\end{aligned} \tag{C.39}$$

$$\begin{aligned}
& +\delta_{i,k}(1-\delta_{j,l})(1-\delta_{j,m})(1-\delta_{j,n})(1-\delta_{l,m})(1-\delta_{l,n})(1-\delta_{m,i})(1-\delta_{n,k}) \\
& +\delta_{j,l}(1-\delta_{i,k})(1-\delta_{i,m})(1-\delta_{i,n})(1-\delta_{k,m})(1-\delta_{k,n})(1-\delta_{m,j})(1-\delta_{n,l}) \\
& +\delta_{i,l}(1-\delta_{j,k})(1-\delta_{j,m})(1-\delta_{j,n})(1-\delta_{k,m})(1-\delta_{k,n})(1-\delta_{m,i})(1-\delta_{n,l})
\end{aligned}$$

$$\begin{aligned}
[B(\equiv)]_{(ij),(kl),(mn)} &= (1-\delta_{i,j})(1-\delta_{k,l})(1-\delta_{m,n})(1-\delta_{i,l})(1-\delta_{i,k}) \times \\
& (1-\delta_{i,m})(1-\delta_{i,n})(1-\delta_{j,k})(1-\delta_{j,l})(1-\delta_{j,m})(1-\delta_{j,n})(1-\delta_{k,n})(1-\delta_{k,m}) \\
& (1-\delta_{l,m})(1-\delta_{l,n}) \tag{C.40}
\end{aligned}$$

There is only one case in the present formalism where it is necessary to distinguish between edges. In Sec D.3, I show that there is one graph $\bullet \circ \bullet$ for which I must distinguish between edges. The binary invariant for the unlabeled graph $B(\bullet \circ \bullet)$ is really the sum of two binary invariants for edge-labeled graphs with two edges to be distinguished (by vertical tic marks) from the third:

$$B(\bullet \circ \bullet) = B(\bullet \overset{\circ}{\circ} \bullet) + B(\bullet \underset{\circ}{\circ} \bullet) \tag{C.41}$$

where

$$\begin{aligned}
[B(\bullet \overset{\circ}{\circ} \bullet)]_{(ij),(kl),(mn)} &= (\delta_{i,k}\delta_{j,l} + \delta_{i,l}\delta_{j,k} + \delta_{i,m}\delta_{j,n} + \delta_{i,n}\delta_{j,m}) \\
& \times (\delta_{k,m}(1-\delta_{l,n}) + \delta_{k,n}(1-\delta_{l,m}) + \delta_{l,m}(1-\delta_{k,n}) + \delta_{l,n}(1-\delta_{k,m}) \tag{C.42}
\end{aligned}$$

$$\begin{aligned}
[B(\bullet \underset{\circ}{\circ} \bullet)]_{(ij),(kl),(mn)} &= (\delta_{k,m}\delta_{l,n} + \delta_{k,n}\delta_{l,m}) (\delta_{i,k}(1-\delta_{j,l}) + \delta_{i,l}(1-\delta_{j,k}) \\
& + \delta_{j,k}(1-\delta_{i,l}) + \delta_{j,l}(1-\delta_{i,k})) . \tag{C.43}
\end{aligned}$$

C.3 Extension of previous work

In previous work (87; 81; 82; 90), the unique values of the Hamiltonian (Eq. 3.38) (each with its own equivalence class of matrix elements) were not labeled by a graph. The present formulation of DPT is a generalization of previous work (81; 87; 90) to higher orders. I have defined “binary invariants”, which are a generalization of the use of structural matrices in (81), and I now employ an extensible notation using graphs. For seasoned fans of DPT, I provide a correspondence between the current notation for the elemental value of each equivalence class, which employs graphs, and previous notation (which was limited to harmonic-order).

$$\begin{aligned}
{}^{(0)}Q(\circ\circ) &= Q_{ii} = Q_a \\
{}^{(0)}Q(\circ\circ) &= Q_{ij} = Q_b \\
{}^{(0)}Q^{\gamma r}(\circ\bullet) &= Q_{ij,i} = Q_c \\
{}^{(0)}Q^{\gamma r}(\circ\bullet) &= Q_{jk,i} = Q_d \\
{}^{(0)}Q^{r\gamma}(\circ\bullet) &= Q_{i,ij} = Q_e \\
{}^{(0)}Q^{r\gamma}(\circ\bullet) &= Q_{i,jk} = Q_f \\
{}^{(0)}Q(\circ\circ) &= Q_{ij,ij} = Q_g \\
{}^{(0)}Q(\bullet\bullet) &= Q_{ij,jk} = Q_h \\
{}^{(0)}Q(\bullet\bullet) &= Q_{ij,kl} = Q_\iota
\end{aligned} \tag{C.44}$$

The elements of the GF matrix are here identified by two-edge graphs, but were referred to as a, b, \dots, ι in References (81; 82; 90).

$$\begin{aligned}
\mathbf{GF}(\circ\circ) &= a \\
\mathbf{GF}(\circ\circ) &= b \\
\mathbf{GF}^{\gamma r}(\circ\rightarrow) &= c \\
\mathbf{GF}^{\gamma r}(\circ\rightarrow) &= d \\
\mathbf{GF}^{r\gamma}(\circ\rightarrow) &= e \\
\mathbf{GF}^{r\gamma}(\circ\rightarrow) &= f \\
\mathbf{GF}(\circ\circ) &= g \\
\mathbf{GF}(\circ\circ) &= h \\
\mathbf{GF}(\circ\circ) &= \iota.
\end{aligned} \tag{C.45}$$

The elements of the FG matrix were referred to as $\tilde{a}, \tilde{b}, \dots, \tilde{i}$ in Eq. (29) in Ref. (87):

$$\begin{aligned}
\tilde{a} &= \mathbf{FG}(\circ\circ) - \mathbf{GF}(\circ\circ) \\
\tilde{b} &= \mathbf{GF}(\circ\circ) \\
\tilde{c} &= \mathbf{GF}^{\gamma r}(\circ\rightarrow) - \mathbf{GF}^{\gamma r}(\circ\rightarrow) \\
\tilde{d} &= \mathbf{GF}^{\gamma r}(\circ\rightarrow) \\
\tilde{e} &= \mathbf{GF}^{r\gamma}(\circ\rightarrow) - \mathbf{GF}^{r\gamma}(\circ\rightarrow) \\
\tilde{f} &= \mathbf{GF}^{r\gamma}(\circ\rightarrow) \\
\tilde{g} &= \mathbf{GF}(\circ\circ) - 2\mathbf{GF}(\circ\circ) + \mathbf{GF}(\circ\circ) \\
\tilde{h} &= \mathbf{GF}(\circ\circ) - 2\mathbf{GF}(\circ\circ) \\
\tilde{i} &= \mathbf{GF}(\circ\circ).
\end{aligned} \tag{C.46}$$

The binary invariants for two-edge graphs correspond to combinations of the so-called ‘‘simple submatrices’’ of previous work (81; 87)

$$\begin{aligned}
B(\circ\circ) &= \mathbf{I}_N \\
B(\circ\circ) &= \mathbf{J}_N - \mathbf{I}_N \\
B^{r\gamma}(\circ\rightarrow) &= \mathbf{R} \\
B^{r\gamma}(\circ\rightarrow) &= \mathbf{J}_{NM} - \mathbf{R} \\
B^{\gamma r}(\circ\rightarrow) &= \mathbf{R}^T \\
B^{\gamma r}(\circ\rightarrow) &= \mathbf{J}_{MN} - \mathbf{R}^T \\
B(\circ\circ) &= \mathbf{I}_M \\
B(\circ\circ) &= \mathbf{R}^T \mathbf{R} - 2\mathbf{I} \\
B(\circ\circ) &= \mathbf{J}_M - \mathbf{R}^T \mathbf{R} - \mathbf{I}.
\end{aligned} \tag{C.47}$$

Here, \mathbf{I}_N is the $N \times N$ identity matrix and \mathbf{J}_{NM} is a $N \times M$ matrix consisting of ones. The matrix \mathbf{R} is the *vertex-edge* incidence matrix from graph theory.

Appendix D

Perturbative expansion of the Hamiltonian coefficient tensors in the basis of binary invariants

The DPT formulation presented in this thesis depends on an intricate structure in the Hamiltonian expansion, due to the requirement of invariance under permutation. Because this structure does not depend on the parameters of the physical system (other than the number of particles N), this formalism can be applied to a broad range of physical systems. The non-derivative “centrifugal” portion of the kinetic term varies from system to system only by a constant, which I denote $\zeta(0)$. With the exception of a few derivatives, most of the effective potential term varies only by $\zeta(0)$ as well.

In this appendix, I calculate the perturbative expansion of the DPT Hamiltonian as well as the expansion of each perturbative term in the basis of binary invariants. In Section D.1, I calculate the perturbative expansion of the kinetic term, and in Section D.2, I derive the expansion of the system potential terms. In Section D.3, I derive the expansion of the kinetic term in the basis of binary invariants, and in Section D.4, I derive the expansion of the potential term in the basis of binary invariants. I do so in a general form, so that any system can be obtained by specifying $\zeta(0)$ and 16 derivatives of the system’s confining and interacting potentials. In Section J.1, I specify the remaining information needed for a Bose-Einstein condensate with a particular hard-sphere interaction model.

The Jacobian-weighted Schrödinger equation from Eqs. (3.20a-3.20d) (with zero angular momentum) reads

$$\bar{H}\Phi = \left(\frac{1}{\kappa(D)}\bar{T} + \bar{U} + \bar{V} \right) \Phi = \bar{E}\Phi,$$

where

$$\begin{aligned} \bar{T} &= \hbar^2 \sum_{i=1}^N \left(-\frac{1}{2m_i} \frac{\partial^2}{\partial \bar{r}_i^2} - \frac{1}{2m_i \bar{r}_i^2} \sum_{j \neq i} \sum_{k \neq i} \frac{\partial}{\partial \gamma_{ij}} (\gamma_{jk} - \gamma_{ij} \gamma_{ik}) \frac{\partial}{\partial \gamma_{ik}} \right) \\ \bar{U} &= \hbar^2 \sum_{i=1}^N \zeta(\delta) \left(\frac{\delta^2 N(N-2) + (1 - \delta(N+1))^2 \left(\frac{\Gamma^{(i)}}{\Gamma} \right)}{8m_i \bar{r}_i^2} \right) \\ \bar{V} &= \sum_{i=1}^N \bar{V}_{\text{conf}}(\bar{r}_i) + \sum_{i=1}^{N-1} \sum_{j=i+1}^N \bar{V}_{\text{int}}(\bar{r}_{ij}) \end{aligned}$$

$$\bar{V}_{\text{eff}} = \bar{U} + \bar{V}.$$

Most of the Hamiltonian coefficient tensor elements may be calculated in general by defining the constant $\zeta(0)$:

$$\zeta(0) = \lim_{D \rightarrow \infty} \frac{D^2}{\kappa(D)}. \quad (\text{D.2})$$

The quantity $\zeta(0)$ is unitless, because $\kappa(D)$ depends only on dimension D .

D.1 Perturbative expansion of the kinetic term

To obtain the perturbation series of the Hamiltonian kinetic term I first transform the internal coordinate derivatives to internal displacement coordinate derivatives:

$$\begin{aligned} \frac{\partial}{\partial \bar{r}_i} &= \delta^{-1/2} \frac{\partial}{\partial \bar{r}'_i} \\ \frac{\partial}{\partial \gamma_{i,j}} &= \delta^{-1/2} \frac{\partial}{\partial \gamma'_{i,j}} \end{aligned}$$

and I obtain (letting the masses be equal and in units where $\hbar = m = 1$)

$$\begin{aligned} \bar{T} = & -\frac{1}{2} \delta \left(\sum_{i=1}^N \frac{\partial^2}{\partial \bar{r}'_i{}^2} + \sum_{i=1}^N \sum_{j \neq i}^N \frac{1 - \gamma_{ij}^2}{\bar{r}_i^2} \frac{\partial^2}{\partial \gamma_{ij}^2} \right. \\ & + \sum_{i=1}^N \sum_{j \neq i}^N \sum_{k \neq i}^N (1 - \delta_{j,k}) \left(\frac{\gamma_{jk} - \gamma_{ij} \gamma_{ik}}{\bar{r}_i^2} \right) \frac{\partial^2}{\partial \gamma'_{ij} \partial \gamma'_{ik}} \\ & \left. - \sum_{i=1}^N \sum_{j \neq i}^N N \frac{\gamma_{ij}}{\bar{r}_i^2} \delta^{1/2} \frac{\partial}{\partial \gamma'_{ij}} \right). \end{aligned} \quad (\text{D.3})$$

I perform a series expansion about the symmetric (large-D) arrangement, expressing the kinetic term in internal displacement coordinates.

$$\begin{aligned} \bar{r}_i - \bar{r}_\infty &= \delta^{1/2} \bar{r}'_i \\ \gamma_{ij} - \gamma_\infty &= \delta^{1/2} \gamma'_{ij} \end{aligned} \quad (\text{D.4})$$

I perform the expansion of three of the summands

$$\frac{1 - \gamma_{ij}^2}{\bar{r}_i^2} = \frac{1 - \gamma_\infty^2}{\bar{r}_\infty^2} + \delta^{1/2} \left(\frac{2(-1 + \gamma_\infty^2)}{\bar{r}_\infty^3} \bar{r}'_i - \frac{2\gamma_\infty}{\bar{r}_\infty^2} \gamma'_{i,j} \right) + O(\delta) \quad (\text{D.5})$$

$$\begin{aligned} \frac{\gamma_{jk} - \gamma_{ij} \gamma_{ik}}{\bar{r}_i^2} &= -\frac{(-1 + \gamma_\infty) \gamma_\infty}{\bar{r}_\infty^2} \\ &+ \delta^{1/2} \left(-\frac{\gamma_\infty}{\bar{r}_\infty^2} (\gamma'_{ij} + \gamma'_{ik}) + \frac{1}{\bar{r}_\infty^2} \gamma'_{jk} + \frac{2(-1 + \gamma_\infty) \gamma_\infty}{\bar{r}_\infty^3} \bar{r}'_i \right) + O(\delta) \end{aligned} \quad (\text{D.6})$$

$$\frac{\gamma_{ij}}{\bar{r}_i^2} = \frac{\gamma_\infty}{\bar{r}_\infty^2} + \delta^{1/2} \frac{(\bar{r}_\infty \gamma'_{ij} - 2\gamma_\infty \bar{r}'_i)}{\bar{r}_\infty^3} + O(\delta) \quad (\text{D.7})$$

Inserting these expansions into (D.3) and collecting by orders of $\delta^{1/2}$, I obtain (3.31), which I reproduce below:

$$\begin{aligned} \mathcal{T} = & -\frac{1}{2}\delta \left(\sum_{i=1}^N \frac{\partial^2}{\partial \bar{r}_i'^2} + \right. \\ & \sum_{i=1}^N \sum_{j \neq i} \frac{1 - \gamma_\infty^2}{\bar{r}_\infty^2} \frac{\partial^2}{\partial \gamma_{ij}'^2} + \sum_{i=1}^N \sum_{j \neq i} \sum_{k \neq i} (1 - \delta_{j,k}) \frac{(1 - \gamma_\infty) \gamma_\infty}{\bar{r}_\infty^2} \frac{\partial^2}{\partial \gamma_{ij}' \partial \gamma_{ik}'} \Big) \\ & - \frac{1}{2} \delta^{3/2} \left(\sum_{i=1}^N \sum_{j \neq i} \left(-\frac{2(1 - \gamma_\infty^2)}{\bar{r}_\infty^3} \bar{r}'_i - \frac{2\gamma_\infty}{\bar{r}_\infty^2} \gamma'_{ij} \right) \frac{\partial^2}{\partial \gamma_{ij}'^2} \right. \\ & + \sum_{i=1}^N \sum_{j \neq i} \sum_{k \neq i} \left(\frac{(2(\gamma_\infty - 1)\gamma_\infty)}{\bar{r}_\infty^3} \bar{r}'_i - \frac{\gamma_\infty}{\bar{r}_\infty^2} (\gamma'_{ij} + \gamma'_{ik}) + \frac{\gamma'_{jk}}{\bar{r}_\infty^2} \right) \frac{\partial^2}{\partial \gamma_{ij}' \gamma_{ik}'} \\ & \left. + \sum_{i=1}^N \sum_{j \neq i} \left(-N \frac{\gamma_\infty}{\bar{r}_\infty^2} \right) \frac{\partial}{\partial \gamma_{ij}'} \right) + O(\delta^2). \end{aligned}$$

D.2 Perturbative expansion of the effective potential

I perform a series expansion of the effective potential about $\delta^{1/2} = 0$. To do so, it will be convenient to express derivatives with respect to $\delta^{1/2}$ in terms of derivatives with respect to δ .

$$\begin{aligned} \frac{\partial}{\partial(\delta^{1/2})} &= \frac{d}{d(\delta^{1/2})} + \sum_{\mu=1}^P \bar{y}'_\mu \frac{\partial}{\partial \bar{y}'_\mu} \\ \frac{\partial^2}{\partial(\delta^{1/2})^2} &= \frac{d^2}{d(\delta^{1/2})^2} + 2 \sum_{\mu=1}^P \bar{y}'_\mu \frac{\partial}{\partial \bar{y}'_\mu} \frac{d}{d(\delta^{1/2})} + \sum_{\mu=1}^P \sum_{\nu=1}^P \bar{y}'_\mu \bar{y}'_\nu \frac{\partial}{\partial \bar{y}'_\mu} \frac{\partial}{\partial \bar{y}'_\nu} \\ \frac{\partial^3}{\partial(\delta^{1/2})^3} &= \frac{d^3}{d(\delta^{1/2})^3} + 3 \sum_{\mu=1}^P \bar{y}'_\mu \frac{\partial}{\partial \bar{y}'_\mu} \frac{d^2}{d(\delta^{1/2})^2} + 3 \sum_{\mu=1}^P \sum_{\nu=1}^P \bar{y}'_\mu \bar{y}'_\nu \frac{\partial}{\partial \bar{y}'_\mu} \frac{\partial}{\partial \bar{y}'_\nu} \frac{d}{d\delta^{1/2}} + \\ &+ \sum_{\mu=1}^P \sum_{\nu=1}^P \sum_{\xi=1}^P \bar{y}'_\mu \bar{y}'_\nu \bar{y}'_\xi \frac{\partial}{\partial \bar{y}'_\mu} \frac{\partial}{\partial \bar{y}'_\nu} \frac{\partial}{\partial \bar{y}'_\xi} \end{aligned} \quad (\text{D.8})$$

The derivatives with respect to $\delta^{1/2}$ in (D.8) may be written as derivatives with respect to δ with the following equations:

$$\frac{d}{d(\delta^{1/2})} = 2\delta^{1/2} \frac{d}{d\delta}$$

$$\begin{aligned}\frac{d^2}{d(\delta^{1/2})^2} &= 2\frac{d}{d\delta} + 4\delta\frac{d^2}{d\delta^2} \\ \frac{d^3}{d(\delta^{1/2})^3} &= 12\delta^{1/2}\frac{d^2}{d\delta^2} + 8\delta^{3/2}\frac{d^3}{d\delta^3}.\end{aligned}\tag{D.9}$$

Using the above derivatives, I calculate the derivatives of the effective potential with respect to $\delta^{1/2}$ to third order.

$$\begin{aligned}\left.\frac{\partial\bar{V}_{\text{eff}}[\bar{\mathbf{y}}';\delta]}{\partial(\delta^{1/2})}\right|_{\infty} &= 0 \\ \left.\frac{\partial^2\bar{V}_{\text{eff}}[\bar{\mathbf{y}}';\delta]}{\partial(\delta^{1/2})^2}\right|_{\infty} &= 2\frac{d}{d\delta}\bar{V}_{\text{eff}}[\bar{\mathbf{y}}';\delta]\Big|_{\infty} + \sum_{\mu=1}^P\sum_{\nu=1}^P\bar{y}'_{\mu}\bar{y}'_{\nu}\frac{\partial}{\partial\bar{y}'_{\mu}}\frac{\partial}{\partial\bar{y}'_{\nu}}\bar{V}_{\text{eff}}[\bar{\mathbf{y}}';\delta]\Big|_{\infty} \\ \left.\frac{\partial^3\bar{V}_{\text{eff}}[\bar{\mathbf{y}}';\delta]}{\partial(\delta^{1/2})^3}\right|_{\infty} &= 6\sum_{\mu=1}^P\bar{y}'_{\mu}\frac{\partial}{\partial\bar{y}'_{\mu}}\frac{d}{d\delta}\bar{V}_{\text{eff}}[\bar{\mathbf{y}}';\delta]\Big|_{\infty} + \sum_{\mu=1}^P\sum_{\nu=1}^P\sum_{\xi=1}^P\bar{y}'_{\mu}\bar{y}'_{\nu}\bar{y}'_{\xi}\frac{\partial}{\partial\bar{y}'_{\mu}}\frac{\partial}{\partial\bar{y}'_{\nu}}\frac{\partial}{\partial\bar{y}'_{\xi}}\bar{V}_{\text{eff}}[\bar{\mathbf{y}}';\delta]\Big|_{\infty}\end{aligned}\tag{D.10}$$

Substituting equations (D.10) into the Taylor series expansion of V_{eff} about $\delta^{1/2} = 0$ (and collecting powers of δ), I obtain Eq. (D.11)

$$\begin{aligned}\bar{V}_{\text{eff}}[\bar{\mathbf{y}}';\delta] &= \bar{V}_{\text{eff}}[\bar{\mathbf{y}}_{\infty};\delta]\Big|_{\infty} + \delta\left(\frac{d}{d\delta}\bar{V}_{\text{eff}}[\bar{\mathbf{y}}';\delta] + \frac{1}{2}\sum_{\mu=1}^P\sum_{\nu=1}^P\bar{y}'_{\mu}\bar{y}'_{\nu}\frac{\partial^2\bar{V}_{\text{eff}}[\bar{\mathbf{y}}';\delta]}{\partial\bar{y}'_{\mu}\partial\bar{y}'_{\nu}}\right)\Big|_{\infty} \\ &+ \delta^{3/2}\left(\sum_{\mu=1}^P\bar{y}'_{\mu}\frac{\partial}{\partial\bar{y}'_{\mu}}\frac{d}{d\delta}\bar{V}_{\text{eff}}[\bar{\mathbf{y}}';\delta]\Big|_{\infty} + \frac{1}{3!}\sum_{\mu=1}^P\sum_{\nu=1}^P\sum_{\xi=1}^P\bar{y}'_{\mu}\bar{y}'_{\nu}\bar{y}'_{\xi}\frac{\partial^3\bar{V}_{\text{eff}}[\bar{\mathbf{y}}';\delta]}{\partial\bar{y}'_{\mu}\partial\bar{y}'_{\nu}\partial\bar{y}'_{\xi}}\Big|_{\infty}\right) \\ &+ O(\delta^2).\end{aligned}\tag{D.11}$$

Equation (D.11) is explicitly written in the form of the Hamiltonian expansions in (3.38) and (3.39), where the F tensors are now revealed to be

$${}^{(0)}_0F = \frac{d}{d\delta}\bar{V}_{\text{eff}}[\bar{\mathbf{y}}';\delta]\Big|_{\infty}\tag{D.12}$$

$${}^{(0)}_2F_{\nu_1,\nu_2} = \frac{\partial^2\bar{V}_{\text{eff}}[\bar{\mathbf{y}}';\delta]}{\partial\bar{y}'_{\nu_1}\partial\bar{y}'_{\nu_2}}\Big|_{\infty}\tag{D.13}$$

and

$${}^{(1)}_1F_{\nu} = \frac{\partial}{\partial\bar{y}'_{\nu}}\frac{d}{d\delta}\bar{V}_{\text{eff}}[\bar{\mathbf{y}}';\delta]\Big|_{\infty}\tag{D.14}$$

$${}^{(1)}_3F_{\nu_1,\nu_2,\nu_3} = \frac{\partial^3\bar{V}_{\text{eff}}[\bar{\mathbf{y}}';\delta]}{\partial\bar{y}'_{\nu_1}\partial\bar{y}'_{\nu_2}\partial\bar{y}'_{\nu_3}}\Big|_{\infty}.\tag{D.15}$$

D.3 Binary invariant expansion the kinetic series

I rewrite the summations in (3.31) in a more general tensor form like (3.39). For each graph in Eq. (3.31), I start by “decoupling” the repeated indices and considering all the possible ways to reconnect them to form the same graph. Take, for example, the term associated with the graph $\bullet\circ\circ$,

$$\sum_{i=1}^N \sum_{j \neq i} \bar{r}'_i \frac{\partial^2}{\partial \gamma'_{ij}}. \quad (\text{D.16})$$

In this term, the indices on the internal coordinates are explicitly repeated. This summation can be written in a more general way by explicitly “decoupling” the repeated indices on the internal coordinates and implicitly coupling them with a Kronecker delta function. The repeated index i in \bar{r}'_i can be decoupled from i in the partial derivative with respect to γ'_{ij} by changing \bar{r}'_i to \bar{r}'_m and adding an additional summation over $\delta_{i,m}$ or over $\delta_{j,m}$.

$$\bullet\circ\circ \rightarrow \bullet\circ + \circ$$
(D.17)

$$\sum_{i=1}^N \sum_{j \neq i} \bar{r}'_i \frac{\partial^2}{\partial \gamma'_{ij}} = \sum_{i=1}^N \sum_{j \neq i} \sum_{m=1}^N \frac{1}{2} (\delta_{i,m} + \delta_{j,m}) \frac{\partial^2}{\partial \gamma'_{ij}} \bar{r}'_m. \quad (\text{D.18})$$

Next, I explicitly decouple the repeated indices in the partial derivatives. Now there are two ways to implicitly couple together $\overset{i}{\bullet} \overset{j}{\bullet}$ and $\overset{k}{\bullet} \overset{l}{\bullet}$ to yield $\bullet\circ$. Therefore, I do it both ways and divide by two.

$$\begin{aligned} \bullet\circ\circ &\rightarrow \circ + \bullet\bullet + \bullet\bullet \\ &\sum_{i=1}^N \sum_{j \neq i} \bar{r}'_i \frac{\partial^2}{\partial \gamma'_{ij}} \\ &= \sum_{i=1}^N \sum_{j \neq i} \sum_{k=1}^N \sum_{l \neq k} \sum_{m=1}^N \frac{1}{4} (\delta_{j,l} \delta_{i,k} + \delta_{j,k} \delta_{i,l}) (\delta_{i,m} + \delta_{j,m}) \frac{\partial^2}{\partial \gamma'_{ij} \partial \gamma'_{kl}} \bar{r}'_m \end{aligned} \quad (\text{D.19})$$

Finally, I rewrite the summations over the indices of γ'_{ij} , using the relation

$$\sum_{j=1}^N \sum_{k \neq j} f_{i,j} = 2 \sum_{j < k} f_{i,j}, \quad (\text{D.20})$$

where $f_{i,j}$ is symmetric in the indices ($f_{i,j} = f_{j,i}$). Written in this summation convention, I obtain

$$\sum_{i=1}^N \sum_{j \neq i} \bar{r}'_i \frac{\partial^2}{\partial \gamma'_{ij}} = \sum_{i < j} \sum_{k < l} \sum_{m=1}^N (\delta_{j,l} \delta_{i,k} + \delta_{j,k} \delta_{i,l}) (\delta_{i,m} + \delta_{j,m}) \frac{\partial^2}{\partial \gamma'_{ij} \partial \gamma'_{kl}} \bar{r}'_m. \quad (\text{D.21})$$

Comparing (D.21) with the binary invariant $B(\bullet\circ\circ)$ in (C.25), I see that I explicitly constructed the binary invariant $[B(\bullet\circ\circ)]_{(ij),(kl),m}$ in the summand! Please note that

$(1 - \delta_{i,j})(1 - \delta_{k,l})$ is not necessary due to the summation restrictions $i < j$ and $k < l$, since it is always unity in the summation one could insert this factor in the summand if desired. Therefore, I write the sum in (D.21) in terms of a binary invariant:

$$\sum_{i=1}^N \sum_{j \neq i} \bar{r}'_i \frac{\partial^2}{\partial \gamma'_{ij}{}^2} = \sum_{i < j} \sum_{k < l} \sum_{m=1}^N [B(\text{---}\odot\text{---})]_{(ij),(kl),m} \frac{\partial^2}{\partial \gamma'_{ij} \partial \gamma'_{kl}} \bar{r}'_m \quad (\text{D.22})$$

Following a similar procedure for the other terms in (3.31), I obtain

$$\begin{aligned} \sum_{i=1}^N \frac{\partial^2}{\partial \bar{r}'_i{}^2} &= \sum_{i=1}^N \sum_{j=1}^N [B(\text{---}\odot\text{---})]_{i,j} \frac{\partial^2}{\partial \bar{r}'_i \partial \bar{r}'_j} \\ \sum_{i=1}^N \sum_{j \neq i} \frac{\partial^2}{\partial \gamma'_{ij}{}^2} &= \sum_{i < j} \sum_{k < l} [B(\text{---}\odot\text{---})]_{(ij),(kl)} \frac{\partial^2}{\partial \gamma'_{ij} \partial \gamma'_{kl}} \\ \sum_{i=1}^N \sum_{j \neq i} \sum_{k \neq i} (1 - \delta_{j,k}) \frac{\partial^2}{\partial \gamma'_{ij} \partial \gamma'_{ik}} &= \sum_{i < j} \sum_{k < l} [B(\text{---}\bullet\text{---})]_{(ij),(kl)} \frac{\partial^2}{\partial \gamma'_{ij} \partial \gamma'_{kl}} \quad (\text{D.23}) \\ \sum_{i=1}^N \sum_{j \neq i} \sum_{k \neq i} (1 - \delta_{j,k}) \bar{r}'_i \frac{\partial^2}{\partial \gamma'_{ij} \partial \gamma'_{ik}} &= \sum_{i < j} \sum_{k < l} \sum_{m=1}^N [B(\text{---}\odot\text{---})]_{(ij),(kl),m} \bar{r}'_m \frac{\partial^2}{\partial \gamma'_{i,j} \partial \gamma'_{k,l}} \\ \sum_{i=1}^N \sum_{j \neq i} \sum_{k \neq i} \delta_{j,k} \gamma'_{i,j} \frac{\partial^2}{\partial \gamma'_{ij} \partial \gamma'_{ik}} &= \sum_{i < j} \sum_{k < l} \sum_{m < n} 2 [B(\text{---}\ominus\text{---})]_{(ij),(kl),(mn)} \gamma'_{i,j} \frac{\partial^2}{\partial \gamma'_{k,l} \partial \gamma'_{m,n}} \\ \sum_{i=1}^N \sum_{j \neq i} \sum_{k \neq i} (1 - \delta_{j,k}) \gamma'_{jk} \frac{\partial^2}{\partial \gamma'_{ij} \partial \gamma'_{ik}} &= \sum_{i < j} \sum_{k < l} \sum_{m < n} [B(\text{---}\triangle\text{---})]_{(ij),(kl),(mn)} \gamma'_{i,j} \frac{\partial^2}{\partial \gamma'_{k,l} \partial \gamma'_{m,n}} \end{aligned}$$

One term in (3.31) warrants closer examination:

$$\begin{aligned} &\sum_{i=1}^N \sum_{j \neq i} \sum_{k \neq i} (1 - \delta_{j,k}) (\gamma'_{ij} + \gamma'_{ik}) \frac{\partial^2}{\partial \gamma'_{ij} \partial \gamma'_{ik}} \\ &= \sum_{i < j} \sum_{k < l} \sum_{m < n} (\delta_{i,k} \delta_{j,l} + \delta_{i,l} \delta_{j,k} + \delta_{i,m} \delta_{j,n} + \delta_{i,n} \delta_{j,m}) \\ &\quad \times (\delta_{k,m} (1 - \delta_{l,n}) + \delta_{k,n} (1 - \delta_{l,m}) + \delta_{l,m} (1 - \delta_{k,n}) + \delta_{l,n} (1 - \delta_{k,m})) \\ &\quad \times \gamma'_{i,j} \frac{\partial^2}{\partial \gamma'_{kl} \partial \gamma'_{mn}}. \quad (\text{D.24}) \end{aligned}$$

In Eq. (D.24), I recognize only part of the binary invariant $B(\text{---}\odot\text{---})$. This is the only graph in this (isotropic confinement, first anharmonic order) DPT implementation for which I must introduce distinguishable edges in our graphs. For this case, I must generalize the mapping from coordinate to graph to distinguish between coordinates and derivatives. I do so by labeling the edges associated with derivatives by a vertical “tic” mark. It will also be necessary to consider distinguishable edges if this formalism is extended to an anisotropic system. The binary invariant for the unlabeled graph $B(\text{---}\odot\text{---})$ is really the sum of two binary invariants for labeled graphs with two edges to be distinguished from the third:

$$B(\text{---}\text{---}) = B(\text{---}\text{---}) + B(\text{---}\text{---}), \quad (\text{D.25})$$

where

$$[B(\text{---}\text{---})]_{(ij),(kl),(mn)} = (\delta_{i,k}\delta_{j,l} + \delta_{i,l}\delta_{j,k} + \delta_{i,m}\delta_{j,n} + \delta_{i,n}\delta_{j,m}) \\ \times (\delta_{k,m}(1 - \delta_{l,n}) + \delta_{k,n}(1 - \delta_{l,n}) + \delta_{l,m}(1 - \delta_{k,n}) + \delta_{l,n}(1 - \delta_{k,m})), \quad (\text{D.26})$$

and

$$[B(\text{---}\text{---})]_{(ij),(kl),(mn)} = (\delta_{k,m}\delta_{l,n} + \delta_{k,n}\delta_{l,m}) \\ \times (\delta_{i,k}(1 - \delta_{j,l}) + \delta_{i,l}(1 - \delta_{j,k}) + \delta_{j,k}(1 - \delta_{i,l}) + \delta_{j,l}(1 - \delta_{i,k})). \quad (\text{D.27})$$

Therefore, I obtain

$$\sum_{i=1}^N \sum_{j \neq i}^N \sum_{k \neq i}^N (1 - \delta_{j,k}) (\gamma'_{ij} + \gamma'_{ik}) \frac{\partial^2}{\partial \gamma'_{ij} \partial \gamma'_{ik}} \\ = \sum_{i < j} \sum_{k < l} \sum_{m < n} [B(\text{---}\text{---})]_{(ij),(kl),(mn)} \gamma'_{i,j} \frac{\partial^2}{\partial \gamma'_{kl} \partial \gamma'_{mn}}. \quad (\text{D.28})$$

Inserting Eqs. (D.22-D.24) and (D.28) into the kinetic-energy expansion (3.31), I obtain a kinetic-energy expansion in terms of binary invariants:

$$\mathcal{T} = -\frac{1}{2} \delta \left(\sum_{i=1}^N \sum_{j=1}^N [B(\text{---}\text{---})]_{i,j} \frac{\partial^2}{\partial \bar{r}'_i \partial \bar{r}'_j} + \sum_{i < j} \sum_{k < l} \frac{1 - \gamma_\infty^2}{\bar{r}_\infty^2} [B(\text{---}\text{---})]_{(ij),(kl)} \frac{\partial^2}{\partial \gamma'_{ij} \partial \gamma'_{kl}} + \right. \\ \left. + \sum_{i < j} \sum_{k < l} \frac{(1 - \gamma_\infty) \gamma_\infty}{\bar{r}_\infty^2} [B(\text{---}\text{---})]_{(ij),(kl)} \frac{\partial^2}{\partial \gamma'_{ij} \partial \gamma'_{kl}} \right) + \\ -\frac{1}{2} \delta^{3/2} \left(\sum_{i=1}^N \sum_{j \neq i}^N \left(-N \frac{\gamma_\infty}{\bar{r}_\infty^2} \right) [B(\text{---}\text{---})]_{(ij)} \frac{\partial}{\partial \gamma'_{ij}} + \right. \\ \left. + \sum_{i=1}^N \sum_{j < k} \sum_{l < m} \left(-\frac{2(1 - \gamma_\infty^2)}{\bar{r}_\infty^3} [B(\text{---}\text{---})]_{(ij),(kl),m} \right. \right. \\ \left. \left. - \frac{2\gamma_\infty(1 - \gamma_\infty)}{\bar{r}_\infty^3} [B(\text{---}\text{---})]_{(ij),(kl),m} \right) \bar{r}'_m \frac{\partial^2}{\partial \gamma'_{ij} \partial \gamma'_{kl}} + \right. \\ \left. + \sum_{i < j} \sum_{k < l} \sum_{m < n} \left(-\frac{4\gamma_\infty}{\bar{r}_\infty^2} [B(\text{---}\text{---})]_{(ij),(kl),(mn)} + \frac{1}{\bar{r}_\infty^2} [B(\text{---}\text{---})]_{(ij),(kl),(mn)} \right. \right. \\ \left. \left. - \frac{\gamma_\infty}{\bar{r}_\infty^2} [B(\text{---}\text{---})]_{(ij),(kl),(mn)} \right) \gamma'_{i,j} \frac{\partial^2}{\partial \gamma'_{k,l} \partial \gamma'_{m,n}} \right) + O(\delta^2). \quad (\text{D.29})$$

I write the above equation in the form of a tensor contraction, by defining tensors ${}^{(0)}_2 G$, ${}^{(0)}_2 G$, and ${}^{(0)}_2 G$ as a linear combination of binary invariants.

For the order- δ harmonic term, I write

$${}^{(0)}_2 G_{\nu_1, \nu_2}^{block} = \sum_{\mathcal{G} \in \mathbb{G}_{block}} G^{block}(\mathcal{G}) [B^{block}(\mathcal{G})]_{\nu_1, \nu_2}, \quad (\text{D.30})$$

with the following coefficients

$${}^{(0)}_2 G^{rr} (\infty\infty) = \zeta(0) \quad (\text{D.31})$$

$${}^{(0)}_2 G^{\gamma\gamma} (\odot\odot) = 2\zeta(0) \frac{1 - \gamma_\infty^2}{\bar{r}_\infty^2} \quad (\text{D.32})$$

$${}^{(0)}_2 G^{\gamma\gamma} (\bullet\bullet) = \zeta(0) \frac{\gamma_\infty(1 - \gamma_\infty)}{\bar{r}_\infty^2}. \quad (\text{D.33})$$

These ${}^{(0)}_2 G$ coefficients were calculated for a BEC in Eq. (120) of Ref. (81) (as well as for other potentials in the same reference). Here, I provide a general calculation of these elements for any potential and for first anharmonic order as well. In this work I label elements by graph, and specify the perturbation order and matrix rank.

The order $\delta^{3/2}$ (first-anharmonic order) term has both a rank-one and a rank-three G tensor. The rank-one tensor has the following trivial decomposition:

$${}^{(1)}_1 G^{\text{block}}_{\nu_1} = \sum_{\mathcal{G} \in \mathbb{G}^{\text{block}}} G^{\text{block}}(\mathcal{G}) [B^{\text{block}}(\mathcal{G})]_{\nu_1}, \quad (\text{D.34})$$

where the only non-zero elements of ${}^{(1)}_1 G$ are

$${}^{(1)}_1 G^r (\odot) = 0 \quad (\text{D.35})$$

$${}^{(1)}_1 G^\gamma (\bullet\rightarrow) = -2\zeta(0) N \frac{\gamma_\infty}{\bar{r}_\infty^2}. \quad (\text{D.36})$$

The rank-three tensor has the decomposition

$${}^{(1)}_3 G^{\text{block}}_{\nu_1, \nu_2, \nu_3} = \sum_{\mathcal{G} \in \mathbb{G}^{\text{block}}} G^{\text{block}}(\mathcal{G}) [B^{\text{block}}(\mathcal{G})]_{\nu_1, \nu_2, \nu_3}, \quad (\text{D.37})$$

where the only non-zero elements of ${}^{(1)}_3 G$ are

$${}^{(1)}_3 G^{r\gamma\gamma} (\infty\infty) = -2\zeta(0) \frac{1 - \gamma_\infty^2}{\bar{r}_\infty^3} \quad (\text{D.38})$$

$${}^{(1)}_3 G^{r\gamma\gamma} (\bullet\infty) = -2\zeta(0) \frac{\gamma_\infty(1 - \gamma_\infty)}{\bar{r}_\infty^3} \quad (\text{D.39})$$

$${}^{(1)}_3 G^{\gamma\gamma\gamma} (\ominus) = -4\zeta(0) \frac{\gamma_\infty}{\bar{r}_\infty^2} \quad (\text{D.40})$$

$${}^{(1)}_3 G^{\gamma\gamma\gamma} (\triangle) = \zeta(0) \frac{1}{\bar{r}_\infty^2} \quad (\text{D.41})$$

$${}^{(1)}_3 G^{\gamma\gamma\gamma} (\odot\bullet) = -\zeta(0) \frac{\gamma_\infty}{\bar{r}_\infty^2}. \quad (\text{D.42})$$

With the above definitions for the G tensors, I have derived a tensor form of the DPT Hamiltonian to first anharmonic order for any ($L = 0$ isotropic identical boson) system:

$$\begin{aligned} \mathcal{T} = & -\frac{1}{2}\delta \sum_{\nu_1} \sum_{\nu_2} {}^{(0)}_2 G_{\nu_1, \nu_2} \frac{\partial^2}{\partial y'_{\nu_1} \partial y'_{\nu_2}} - \frac{1}{2}\delta^{3/2} \left(\sum_{\nu_1} {}^{(1)}_1 G_{\nu_1} \frac{\partial}{\partial y'_{\nu_1}} + \right. \\ & \left. + \sum_{\nu_1} \sum_{\nu_2} \sum_{\nu_3} {}^{(1)}_3 G_{\nu_1, \nu_2, \nu_3} y'_{\nu_1} \frac{\partial^2}{\partial y'_{\nu_2} \partial y'_{\nu_3}} \right) + O(\delta^2). \end{aligned} \quad (\text{D.43})$$

D.4 Binary invariant expansion of the effective potential series

The calculation of the binary invariant expansion of the effective potential perturbative expressions in Eqs. (D.11) is much more straightforward than for the kinetic term, although one must calculate many derivatives.

D.4.1 Calculation of derivatives

Due to number of derivatives and the extensive arithmetic involved, I use a symbolic *Mathematica* program to derive the derivatives for each graph (107). Some of these derivatives cannot be simply calculated by this program. Derivatives of the Grammian determinant Γ in the “centrifugal” portion of the effective potential are too complicated. The definition and relevance of the Grammian determinant, as well as derivatives (up to second order) are given in Appendix D of Ref. (81). The program uses graph theory to look these derivatives up in a table. I have derived the necessary third-order derivatives, and the nonzero derivatives are listed here:

$$\left. \frac{\partial^3 \Gamma}{\partial \gamma_{ij} \partial \gamma_{jk} \partial \gamma_{kl}} \right|_{D=\infty} = -2\gamma_\infty (1 - \gamma_\infty)^{N-4} \quad (\text{D.44})$$

$$\left. \frac{\partial^3 \Gamma}{\partial \gamma_{ij} \partial \gamma_{jk} \partial \gamma_{ik}} \right|_{D=\infty} = 2(1 + (N - 4)\gamma_\infty)(1 - \gamma_\infty)^{N-4} \quad (\text{D.45})$$

$$\left. \frac{\partial^3 \Gamma}{\partial \gamma_{ij}^2 \partial \gamma_{kl}} \right|_{D=\infty} = 4\gamma_\infty (1 - \gamma_\infty)^{N-4}. \quad (\text{D.46})$$

Since most of the derivatives in the F tensors are derivatives of the centrifugal term (which varies from system to system only by the constant $\zeta(0)$), I express the F tensors for any ($L = 0$) 2-body system below.

In the special case of a power-law potential,

$$\bar{V}_{\text{conf}}(\bar{r}_i) = \frac{\beta_V}{n} \bar{r}_i^n,$$

these results may be further simplified by making the following substitution for \bar{r}_∞ :

$$\bar{r}_\infty = \frac{\left(\frac{\zeta(0)}{4\beta_V}\right)^{\frac{1}{n+2}}}{(1 + (N - 1)\gamma_\infty)^{\frac{2}{n+2}}}. \quad (\text{D.47})$$

In the interest of preserving generality, I do not do so here.

D.4.2 Elements of the harmonic-order Hamiltonian

I list the harmonic-order F elements. These have been calculated for three different specific systems (the N -electron atom, the N -electron quantum dot, and a Bose-Einstein condensate) in Ref. (81). In order to apply these general results to a specific system, one must only specify six additional potential derivatives.

$$\begin{aligned}
{}^{(0)}_0 F &= \left. \frac{d\bar{U}}{d\delta} \right|_{\infty} + \left. \frac{d\bar{V}_{\text{conf}}}{d\delta} \right|_{\infty} + \left. \frac{d\bar{V}_{\text{int}}}{d\delta} \right|_{\infty} \\
&= -\frac{\zeta(0) N(N+1)(1+(N-2)\gamma_{\infty})}{4\bar{r}_{\infty}^2 (1-\gamma_{\infty})(1+(N-1)\gamma_{\infty})} + \left. \frac{d\bar{V}_{\text{conf}}}{d\delta} \right|_{\infty} + \left. \frac{d\bar{V}_{\text{int}}}{d\delta} \right|_{\infty} \quad (\text{D.48})
\end{aligned}$$

In the present notation, ${}^{(0)}_0 F$ replaces ν_0 in Eq. (125) of Ref. (81).

$$\begin{aligned}
{}^{(0)}_2 F(\bigcirc\bigcirc) &= \frac{\partial^2 \bar{V}_{\text{eff}}}{\partial \bar{r}_i^2} \\
&= \frac{3\zeta(0) ((N-2)\gamma_{\infty} + 1)}{4(1-\gamma_{\infty})\bar{r}_{\infty}^4 ((N-1)\gamma_{\infty} + 1)} + \left(\frac{\partial^2 \bar{V}_{\text{conf}}}{\partial \bar{r}_i^2} \right) \Big|_{\infty} \\
&\quad + (N-1) \left(\frac{\partial^2 \bar{V}_{\text{int}}}{\partial \bar{r}_i^2} \right) \Big|_{\infty} \quad (\text{D.49})
\end{aligned}$$

$${}^{(0)}_2 F(\bigcirc \bigcirc) = \left(\frac{\partial^2 \bar{V}_{\text{int}}}{\partial \bar{r}_i \partial \bar{r}_j} \right) \Big|_{\infty} \quad (\text{D.50})$$

$${}^{(0)}_2 F(\bigcirc \bullet) = \left(\frac{\partial^2 \bar{V}_{\text{eff}}}{\partial \gamma_{ij} \partial \bar{r}_i} \right) \Big|_{\infty} = -\frac{\zeta(0)\gamma_{\infty} ((N-2)\gamma_{\infty} + 1)}{2(1-\gamma_{\infty})^2 \bar{r}_{\infty}^3 ((N-1)\gamma_{\infty} + 1)^2} \quad (\text{D.51})$$

$${}^{(0)}_2 F(\bigcirc \bullet) = \left(\frac{\partial^2 \bar{V}_{\text{eff}}}{\partial \gamma_{ij} \partial \bar{r}_k} \right) \Big|_{\infty} = \frac{\zeta(0)\gamma_{\infty}^2}{2(1-\gamma_{\infty})^2 \bar{r}_{\infty}^3 ((N-1)\gamma_{\infty} + 1)^2} \quad (\text{D.52})$$

$$\begin{aligned}
{}^{(0)}_2 F(\bigcirc \bullet) &= \frac{\zeta(0)}{2(1-\gamma_{\infty})^3 \bar{r}_{\infty}^2 ((N-1)\gamma_{\infty} + 1)^3} ((N^3 - 5N^2 + 10N - 8) \gamma_{\infty}^3 \\
&\quad + (3N^2 - 11N + 13) \gamma_{\infty}^2 + 3(N-2)\gamma_{\infty} + 1) + \left(\frac{\partial^2 \bar{V}_{\text{int}}}{\partial \gamma_{ij}^2} \right) \Big|_{\infty} \quad (\text{D.53})
\end{aligned}$$

$${}^{(0)}_2 F(\bullet \downarrow) = -\frac{\zeta(0)\gamma_{\infty} ((2N^2 - 9N + 11) \gamma_{\infty}^2 + (5N - 14)\gamma_{\infty} + 3)}{4(1-\gamma_{\infty})^3 \bar{r}_{\infty}^2 ((N-1)\gamma_{\infty} + 1)^3} \quad (\text{D.54})$$

$${}^{(0)}_2 F(\bullet \bullet) = \frac{\zeta(0)\gamma_{\infty}^2 ((N-2)\gamma_{\infty} + 2)}{(1-\gamma_{\infty})^3 \bar{r}_{\infty}^2 ((N-1)\gamma_{\infty} + 1)^3} \quad (\text{D.55})$$

D.4.3 Elements of the first anharmonic-order Hamiltonian

I report the calculation of the elements of the first-anharmonic-order F tensors in general. In order to apply these results to a specific system, one must only calculate 10 additional potential derivatives.

D.4.3.1 Rank-one Hamiltonian elements

$$\begin{aligned} {}_1^{(1)}F(\odot) &= \frac{\zeta(0)(N+1)((N-2)\gamma_\infty+1)}{2(1-\gamma_\infty)\bar{r}_\infty^3((N-1)\gamma_\infty+1)} + \left(\frac{\partial}{\partial \bar{r}'_i} \frac{d\bar{V}_{\text{conf}}(\bar{\mathbf{y}}')}{d\delta} \right) \Big|_\infty + \\ &+ \left(\frac{\partial}{\partial \bar{r}'_i} \frac{d\bar{V}_{\text{int}}(\bar{\mathbf{y}}')}{d\delta} \right) \Big|_\infty \end{aligned} \quad (\text{D.56})$$

$${}_1^{(1)}F(\bullet\leftarrow) = -\frac{\zeta(0)(N+1)\gamma_\infty((N-2)\gamma_\infty+2)}{2(1-\gamma_\infty)^2\bar{r}_\infty^2((N-1)\gamma_\infty+1)^2} + \left(\frac{\partial}{\partial \gamma'_{ij}} \frac{d\bar{V}_{\text{int}}(\bar{\mathbf{y}}')}{d\delta} \right) \Big|_\infty \quad (\text{D.57})$$

D.4.3.2 Rank-three Hamiltonian elements

$$\begin{aligned} {}_3^{(1)}F(\text{⊗}) &= -\frac{3\zeta(0)((N-2)\gamma_\infty+1)}{(1-\gamma_\infty)\bar{r}_\infty^5((N-1)\gamma_\infty+1)} + \left(\frac{\partial^3 \bar{V}_{\text{conf}}}{\partial \bar{r}_i^3} \right) \Big|_\infty \\ &+ (N-1) \left(\frac{\partial^3 \bar{V}_{\text{int}}}{\partial \bar{r}_i^3} \right) \Big|_\infty \end{aligned} \quad (\text{D.58})$$

$${}_3^{(1)}F(\text{⊗} \odot) = \left(\frac{\partial^3 \bar{V}_{\text{int}}}{\partial \bar{r}_i^2 \partial \bar{r}_j} \right) \Big|_\infty \quad (\text{D.59})$$

$${}_3^{(1)}F(\odot \odot \odot) = 0 \quad (\text{D.60})$$

$${}_3^{(1)}F(\text{⊗} \bullet\leftarrow) = \frac{3\zeta(0)\gamma_\infty((N-2)\gamma_\infty+1)}{2(1-\gamma_\infty)^2\bar{r}_\infty^4((N-1)\gamma_\infty+1)^2} + \left(\frac{\partial^3 \bar{V}_{\text{int}}}{\partial \gamma_{ij} \partial^2 \bar{r}_i} \right) \Big|_\infty \quad (\text{D.61})$$

$${}_3^{(1)}F(\odot \bullet\leftarrow \odot) = \left(\frac{\partial^3 \bar{V}_{\text{int}}}{\partial \gamma_{ij} \partial \bar{r}_i \partial \bar{r}_j} \right) \Big|_\infty \quad (\text{D.62})$$

$${}_3^{(1)}F(\odot \bullet\leftarrow \bullet\leftarrow) = 0 \quad (\text{D.63})$$

$${}_3^{(1)}F(\text{⊗} \text{⊗}) = -\frac{3\zeta(0)\gamma_\infty^2}{2(1-\gamma_\infty)^2\bar{r}_\infty^4((N-1)\gamma_\infty+1)^2} \quad (\text{D.64})$$

$${}_3^{(1)}F(\odot \odot \bullet\leftarrow) = 0 \quad (\text{D.65})$$

$$\begin{aligned} {}_3^{(1)}F(\text{⊗} \text{⊗}) &= -\frac{\zeta(0)((N-2)\gamma_\infty+1)((N^2-4N+7)\gamma_\infty^2+2(N-2)\gamma_\infty+1)}{2(1-\gamma_\infty)^3\bar{r}_\infty^3((N-1)\gamma_\infty+1)^3} \\ &+ \left(\frac{\partial^3 \bar{V}_{\text{int}}}{\partial \gamma_{ij}^2 \partial \bar{r}_i} \right) \Big|_\infty \end{aligned} \quad (\text{D.66})$$

$${}_3^{(1)}F(\text{⊗} \odot) = -\frac{\zeta(0)\gamma_\infty^2((N-3)\gamma_\infty+1)}{(1-\gamma_\infty)^3\bar{r}_\infty^3((N-1)\gamma_\infty+1)^3} \quad (\text{D.67})$$

$${}_3^{(1)}F(\bullet\leftarrow \bullet\leftarrow) = \frac{\zeta(0)\gamma_\infty((N-5)\gamma_\infty+1)((N-2)\gamma_\infty+1)}{2(1-\gamma_\infty)^3\bar{r}_\infty^3((N-1)\gamma_\infty+1)^3} \quad (\text{D.68})$$

$${}^{(1)}_3F(\text{L}\text{---}\text{O}) = \frac{\zeta(0)\gamma_\infty((N^2 - 5N + 8)\gamma_\infty^2 + (2N - 5)\gamma_\infty + 1)}{2(1 - \gamma_\infty)^3 \bar{r}_\infty^3 ((N - 1)\gamma_\infty + 1)^3} \quad (\text{D.69})$$

$${}^{(1)}_3F(\text{L}\text{---}\text{O}) = -\frac{\zeta(0)\gamma_\infty^2((N - 5)\gamma_\infty + 1)}{2(1 - \gamma_\infty)^3 \bar{r}_\infty^3 ((N - 1)\gamma_\infty + 1)^3} \quad (\text{D.70})$$

$${}^{(1)}_3F(\text{---}\text{O}) = -\frac{\zeta(0)\gamma_\infty^2((N - 3)\gamma_\infty + 1)}{(1 - \gamma_\infty)^3 \bar{r}_\infty^3 ((N - 1)\gamma_\infty + 1)^3} \quad (\text{D.71})$$

$${}^{(1)}_3F(\text{---}\text{O}) = \frac{2\zeta(0)\gamma_\infty^3}{(1 - \gamma_\infty)^3 \bar{r}_\infty^3 ((N - 1)\gamma_\infty + 1)^3} \quad (\text{D.72})$$

$$(\text{D.73})$$

$${}^{(1)}_3F(\ominus) = \frac{3\zeta(0)\gamma_\infty}{2(1 - \gamma_\infty)^4 \bar{r}_\infty^2 ((N - 1)\gamma_\infty + 1)^4} ((3N^3 - 16N^2 + 31N - 22)\gamma_\infty^3 + 2(5N^2 - 19N + 20)\gamma_\infty^2 + 11(N - 2)\gamma_\infty + 4) \left(\frac{\partial^3 \bar{V}_{\text{int}}}{\partial \gamma_{ij}^3} \right) \Big|_\infty \quad (\text{D.74})$$

$${}^{(1)}_3F(\triangle) = -\frac{3\zeta(0)}{4(1 - \gamma_\infty)^4 \bar{r}_\infty^2 ((N - 1)\gamma_\infty + 1)^4} \times ((N^4 - 7N^3 + 22N^2 - 39N + 31)\gamma_\infty^4 + (4N^3 - 22N^2 + 50N - 52)\gamma_\infty^3 + (6N^2 - 23N + 28)\gamma_\infty^2 + 4(N - 2)\gamma_\infty + 1) \quad (\text{D.75})$$

$${}^{(1)}_3F(\text{O}\text{---}\text{---}) = \frac{\zeta(0)\gamma_\infty((N - 3)\gamma_\infty + 1)}{2(1 - \gamma_\infty)^4 \bar{r}_\infty^2 ((N - 1)\gamma_\infty + 1)^4} ((3N^2 - 13N + 16)\gamma_\infty^2 + (7N - 20)\gamma_\infty + 4) \quad (\text{D.76})$$

$${}^{(1)}_3F(\text{---}\text{---}\text{---}) = -\frac{3\zeta(0)\gamma_\infty^2}{2(1 - \gamma_\infty)^4 \bar{r}_\infty^2 ((N - 1)\gamma_\infty + 1)^4} ((3N^2 - 12N + 13)\gamma_\infty^2 + 2(4N - 9)\gamma_\infty + 5) \quad (\text{D.77})$$

$${}^{(1)}_3F(\text{---}\text{---}\text{---}) = \frac{\zeta(0)\gamma_\infty}{4(1 - \gamma_\infty)^4 \bar{r}_\infty^2 ((N - 1)\gamma_\infty + 1)^4} ((3N^3 - 22N^2 + 67N - 72)\gamma_\infty^3 + 2(5N^2 - 27N + 50)\gamma_\infty^2 + (11N - 32)\gamma_\infty + 4) \quad (\text{D.78})$$

$${}^{(1)}_3F(\text{---}\text{---}\text{---}) = -\frac{\zeta(0)\gamma_\infty^2}{(1 - \gamma_\infty)^4 \bar{r}_\infty^2 ((N - 1)\gamma_\infty + 1)^4} ((3N^2 - 14N + 17)\gamma_\infty^2 + (8N - 22)\gamma_\infty + 5) \quad (\text{D.79})$$

$${}^{(1)}_3F(\text{---}\text{---}\text{---}) = -\frac{\zeta(0)\gamma_\infty^2}{2(1 - \gamma_\infty)^4 \bar{r}_\infty^2 ((N - 1)\gamma_\infty + 1)^4} ((3N^2 - 20N + 29)\gamma_\infty^2 + (8N - 34)\gamma_\infty + 5) \quad (\text{D.80})$$

$${}^{(1)}_3F(\text{---}\text{---}\text{---}) = \frac{6\zeta(0)\gamma_\infty^3((N - 2)\gamma_\infty + 2)}{(1 - \gamma_\infty)^4 \bar{r}_\infty^2 ((N - 1)\gamma_\infty + 1)^4} \quad (\text{D.81})$$

Appendix E

The S_N Clebsch-Gordon coefficients

E.1 Harmonic order

In Reference (87) it was shown that the transformation of the harmonic-order G and F matrix to symmetry coordinates is proportional to one of three matrices. These matrices are actually the Clebsch-Gordon coefficients which couple together the two irreps of the matrix transformation to yield something that is scalar under S_N , and hence transforms under the $[N]$ irrep. These Clebsch-Gordon coefficients were shown to have a simple form:

$$C^{[N][N]} = 1 \tag{E.1}$$

$$C^{[N-1,1][N-1,1]} = \mathbf{I}_{[N-1,1]} \tag{E.2}$$

$$C^{[N-2,2][N-2,2]} = \mathbf{I}_{[N-2,2]} \tag{E.3}$$

where $\mathbf{I}_{[N-1,1]}$ and $\mathbf{I}_{[N-2,2]}$ are identity matrices of dimension $N-1$ and $N(N-3)/2$, respectively. All other transformations yielded zero (or a zero matrix).

This result can be obtained by simply performing all the transformations and noting the results. This result can also be anticipated from group representation theory. There are only three ways one can couple two irreducible representations drawn from $[N]$, $[N-1,1]$, and $[N-2,2]$ irreps to form a scalar $[N]$ irrep,

$$\begin{aligned} [N] \otimes [N] &= [N] + \dots \\ [N-1,1] \otimes [N-1,1] &= [N] + \dots \\ [N-2,2] \otimes [N-2,2] &= [N] + \dots \end{aligned} \tag{E.4}$$

Therefore one expects only three corresponding Clebsch-Gordon coefficients at harmonic order.

E.2 First anharmonic order

E.2.1 Rank-one Clebsch-Gordon coefficients

Of the $[N]$, $[N-1,1]$, and $[N-2,2]$ irreps in the linear first-anharmonic term, only $[N]$ is scalar under S_N . Clearly

$$C^{[N]} = 1 \quad (\text{E.5})$$

$$C_{\xi}^{[N-1,1]} = 0 \quad (\text{E.6})$$

$$C_{\xi}^{[N-2,2]} = 0. \quad (\text{E.7})$$

E.2.2 Rank-three Clebsch-Gordon coefficients for S_N

We can know how many rank-three, first-anharmonic-order Clebsch-Gordon coefficients to expect from the theory of group representations, because there are only so many ways that three of the $[N]$, $[N-1, 1]$, and $[N-2, 2]$ irreps can be coupled together to form a scalar $[N]$ irrep. From the Clebsch-Gordon series for S_N (in Ref. (95) and others), there are eight ways:

$$\begin{aligned} [N] \otimes [N] \otimes [N] &= [N] + \dots \\ [N] \otimes [N-1, 1] \otimes [N-1, 1] &= [N] + \dots \\ [N] \otimes [N-2, 2] \otimes [N-2, 2] &= [N] + \dots \\ [N-1, 1] \otimes [N-1, 1] \otimes [N-1, 1] &= [N] + \dots \\ [N-1, 1] \otimes [N-1, 1] \otimes [N-2, 2] &= [N] + \dots \\ [N-1, 1] \otimes [N-2, 2] \otimes [N-2, 2] &= [N] + \dots \end{aligned} \quad (\text{E.8})$$

and two linearly independent couplings

$$[N-2, 2] \otimes [N-2, 2] \otimes [N-2, 2] = 2[N] + \dots \quad (\text{E.9})$$

In what follows we denote these two different couplings of three $[N-2, 2]$ irreps together to form an $[N]$ irrep by the roman numerals for the numbers 1 and 2, i.e. I and II respectively.

These Clebsch-Gordon coefficients are actually calculated (to within a normalization constant) by performing the relevant W transformations to symmetry coordinates of some binary invariant $B(\mathcal{G})$. This transformation is performed symbolically in *Mathematica*(101), using closed-form expressions for the W transformation matrices and the binary invariant. The W matrices are composed of step and Kronecker delta functions, and the binary invariants are composed of products of Kronecker delta functions. In order to perform this transformation analytically, we developed a *Mathematica* package which expands the native symbolic summation capability to include summands with step and Kronecker delta functions (106).

The Clebsch-Gordon coefficients may be normalized, using

$$C_{\xi_1, \xi_2, \xi_3}^{\alpha_1 \alpha_2 \alpha_3, k} C_{\xi_1, \xi_2, \xi_3}^{\alpha_1 \alpha_2 \alpha_3, k} = 1. \quad (\text{E.10})$$

We do not, however, need the above normalization relationship: we only need the coefficients to be linearly independent and to span the required space. Therefore, we drop the unitarity requirement and use unnormalized Clebsch-Gordon coefficients. The Clebsch-Gordon coefficient which couples together $[N][N][N]$ to yield an $[N]$ irrep is simply one:

$$C_{i,j,k}^{[N][N][N]} = 1, \quad (\text{E.11})$$

where $i = j = k = 1$. The Clebsch-Gordon coefficient which couples together $[N - 1, 1][N - 1, 1][N]$ to yield an $[N]$ irrep is an $(N - 1) \times (N - 1)$ matrix:

$$C_{i,j,k}^{[N-1,1][N-1,1][N]} = \delta_{i,j}, \quad (\text{E.12})$$

where $1 \leq i \leq N - 1$, $1 \leq j \leq N - 1$, and $k = 1$. The Clebsch-Gordon coefficient which couples together $[N - 1, 1][N - 1, 1][N - 1, 1]$ to yield an $[N]$ irrep is an $(N - 1) \times (N - 1) \times (N - 1)$ tensor:

$$C_{i,j,k}^{[N-1,1][N-1,1][N-1,1]} = \frac{1}{\sqrt{i(i+1)j(j+1)k(k+1)}} \left(-i(i^2 - 1)\delta_{ij}\delta_{ik} + i(i+1)\Theta_{k-i}\delta_{i,j} + k(k+1)\Theta_{j-k}\delta_{i,k} + j(j+1)\Theta_{i-j}\delta_{j,k} \right), \quad (\text{E.13})$$

where $1 \leq i \leq N - 1$, $1 \leq j \leq N - 1$, and $1 \leq k \leq N - 1$. We have five more Clebsch-Gordon coefficients.

$$C_{(ij),k,l}^{[N-2,2][N-1,1][N-1,1]} = \frac{1}{\sqrt{i(i+1)(j-3)(j-2)k(k+1)l(l+1)}} \times \left(2i(i+1)(\Theta_{-j+l+1} - \Theta_{l-k})\delta_{i,k} + 2i(i+1)(\Theta_{-j+k+1} - \Theta_{k-l})\delta_{i,l} + i(i+1)(j-2)(j-1)(\delta_{i,l}\delta_{j-1,k} + \delta_{i,k}\delta_{j-1,l}) - 2l(l+1)\Theta_{i-k}\delta_{k,l} + 2i(i^2 - 1)\delta_{i,k,l} \right), \quad (\text{E.14})$$

where $1 \leq i \leq j - 2$, $4 \leq j \leq N$, $1 \leq k \leq N - 1$, and $1 \leq l \leq N - 1$ (therefore $i \leq N - 2$).

$$C_{(ij)(kl),m}^{[N-2,2][N-2,2][N]} = \delta_{i,k}\delta_{j,l} \quad (\text{E.15})$$

where $1 \leq i \leq j - 2$, $4 \leq j \leq N$, $1 \leq k \leq l - 2$, $4 \leq l \leq N$ (therefore $i \leq N - 2$, $k \leq N - 2$), and $m = 1$.

We have also derived the remaining Clebsch-Gordon coefficients in closed form, but the result is too large to print here. The worst offender is $C^{[N-2,2][N-2,2][N-2,2],II}$, which contains 6,082 terms. All of the Clebsch-Gordon coefficients are available in a MATHEMATICA package (102), including the remaining coefficients:

$$C_{(i,j),(k,l),m}^{[N-2,2][N-2,2][N-1,1]}$$

(where $1 \leq i \leq j - 2$, $4 \leq j \leq N$, $1 \leq k \leq l - 2$, $4 \leq l \leq N$, $1 \leq m \leq N - 1$ and therefore $i \leq N - 2$, $k \leq N - 2$),

$$C_{(i,j),(k,l),(m,n)}^{[N-2,2][N-2,2][N-2,2],I}$$

and

$$C_{(i,j),(k,l),(m,n)}^{[N-2,2][N-2,2][N-2,2],II}$$

(where $1 \leq i \leq j - 2$, $4 \leq j \leq N$, $1 \leq k \leq l - 2$, $4 \leq l \leq N$, $1 \leq m \leq n - 2$, $4 \leq n \leq N$).

Appendix F

Binary invariants transformed to symmetry coordinates

Although the N -dependence of the Hamiltonian is contained within the Clebsch-Gordon coefficients, there remains the computation of the matrix transformations implicit in the proportionality tensors ${}^{(1)}_1\sigma^Q$ and ${}^{(1)}_3\sigma^Q$. Although these are small tensors, this is not a task I wish to repeat each time some detail of the physical system changes, such as an increase in the number of particles. This is where the decomposition of the DPT Hamiltonian tensors in the basis of binary invariants becomes indispensable. In order to derive the transformed Hamiltonian tensors F and G , I derive the transformed binary invariant basis tensors. These transformed binary invariant tensors must also be proportional to the appropriate Clebsch-Gordon coefficients.

F.1 Harmonic order

At harmonic order, there are three distinct blocks which may be resolved as a linear combination of the binary invariants of the graphs of those blocks,

$${}^{(0)}_2Q^{rr} = Q(\textcircled{\circ}\textcircled{\circ})B(\textcircled{\circ}\textcircled{\circ}) + Q(\textcircled{\circ}\textcircled{\circ})B(\textcircled{\circ}\textcircled{\circ}) \quad (\text{F.1})$$

$${}^{(0)}_2Q^{\gamma r} = Q(\textcircled{\circ}\textcircled{\circ})B(\textcircled{\circ}\textcircled{\circ}) + Q(\textcircled{\circ}\textcircled{\circ})B(\textcircled{\circ}\textcircled{\circ}) \quad (\text{F.2})$$

$${}^{(0)}_2Q^{\gamma\gamma} = Q(\textcircled{\circ}\textcircled{\circ})B(\textcircled{\circ}\textcircled{\circ}) + Q(\textcircled{\circ}\textcircled{\circ})B(\textcircled{\circ}\textcircled{\circ}) + Q(\textcircled{\circ}\textcircled{\circ})B(\textcircled{\circ}\textcircled{\circ}). \quad (\text{F.3})$$

The harmonic $\beta(G)$ is calculated by combining Eq.'s (5.31), (5.35), and (5.38):

$$\left[{}^{(0)}_2\beta^{\alpha_1\alpha_2}(\mathcal{G}) \right]_{X_1, X_2} = [W_{X_1}^{\alpha_1} W_{X_2}^{\alpha_2} B(\mathcal{G})]_{\xi, \xi} \quad (\text{F.4})$$

for any choice of ξ (so one makes a convenient choice).

For example, ${}^{(0)}_2Q^{rr}$ is resolved as a linear combination of two binary invariants:

$${}^{(0)}_2Q^{rr} = Q(\textcircled{\circ}\textcircled{\circ})B(\textcircled{\circ}\textcircled{\circ}) + Q(\textcircled{\circ}\textcircled{\circ})B(\textcircled{\circ}\textcircled{\circ}).$$

There are two harmonic σ^Q tensors with $\vec{r}'\vec{r}'$ elements:

$$\left[{}^{(0)}_2\sigma^Q_{[N][N]} \right]_{\vec{r}', \vec{r}'} = Q(\textcircled{\circ}\textcircled{\circ}) + (N-1)Q(\textcircled{\circ}\textcircled{\circ}) \quad (\text{F.5})$$

$$\left[\begin{matrix} (0) \\ 2 \end{matrix} \sigma_{[N-1,1][N-1,1]}^Q \right]_{\bar{r}', \bar{r}'} = Q(\infty) - Q(\odot \odot). \quad (\text{F.6})$$

Using Eq. (F.4), I generate the coefficients of the transformed binary invariants, $\left[\begin{matrix} (0) \\ 2 \end{matrix} \beta^{\alpha_1 \alpha_2}(\mathcal{G}) \right]_{X_1, X_2}$, in Table F.1. These results are consistent with Ref. (81; 82).

F.2 First anharmonic order

The transformation of the F and G tensors results from the transformation properties of the binary invariants,

$$\left[\begin{matrix} (1) \\ 1 \end{matrix} Q_W^{block} \right]_{\nu} = \sum_{\mathcal{G} \in \mathbb{G}_{block}} Q^{block}(\mathcal{G}) [B_W^{block}(\mathcal{G})]_{\nu} \quad (\text{F.7})$$

$$\left[\begin{matrix} (1) \\ 3 \end{matrix} Q_W^{block} \right]_{\nu_1, \nu_2, \nu_3} = \sum_{\mathcal{G} \in \mathbb{G}_{block}} Q^{block}(\mathcal{G}) [B_W^{block}(\mathcal{G})]_{\nu_1, \nu_2, \nu_3}. \quad (\text{F.8})$$

The rank-one binary invariants transform as (summation over repeated indices η from 1 to P implied)

$$[B_W(\mathcal{G})]_{\nu} = W_{\nu, \eta} [B(\mathcal{G})]_{\eta}, \quad (\text{F.9})$$

and the rank-three binary invariants transform as

$$[B_W(\mathcal{G})]_{\nu_1, \nu_2, \nu_3} = W_{\nu_1, \eta_1} W_{\nu_2, \eta_2} W_{\nu_3, \eta_3} [B(\mathcal{G})]_{\eta_1, \eta_2, \eta_3}. \quad (\text{F.10})$$

Each transformed binary invariant, in turn, may be written in terms of the appropriate Clebsch-Gordon coefficient with some multiplier $\beta(\mathcal{G})$.

F.2.1 Rank one first anharmonic



The Clebsch-Gordon coefficients for the symmetry transformations of $B(\odot)$ and $B(\leftrightarrow)$ are simply unity or zero. Therefore, the rank-one binary invariants transformed to symmetry coordinates have a block structure



$$B_W = \begin{pmatrix} \left[\begin{matrix} (1) \\ 1 \end{matrix} \beta^{\mathbf{0}}(\odot) \right]_r \\ \left[\begin{matrix} (1) \\ 1 \end{matrix} \beta^{\mathbf{0}}(\leftrightarrow) \right]_{\gamma} \\ \hline 0 \\ 0 \\ \hline 0 \end{pmatrix}, \quad (\text{F.11})$$

where the $\beta(\mathcal{G})$ multipliers are obtained from solving (for any ξ)

$$\left[\begin{matrix} (1) \\ 1 \end{matrix} \beta^{\alpha_1}(\mathcal{G}) \right]_{X_1} = [W_{X_1}^{\alpha_1} B(\mathcal{G})]_{\xi_1} \quad (\text{F.12})$$

for any ξ_1 . The two non-zero $\beta(\mathcal{G})$ multipliers are given in Table F.2.

$\left[\begin{smallmatrix} (0) \\ 2 \end{smallmatrix} \beta^{\alpha\alpha}(\mathcal{G}) \right]_{rr}$	00	11
	$(1 \leq N)$	$(1 \leq N)$
	1	1
	$N - 1$	-1

$\left[\begin{smallmatrix} (0) \\ 2 \end{smallmatrix} \beta^{\alpha\alpha}(\mathcal{G}) \right]_{\gamma r}$	00	11
	$(2 \leq N)$	$(3 \leq N)$
	$\sqrt{2(N-1)}$	$\sqrt{N-2}$
	$\frac{1}{2}(N-2)\sqrt{2(N-1)}$	$-\sqrt{N-2}$




$\left[\begin{smallmatrix} (0) \\ 2 \end{smallmatrix} \beta^{\alpha\alpha}(\mathcal{G}) \right]_{\gamma\gamma}$	00	11	22
	$(2 \leq N)$	$(3 \leq N)$	$(4 \leq N)$
	1	1	1
	$2(N-2)$	$N-4$	-2
	$\frac{1}{2}(N-3)(N-2)$	$-(N-3)$	1

Table F.1: Multipliers of the Clebsch-Gordon coefficients of the harmonic-order transformed binary invariants.

F.2.2 Rank-three first anharmonic order

The third-rank binary invariants transformed to symmetry coordinates $B_W(\mathcal{G})$ have a block form

$$B_W(\mathcal{G}) = \begin{pmatrix} \begin{pmatrix} B_W^{000}(\mathcal{G}) \\ B_W^{010}(\mathcal{G}) = 0 \\ B_W^{020}(\mathcal{G}) = 0 \end{pmatrix} & \begin{pmatrix} B_W^{001}(\mathcal{G}) = 0 \\ B_W^{011}(\mathcal{G}) \\ B_W^{021}(\mathcal{G}) = 0 \end{pmatrix} & \begin{pmatrix} B_W^{002}(\mathcal{G}) = 0 \\ B_W^{012}(\mathcal{G}) = 0 \\ B_W^{022}(\mathcal{G}) \end{pmatrix} \\ \begin{pmatrix} B_W^{100}(\mathcal{G}) = 0 \\ B_W^{110}(\mathcal{G}) \\ B_W^{120}(\mathcal{G}) = 0 \end{pmatrix} & \begin{pmatrix} B_W^{101}(\mathcal{G}) \\ B_W^{111}(\mathcal{G}) \\ B_W^{121}(\mathcal{G}) \end{pmatrix} & \begin{pmatrix} B_W^{102}(\mathcal{G}) = 0 \\ B_W^{112}(\mathcal{G}) \\ B_W^{122}(\mathcal{G}) \end{pmatrix} \\ \begin{pmatrix} B_W^{200}(\mathcal{G}) = 0 \\ B_W^{210}(\mathcal{G}) = 0 \\ B_W^{220}(\mathcal{G}) \end{pmatrix} & \begin{pmatrix} B_W^{201}(\mathcal{G}) = 0 \\ B_W^{211}(\mathcal{G}) \\ B_W^{221}(\mathcal{G}) \end{pmatrix} & \begin{pmatrix} B_W^{202}(\mathcal{G}) \\ B_W^{212}(\mathcal{G}) \\ B_W^{222}(\mathcal{G}) \end{pmatrix} \end{pmatrix}, \quad (\text{F.13})$$

where each block $B_W^{\alpha_1\alpha_2\alpha_3}(\mathcal{G})$ is related to the appropriate Clebsch-Gordan coefficient by a scalar multiplier $\beta^{\alpha_1\alpha_2\alpha_3,k}(\mathcal{G})$,

$$B_W^{\alpha_1\alpha_2\alpha_3}(\mathcal{G}) = \sum_k \binom{(1)}{3} \beta^{\alpha_1\alpha_2\alpha_3,k}(\mathcal{G}) C^{\alpha_1\alpha_2\alpha_3,k}. \quad (\text{F.14})$$

Therefore, I calculate each $\beta(\mathcal{G})$ coefficient using the following formula:

$$\sum_k^{t(\alpha_1,\alpha_2,\alpha_3)} \left[\binom{(1)}{3} \beta^{\alpha_1\alpha_2\alpha_3,k}(\mathcal{G}) \right]_{X_1,X_2,X_3} = \sum_k^{t(\alpha_1,\alpha_2,\alpha_3)} [W_{X_1}^{\alpha_1} W_{X_2}^{\alpha_2} W_{X_3}^{\alpha_3} B(\mathcal{G})]_{\xi_1,\xi_2,\xi_3} / C_{\xi_1,\xi_2,\xi_3}^{\alpha_1\alpha_2,\alpha_3,k} \quad (\text{F.15})$$

for any triple (ξ_1, ξ_2, ξ_3) where $C_{\xi_1,\xi_2,\xi_3}^{\alpha_1\alpha_2,\alpha_3,k} \neq 0$.

With implicit assumptions on the lower bound of N, given by the highest number of vertices in the corresponding sets of graphs, I list all coefficients of the transformed rank-three binary invariants in Tables F.3 through F.7.

$\left[\begin{smallmatrix} (1) \\ 1 \end{smallmatrix} \beta^\alpha(\mathcal{G}) \right]_X$	0	1	2
	\sqrt{N}	0	0
	$\sqrt{\frac{N(N-1)}{2}}$	0	0

Table F.2: Multipliers of the Clebsch-Gordon coefficients of the linear, first-anharmonic-order transformed binary invariants.

$\left[\begin{smallmatrix} (1) \\ 3 \end{smallmatrix} \beta^{\alpha_1 \alpha_2 \alpha_3, k}(\mathcal{G}) \right]_{r, r, r}$	000 ($1 \leq N$)	110, 101, 011 ($2 \leq N$)	111 ($3 \leq N$)
	$\frac{1}{\sqrt{N}}$	$\frac{1}{\sqrt{N}}$	1
	$\frac{3(N-1)}{\sqrt{N}}$	$\frac{N-3}{\sqrt{N}}$	-3
	$\frac{(N-2)(N-1)}{\sqrt{N}}$	$\frac{2-N}{\sqrt{N}}$	2

Table F.3: Multipliers of the Clebsch-Gordon coefficients of the first-anharmonic-order transformed binary invariants: $\left[\begin{smallmatrix} (1) \\ 3 \end{smallmatrix} \beta^{\alpha_1 \alpha_2 \alpha_3, R}(\mathcal{G}) \right]_{r, r, r}$.

$\left[\begin{smallmatrix} (1) \\ 3 \end{smallmatrix} \beta^{\alpha_1 \alpha_2 \alpha_3, k}(\mathcal{G}) \right]_{\gamma, r, r}$	000 ($2 \leq N$)	011 ($2 \leq N$)	110, 101 ($3 \leq N$)	111 ($3 \leq N$)	211 ($4 \leq N$)
	$2\sqrt{\frac{N-1}{2N}}$	$\frac{\sqrt{2}\sqrt{N-1}}{\sqrt{N}}$	$\sqrt{\frac{N-2}{N}}$	$\sqrt{N-2}$	0
	$2\sqrt{\frac{N-1}{2N}}$	$-\frac{\sqrt{2}}{\sqrt{N-1}\sqrt{N}}$	$\sqrt{\frac{N-2}{N}}$	$-\frac{2}{\sqrt{N-2}}$	1
	$4\sqrt{\frac{N-1}{2N}}$	$-\frac{2\sqrt{2}(N-2)}{\sqrt{N-1}\sqrt{N}}$	$(N-4)\sqrt{\frac{N-2}{N}}$	$-\frac{2(N-4)}{\sqrt{N-2}}$	-2
	$(N-2)\sqrt{\frac{N-1}{2N}}$	$\frac{(N-2)\sqrt{N-1}}{\sqrt{2}\sqrt{N}}$	$-\sqrt{\frac{N-2}{N}}$	$-\sqrt{N-2}$	0
	$(N-2)(N-3)\sqrt{\frac{N-1}{2N}}$	$\frac{(3-N)(N-2)}{\sqrt{2}\sqrt{N-1}\sqrt{N}}$	$-(N-3)\sqrt{\frac{N-2}{N}}$	$\frac{2(N-3)}{\sqrt{N-2}}$	1

Table F.4: Multipliers of the Clebsch-Gordon coefficients of the first-anharmonic-order transformed binary invariants: $\left[\begin{smallmatrix} (1) \\ 3 \end{smallmatrix} \beta^{\alpha_1 \alpha_2 \alpha_3, R}(\mathcal{G}) \right]_{\gamma, r, r}$.

$\left[\begin{smallmatrix} (1) \\ 3 \end{smallmatrix} \beta^{\alpha_1 \alpha_2 \alpha_3, k} (G) \right]_{\gamma, \gamma, r}$	000	110	011, 101	111
	$(2 \leq N)$	$(3 \leq N)$	$(3 \leq N)$	$(3 \leq N)$
	$\frac{2}{\sqrt{N}}$	$\frac{2}{\sqrt{N}}$	$\sqrt{2} \sqrt{\frac{N-2}{(N-1)N}}$	$\frac{N-4}{N-2}$
	$\frac{N-2}{\sqrt{N}}$	$\frac{N-2}{\sqrt{N}}$	$-\sqrt{2} \sqrt{\frac{N-2}{(N-1)N}}$	$\frac{4-N}{N-2}$
	$\frac{2(N-2)}{\sqrt{N}}$	$\frac{N-4}{\sqrt{N}}$	$\sqrt{2}(N-2) \sqrt{\frac{N-2}{(N-1)N}}$	$\frac{N^2-5N+8}{N-2}$
	$\frac{4(N-2)}{\sqrt{N}}$	$\frac{2(N-4)}{\sqrt{N}}$	$\sqrt{2}(N-4) \sqrt{\frac{N-2}{(N-1)N}}$	$\frac{16-6N}{N-2}$
	$\frac{2(N-3)(N-2)}{\sqrt{N}}$	$\frac{(N-4)(N-3)}{\sqrt{N}}$	$-2\sqrt{2}(N-3) \sqrt{\frac{N-2}{(N-1)N}}$	$-\frac{(N-8)(N-3)}{N-2}$
	$\frac{2(N-3)(N-2)}{\sqrt{N}}$	$-\frac{4(N-3)}{\sqrt{N}}$	$(N-4)(N-3) \sqrt{\frac{N-2}{2(N-1)N}}$	$-\frac{2(N-4)(N-3)}{N-2}$
	$\frac{(N-4)(N-3)(N-2)}{2\sqrt{N}}$	$-\frac{(N-4)(N-3)}{\sqrt{N}}$	$-(N-4)(N-3) \sqrt{\frac{N-2}{2(N-1)N}}$	$\frac{2(N-4)(N-3)}{N-2}$


$\left[\begin{smallmatrix} (1) \\ 3 \end{smallmatrix} \beta^{\alpha_1 \alpha_2 \alpha_3, k} (G) \right]_{\gamma, \gamma, r}$	211, 121	220	221
	$(4 \leq N)$	$(4 \leq N)$	$(5 \leq N)$
	$\frac{1}{\sqrt{N-2}}$	$\frac{2}{\sqrt{N}}$	$\frac{1}{\sqrt{N}}$
	$-\frac{1}{\sqrt{N-2}}$	$\frac{N-2}{\sqrt{N}}$	$\frac{-1}{\sqrt{N}}$
	$-\frac{1}{\sqrt{N-2}}$	$-\frac{2}{\sqrt{N}}$	$\frac{-1}{\sqrt{N}}$
	$\frac{N-4}{\sqrt{N-2}}$	$-\frac{4}{\sqrt{N}}$	$\frac{-2}{\sqrt{N}}$
	$\frac{5-N}{\sqrt{N-2}}$	$-\frac{2(N-3)}{\sqrt{N}}$	$\frac{3}{\sqrt{N}}$
	$\frac{4-N}{\sqrt{N-2}}$	$\frac{4}{\sqrt{N}}$	$\frac{2}{\sqrt{N}}$
	$\frac{N-4}{\sqrt{N-2}}$	$\frac{N-4}{\sqrt{N}}$	$\frac{-2}{\sqrt{N}}$

Table F.5: Multipliers of the Clebsch-Gordan coefficients of the first-anharmonic-order transformed binary invariants: $\left[\begin{smallmatrix} (1) \\ 3 \end{smallmatrix} \beta^{\alpha_1 \alpha_2 \alpha_3, R} (\mathcal{G}) \right]_{\gamma, \gamma, r}$

$\left[\begin{smallmatrix} (1) \\ 3 \end{smallmatrix} \beta^{\alpha_1 \alpha_2 \alpha_3, k} (\mathcal{G}) \right]_{\gamma, \gamma, \gamma}$	000	110, 101, 011	111	211, 121, 112
	$(2 \leq N)$	$(3 \leq N)$	$(3 \leq N)$	$(4 \leq N)$
\ominus	$\frac{1}{2} N P_2 \left(\frac{2}{N(N-1)} \right)^{\text{obj}}$	$\frac{\sqrt{2}}{\sqrt{(N-1)N}}$	$\frac{N-4}{(N-2)^{3/2}}$	$\frac{1}{N-2}$
\triangle	$N P_3 \left(\frac{2}{N(N-1)} \right)^{\text{obj}}$	$\frac{\sqrt{2}(N-4)}{\sqrt{(N-1)N}}$	$\frac{16-6N}{(N-2)^{3/2}}$	$\frac{N-4}{N-2}$
\circ	$3_N P_3 \left(\frac{2}{N(N-1)} \right)^{\text{obj}}$	$\frac{4\sqrt{2}(N-3)}{\sqrt{(N-1)N}}$	$\frac{3(N-4)^2}{(N-2)^{3/2}}$	$\frac{2(N-5)}{N-2}$
\vdash	$N P_4 \left(\frac{2}{N(N-1)} \right)^{\text{obj}}$	$\frac{\sqrt{2}(N-4)(N-3)}{\sqrt{(N-1)N}}$	$\frac{(N-3)(N^2-6N+16)}{(N-2)^{3/2}}$	$-\frac{2(N-4)}{N-2}$
\sqcup	$3_N P_4 \left(\frac{2}{N(N-1)} \right)^{\text{obj}}$	$\frac{2\sqrt{2}(N-6)(N-3)}{\sqrt{(N-1)N}}$	$-\frac{12(N-4)(N-3)}{(N-2)^{3/2}}$	$\frac{(N-6)(N-5)}{N-2}$
$\circ \circ$	$\frac{3}{4} N P_4 \left(\frac{2}{N(N-1)} \right)^{\text{obj}}$	$\frac{(N-6)(N-3)}{\sqrt{2}\sqrt{(N-1)N}}$	$-\frac{3(N-4)(N-3)}{(N-2)^{3/2}}$	$\frac{7-2N}{N-2}$
$\sqcup \sqcup$	$\frac{3}{2} N P_5 \left(\frac{2}{N(N-1)} \right)^{\text{obj}}$	$\frac{(N-12)(N-4)(N-3)}{\sqrt{2}\sqrt{(N-1)N}}$	$-\frac{3(N-8)(N-4)(N-3)}{(N-2)^{3/2}}$	$-\frac{(N-4)(2N-13)}{N-2}$
\equiv	$\frac{1}{8} N P_6 \left(\frac{2}{N(N-1)} \right)^{\text{obj}}$	$-\frac{(N-5)(N-4)(N-3)}{\sqrt{2}\sqrt{(N-1)N}}$	$\frac{2(N-5)(N-4)(N-3)}{(N-2)^{3/2}}$	$\frac{(N-5)(N-4)}{N-2}$

$\left[\begin{smallmatrix} (1) \\ 3 \end{smallmatrix} \beta^{\alpha_1 \alpha_2 \alpha_3, k} (\mathcal{G}) \right]_{\gamma, \gamma, \gamma}$	220, 202, 022	221, 212, 122	222	222(i)	222(ii)
	$(4 \leq N)$	$(5 \leq N)$	$(4 \leq N \leq 5)$	$(6 \leq N)$	$(6 \leq N)$
\ominus	$\sqrt{\frac{2}{N(N-1)}}$	$\frac{1}{\sqrt{N-2}}$	$\frac{1}{4}$	0	$\frac{1}{4}$
\triangle	$-2\sqrt{\frac{2}{N(N-1)}}$	$-\frac{2}{\sqrt{N-2}}$	1	1	0
\circ	$2(N-4)\sqrt{\frac{2}{N(N-1)}}$	$\frac{N-8}{\sqrt{N-2}}$	$-\frac{3}{2}$	0	$-\frac{3}{2}$
\vdash	$-2(N-3)\sqrt{\frac{2}{N(N-1)}}$	$\frac{6-N}{\sqrt{N-2}}$	1	0	1
\sqcup	$-4(N-4)\sqrt{\frac{2}{N(N-1)}}$	$-\frac{2(N-8)}{\sqrt{N-2}}$	$-\frac{3}{2}$	-3	$\frac{3}{2}$
$\circ \circ$	$\frac{1}{2} (N^2 - 5N + 10) \sqrt{\frac{2}{N(N-1)}}$	$\frac{5-N}{\sqrt{N-2}}$	$\frac{3}{4}$	0	$\frac{3}{4}$
$\sqcup \sqcup$	$-(N-7)(N-4)\sqrt{\frac{2}{N(N-1)}}$	$\frac{5N-28}{\sqrt{N-2}}$	0	3	-3
\equiv	$\frac{1}{2} (N-5)(N-4)\sqrt{\frac{2}{N(N-1)}}$	$-\frac{2(N-5)}{\sqrt{N-2}}$	0	-1	1

Table F.6: Multipliers of the Clebsch-Gordan coefficients of the first-anharmonic-order transformed binary invariants: $\left[\begin{smallmatrix} (1) \\ 3 \end{smallmatrix} \beta^{\alpha_1 \alpha_2 \alpha_3, k} (\mathcal{G}) \right]_{\gamma, \gamma, \gamma}$. The quantity ${}_N P_v$ is the number of ways to choose v vertices from N , without replacement (${}_N P_v = N!/(N-v)!$).

$\left[\begin{smallmatrix} (1) \\ 3 \end{smallmatrix} \beta^{\alpha_1 \alpha_2 \alpha_3, k}(\mathcal{G}) \right]_{\gamma, \gamma, \gamma}$	000 ($2 \leq N$)	110, 101 ($3 \leq N$)	011 ($3 \leq N$)	111 ($3 \leq N$)	211 ($4 \leq N$)	121, 112 ($4 \leq N$)
	$2_N P_3 \left(\frac{2}{N(N-1)} \right)^{\frac{3}{2}}$	$\frac{\sqrt{2}(3N-8)}{\sqrt{(N-1)N}}$	$\frac{2\sqrt{2}(N-4)}{\sqrt{(N-1)N}}$	$\frac{2(N-4)^2}{(N-2)^{3/2}}$	$\frac{2(-4+N)}{N-2}$	$\frac{N-6}{N-2}$


$\left[\begin{smallmatrix} (1) \\ 3 \end{smallmatrix} \beta^{\alpha_1 \alpha_2 \alpha_3, k}(\mathcal{G}) \right]_{\gamma, \gamma, \gamma}$	022 ($4 \leq N$)	202, 220 ($4 \leq N$)	122 ($5 \leq N$)	221, 212 ($5 \leq N$)	222 ($4 \leq N \leq 5$)	222(i) ($6 \leq N$)	222(ii) ($6 \leq N$)
	$-\frac{4\sqrt{2}}{\sqrt{(N-1)N}}$	$\frac{2\sqrt{2}(N-3)}{\sqrt{(N-1)N}}$	$-\frac{4}{\sqrt{N-2}}$	$\frac{N-6}{\sqrt{N-2}}$	-1	0	-1

Table F.7: Multipliers of the Clebsch-Gordon coefficients of the first-anharmonic-order transformed binary invariants with distinguishable edges: relevant graphs. The quantity ${}_N P_3$ is the number of ways to choose three vertices from N , without replacement (${}_N P_3 = N(N-1)(N-2)$).

Appendix G

Derivation of the probability density profile

In this appendix, we provide the details of the derivation of the harmonic-order density profile and of the first-anharmonic-order density profile derived in References (90) and (103), respectively.

G.1 Harmonic-order density profile

Defining $S(D)$ to be the total D -dimensional solid angle(92),

$$S(D) = \frac{2 \pi^{\frac{D}{2}}}{\Gamma(\frac{D}{2})}, \quad (\text{G.1})$$

where we note that $S(1) = 2$, $S(2) = 2\pi$, $S(3) = 4\pi$, $S(4) = 2\pi^2$, the harmonic-order Jacobian-weighted ground-state density profile, $N_0(r)$, is

$$\begin{aligned} S(D) N_0(r) &= S(D) r^{(D-1)} \rho_0(r) \\ &= \sum_{i=1}^N \int_{-\infty}^{\infty} \cdots \int_{-\infty}^{\infty} \delta_f(r - r_i) [{}_g\Phi_0(\bar{\mathbf{y}}')]^2 \prod_{\mu=\mathbf{0}^\pm, \mathbf{1}^\pm, \mathbf{2}} \prod_{\xi=1}^{d_\mu} d[q'_\mu]_\xi, \end{aligned} \quad (\text{G.2})$$

where $\rho_0(r)$ is the unweighted harmonic-order ground-state density profile and the Dirac delta function $\delta_f(r - r_i)$ is differentiated from the inverse dimension, δ , by the subscript f . We must perform a change of coordinates to evaluate this integral, due to the presence of r_i in the delta function. Since ${}_g\Phi_0(\bar{\mathbf{y}}')$ is invariant under particle interchange we choose $r_i = r_N$, since there are only four of the $P = N(N+1)/2$ normal coordinates which involve r_N : $\mathbf{q}'_{\mathbf{0}^+}$, $\mathbf{q}'_{\mathbf{0}^-}$, $[\mathbf{q}'_{\mathbf{1}^+}]_{d_{\mathbf{1}^+}}$ and $[\mathbf{q}'_{\mathbf{1}^-}]_{d_{\mathbf{1}^-}}$ (87). Therefore, we write the ground-state harmonic-order Jacobian-weighted probability density profile $N_0(r)$ as

$$\begin{aligned} S(D) N_0(r) &= N \int_{-\infty}^{\infty} \cdots \int_{-\infty}^{\infty} \delta_f(r - r_N) [{}_g\Phi_0(\bar{\mathbf{y}}')]^2 \prod_{\mu=\mathbf{0}^\pm, \mathbf{1}^\pm, \mathbf{2}} \prod_{\xi=1}^{d_\mu} d[q'_\mu]_\xi. \end{aligned} \quad (\text{G.3})$$

Upon substituting the form of the ground-state wavefunction using Eq. (6.3) and the fact that r_N only appears in $\mathbf{q}'_{\mathbf{0}^+}$, $\mathbf{q}'_{\mathbf{0}^-}$, $[\mathbf{q}'_{\mathbf{1}^+}]_{d_{\mathbf{1}^+}}$ and $[\mathbf{q}'_{\mathbf{1}^-}]_{d_{\mathbf{1}^-}}$ (87) we obtain

$$\begin{aligned}
& S(D) N_0(r) \\
&= N \int_{-\infty}^{\infty} \int_{-\infty}^{\infty} \int_{-\infty}^{\infty} \int_{-\infty}^{\infty} \delta_f(r - r_N) \\
&\quad \times \prod_{\mu=0^\pm, 1^\pm} [\phi_0(\sqrt{\bar{\omega}_\mu} [q'_\mu]_{d_\mu})]^2 d[q'_\mu]_{d_\mu} \\
&= \frac{N \sqrt{\bar{\omega}_{0^+} \bar{\omega}_{0^-} \bar{\omega}_{1^+} \bar{\omega}_{1^-}}}{\pi^2} \int_{-\infty}^{\infty} \int_{-\infty}^{\infty} \int_{-\infty}^{\infty} \int_{-\infty}^{\infty} \delta_f(r - r_N) \\
&\quad \times \exp \left(- \sum_{\mu_1=0^\pm, 1^\pm} \bar{\omega}_{\mu_1} [q'_{\mu_1}]_{d_{\mu_1}}^2 \right) \prod_{\mu_2=0^\pm, 1^\pm} d[q'_{\mu_2}]_{d_{\mu_2}}. \tag{G.4}
\end{aligned}$$

The delta function $\delta_f(r - r_N)$ is a function of r_N , while the integral is over the normal coordinates \mathbf{q}'^{0^+} , \mathbf{q}'^{0^-} , $[\mathbf{q}'^{1^+}]_{N-1}$, and $[\mathbf{q}'^{1^-}]_{N-1}$. Thus we need a change of variables to perform the integral. We change the variables of the integral to \bar{r}'_N , \bar{r}'_S , $\mathbf{S}'_{\bar{\gamma}}^{[N]}$, and $[\mathbf{S}'_{\bar{\gamma}}^{[N-1, 1]}]_{(N-1)}$, where

$$\bar{r}'_S = \sum_{i=1}^{N-1} \bar{r}'_i, \tag{G.5}$$

and $\mathbf{S}'_{\bar{\gamma}}^{[N]}$ and $[\mathbf{S}'_{\bar{\gamma}}^{[N-1, 1]}]_{(N-1)}$ are defined in Reference (87). Thus from Eq. (G.5) we obtain

$$\begin{pmatrix} \mathbf{q}'^{0^+} \\ \mathbf{q}'^{0^-} \\ [\mathbf{q}'^{1^+}]_{N-1} \\ [\mathbf{q}'^{1^-}]_{N-1} \end{pmatrix} = \mathbf{T} \mathbf{a}', \tag{G.6}$$

where

$$\mathbf{a}' = \begin{pmatrix} \bar{r}'_N \\ \bar{r}'_S \\ \mathbf{S}'_{\bar{\gamma}}^{[N]} \\ [\mathbf{S}'_{\bar{\gamma}}^{[N-1, 1]}]_{(N-1)} \end{pmatrix}, \tag{G.7}$$

$$\mathbf{T} = \begin{pmatrix} T_{11} & T_{11} & T_{13} & 0 \\ T_{21} & T_{21} & T_{23} & 0 \\ -(N-1)T_{31} & T_{31} & 0 & T_{34} \\ -(N-1)T_{41} & T_{41} & 0 & T_{44} \end{pmatrix},$$

and

$$\begin{aligned} T_{11} &= \frac{c_+^{[N]} \cos \theta_+^{[N]}}{\sqrt{N}}, & T_{13} &= c_+^{[N]} \sin \theta_+^{[N]}, \\ T_{21} &= \frac{c_-^{[N]} \cos \theta_-^{[N]}}{\sqrt{N}}, & T_{23} &= c_-^{[N]} \sin \theta_-^{[N]}, \\ T_{31} &= \frac{c_+^{[N-1, 1]} \cos \theta_+^{[N-1, 1]}}{\sqrt{N(N-1)}}, & T_{34} &= c_+^{[N-1, 1]} \sin \theta_+^{[N-1, 1]}, \\ T_{41} &= \frac{c_-^{[N-1, 1]} \cos \theta_-^{[N-1, 1]}}{\sqrt{N(N-1)}}, & T_{44} &= c_-^{[N-1, 1]} \sin \theta_-^{[N-1, 1]}. \end{aligned} \quad (\text{G.8})$$

The Jacobian, J_T , of the T transformation is thus

$$\begin{aligned} J_T = \det T &= -\frac{c_+^{[N]} c_-^{[N]} c_+^{[N-1, 1]} c_-^{[N-1, 1]}}{\sqrt{N-1}} \\ &\times \sin(\theta_+^{[N]} - \theta_-^{[N]}) \sin(\theta_+^{[N-1, 1]} - \theta_-^{[N-1, 1]}). \end{aligned} \quad (\text{G.9})$$

Defining a matrix of the normal-mode frequencies $\bar{\Omega}$,

$$\bar{\Omega} = \begin{pmatrix} \bar{\omega}_{\mathbf{0}+} & 0 & 0 & 0 \\ 0 & \bar{\omega}_{\mathbf{0}-} & 0 & 0 \\ 0 & 0 & \bar{\omega}_{\mathbf{1}+} & 0 \\ 0 & 0 & 0 & \bar{\omega}_{\mathbf{1}-} \end{pmatrix}, \quad (\text{G.10})$$

we can write the polynomial in the argument of the exponential in a more compact form (which is called bilinear form),

$$\begin{aligned} &S(D) N_0(r) \\ &= \frac{N J_T \sqrt{\bar{\omega}_{\mathbf{0}+} \bar{\omega}_{\mathbf{0}-} \bar{\omega}_{\mathbf{1}+} \bar{\omega}_{\mathbf{1}-}}}{\pi^2} \int_{-\infty}^{\infty} \int_{-\infty}^{\infty} \int_{-\infty}^{\infty} \int_{-\infty}^{\infty} \delta_f(r - r_N) \\ &\quad \times \exp\left(-\mathbf{a}'^T \mathbf{T}^T \bar{\Omega} \mathbf{T} \mathbf{a}'\right) d\bar{r}'_N d^3 \mathbf{b}', \end{aligned} \quad (\text{G.11})$$

where $d^3 \mathbf{b}' = d\bar{r}'_S d\mathbf{S}'_{\bar{\gamma}} d[\mathbf{S}'_{\bar{\gamma}}^{[N-1, 1]}]_{(N-1)}$.

The matrix $\mathbf{T}^T \overline{\boldsymbol{\Omega}} \mathbf{T}$ has a block form, which we must elucidate in order to separate the parts that do not act on \bar{r}'_N in the column vector \mathbf{a}' . Thus we write $\mathbf{T}^T \overline{\boldsymbol{\Omega}} \mathbf{T}$ in the following block form:

$$\mathbf{T}^T \overline{\boldsymbol{\Omega}} \mathbf{T} = \begin{pmatrix} K_0 & \mathbf{K}^T \\ \mathbf{K} & \boldsymbol{\kappa} \end{pmatrix}, \quad (\text{G.12})$$

where the blocks K_0 (a scalar), \mathbf{K} (a column vector of length 3), and $\boldsymbol{\kappa}$ (a 3×3 matrix) are defined as

$$K_0 = \bar{\omega}_{\mathbf{0}+} T_{11}^2 + \bar{\omega}_{\mathbf{0}-} T_{21}^2 + (N-1)^2 (\bar{\omega}_{\mathbf{1}+} T_{31}^2 + \bar{\omega}_{\mathbf{1}-} T_{41}^2), \quad (\text{G.13})$$

$$\mathbf{K} = \begin{pmatrix} \bar{\omega}_{\mathbf{0}+} T_{11}^2 + \bar{\omega}_{\mathbf{0}-} T_{21}^2 - (N-1)(\bar{\omega}_{\mathbf{1}+} T_{31}^2 + \bar{\omega}_{\mathbf{1}-} T_{41}^2) \\ \bar{\omega}_{\mathbf{0}+} T_{11} T_{13} + \bar{\omega}_{\mathbf{0}-} T_{21} T_{23} \\ -(N-1)(\bar{\omega}_{\mathbf{1}+} T_{31} T_{34} + \bar{\omega}_{\mathbf{1}-} T_{41} T_{44}) \end{pmatrix}, \quad (\text{G.14})$$

and the matrix $\boldsymbol{\kappa}$ has components

$$\begin{aligned} \boldsymbol{\kappa}_{11} &= \bar{\omega}_{\mathbf{0}+} T_{11}^2 + \bar{\omega}_{\mathbf{0}-} T_{21}^2 + \bar{\omega}_{\mathbf{1}+} T_{31}^2 + \bar{\omega}_{\mathbf{1}-} T_{41}^2, \\ \boldsymbol{\kappa}_{12} &= \boldsymbol{\kappa}_{21} = \bar{\omega}_{\mathbf{0}+} T_{11} T_{13} + \bar{\omega}_{\mathbf{0}-} T_{21} T_{23}, \\ \boldsymbol{\kappa}_{13} = \boldsymbol{\kappa}_{31} &= \bar{\omega}_{\mathbf{1}+} T_{31} T_{34} + \bar{\omega}_{\mathbf{1}-} T_{41} T_{44}, \quad \boldsymbol{\kappa}_{22} = \bar{\omega}_{\mathbf{0}+} T_{13}^2 + \bar{\omega}_{\mathbf{0}-} T_{23}^2, \\ \boldsymbol{\kappa}_{23} = \boldsymbol{\kappa}_{32} &= 0, \quad \boldsymbol{\kappa}_{33} = \bar{\omega}_{\mathbf{1}+} T_{34}^2 + \bar{\omega}_{\mathbf{1}-} T_{44}^2. \end{aligned} \quad (\text{G.15})$$

Using Eqs. (G.7) and (G.12) in Eq. (G.11), we obtain

$$\begin{aligned} &S(D) N_0(r) \\ &= \frac{N J_T \sqrt{\bar{\omega}_{\mathbf{0}+} \bar{\omega}_{\mathbf{0}-} \bar{\omega}_{\mathbf{1}+} \bar{\omega}_{\mathbf{1}-}}}{\pi^2} \int_{-\infty}^{\infty} \int_{-\infty}^{\infty} \int_{-\infty}^{\infty} \int_{-\infty}^{\infty} \delta_f(r - r_N) \\ &\quad \times \exp \left(-K_0 \bar{r}'_N{}^2 - 2\bar{r}'_N \mathbf{K}^T \mathbf{b}' - \mathbf{b}'^T \boldsymbol{\kappa} \mathbf{b}' \right) d\bar{r}'_N d^3 \mathbf{b}', \end{aligned} \quad (\text{G.16})$$

where

$$\mathbf{b}' = \begin{pmatrix} \bar{r}'_S \\ \mathbf{S}_{\bar{\gamma}'}^{[N]} \\ [\mathbf{S}_{\bar{\gamma}'}^{[N-1, 1]}]_{(N-1)} \end{pmatrix}. \quad (\text{G.17})$$

The delta function is written in terms of the radius r_N , not the internal displacement coordinate \bar{r}'_N in the integral. We rewrite the delta function in terms of the coordinate \bar{r}'_N using the identity

$$\delta_f(r - r_N) = \left(\sqrt{\delta} \kappa(D) \right)^{-1} \delta_f \left(\delta^{-\frac{1}{2}} \left(\frac{r}{\kappa(D)} - \bar{r}_\infty \right) - \bar{r}'_N \right). \quad (\text{G.18})$$

(Note that Eq. (G.18) corrects a mistake between Eqs (63) and (64) in Reference (90)). We obtain

$$\begin{aligned} S(D) N_0(r) &= \frac{N}{\pi^2} \sqrt{\frac{\bar{\omega}_{0+} \bar{\omega}_{0-} \bar{\omega}_{1+} \bar{\omega}_{1-} J_T^2}{\delta \kappa^2(D)}} \\ &\times \int_{-\infty}^{\infty} \int_{-\infty}^{\infty} \int_{-\infty}^{\infty} \int_{-\infty}^{\infty} \exp \left(-\delta^{-1} K_0 \left(\frac{r}{\kappa(D)} - \bar{r}_\infty \right)^2 \right. \\ &\quad \left. - 2\delta^{-\frac{1}{2}} \left(\frac{r}{\kappa(D)} - \bar{r}_\infty \right) \mathbf{K}^T \mathbf{b}' - \mathbf{b}'^T \mathbf{K} \mathbf{b}' \right) d^3 \mathbf{b}'. \end{aligned} \quad (\text{G.19})$$

Using the integral identity

$$\begin{aligned} \int_{-\infty}^{\infty} \cdots \int_{-\infty}^{\infty} \exp(-\mathbf{b}'^T \mathbf{A} \mathbf{b}' - 2\mathbf{B}^T \mathbf{b}') d^n \mathbf{b}' \\ = \frac{\pi^{\frac{n}{2}}}{\sqrt{\det \mathbf{A}}} \exp(\mathbf{B}^T \mathbf{A}^{-1} \mathbf{B}). \end{aligned} \quad (\text{G.20})$$

We finally evaluate the integral in Eq. (G.19), obtaining

$$\begin{aligned} S(D) N_0(r) &= N \sqrt{\frac{\bar{\omega}_{0+} \bar{\omega}_{0-} \bar{\omega}_{1+} \bar{\omega}_{1-} J_T^2}{\delta \kappa^2(D) \pi \det \mathbf{K}}} \\ &\times \exp \left(-\delta^{-1} \left(\frac{r}{\kappa(D)} - \bar{r}_\infty \right)^2 (K_0 - \mathbf{K}^T \mathbf{K}^{-1} \mathbf{K}) \right). \end{aligned} \quad (\text{G.21})$$

The number of constants floating around in the above equation may be significantly reduced. For one thing, if the above density profile is to be normalized to N , then there should be a relation between the factors in the exponential and those in front. That relationship is expressed in the following definition for the constant R :

$$R = \frac{\bar{\omega}_{0+} \bar{\omega}_{0-} \bar{\omega}_{1+} \bar{\omega}_{1-} J_T^2}{\det \mathbf{K}} = (K_0 - \mathbf{K}^T \mathbf{K}^{-1} \mathbf{K}). \quad (\text{G.22})$$

Writing $N_0(r)$ in terms of the constant R , we obtain a relatively simple expression for $N_0(r)$,

$$S(D) N_0(r) = N \sqrt{\frac{D}{\kappa^2(D)} \frac{R}{\pi}} \exp \left(-R \left(r \frac{\sqrt{D}}{\kappa(D)} - \sqrt{D} \bar{r}_\infty \right)^2 \right). \quad (\text{G.23})$$

Notice that the harmonic-order DPT density profile is a Gaussian (normalized to N) centered around $r = \kappa(D) \bar{r}_\infty$, the $D \rightarrow \infty$ configuration radius.

G.2 First anharmonic density profile

The derivation of the first-anharmonic density profile is similar to that of the harmonic density profile in that the same transformations are used to perform a change of coordinates. Integrals over the normal coordinates \mathbf{q}'_{0+} , \mathbf{q}'_{0-} , $[\mathbf{q}'_{1+}]_{N-1}$, and $[\mathbf{q}'_{1-}]_{N-1}$ are transformed to \bar{r}'_N , \bar{r}'_S , $\mathbf{S}'_{\bar{r}'}$, and $[\mathbf{S}'_{\bar{r}'}]_{(N-1)}$.

The first-anharmonic-order density profile is derived from the first-anharmonic-order wavefunction in a similar way to harmonic order, starting by simply substituting $[_g\Phi_1(\bar{\mathbf{q}}')]^2 = (1 + \delta^{1/2})^2 [_g\Phi_0(\bar{\mathbf{q}}')]^2$ for $[_g\Phi_0(\bar{\mathbf{q}}')]^2$ in Eq. (G.3):

$$N_1(r) = \frac{N}{S(D)} \int_{-\infty}^{\infty} \cdots \int_{-\infty}^{\infty} \prod_{\mu=\mathbf{0}^{\pm}, \mathbf{1}^{\pm}, \mathbf{2}} \prod_{\xi=1}^{d_{\mu}} d[q'^{\mu}]_{\xi} \times \delta_f(r - r_N) (1 + 2\delta^{1/2}\Delta + \delta\Delta^2) [_g\Phi_0(\bar{\mathbf{q}}')]^2, \quad (\text{G.24})$$

We are interested in deriving the density profile to order $\delta^{1/2}$, and the $\delta\Delta^2$ term is much more difficult to derive (due to the presence of a sixth-order polynomial). Dropping the order δ term is expedient, but it introduces a liability: it will be possible for the density profile to become negative. We drop the order δ term for now, obtaining Eq. (6.28)

$$N_1(r) = N_0(r) + \frac{N}{S(D)} 2\delta^{1/2} \int_{-\infty}^{\infty} \cdots \int_{-\infty}^{\infty} \prod_{\mu=\mathbf{0}^{\pm}, \mathbf{1}^{\pm}, \mathbf{2}} \prod_{\xi=1}^{d_{\mu}} d[q'_{\mu}]_{\xi} \times \delta_f(r - r_N) \Delta [_g\Phi_0(\bar{\mathbf{q}}')]^2. \quad (\text{G.25})$$

Substituting Δ from Eq. (6.15), we obtain

$$N_1(r) = N_0(r) + \frac{N}{S(D)} 2\delta^{1/2} \int_{-\infty}^{\infty} \cdots \int_{-\infty}^{\infty} \prod_{\mu=\mathbf{0}^{\pm}, \mathbf{1}^{\pm}, \mathbf{2}} \prod_{\xi=1}^{d_{\mu}} d[q'_{\mu}]_{\xi} \delta_f(r - r_N) \times \left(\sum_{\mu_1, \mu_2, \mu_3, k} \sum_{\xi_1, \xi_2, \xi_3} {}^{(1)}_3\tau_{\mu_1, \mu_2, \mu_3, k}^{\Delta} C_{\xi_1, \xi_2, \xi_3}^{\mu_1 \mu_2 \mu_3, k} [q'_{\mu_1}]_{\xi_1} [q'_{\mu_2}]_{\xi_2} [q'_{\mu_3}]_{\xi_3} + \sum_{\mu_1, \xi_1} {}^{(1)}_1\tau_{\mu_1}^{\Delta} [q'_{\mu_1}]_{\xi_1} \right) \times [_g\Phi_0(\bar{\mathbf{q}}')]^2. \quad (\text{G.26})$$

G.2.1 Normal-coordinate integrals

Let us separate the problem of evaluating the integrals over the third-order polynomial in q'_{ν_i} from the problem of summing over ${}^{(1)}_3\tau_{\mu_1, \mu_2, \mu_3, k}^{\Delta} C_{\xi_1, \xi_2, \xi_3}^{\mu_1 \mu_2 \mu_3, k}$ and ${}^{(1)}_1\tau_{\mu_1}^{\Delta}$ by defining the $(P \times P \times P)$ tensor ${}_3M_{\nu_1, \nu_2, \nu_3}$ and the length P column vector ${}_1M_{\nu}$:

$${}_3M_{\nu_1 \nu_2 \nu_3} = \int_{-\infty}^{\infty} \cdots \int_{-\infty}^{\infty} \prod_{\nu'=1}^P dq'_{\nu'} \delta_f(r - r_N) q'_{\nu_1} q'_{\nu_2} q'_{\nu_3} [_g\Phi_0(\bar{\mathbf{q}}')]^2 \quad (\text{G.27})$$

$${}_1M_{\nu} = \int_{-\infty}^{\infty} \cdots \int_{-\infty}^{\infty} \prod_{\nu'=1}^P dq'_{\nu'} \delta_f(r - r_N) q'_{\nu} [_g\Phi_0(\bar{\mathbf{q}}')]^2. \quad (\text{G.28})$$

Indexing ${}_3M$ and ${}_1M$ by (μ_i, ξ_i) rather than ν_i , we can write the density profile as a tensor contraction:

$$N_1(r) = N_0(r) + \frac{2\delta^{1/2} N}{S(D)} \left(\sum_{\mu_1, \mu_2, \mu_3, k} \sum_{\xi_1, \xi_2, \xi_3} \binom{(1)}{3} \tau_{\mu_1, \mu_2, \mu_3, k}^\Delta C_{\xi_1, \xi_2, \xi_3}^{\mu_1 \mu_2 \mu_3, k} {}_3M_{\xi_1, \xi_2, \xi_3}^{\mu_1 \mu_2 \mu_3} + \sum_{\mu_1'} \binom{(1)}{1} \tau_{\mu_1'}^\Delta {}_1M_1^{\mu_1'} \right), \quad (\text{G.29})$$

where we have used the fact that since $N_1(r)$ is a scalar under S_N , μ_1' only ranges over $\mathbf{0}^+$ and $\mathbf{0}^-$. Each element of the M tensor is an integral.

Because the integrals in both ${}_3M$ and ${}_1M$ are odd, each element of ${}_3M$ and ${}_1M$ would be zero were it not for the presence of the Kronecker delta function which depends on radius of the N -th particle r_N . Still, many of the normal coordinates do not depend on r_N . The normal coordinates of the $\mathbf{2}$ sector are entirely angular and do not depend on r_N .

For the column vector ${}_1M$, there are only two types of elements, those which are independent of r_N and are indexed by $(\bar{\mu}, \bar{\xi})$, and those four which depend on r_N and are indexed by $(\mu', d_{\mu'})$. The integrals for the $(\bar{\mu}, \bar{\xi})$ elements are zero because the delta function has no effect and the integral is odd. The remaining four integrals must be transformed to internal coordinates to be evaluated.

For the rank-three tensor ${}_3M$, there are more cases to consider. Integrals in which all three normal coordinates are independent of r_N are zero (because at least one integrand will always be odd) and hence ${}_3M_{\bar{x}i_1, \bar{x}i_2, \bar{x}i_3}^{\bar{\mu}_1, \bar{\mu}_2, \bar{\mu}_3} = 0$. Integrals in which two coordinates are independent of r_N are odd unless the coordinates are the same. Therefore there will be some non-zero elements of the form ${}_3M_{\bar{x}i, \bar{x}i, d_{\mu'}}^{\bar{\mu}, \bar{\mu}, \mu'}$ that are yet to be determined. The final case is when all three coordinates are one of the four that depend on r_N : ${}_3M_{d_{\mu'_1}, d_{\mu'_2}, d_{\mu'_3}}^{\mu'_1, \mu'_2, \mu'_3}$.

All of the remaining elements of ${}_3M$ and ${}_1M$ that do not involve r_N may be evaluated using the following integrals:

$$\int_{-\infty}^{\infty} \sqrt{\frac{\bar{\omega}_\nu}{\pi}} e^{-\bar{\omega}_\nu (q'_\nu)^2} dq'_\nu = 1 \quad (\text{G.30})$$

$$\int_{-\infty}^{\infty} \sqrt{\frac{\bar{\omega}_\nu}{\pi}} (q'_\nu)^2 e^{-\bar{\omega}_\nu (q'_\nu)^2} dq'_\nu = \frac{1}{2\bar{\omega}_\nu}. \quad (\text{G.31})$$

Thus from Eqs. (G.29) and (G.30) we find

$$\begin{aligned} \mathcal{N}_1(r) = N_0(r) + \frac{2\delta^{1/2} N}{S(D)} & \left(\sum_{\mu'_1, \mu'_2, \mu'_3} \binom{(1)}{3} \tau_{\mu'_1, \mu'_2, \mu'_3, i}^\Delta C_{d_{\mu'_1}, d_{\mu'_2}, d_{\mu'_3}}^{\mu'_1, \mu'_2, \mu'_3, i} {}_3M_{d_{\mu'_1}, d_{\mu'_2}, d_{\mu'_3}}^{\mu'_1, \mu'_2, \mu'_3} \right. \\ & + \sum_{\mu'} \left\{ \sum_{\bar{\mu}} \frac{1}{2\bar{\omega}_{\bar{\mu}}} \left(\binom{(1)}{3} \tau_{\bar{\mu}, \bar{\mu}, \mu', i}^\Delta + \binom{(1)}{3} \tau_{\bar{\mu}, \mu', \bar{\mu}, i}^\Delta + \binom{(1)}{3} \tau_{\mu', \bar{\mu}, \bar{\mu}, i}^\Delta \right) C_{\bar{\xi}, \bar{\xi}, d_{\mu'}}^{\bar{\mu}, \bar{\mu}, \mu', i} + \sum_{\bar{\mu}=\mathbf{0}^+}^{\mathbf{0}^-} \binom{(1)}{1} \tau_{\mu'}^\Delta \right\} \\ & \left. \times {}_1M_{d_{\mu'}}^{\mu'} \right), \quad (\text{G.32}) \end{aligned}$$

where μ' ranges over $\mathbf{0}^\pm$ and $\mathbf{1}^\pm$, $\delta_{\mu', \mathbf{0}^\pm}$ equals one when $\mu' = \mathbf{0}^\pm$ but is zero otherwise, $\bar{\mu}$ ranges over $\mathbf{1}^\pm$ and $\mathbf{2}$, and $1 \leq \bar{\xi} \leq d_{\mathbf{1}^\pm} - 1 = N - 2$ when $\bar{\mu} = \mathbf{1}^\pm$, or $1 \leq \bar{\xi} \leq d_{\mathbf{2}} = N(N - 3)/2$ when $\bar{\mu} = \mathbf{2}$.

G.2.2 Clebsch-Gordon tensor contractions

The relevant Clebsch-Gordon elements and sums in the above equation are

$$\begin{aligned}
C_{1\ 1\ 1}^{\mathbf{0}\ \mathbf{0}\ \mathbf{0},i} &= 1 \\
C_{N-1\ 1\ 1}^{\mathbf{1}\ \mathbf{0}\ \mathbf{0},i} &= C_{1\ N-1\ 1}^{\mathbf{0}\ \mathbf{1}\ \mathbf{0},i} = C_{1\ 1\ N-1}^{\mathbf{0}\ \mathbf{0}\ \mathbf{1},i} = 0 \\
C_{N-1\ N-1\ 1}^{\mathbf{1}\ \mathbf{1}\ \mathbf{0},i} &= C_{N-1\ 1\ N-1}^{\mathbf{1}\ \mathbf{0}\ \mathbf{1},i} = C_{1\ N-1\ N-1}^{\mathbf{0}\ \mathbf{1}\ \mathbf{1},i} = 1 \\
C_{N-1\ N-1\ N-1}^{\mathbf{1}\ \mathbf{1}\ \mathbf{1},i} &= \frac{-(N-2)}{\sqrt{N(N-1)}}
\end{aligned} \tag{G.33}$$

$$\sum_{\bar{\xi}=1}^{N-2} C_{\bar{\xi}\ \bar{\xi}\ 1}^{\mathbf{1}\ \mathbf{1}\ \mathbf{0},i} = N-2 \tag{G.34}$$

$$\sum_{\bar{\xi}=1}^{N(N-3)/2} C_{\bar{\xi}\ \bar{\xi}\ 1}^{\mathbf{2}\ \mathbf{2}\ \mathbf{0},i} = \frac{N(N-3)}{2} \tag{G.35}$$

$$\sum_{\bar{\xi}=1}^{N-2} C_{\bar{\xi}\ \bar{\xi}\ N-1}^{\mathbf{1}\ \mathbf{1}\ \mathbf{1},i} = \frac{N-2}{\sqrt{N(N-1)}} \tag{G.36}$$

$$\sum_{\bar{\xi}=1}^{N(N-3)/2} C_{\bar{\xi}\ \bar{\xi}\ N-1}^{\mathbf{2}\ \mathbf{2}\ \mathbf{1},i} = 0. \tag{G.37}$$

Equation (G.37) simply follows from the fact that since the $\mathbf{2}$ indices are saturated, there is nothing to couple the $\mathbf{1}$ index with to form a scalar $\mathbf{0}$ irrep.

The indices ν_i of the tensor ${}_3M_{\nu_1,\nu_2,\nu_3}$ run from 1 to P , but since so many of the elements are zero we find it convenient to define two smaller tensors indexed by μ' : a $4 \times 4 \times 4$ tensor ${}^3E_{\mu'_1,\mu'_2,\mu'_3}$ to be the non-zero coefficients of the elements of ${}_3M$ which are cubic in r_N . In what follows we find it useful to define a $4 \times 4 \times 4$ tensor ${}^3E_{\mu'_1,\mu'_2,\mu'_3}$:

$${}^3E_{\mu'_1,\mu'_2,\mu'_3} = {}_3\tau_{\mu'_1,\mu'_2,\mu'_3,i}^{\Delta} C_{d_{\mu'_1},d_{\mu'_2},d_{\mu'_3}}^{\mu'_1\mu'_2\mu'_3,i}. \tag{G.38}$$

We emphasize that the above equation is a simple elemental multiplication, no summation is implied. Using the above Clebsch-Gordon sums, we obtain

$${}^3E_{\mathbf{0}\pm,\mathbf{0}\pm,\mathbf{0}\pm} = \tau_{\mathbf{0}\pm,\mathbf{0}\pm,\mathbf{0}\pm}^{\Delta} \tag{G.39}$$

$${}^3E_{\mathbf{1}\pm,\mathbf{0}\pm,\mathbf{0}\pm} = {}^3E_{\mathbf{0}\pm,\mathbf{1}\pm,\mathbf{0}\pm} = {}^3E_{\mathbf{0}\pm,\mathbf{0}\pm,\mathbf{1}\pm} = 0 \tag{G.40}$$

$${}^3E_{\mathbf{1}\pm,\mathbf{1}\pm,\mathbf{0}\pm} = \tau_{\mathbf{1}\pm,\mathbf{1}\pm,\mathbf{0}\pm}^{\Delta} \tag{G.41}$$

$${}^3E_{\mathbf{1}\pm,\mathbf{0}\pm,\mathbf{1}\pm} = \tau_{\mathbf{1}\pm,\mathbf{0}\pm,\mathbf{1}\pm}^{\Delta} \tag{G.42}$$

$${}^3E_{\mathbf{0}\pm,\mathbf{1}\pm,\mathbf{1}\pm} = \tau_{\mathbf{0}\pm,\mathbf{1}\pm,\mathbf{1}\pm}^{\Delta} \tag{G.43}$$

$${}^3E_{\mathbf{1}\pm,\mathbf{1}\pm,\mathbf{1}\pm} = \frac{-(N-2)}{\sqrt{N(N-1)}} \tau_{\mathbf{1}\pm,\mathbf{1}\pm,\mathbf{1}\pm}^{\Delta}. \tag{G.44}$$

In Eqs. G.39, each \pm associated with a sector ν_i is taken to be independent of the \pm associated with the other two sectors.

We also define a length-four column vector ${}^1E_{\mu'}$ to be those nonzero terms which are linear in r_N .

$${}^1E_{\mu'} = \sum_{\bar{\mu}} \frac{1}{2\bar{\omega}_{\bar{\mu}}} \left(\binom{(1)}{3} \tau_{\bar{\mu}, \bar{\mu}, \mu', i}^{\Delta} + \binom{(1)}{3} \tau_{\bar{\mu}, \mu', \bar{\mu}, i}^{\Delta} + \binom{(1)}{3} \tau_{\mu', \bar{\mu}, \bar{\mu}, i}^{\Delta} \right) \sum_{\bar{\xi}} C_{\bar{\xi}, \bar{\xi}, d_{\mu'}}^{\bar{\mu}, \bar{\mu}, \mu', i} + \sum_{\mu'=\mathbf{0}+}^{\mathbf{0}-} \binom{(1)}{1} \tau_{\mu'}^{\Delta}, \quad (\text{G.45})$$

i.e.

$$\begin{aligned} {}^1E_{\mathbf{0}\pm} &= \frac{(N-2)}{2} \frac{1}{\omega_{\mathbf{1}+}} (\tau_{\mathbf{1}+\mathbf{1}+\mathbf{0}\pm}^{\Delta} + \tau_{\mathbf{1}+\mathbf{0}\pm\mathbf{1}+}^{\Delta} + \tau_{\mathbf{0}\pm\mathbf{1}+\mathbf{1}+}^{\Delta}) \\ &\quad + \frac{(N-2)}{2} \frac{1}{\omega_{\mathbf{1}-}} (\tau_{\mathbf{1}-\mathbf{1}-\mathbf{0}\pm}^{\Delta} + \tau_{\mathbf{1}-\mathbf{0}\pm\mathbf{1}-}^{\Delta} + \tau_{\mathbf{0}\pm\mathbf{1}-\mathbf{1}-}^{\Delta}) \\ &\quad + \frac{N(N-3)}{4} \frac{1}{\omega_{\mathbf{2}}} (\tau_{\mathbf{2}\mathbf{2}\mathbf{0}\pm}^{\Delta} + \tau_{\mathbf{2}\mathbf{0}\pm\mathbf{2}}^{\Delta} + \tau_{\mathbf{0}\pm\mathbf{2}\mathbf{2}}^{\Delta}) + \binom{(1)}{1} \tau_{\mathbf{0}\pm}^{\Delta} \end{aligned} \quad (\text{G.46})$$

$$\begin{aligned} {}^1E_{\mathbf{1}\pm} &= \frac{N-2}{2\sqrt{N(N-1)}} \frac{1}{\omega_{\mathbf{1}+}} \left(\binom{(1)}{3} \tau_{\mathbf{1}+\mathbf{1}+\mathbf{1}\pm}^{\Delta} + \binom{(1)}{3} \tau_{\mathbf{1}+\mathbf{1}\pm\mathbf{1}+}^{\Delta} + \binom{(1)}{3} \tau_{\mathbf{1}\pm\mathbf{1}+\mathbf{1}+}^{\Delta} \right) \\ &\quad + \frac{N-2}{2\sqrt{N(N-1)}} \frac{1}{\omega_{\mathbf{1}-}} \left(\binom{(1)}{3} \tau_{\mathbf{1}-\mathbf{1}-\mathbf{1}\pm}^{\Delta} + \binom{(1)}{3} \tau_{\mathbf{1}-\mathbf{1}\pm\mathbf{1}-}^{\Delta} + \binom{(1)}{3} \tau_{\mathbf{1}\pm\mathbf{1}-\mathbf{1}-}^{\Delta} \right) \end{aligned} \quad (\text{G.47})$$

Using Eqs. (G.38) and (G.45), Eq. (G.32) may be written in a simpler form as

$$N_1(r) = N_0(r) + \frac{2\delta^{1/2} N}{S(D)} \left(\sum_{\mu'_1, \mu'_2, \mu'_3} {}^3E_{\mu'_1, \mu'_2, \mu'_3} {}^3M_{d_{\mu'_1}, d_{\mu'_2}, d_{\mu'_3}}^{\mu'_1, \mu'_2, \mu'_3} + \sum_{\mu'} {}^1E_{\mu'} {}^1M_{d_{\mu'}}^{\mu'} \right) \quad (\text{G.48})$$

G.2.3 Transformation of the integrals to symmetry coordinates

The elements of the M tensors are integrals over the normal coordinates. We use the T transformation in Eq. (G.6) to write these M tensors in terms of integrals over the coordinates of \mathbf{a}' :

$${}^nM_{d_{\mu'_1}, d_{\mu'_2}, \dots, d_{\mu'_n}}^{\mu'_1, \mu'_2, \dots, \mu'_n} = \sum_{i_1, i_2, \dots, i_n} T_{\mu'_1, i_1} T_{\mu'_2, i_2} \cdots T_{\mu'_n, i_n} {}^n\mathcal{M}_{i_1 i_2 \dots i_n}, \quad (\text{G.49})$$

where

$$\begin{aligned} {}^n\mathcal{M}_{i_1 i_2 \dots i_n} &= \frac{J_T \sqrt{\bar{\omega}_{\mathbf{0}+} \bar{\omega}_{\mathbf{0}-} \bar{\omega}_{\mathbf{1}+} \bar{\omega}_{\mathbf{1}-}}}{\pi^2} \int_{-\infty}^{\infty} \int_{-\infty}^{\infty} \int_{-\infty}^{\infty} \int_{-\infty}^{\infty} \delta_f(r - r_N) \\ &\quad \times a_{i_1} a_{i_2} \cdots a_{i_n} \exp(-K_0 a_1^2 - 2a_1 \mathbf{K}^T \mathbf{b}' - \mathbf{b}'^T \boldsymbol{\kappa} \mathbf{b}') da_1 d^3 \mathbf{b}', \end{aligned} \quad (\text{G.50})$$

and we have defined a new column vector \mathbf{b}'

$$\mathbf{b}' = \begin{pmatrix} \bar{r}'_S \\ \mathbf{S}_{\bar{\gamma}'}^{[N]} \\ \left[\mathbf{S}_{\bar{\gamma}'}^{[N-1, 1]} \right]_{(N-1)} \end{pmatrix}. \quad (\text{G.51})$$

Performing a similar transformation on the coefficients of the density profile ${}^1E_{\mu'}$ and ${}^3E_{\mu'_1, \mu'_2, \mu'_3}$, we obtain the (length 3) column vector ${}^1\Xi_i$ and the $(3 \times 3 \times 3)$ tensor ${}^3\Xi_{i,j,k}$:

$${}^1\Xi_i = \sum_{\mu'} {}^1E_{\mu'} T_{\mu', i} \quad (\text{G.52})$$

$${}^3\Xi_{i_1 i_2 i_3} = \sum_{\mu'_1, \mu'_2, \mu'_3} {}^3E_{\mu'_1, \mu'_2, \mu'_3} T_{\mu'_1, i_1} T_{\mu'_2, i_2} T_{\mu'_3, i_3}. \quad (\text{G.53})$$

Thus we have transform the density profile in Eq. (G.48) to internal coordinates and can now write

$$N_1(r) = N_0(r) + \frac{2\delta^{1/2} N}{S(D)} \left(\sum_{i_1, i_2, i_3} {}^3\Xi_{i_1 i_2 i_3} {}^3\mathcal{M}_{i_1 i_2 i_3} + \sum_i {}^1\Xi_i {}^1\mathcal{M}_i \right). \quad (\text{G.54})$$

G.2.4 Evaluation of the integrals

What remains now is to perform the integrals of Eq. (G.50) for ${}^3\mathcal{M}_{i_1 i_2 i_3}$ and ${}^1\mathcal{M}_i$ in Eq. (G.54). Defining the four component vector

$$\mathbf{V} = \begin{pmatrix} \frac{1}{2} K_0 \\ \mathbf{K} \end{pmatrix}, \quad (\text{G.55})$$

Eq. (G.50) can be written as a series of derivatives of a term proportional to $N_0(r)$

$$\begin{aligned} {}^n\mathcal{M}_{i_1 i_2 \dots i_n} &= \frac{J_T \sqrt{\bar{\omega}_0^+ \bar{\omega}_0^- \bar{\omega}_1^+ \bar{\omega}_1^-}}{\pi^2} \\ &\times \left(\frac{-1}{2\bar{r}'} \frac{\partial}{\partial V_{i_1}} \right) \left(\frac{-1}{2\bar{r}'} \frac{\partial}{\partial V_{i_2}} \right) \dots \left(\frac{-1}{2\bar{r}'} \frac{\partial}{\partial V_{i_n}} \right) \int_{-\infty}^{\infty} \int_{-\infty}^{\infty} \int_{-\infty}^{\infty} \int_{-\infty}^{\infty} \delta_f(r - r_N) \\ &\times \exp(-K_0 a_1^2 - 2a_1 \mathbf{K}^T \mathbf{b}' - \mathbf{b}'^T \mathbf{K} \mathbf{b}') da_1 d^3 \mathbf{b}', \end{aligned} \quad (\text{G.56})$$

From Eq. (6.26) we obtain

$$\begin{aligned} {}^n\mathcal{M}_{i_1 i_2 \dots i_n} &= \sqrt{\frac{D}{\pi \kappa^2(D)} \frac{\bar{\omega}_0^+ \bar{\omega}_0^- \bar{\omega}_1^+ \bar{\omega}_1^- J_T^2}{\det \mathbf{K}}} \\ &\times \left(\frac{-1}{2\bar{r}'} \frac{\partial}{\partial V_{i_1}} \right) \left(\frac{-1}{2\bar{r}'} \frac{\partial}{\partial V_{i_2}} \right) \dots \left(\frac{-1}{2\bar{r}'} \frac{\partial}{\partial V_{i_n}} \right) \exp(-(K_0 - \mathbf{K}^T \mathbf{K}^{-1} \mathbf{K}) \bar{r}'^2), \end{aligned} \quad (\text{G.57})$$

which yields

$$\begin{aligned} {}^n\mathcal{M}_{i_1 i_2 \dots i_n} &= \hat{C} \left({}^1\chi_{i_1} {}^1\chi_{i_2} \times \dots \times {}^1\chi_{i_n} \bar{r}'^n + 2\chi_{i_1 i_2} {}^1\chi_{i_3} {}^1\chi_{i_4} \times \dots \times {}^1\chi_{i_n} \bar{r}'^{n-2} \right. \\ &\quad \left. + 2\chi_{i_1 i_2} 2\chi_{i_3 i_4} {}^1\chi_{i_5} {}^1\chi_{i_6} \times \dots \times {}^1\chi_{i_n} \bar{r}'^{n-4} \right. \\ &\quad \left. + \dots + 2\chi_{i_1 i_2} 2\chi_{i_3 i_4} \times \dots \times 2\chi_{i_{n-1} i_n} \right) \quad \text{when } n \text{ is even,} \\ &\quad 2\chi_{i_1 i_2} 2\chi_{i_3 i_4} \times \dots \times 2\chi_{i_{n-2} i_{n-1}} {}^1\chi_{i_n} \bar{r}' \quad \text{when } n \text{ is odd,} \end{aligned} \quad (\text{G.58})$$

where

$${}_1\mathcal{X} = -\frac{1}{2}\nabla_{\mathbf{V}}(-R) = \begin{pmatrix} 1 \\ -\mathcal{K}^{-1}\mathbf{K} \end{pmatrix} \quad (\text{G.59})$$

$${}_2\mathcal{X} = -\frac{1}{2}\nabla_{\mathbf{V}} \otimes {}_1\mathcal{X} = \frac{1}{2} \begin{pmatrix} 0 & 0 \\ 0 & \mathcal{K}^{-1} \end{pmatrix}, \quad (\text{G.60})$$

and

$$R = (K_0 - \mathbf{K}^T \mathcal{K}^{-1} \mathbf{K}). \quad (\text{G.61})$$

The \hat{C} operator acts on each term in Eq. (G.59) to produce a sum of terms over all the distinct combinations of indices.

From Eq. (G.59) we can now evaluate each element of the \mathcal{M} tensors:

$${}_1\mathcal{M}_i = {}_1\chi_i \bar{r}' \quad (\text{G.62})$$

$${}_3\mathcal{M}_{i_1 i_2 i_3} = {}_1\chi_{i_1} {}_1\chi_{i_2} {}_1\chi_{i_3} \bar{r}'^3 + (2\chi_{i_1 i_2} {}_1\chi_{i_3} + 2\chi_{i_1 i_3} {}_1\chi_{i_2} + 2\chi_{i_2 i_3} {}_1\chi_{i_1}) \bar{r}' \quad (\text{G.63})$$

G.2.5 Result: first-anharmonic-order density profile

Using Eqs. (G.62) and (G.62) in Eq. (G.54) we finally arrive at the density profile

$$N_1(r) = \frac{N}{S(D)} \sqrt{\frac{R}{\delta\kappa(D)2\pi}} (1 + \delta^{\frac{1}{2}}(A_1 \bar{r}' + A_3 \bar{r}'^2)) \exp(-R\bar{r}'^2), \quad (\text{G.64})$$

where

$$\bar{r}'(r; D) = \sqrt{D} \left(\frac{r}{\kappa(D)} - \bar{r}_\infty \right). \quad (\text{G.65})$$

The coefficients A_1 and A_3 of the polynomial are

$$A_1 = 2 \sum_i {}_1\chi_i {}_1\Xi_i + 2 \sum_{i_1, i_2, i_3} (2\chi_{i_1 i_2} {}_1\chi_{i_3} + 2\chi_{i_1 i_3} {}_1\chi_{i_2} + 2\chi_{i_2 i_3} {}_1\chi_{i_1}) {}_3\Xi_{i_1 i_2 i_3} \quad (\text{G.66})$$

$$A_3 = 2 \sum_{i_1, i_2, i_3} {}_1\chi_{i_1} {}_1\chi_{i_2} {}_1\chi_{i_3} {}_3\Xi_{i_1 i_2 i_3}, \quad (\text{G.67})$$

where

$${}_1\Xi_i = \sum_{\mu=\{\mathbf{0}\pm, \mathbf{1}\pm\}} T_{\mu, i} {}^1E_\mu \quad (\text{G.68})$$

$${}_3\Xi_{i, j, k} = \sum_{\mu_1=\{\mathbf{0}\pm, \mathbf{1}\pm\}} \sum_{\mu_2=\{\mathbf{0}\pm, \mathbf{1}\pm\}} \sum_{\mu_3=\{\mathbf{0}\pm, \mathbf{1}\pm\}} T_{\mu_1, i} T_{\mu_2, j} T_{\mu_3, k} {}^3E_{\mu_1, \mu_2, \mu_3}, \quad (\text{G.69})$$

$${}_1\chi_i = \begin{cases} 1 & i = 1 \\ -(\mathcal{K}^{-1}\mathbf{K})_{i-1} & 1 < i \leq 4 \end{cases}, \quad (\text{G.70})$$

and

$$\begin{aligned}
2\chi_{i,j} \chi_k &= \mathcal{K}_{i-1,j-1}^{-1} \chi_k \Theta_{i-1} \Theta_{j-1} + \mathcal{K}_{j-1,k-1}^{-1} \chi_i \Theta_{j-1} \Theta_{k-1} \\
&\quad + \mathcal{K}_{k-1,i-1}^{-1} \chi_j \Theta_{k-1} \Theta_{i-1}.
\end{aligned} \tag{G.71}$$

The first-anharmonic-order density profile is a cubic polynomial multiplied by the harmonic order density profile. Note that the density profile is a function of the coordinate r , which is not the dimensionally-scaled internal displacement coordinate $\bar{r}'(r; D)$. Thus one must make the following substitution to obtain the density profile as an explicit function of r :

$$\bar{r}'(r; D) = \delta^{-\frac{1}{2}} \left(\frac{r}{\kappa(D)} - \bar{r}_\infty \right). \tag{G.72}$$

In this Appendix, we have derived the N -body density profile through first-anharmonic order using DPT. In doing so, we have neglected the Δ^2 term in Eq. (6.27).

Appendix H

Calculation of the Δ^2 term

In this Appendix, we set up the calculation of Δ^2 term in the density profile Eq. 6.27 which was initially neglected because it is of order δ (second anharmonic order), whereas we have calculated the wavefunction and density profile only to order $\delta^{1/2}$ (first anharmonic order). This “extra term” ensures that the density profile is positive definite, a feature that was seen to be critical in the preliminary application to the BEC.

We start with Eq. (6.27), in which the order δ term Δ^2 is not yet neglected:

$$N_1(r) = \frac{N}{S(D)} \int_{-\infty}^{\infty} \cdots \int_{-\infty}^{\infty} \prod_{\mu=\mathbf{0}^{\pm}, \mathbf{1}^{\pm}, \mathbf{2}} \prod_{\xi=1}^{d_{\mu}} d[q'^{\mu}]_{\xi} \\ \times \delta_f(r - r_N) (1 + 2\delta^{1/2}\Delta + \delta\Delta^2) [{}_g\Phi_0(\bar{\mathbf{q}}')]^2.$$

The third order, multivariate polynomial Δ is defined in Eq. (6.15)

$$\Delta = \sum_{\mu_1, \mu_2, \mu_3, k} \sum_{\xi_1, \xi_2, \xi_3} \left({}_3^{(1)}\tau_{\mu_1, \mu_2, \mu_3, k}^{\Delta} C_{\xi_1, \xi_2, \xi_3}^{\mu_1 \mu_2 \mu_3, k} \right) [q'_{\mu_1}]_{\xi_1} [q'_{\mu_2}]_{\xi_2} [q'_{\mu_3}]_{\xi_3} + \sum_{\mu''=\mathbf{0}^+}^{\mathbf{0}^-} {}_1^{(1)}\tau_{\mu''}^{\Delta} q'_{\mu''},$$

where μ'' only ranges over $\mathbf{0}^+$ and $\mathbf{0}^-$.

Adopting a more compact notation, where summation over repeated indices μ and ξ implied, the sixth-order, multivariate polynomial Δ^2 is therefore

$$\Delta^2 = {}_3^{(1)}\tau_{\mu_1, \mu_2, \mu_3, k_1}^{\Delta} C_{\xi_1, \xi_2, \xi_3}^{\mu_1 \mu_2 \mu_3, k} {}_3^{(1)}\tau_{\mu_4, \mu_5, \mu_6, k_1}^{\Delta} C_{\xi_4, \xi_5, \xi_6}^{\mu_4 \mu_5 \mu_6, k} [q'_{\mu_1}]_{\xi_1} [q'_{\mu_2}]_{\xi_2} [q'_{\mu_3}]_{\xi_3} [q'_{\mu_4}]_{\xi_4} [q'_{\mu_5}]_{\xi_5} [q'_{\mu_6}]_{\xi_6} \\ + 2 {}_3^{(1)}\tau_{\mu_1, \mu_2, \mu_3, k_1}^{\Delta} C_{\xi_1, \xi_2, \xi_3}^{\mu_1 \mu_2 \mu_3, k} \delta_{\mu_1, \mathbf{0}^{\pm}} {}_1^{(1)}\tau_{\mu_4}^{\Delta} [q'_{\mu_1}]_{\xi_1} [q'_{\mu_2}]_{\xi_2} [q'_{\mu_3}]_{\xi_3} q'_{\mu_4} \\ + {}_1^{(1)}\tau_{\mu_1''}^{\Delta} {}_1^{(1)}\tau_{\mu_2''}^{\Delta} q'_{\mu_1''} q'_{\mu_2''}, \quad (\text{H.1})$$

where μ'' only ranges over $\mathbf{0}^+$ and $\mathbf{0}^-$.

As before, we separate the problem of evaluating the integrals over the sixth-order polynomial in q'_{ν_i} from the problem of summing over ${}_3^{(1)}\tau_{\mu_1, \mu_2, \mu_3, k}^{\Delta} C_{\xi_1, \xi_2, \xi_3}^{\mu_1 \mu_2 \mu_3, k}$ and ${}_1^{(1)}\tau_{\mu_1}^{\Delta}$ by defining the rank- n tensors ${}_n M_{\nu_1, \nu_2, \dots, \nu_n}$:

$${}_n M_{\nu_1, \nu_2, \dots, \nu_n} = \int_{-\infty}^{\infty} \cdots \int_{-\infty}^{\infty} \prod_{\mu=\mathbf{0}^{\pm}, \mathbf{1}^{\pm}, \mathbf{2}} \prod_{\xi=1}^{d_{\mu}} d[q'_{\mu}]_{\xi} \delta_f(r - r_N) q'_{\nu_1} q'_{\nu_2} \cdots q'_{\nu_n} [{}_g\Phi_0(\bar{\mathbf{q}}')]^2 \quad (\text{H.2})$$

Indexing ${}_nM$ by (μ_i, ξ_i) rather than ν_i , we can write the density profile as a tensor contraction

$$N_1(r)S(D)/N = {}_0M + 2\delta^{1/2} \left(\sum_{\mu_1, \mu_2, \mu_3, k} \sum_{\xi_1, \xi_2, \xi_3} \binom{(1)}{3} \tau_{\mu_1, \mu_2, \mu_3, k}^\Delta C_{\xi_1, \xi_2, \xi_3}^{\mu_1 \mu_2 \mu_3, k} {}_3M_{\xi_1, \xi_2, \xi_3}^{\mu_1 \mu_2 \mu_3} + \sum_{\mu_1''} \binom{(1)}{1} \tau_{\mu_1''}^\Delta {}_1M_1^{\mu_1''} \right) + \delta \left(\sum_{\mu_1, \mu_2, \mu_3, k_1} \sum_{\xi_1, \xi_2, \xi_3} \sum_{\mu_4, \mu_5, \mu_6, k_2} \sum_{\xi_4, \xi_5, \xi_6} \binom{(1)}{3} \tau_{\mu_1, \mu_2, \mu_3, k_1}^\Delta \binom{(1)}{3} \tau_{\mu_4, \mu_5, \mu_6, k_2}^\Delta \times \right. \quad (H.3)$$

$$C_{\xi_1, \xi_2, \xi_3}^{\mu_1 \mu_2 \mu_3, k} \times C_{\xi_4, \xi_5, \xi_6}^{\mu_4 \mu_5 \mu_6, k} {}_6M_{\xi_1, \xi_2, \xi_3, \xi_4, \xi_5, \xi_6}^{\mu_1, \mu_2, \mu_3, \mu_4, \mu_5, \mu_6} + 2 \binom{(1)}{3} \tau_{\mu_1, \mu_2, \mu_3, k_1}^\Delta \binom{(1)}{1} \tau_{\mu_4''}^\Delta C_{\xi_1, \xi_2, \xi_3}^{\mu_1 \mu_2 \mu_3, k} [q'_{\mu_1}]_{\xi_1} [q'_{\mu_2}]_{\xi_2} [q'_{\mu_3}]_{\xi_3} q'_{\mu_4''} + \binom{(1)}{1} \tau_{\mu_1''}^\Delta \binom{(1)}{1} \tau_{\mu_2''}^\Delta q'_{\mu_1''} q'_{\mu_2''} \right) \quad (H.4)$$

Due to the presence of the Dirac delta function in the integrals in each element of the M tensors, we must treat integrals over normal coordinates involving r_N differently from those that don't.

We have noted that r_N only appears in four normal coordinates, i.e. in $\mathbf{q}'_{\mathbf{0}+}$, $\mathbf{q}'_{\mathbf{0}-}$, $[\mathbf{q}'_{\mathbf{1}+}]_{d_{\mathbf{1}+}}$ and $[\mathbf{q}'_{\mathbf{1}-}]_{d_{\mathbf{1}-}}$. We adopt an index convention that distinguishes between normal coordinates which do and do not depend on r_N : normal coordinates which do not depend on r_N are indexed by $(\bar{\mu}, \bar{\xi})$ and normal coordinates which do depend on r_N by $(\mu', d_{\mu'})$. Therefore $\bar{\mu} \in \{\mathbf{0}+, \mathbf{0}-, \mathbf{1}+, \mathbf{1}-, \mathbf{2}\}$ and $\bar{\xi}$ has a range determined by $\bar{\mu}$

Most of the integrals do not depend on r_N and are easily evaluated. Integrals which are odd in one coordinate are zero. Integrals which are even can be evaluated using the integral identity

$$\int_{-\infty}^{\infty} \sqrt{\frac{\bar{\omega}_\nu}{\pi}} (q'_\nu)^{2n} e^{-\bar{\omega}_\nu (q'_\nu)^2} dq'_\nu = \frac{1}{\bar{\omega}_\nu^n} \frac{(2n-1)!!}{2^n}. \quad (H.5)$$

Thus many terms are zeroed out, only those terms involving even powers of the normal coordinates which are independent of r_N contribute to the density profile.

What remains is to show all the possible ways some of the indices μ and ξ may depend on r_N (and therefore be denoted μ' and d_μ), leaving the other indices as summations over the barred indices (corresponding to coordinates which do not depend on r_N). There are many such combinations possible. Then one must perform the summations over barred indices, which requires contractions of the product of Clebsch-Gordon terms in the above equation. This is a significant challenge for a symbolic calculation, given the complexity of some of the larger Clebsch-Gordon coefficients.

Appendix I

Derivation of the Hooke's law gas wave function and density profile

In this Appendix we derive the exact ground-state wave function for a harmonically-confined, harmonically-interacting system of N particles in D dimensions as in Reference (104). The exact density profile was derived in Reference (103). From these exact expressions, we derive a perturbation series for the wave function and density profile (exact at each order) through first order in $\delta^{1/2}$, where $\delta = 1/D$.

I.1 First-anharmonic-order wavefunction

The Hamiltonian of the harmonically-interacting model system of identical particles is

$$H = \frac{1}{2} \left(\sum_i^N \left[-\frac{\partial^2}{\partial \mathbf{r}_i^2} + \omega_t^2 \mathbf{r}_i^2 \right] + \sum_{i < j}^N \omega_p^2 \mathbf{r}_{ij}^2 \right). \quad (\text{I.1})$$

Making the orthogonal transformation to center-of-mass and Jacobi coordinates,

$$\mathbf{R} = \frac{1}{\sqrt{N}} \sum_{k=1}^N \mathbf{r}_k \quad \text{and} \quad \boldsymbol{\rho}_i = \frac{1}{\sqrt{i(i+1)}} \left(\sum_{j=1}^i \mathbf{r}_j - i \mathbf{r}_{i+1} \right), \quad (\text{I.2})$$

where $1 \leq i \leq N-1$, the Hamiltonian becomes

$$H = \frac{1}{2} \left(-\frac{\partial^2}{\partial \mathbf{R}^2} + \omega_t^2 \mathbf{R}^2 \right) + \frac{1}{2} \sum_{i=1}^{N-1} \left(-\frac{\partial^2}{\partial \boldsymbol{\rho}_i^2} + \omega_{\text{int}}^2 \boldsymbol{\rho}_i^2 \right), \quad (\text{I.3})$$

the sum of N , D -dimensional, harmonic-oscillator Hamiltonians, where

$$\omega_{\text{int}} = \sqrt{\omega_t^2 + N \omega_p^2}. \quad (\text{I.4})$$

Notice two things about the Hamiltonian: it is separable and each component has the form of a D -dimensional harmonic oscillator. Therefore the ground-state solution to the wave function in the Schrödinger equation

$$H \Psi = E \Psi \quad (\text{I.5})$$

is the product of harmonic-oscillator wavefunctions

$$\Psi(\mathbf{R}, \{\boldsymbol{\rho}_i\}; D) = \psi(R; \omega_t, D) \prod_{i=1}^{N-1} \psi(\rho_i; \omega_{\text{int}}, D), \quad (\text{I.6})$$

where $\psi(\rho_i; \omega_{\text{int}}, D)$ is the D -dimensional, harmonic-oscillator, ground-state wave function

$$\psi(r; \omega, D) = \sqrt{\frac{\omega^{\frac{D}{2}}}{\pi^{\frac{D}{2}}}} \exp\left(-\frac{\omega}{2} r^2\right) \quad (\text{I.7})$$

where $\psi(r; \omega, D)$ satisfies the normalization condition

$$\int_0^\infty [\psi(r; \omega, D)]^2 r^{D-1} d^D \mathbf{r} = 1 \quad (\text{I.8})$$

so that

$$\int_{-\infty}^\infty [\Psi(\mathbf{R}, \{\boldsymbol{\rho}_i\}; D)]^2 \prod_{i=1}^{N-1} d^D \boldsymbol{\rho}_i d^D \mathbf{R} = 1. \quad (\text{I.9})$$

The Jacobian-weighted, $L = 0$ wave function Ψ_J is obtained by folding into the wavefunction the square root of that portion of the Jacobian which depends on the internal coordinates; i.e. the square root of

$$\Gamma^{(D-N-1)/2} \prod_{j=1}^N r_j^{(D-1)}, \quad (\text{I.10})$$

where Γ is the Gramian determinant, so that

$$\Psi_J = \mathcal{N} \Gamma^{(D-N-1)/4} \prod_{j=1}^N r_j^{(D-1)/2} \psi(R; \omega_t, D) \prod_{i=1}^{N-1} \psi(\rho_i; \omega_{\text{int}}, D), \quad (\text{I.11})$$

where \mathcal{N} is a normalization constant ensuring that

$$\int [\Psi_J(\{r_i\}, \{\gamma_{jl}\}; D)]^2 \prod_i dr_i \prod_{j<k} d\gamma_{jk} = 1. \quad (\text{I.12})$$

I.1.1 A perturbation series in $1/\sqrt{D}$ for the exact wavefunction

I.1.1.1 Dimensional scaling

First we need to regularize the large-dimension limit by dimensionally scaling the parameters and variables as in Eq. (3.19). We choose a scaling $\kappa(D)$ and define the dimensionally-scaled frequency $\bar{\omega}_t$,

$$\kappa(D) = \frac{1}{\sqrt{\bar{\omega}_t}} D^2 \quad (\text{I.13})$$

$$\bar{\omega}_t = D^3 \omega_t. \quad (\text{I.14})$$

Now consider transforming to dimensionally-scaled oscillator coordinates

$$\begin{aligned} r &= \kappa(D)\bar{r} & \rho &= \kappa(D)\bar{\rho} & R &= \kappa(D)\bar{R} \\ &= \frac{D^{1/2}\bar{r}}{\sqrt{\omega_t}} & &= \frac{D^{1/2}\bar{\rho}}{\sqrt{\omega_t}} & &= \frac{D^{1/2}\bar{R}}{\sqrt{\omega_t}}, \end{aligned} \quad (\text{I.15})$$

From Eq. (I.11) we obtain

$$\begin{aligned} \Psi_J &= \mathcal{N} \Gamma^{(D-N-1)/4} \prod_{j=1}^N \bar{r}_j^{(D-1)/2} \sqrt{\frac{2}{\Gamma(\frac{D}{2})}} D^{\frac{D}{4}} \exp\left(-\frac{D}{2} \bar{R}^2\right) \\ &\times \left(\frac{2}{\Gamma(\frac{D}{2})}\right)^{\frac{N-1}{2}} [(\lambda D)^{\frac{D}{2}}]^{\frac{N-1}{2}} \prod_{i=1}^{N-1} \exp\left(-\frac{\lambda D}{2} \bar{\rho}_i^2\right), \end{aligned} \quad (\text{I.16})$$

where

$$\lambda = \frac{\omega_{\text{int}}}{\omega_t}. \quad (\text{I.17})$$

I.1.1.2 The large-dimension limit

To test the general formalism of Reference (100) we need to expand Eq. (I.16) about the large-dimension limit through first order in $\delta^{1/2}$. In the large-dimension limit the system localizes about a structure where all the radii are equal to \bar{r}_∞ and angle cosines are equal to γ_∞ . To derive \bar{r}_∞ and γ_∞ , one applies the condition

$$\left. \frac{\partial \Psi_J}{\partial \bar{r}_i} \right|_{D=\infty} = \left. \frac{\partial \Psi_J}{\partial \gamma_{jk}} \right|_{D=\infty} = 0. \quad (\text{I.18})$$

In this endeavor the following results are useful:

$$\Gamma|_{D=\infty} = (1 + (N-1)\gamma_\infty)(1 - \gamma_\infty)^{N-1} \quad (\text{I.19})$$

$$\left. \frac{\partial \Gamma}{\partial \gamma_{jk}} \right|_{D=\infty} = -2\gamma_\infty(1 - \gamma_\infty)^{N-2} \quad (\text{I.20})$$

$$\bar{R}^2|_{D=\infty} = \bar{r}_\infty^2(1 + (N-1)\gamma_\infty) \quad (\text{I.21})$$

$$\left. \frac{\partial \bar{R}^2}{\partial \bar{r}_i} \right|_{D=\infty} = 2\bar{r}_\infty \frac{(1 + (N-1)\gamma_\infty)}{N} \quad (\text{I.22})$$

$$\left. \frac{\partial \bar{R}^2}{\partial \gamma_{jk}} \right|_{D=\infty} = 2 \frac{\bar{r}_\infty^2}{N} \quad (\text{I.23})$$

$$\sum_{i=1}^{N-1} \bar{\rho}_i^2 = \sum_{j=1}^N \bar{\rho}_j^2 - \bar{R}^2 \quad (\text{I.24})$$

$$\left. \sum_{i=1}^{N-1} \bar{\rho}_i^2 \right|_{D=\infty} = (N-1)\bar{r}_\infty^2(1 - \gamma_\infty) = (N-1)\bar{\rho}_\infty \quad (\text{I.25})$$

$$\left. \frac{\partial \sum_{i=1}^{N-1} \bar{\rho}_i^2}{\partial r_k} \right|_{D=\infty} = \frac{2(N-1)}{N} \bar{r}_\infty (1 - \gamma_\infty) \quad (\text{I.26})$$

$$\left. \frac{\partial \sum_{i=1}^{N-1} \bar{\rho}_i^2}{\partial \gamma_{jk}} \right|_{D=\infty} = -\frac{2}{N} \bar{r}_\infty^2. \quad (\text{I.27})$$

From Eq. (I.18) we obtain the parameters \bar{r}_∞ and γ_∞

$$\gamma_\infty = \frac{(\lambda - 1)}{(N + (\lambda - 1))} \quad (\text{I.28})$$

$$\bar{r}_\infty^2 = \frac{1}{2(1 + (N - 1)\gamma_\infty)} = \frac{N + (\lambda - 1)}{2\lambda N}. \quad (\text{I.29})$$

Equations (I.28) and (I.29) define the $D \rightarrow \infty$ structure about which the system oscillates at finite dimension.

I.1.1.3 A series expansion about the large- D limit

To derive the wave function through order $\delta^{1/2}$ we perform a series expansion of each of the D -dependent terms in Eq. (I.16):

$$\sqrt{\frac{1}{\Gamma\left(\frac{D}{2}\right)}} = \frac{2^{\frac{D-2}{4}} \exp\left(\frac{D}{4}\right)}{\sqrt[4]{\pi} D^{\frac{D-1}{4}}} + O(\delta), \quad (\text{I.30})$$

$$\begin{aligned} \prod_{i=1}^N \bar{r}_i^{\frac{D-1}{2}} &= \bar{r}_\infty^{\frac{N(D-1)}{2}} \exp\left(\sum_{i=1}^N \frac{D^{\frac{1}{2}} \bar{r}'_i}{2\bar{r}_\infty}\right) \exp\left(-\frac{1}{4\bar{r}_\infty^2} \sum_{i=1}^N \bar{r}'_i{}^2\right) \\ &\times \left(1 + \frac{\delta^{\frac{1}{2}}}{2} \sum_{i=1}^N \left(\frac{\bar{r}'_i{}^3}{3\bar{r}_\infty^3} - \frac{\bar{r}'_i}{\bar{r}_\infty}\right) + O(\delta)\right). \end{aligned} \quad (\text{I.31})$$

We also have

$$\bar{R}^2 = \bar{R}_\infty^2 + \delta^{1/2} \bar{R}'_2(\delta^{1/2}) \quad (\text{I.32})$$

$$\sum_{i=1}^{N-1} \bar{\rho}_i^2 = (N-1) \bar{\rho}_\infty^2 + \delta^{1/2} \sum_{\Sigma} \bar{\rho}'_2(\delta^{1/2}), \quad (\text{I.33})$$

where

$$\bar{R}^2 \Big|_{D \rightarrow \infty} \equiv \bar{R}_\infty^2 = \bar{r}_\infty^2 (1 + (N-1)\gamma_\infty) \quad (\text{I.34})$$

$$\sum_{i=1}^{N-1} \bar{\rho}_i^2 \Big|_{D \rightarrow \infty} \equiv (N-1) \bar{\rho}_\infty^2 = (N-1) \bar{r}_\infty^2 (1 - \gamma_\infty) \quad (\text{I.35})$$

and

$$\begin{aligned}
\bar{R}'_2(\delta^{1/2}) &= \frac{2\bar{r}_\infty}{N} \left((1 + (N-1)\gamma_\infty) \sum_{i=1}^N \bar{r}'_i + \sum_{i<j=1}^N \bar{r}_\infty \bar{\gamma}'_{ij} \right) \\
&+ \frac{\delta^{1/2}}{N} \left(\sum_{i=1}^N (\bar{r}'_i)^2 + 2\gamma_\infty \sum_{i<j=1}^N \bar{r}'_i \bar{r}'_j + 2\bar{r}_\infty \sum_{i<j=1}^N (\bar{r}'_i + \bar{r}'_j) \bar{\gamma}'_{ij} \right) \\
&+ \delta \frac{2}{N} \sum_{i<j=1}^N \bar{r}'_i \bar{r}'_j \bar{\gamma}'_{ij}
\end{aligned} \tag{I.36}$$

$$\begin{aligned}
{}_\Sigma \bar{\rho}'_2(\delta^{1/2}) &= \frac{2\bar{r}_\infty}{N} \left((N-1)(1-\gamma_\infty) \sum_{i=1}^N \bar{r}'_i - \sum_{i<j=1}^N \bar{r}_\infty \bar{\gamma}'_{ij} \right) \\
&+ \frac{\delta^{1/2}}{N} \left((N-1) \sum_{i=1}^N (\bar{r}'_i)^2 - 2\gamma_\infty \sum_{i<j=1}^N \bar{r}'_i \bar{r}'_j - 2\bar{r}_\infty \sum_{i<j=1}^N (\bar{r}'_i + \bar{r}'_j) \bar{\gamma}'_{ij} \right) \\
&- \delta \frac{2}{N} \sum_{i<j=1}^N \bar{r}'_i \bar{r}'_j \bar{\gamma}'_{ij},
\end{aligned} \tag{I.37}$$

so that

$$\begin{aligned}
&\exp\left(-\frac{D}{2} \bar{R}^2\right) \prod_{i=1}^{N-1} \exp\left(-\frac{\lambda D}{2} \bar{\rho}_i^2\right) = \exp\left(-\frac{DN}{4}\right) \exp\left(-\sum_{i=1}^N \frac{D^{\frac{1}{2}} \bar{r}'_i}{2\bar{r}_\infty}\right) \\
&\times \exp\left(-\frac{D^{\frac{1}{2}} \bar{r}_\infty^2}{N} (1-\lambda) \sum_{i<j=1}^N \bar{\gamma}'_{ij}\right) \exp\left(-\frac{1}{2} \left(\left(\lambda - \frac{\lambda-1}{N}\right) \sum_{i=1}^N \bar{r}'_i{}^2 + \right. \right. \\
&\quad \left. \left. - \frac{2(\lambda-1)}{N} \bar{\gamma}_\infty \sum_{i<j=1}^N \bar{r}'_i \bar{r}'_j + -\frac{2(\lambda-1)}{N} \bar{r}_\infty \sum_{i<j=1}^N (\bar{r}'_i + \bar{r}'_j) \bar{\gamma}'_{ij} \right)\right) \\
&\times \left(1 + \delta^{\frac{1}{2}} \left(\frac{\lambda-1}{N} \right) \sum_{i<j=1}^N \bar{r}'_i \bar{r}'_j \bar{\gamma}'_{ij} + O(\delta) \right).
\end{aligned} \tag{I.38}$$

The final bit of the puzzle in the dimensional expansion of Eq. (I.16) is the dimensional expansion of $\Gamma^{(D-N-1)/4}$. For this we need Eqs. (I.19), (I.20), and

$$\left. \frac{\partial^2 \Gamma}{\partial \gamma_{ij} \partial \gamma_{kl}} \right|_{D=\infty} = 0 \tag{I.39}$$

$$\left. \frac{\partial^2 \Gamma}{\partial \gamma_{ij} \partial \gamma_{jk}} \right|_{D=\infty} = 2\gamma_\infty (1-\gamma_\infty)^{N-3} \tag{I.40}$$

$$\left. \frac{\partial^2 \Gamma}{\partial \gamma_{ij}^2} \right|_{D=\infty} = -2(1+(N-3)\gamma_\infty)(1-\gamma_\infty)^{N-3} \tag{I.41}$$

$$\left. \frac{\partial^3 \Gamma}{\partial \gamma_{ij} \partial \gamma_{kl} \partial \gamma_{mn}} \right|_{D=\infty} = 0 \tag{I.42}$$

$$\left. \frac{\partial^3 \Gamma}{\partial \gamma_{ij} \partial \gamma_{jk} \partial \gamma_{lm}} \right|_{D=\infty} = 0 \tag{I.43}$$

$$\left. \frac{\partial^3 \Gamma}{\partial \gamma_{ij} \partial \gamma_{jk} \partial \gamma_{kl}} \right|_{D=\infty} = -2\gamma_\infty (1 - \gamma_\infty)^{N-4} \quad (\text{I.44})$$

$$\left. \frac{\partial^3 \Gamma}{\partial \gamma_{ij} \partial \gamma_{jk} \partial \gamma_{jl}} \right|_{D=\infty} = 0 \quad (\text{I.45})$$

$$\left. \frac{\partial^3 \Gamma}{\partial \gamma_{ij} \partial \gamma_{jk} \partial \gamma_{ik}} \right|_{D=\infty} = 2(1 + (N - 4)\gamma_\infty)(1 - \gamma_\infty)^{N-4} \quad (\text{I.46})$$

$$\left. \frac{\partial^3 \Gamma}{\partial \gamma_{ij}^2 \partial \gamma_{kl}} \right|_{D=\infty} = 4\gamma_\infty (1 - \gamma_\infty)^{N-4} \quad (\text{I.47})$$

$$\left. \frac{\partial^3 \Gamma}{\partial \gamma_{ij}^2 \partial \gamma_{jk}} \right|_{D=\infty} = 0 \quad (\text{I.48})$$

$$\left. \frac{\partial^3 \Gamma}{\partial \gamma_{ij}^3} \right|_{D=\infty} = 0, \quad (\text{I.49})$$

from which we obtain

$$\begin{aligned} \Gamma^{(D-N-1)/4} &= ((1 - \gamma_\infty)^{N-1} (1 + (N - 1)\gamma_\infty))^{\frac{D-N-1}{4}} \times \\ &\times \left(1 + \frac{\delta^{\frac{1}{2}}}{12(1 - \gamma_\infty)(1 + (N - 1)\gamma_\infty)} \left(6(N + 1)\gamma_\infty [B(\bullet \leftrightarrow) \bar{\gamma}'] + \right. \right. \\ &- \frac{8\gamma_\infty^3}{(1 - \gamma_\infty)^2 (1 + (N - 1)\gamma_\infty)^2} [B(\bullet \leftrightarrow) \bar{\gamma}']^3 - \frac{6\gamma_\infty}{(1 - \gamma_\infty)^2 (1 + (N - 1)\gamma_\infty)} [B(\bullet \leftrightarrow) \bar{\gamma}'] \times \\ &\times ((1 + (N - 3)\gamma_\infty) B(\odot) - \gamma_\infty B(\bullet \downarrow)) \bar{\gamma}' \bar{\gamma}' + \\ &\left. + \frac{1}{(1 - \gamma_\infty)^2} \left((1 + (N - 4)\gamma_\infty) B(\triangle) - \gamma_\infty B(\blacksquare) + 2\gamma_\infty B(\odot) \right) \bar{\gamma}' \bar{\gamma}' \bar{\gamma}' \right) + \\ &+ O(\delta) \exp \left(-D^{\frac{1}{2}} \frac{(\lambda - 1)\bar{r}_\infty^2}{N} \sum_{i < j=1}^N \bar{\gamma}'_{ij} \right) \times \\ &\times \exp \left(-\frac{1}{2(1 - \gamma_\infty)^2 (1 + (N - 1)\gamma_\infty)} \left(-\frac{\gamma_\infty^2}{(1 + (N - 1)\gamma_\infty)} [B(\bullet \leftrightarrow) \bar{\gamma}']^2 + \right. \right. \\ &\left. \left. + \left[\frac{(1 + (N - 3)\gamma_\infty)}{2} B(\odot) - \frac{\gamma_\infty}{2} B(\bullet \downarrow) \right] \bar{\gamma}' \bar{\gamma}' \right) \right), \quad (\text{I.50}) \end{aligned}$$

where the $[B(\mathcal{G})]_{\nu_1, \nu_2, \dots}$ are the binary invariants introduced in Chapter 4 and \mathcal{G} is the graph labeling the binary invariant. The expression $B(\mathcal{G}) \bar{\mathbf{X}}'_1 \bar{\mathbf{X}}'_2 \bar{\mathbf{X}}'_3$ is shorthand for $[B(\mathcal{G})]_{\nu_1, \nu_2, \nu_3} [\bar{\mathbf{X}}'_1]_{\nu_1} [\bar{\mathbf{X}}'_2]_{\nu_2} [\bar{\mathbf{X}}'_3]_{\nu_3}$, where repeated indices ν_i are summed over, $\bar{\mathbf{X}}'$ is the $\bar{\mathbf{r}}'$ or $\bar{\gamma}'$ vector from Eq. (3.29), likewise for $B(\mathcal{G}) \bar{\mathbf{X}}'_1 \bar{\mathbf{X}}'_2$ and $B(\mathcal{G}) \bar{\mathbf{X}}'_1$. Using Eqs. (I.30), (I.31), (I.38), and (I.50), along with

$$B(\bullet \leftrightarrow) \otimes B(\bullet \leftrightarrow) = B(\odot) + B(\bullet \downarrow) + B(\bullet \leftrightarrow) \quad (\text{I.51})$$

$$\begin{aligned} B(\bullet \leftrightarrow) \otimes B(\bullet \leftrightarrow) \otimes B(\bullet \leftrightarrow) &= B(\odot) + B(\triangle) + B(\odot \leftrightarrow) + B(\bullet \downarrow) + B(\blacksquare) \\ &+ B(\odot) + B(\bullet \downarrow) + B(\equiv) \quad (\text{I.52}) \end{aligned}$$

$$B(\bullet\rightarrow) \otimes B(\bullet\circ) = B(\bullet\ominus) + \frac{B(\bullet\circ\rightarrow)}{3} + \frac{B(\bullet\circ\circ)}{3} \quad (\text{I.53})$$

$$B(\bullet\rightarrow) \otimes \frac{B(\bullet\downarrow)}{2} = \frac{B(\bullet\circ\rightarrow)}{3} + \frac{B(\triangle)}{2} + \frac{B(\bullet\downarrow\downarrow)}{2} + \frac{B(\downarrow\downarrow)}{3} + \frac{B(\downarrow\downarrow)}{6} \quad (\text{I.54})$$

in Eq. (I.16), with

$$\mathcal{N} = \frac{1}{\bar{r}_\infty^{\frac{N(D-1)}{2}} ((1-\gamma_\infty)^{N-1} (1+(N-1)\gamma_\infty))^{\frac{D-N-1}{4}}} + O(\delta), \quad (\text{I.55})$$

we obtain the Jacobian-weighted N -body wavefunction in Eq. (7.14) for a system of identical particles under harmonic confinement with harmonic interactions:

$$\Psi_J = \left(\frac{1}{\sqrt[4]{\pi}} \right)^{\frac{N(N+1)}{2}} \left(1 + \frac{1}{2} \delta^{\frac{1}{2}} \Delta_{\bar{\mathbf{y}}'} + O(\delta) \right) \exp(-[\bar{\mathbf{y}}']^T \bar{\Omega}_{\bar{\mathbf{y}}'} \bar{\mathbf{y}}'),$$

where we have defined $\bar{\Omega}_{\bar{\mathbf{y}}'}$ as $\bar{\Omega}$ (the matrix whose diagonal elements are frequencies) from the normal-coordinate basis to the internal coordinate basis,

$$\begin{aligned} \bar{\Omega}_{\bar{\mathbf{y}}'} &= \mathbf{V}^T \bar{\Omega} \mathbf{V} \\ \bar{\Omega}_{\nu_1, \nu_2} &= \delta_{\nu_1, \nu_2} \bar{\omega}_{\nu_1}. \end{aligned}$$

Similarly, have transformed the polynomial Δ from a normal-coordinate basis to a internal-coordinate basis

$$\begin{aligned} \Delta_{\bar{\mathbf{y}}'} &= \Delta(\circ) [B(\circ)]_i \bar{r}'_i + \Delta(\bullet\rightarrow) [B(\bullet\rightarrow)]_{(ij)} \bar{\gamma}'_{(ij)} + \Delta(\circ\circ) [B(\circ\circ)]_{i,j,k} \bar{r}'_i \bar{r}'_j \bar{r}'_k \\ &+ \Delta(\circ\rightarrow\circ) [B(\circ\rightarrow\circ)]_{(ij),k,l} \bar{\gamma}'_{(ij)} \bar{r}'_k \bar{r}'_l + \left(\Delta(\bullet\ominus) [B(\bullet\ominus)]_{(ij),(kl),(mn)} + \right. \\ &+ \Delta(\triangle) [B(\triangle)]_{(ij),(kl),(mn)} + \Delta(\bullet\circ\rightarrow) [B(\bullet\circ\rightarrow)]_{(ij),(kl),(mn)} + \\ &+ \Delta(\bullet\downarrow\downarrow) [B(\bullet\downarrow\downarrow)]_{(ij),(kl),(mn)} + \Delta(\downarrow\downarrow) [B(\downarrow\downarrow)]_{(ij),(kl),(mn)} \\ &+ \Delta(\circ\circ) [B(\circ\circ)]_{(ij),(kl),(mn)} + \Delta(\downarrow\downarrow) [B(\downarrow\downarrow)]_{(ij),(kl),(mn)} + \\ &\left. + \Delta(\equiv) [B(\equiv)]_{(ij),(kl),(mn)} \right) \bar{\gamma}'_{(ij)} \bar{\gamma}'_{(kl)} \bar{\gamma}'_{(mn)} \end{aligned}$$

and $\bar{\Omega}$ has also been transformed to an internal coordinate basis

$$\begin{aligned} \bar{\Omega}_{\bar{\mathbf{y}}'} &= \left(\Delta(\circ\circ) [B(\circ\circ)]_{i,j} + \Delta(\circ\circ\circ) [B(\circ\circ\circ)]_{i,j} \right) \bar{r}'_i \bar{r}'_j + \\ &+ \Delta(\circ\rightarrow) [B(\circ\rightarrow)]_{(ij),k} \bar{\gamma}'_{(ij)} \bar{r}'_k + \left(\Delta(\bullet\circ) [B(\bullet\circ)]_{(ij),(kl)} + \right. \\ &\left. + \Delta(\bullet\downarrow) [B(\bullet\downarrow)]_{(ij),(kl)} + \Delta(\bullet\rightarrow) [B(\bullet\rightarrow)]_{(ij),(kl)} \right) \bar{\gamma}'_{(ij)} \bar{\gamma}'_{(kl)}. \end{aligned}$$

The scalar coefficients, $\Delta(\mathcal{G})$ are

$$\Delta(\circ) = -\frac{1}{\bar{r}_\infty} \quad (\text{I.56})$$

$$\Delta(\bullet\rightarrow) = \mathcal{A}6(N+1)\gamma_\infty \quad (\text{I.57})$$

$$\Delta(\text{figure}) = \frac{1}{3\bar{r}_\infty^3} \quad (\text{I.58})$$

$$\Delta(\text{figure}) = \frac{\lambda-1}{N} \quad (\text{I.59})$$

$$\Delta(\text{figure}) = \mathcal{A}(\mathcal{B} + \mathcal{C}\mathcal{D}) \quad (\text{I.60})$$

$$\Delta(\text{figure}) = \mathcal{A}(\mathcal{B} + \mathcal{C}\mathcal{E} + \mathcal{F}) \quad (\text{I.61})$$

$$\Delta(\text{figure}) = \mathcal{A}\left(\mathcal{B} + \mathcal{C}\left(\frac{\mathcal{D}}{3} + \frac{2\mathcal{E}}{3}\right)\right) \quad (\text{I.62})$$

$$\Delta(\text{figure}) = \mathcal{A}(\mathcal{B} + \mathcal{C}\mathcal{E}) \quad (\text{I.63})$$

$$\Delta(\text{figure}) = \mathcal{A}\left(\mathcal{B} + \frac{2\mathcal{C}\mathcal{E}}{3} - \mathcal{G}\right) \quad (\text{I.64})$$

$$\Delta(\text{figure}) = \mathcal{A}\left(\mathcal{B} + \frac{\mathcal{C}\mathcal{D}}{3} + 2\mathcal{G}\right) \quad (\text{I.65})$$

$$\Delta(\text{figure}) = \mathcal{A}\left(\mathcal{B} + \frac{\mathcal{C}\mathcal{E}}{3}\right) \quad (\text{I.66})$$

$$\Delta(\text{figure}) = \mathcal{A}\mathcal{B} \quad (\text{I.67})$$

$$\Delta(\text{figure}) = \lambda_{\text{eff}} + \frac{\lambda-1}{2N}(\lambda_{\text{eff}} - 1) \quad (\text{I.68})$$

$$\Delta(\text{figure}) = \frac{\gamma_\infty}{2} \quad (\text{I.69})$$

$$\Delta(\text{figure}) = \bar{r}_\infty \quad (\text{I.70})$$

$$\Delta(\text{figure}) = \mathcal{H}(\mathcal{I} + \mathcal{J}) \quad (\text{I.71})$$

$$\Delta(\text{figure}) = \mathcal{H}\left(\mathcal{I} - \frac{\gamma_\infty}{2}\right) \quad (\text{I.72})$$

$$\Delta(\text{figure}) = \mathcal{H}. \quad (\text{I.73})$$

I.1.2 Comparison of direct derivation to DPT

The DPT wavefunction in Eq. (6.19) is written in the basis of normal coordinates. The directly derived wavefunction above and in Eq. (7.14) is written in the basis of internal coordinates. In order to directly compare the two expressions, a transformation must be made. We choose to reverse the process described in this thesis and transformed the DPT wavefunction polynomials back to an internal coordinate basis.

In Tables I.1–I.4 we compare the binary invariant coefficients, $\Delta(\mathcal{G})$, from the general formalism with the above results derived from the full analytical solution above for $N = 10,000$ particles.

\mathcal{G}	$\Delta[\Delta(\mathcal{G})]$	\mathcal{G}	$\Delta[\Delta(\mathcal{G})]$	\mathcal{G}	$\Delta[\Delta(\mathcal{G})]$
	7.0×10^{-16}		-1.5×10^{-16}		-3.6×10^{-16}
	2.3×10^{-11}		-6.0×10^{-13}		-5.1×10^{-11}
	-4.1×10^{-16}		3.7×10^{-16}		9.6×10^{-15}
	-1.3×10^{-16}		-2.1×10^{-13}		-3.7×10^{-16}
	-6.1×10^{-16}		-8.4×10^{-7}		-2.2×10^{-16}
	1.2×10^{-16}		8.4×10^{-10}		2.5×10^{-14}

Table I.1: Fractional difference, $\Delta\Delta(\mathcal{G}) = (\Delta_{analytic}(\mathcal{G}) - \Delta_{DPT}(\mathcal{G}))/\Delta_{analytic}(\mathcal{G})$, between the analytic and DPT rank-three, rank-two, and rank-one binary invariant coefficients when $N = 10,000$ and $\lambda = 10$.

\mathcal{G}	$\Delta(\mathcal{G})$	\mathcal{G}	$\Delta(\mathcal{G})$
	2.3×10^{-11}		-2.9×10^{-15}
	1.1×10^{-11}		7.8×10^{-19}
	2.4×10^{-15}		4.1×10^{-19}
	2.2×10^{-15}		9.8×10^{-17}
	2.0×10^{-15}		1.0×10^{-19}
	8.2×10^{-16}		6.2×10^{-20}
	-1.2×10^{-17}		2.1×10^{-20}

Table I.2: Rank-three and rank-two binary invariant coefficient, $\Delta_{DPT}(\mathcal{G})$, from the general *Mathematica* code when $N = 10,000$ and $\lambda = 10$. All of these coefficients are exactly zero in the exactly soluble analytic solution.

\mathcal{G}	$\Delta[\Delta(\mathcal{G})]$	\mathcal{G}	$\Delta[\Delta(\mathcal{G})]$	\mathcal{G}	$\Delta[\Delta(\mathcal{G})]$
	1.6×10^{-11}		-2.0×10^{-8}		-2.6×10^{-11}
	-3.8×10^{-8}		1.7×10^{-13}		-1.1×10^{-9}
	2.5×10^{-8}		2.1×10^{-11}		6.8×10^{-13}
	-3.8×10^{-8}		-3.0×10^{-14}		-1.6×10^{-7}
	2.5×10^{-8}		1.7×10^{-3}		1.6×10^{-10}
	2.2×10^{-5}		-1.7×10^{-10}		-3.8×10^{-13}

Table I.3: Fractional difference, $\Delta\Delta(\mathcal{G}) = (\Delta_{analytic}(\mathcal{G}) - \Delta_{DPT}(\mathcal{G}))/\Delta_{analytic}(\mathcal{G})$, between the analytic and DPT rank-three, rank-two and rank-one binary invariant coefficients when $N = 10,000$ and $\lambda^2 = -1/10,000 + 10^{-10}$.







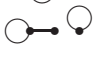

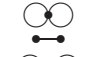



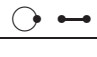
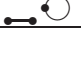
\mathcal{G}	$\Delta(\mathcal{G})$	\mathcal{G}	$\Delta(\mathcal{G})$
	-4.8×10^{-20}		2.8×10^{-10}
	7.9×10^{-24}		-1.7×10^{-14}
	1.9×10^{-12}		-2.8×10^{-14}
	-1.9×10^{-16}		5.3×10^{-14}
	-2.6×10^{-19}		-1.2×10^{-17}
	3.8×10^{-20}		-5.0×10^{-18}
	8.1×10^{-20}		3.3×10^{-20}

Table I.4: Rank-three and rank-two binary invariant coefficient, $\Delta_{DPT}(\mathcal{G})$, from the general *Mathematica* code when $N = 10,000$ and $\lambda^2 = -1/10,000 + 10^{-10}$. All of these coefficients are exactly zero in the exactly soluble analytic solution.

I.2 First-anharmonic-order density profile

In Reference (103), we derive the N -body density profile for the exact wavefunction. In this reference, the number density

$$\mathcal{N}(r) = N(r)/N \quad (\text{I.74})$$

is used, which differs from the density profile $N(r)$ used elsewhere in this thesis in that $\mathcal{N}(r)$ is normalized to unity, not N :

$$\int_0^\infty \mathcal{N}(r) dr = 1. \quad (\text{I.75})$$

The exact number density derived in Reference (103) is

$$\mathcal{N}(r) = \frac{2(\lambda_{\text{eff}}\omega_t)^{\frac{D}{2}}}{\Gamma(\frac{D}{2})} r^{D-1} \exp(-\lambda_{\text{eff}}\omega_t r^2), \quad (\text{I.76})$$

where

$$\lambda_{\text{eff}} = \frac{N\omega_{\text{int}}}{\omega_{\text{int}} + (N-1)\omega_t} = \frac{1}{2\bar{r}_\infty^2}. \quad (\text{I.77})$$

I.2.1 Dimensional scaling

As for the wavefunction in the previous section and in Eq. (3.19), we regularize the large-dimension limit by dimensionally scaling the parameters and variables. We choose a scaling $\kappa(D)$ and define dimensionally-scaled frequency $\bar{\omega}_t$,

$$\kappa(D) = \frac{1}{\sqrt{\bar{\omega}_t}} D^2 \quad (\text{I.78})$$

$$\bar{\omega}_t = D^3 \omega_t. \quad (\text{I.79})$$

Therefore the dimensionally-scaled radius \bar{r} in Eq. (3.19) is

$$\bar{r} = \sqrt{\bar{\omega}_t} \frac{r}{D^2} = \sqrt{\frac{\omega_t}{D}} r, \quad (\text{I.80})$$

from which we derive

$$(\lambda_{\text{eff}}\omega_t)^{\frac{D}{2}} r^{D-1} dr = (\lambda_{\text{eff}} D)^{\frac{D}{2}} \bar{r}^{D-1} d\bar{r}. \quad (\text{I.81})$$

Thus the number density in dimensionally scaled coordinates is

$$\mathcal{N}(\bar{r}) = \frac{2(\lambda_{\text{eff}} D)^{\frac{D}{2}}}{\Gamma(\frac{D}{2})} \bar{r}^{D-1} \exp(-\lambda_{\text{eff}} D \bar{r}^2). \quad (\text{I.82})$$

Equation (I.82) implies (as does Eq. (I.76)) that the density profiles for harmonically-interacting particles in a harmonic confining potential follow a universal curve for any

N or interparticle interaction strength $\lambda_p = \omega_p/\omega_t$. This is simply seen by scaling the dimensionally scaled radius \bar{r} :

$$\bar{r}_{\text{eff}} = \sqrt{\lambda_{\text{eff}}} \bar{r} \quad (\text{I.83})$$

and scaling the wavefunction by the multiplier $1/\sqrt{\lambda_{\text{eff}}}$ from the change of variables

$$d\bar{r} = \frac{1}{\sqrt{\lambda_{\text{eff}}}} d\bar{r}_{\text{eff}}, \quad (\text{I.84})$$

which gives

$$\mathcal{N}(\bar{r}_{\text{eff}}) = \frac{2 D^{\frac{D}{2}}}{\Gamma(\frac{D}{2})} \bar{r}_{\text{eff}}^{D-1} \exp(-D \bar{r}_{\text{eff}}^2). \quad (\text{I.85})$$

I.2.2 Series expansion

As in Eq. (3.30), we introduce the dimensionally scaled-displacement coordinate

$$\bar{r}_{\text{eff}} = \frac{1}{D^{\frac{1}{2}}} (\bar{r}'_{\text{eff}} + D^{\frac{1}{2}} (\bar{r}_{\text{eff}})_{\infty}) \quad (\text{I.86})$$

so that

$$d\bar{r}_{\text{eff}} = \frac{1}{D^{\frac{1}{2}}} d\bar{r}'_{\text{eff}}. \quad (\text{I.87})$$

Thus

$$\mathcal{N}(\bar{r}'_{\text{eff}}) = \frac{2}{\Gamma(\frac{D}{2})} (\bar{r}'_{\text{eff}} + D^{\frac{1}{2}} (\bar{r}_{\text{eff}})_{\infty})^{D-1} \exp\left(-(\bar{r}'_{\text{eff}} + D^{\frac{1}{2}} (\bar{r}_{\text{eff}})_{\infty})^2\right), \quad (\text{I.88})$$

where

$$\int_{-\infty}^{\infty} \mathcal{N}(\bar{r}'_{\text{eff}}) d\bar{r}'_{\text{eff}} = 1. \quad (\text{I.89})$$

To derive the dimensional expansion of Eq. (I.88), let's first consider expanding $(\bar{r}'_{\text{eff}} + D^{\frac{1}{2}} (\bar{r}_{\text{eff}})_{\infty})^{D-1}$. We derive

$$\begin{aligned} (\bar{r}'_{\text{eff}} + D^{\frac{1}{2}} (\bar{r}_{\text{eff}})_{\infty})^{D-1} &= \left(\frac{D}{2}\right)^{\frac{D-1}{2}} \left(1 + \delta^{\frac{1}{2}} \left(\frac{\bar{r}'_{\text{eff}}{}^3}{3(\bar{r}_{\text{eff}})_{\infty}^3} - \frac{\bar{r}'_{\text{eff}}}{(\bar{r}_{\text{eff}})_{\infty}}\right) + O(\delta)\right) \\ &\times \exp\left(\frac{D^{\frac{1}{2}} \bar{r}'_{\text{eff}}}{(\bar{r}_{\text{eff}})_{\infty}}\right) \exp(-\bar{r}'_{\text{eff}}{}^2). \end{aligned} \quad (\text{I.90})$$

Likewise we also have

$$\exp\left(-(\bar{r}'_{\text{eff}} + D^{\frac{1}{2}} (\bar{r}_{\text{eff}})_{\infty})^2\right) = \exp\left(-\frac{D}{2}\right) \exp\left(-D^{\frac{1}{2}} \frac{\bar{r}'_{\text{eff}}}{(\bar{r}_{\text{eff}})_{\infty}}\right) \exp(-\bar{r}'_{\text{eff}}{}^2). \quad (\text{I.91})$$

Equations (I.90) and (I.91), along with Eq. (I.30), give us the result we are after, Eq. (7.19) in Chapter 7:

$$\mathcal{N}(\bar{r}'_{\text{eff}}) = \left(1 + \delta^{\frac{1}{2}} \sqrt{2} \left(\frac{2\bar{r}'_{\text{eff}}{}^3}{3} - \bar{r}'_{\text{eff}}\right) + O(\delta)\right) \left(\frac{2}{\pi}\right)^{\frac{1}{2}} \exp(-2\bar{r}'_{\text{eff}}{}^2),$$

where the normalization condition

$$\int_{-\infty}^{\infty} \mathcal{N}(\bar{r}'_{\text{eff}}) d\bar{r}'_{\text{eff}} = 1 \quad (\text{I.92})$$

is still satisfied through order $\delta^{\frac{1}{2}}$.

Here we have expanded the exact number density profile derived in Reference (103) through first order in $\delta^{1/2}$ to yield the exact density profile through first order (see Eq. (7.19)). This analysis shows that the density profile for any N or interaction strength follows a universal curve when a simple scaling is applied to the radial variable.

Appendix J

Details of the application to BEC

J.1 Hamiltonian Elements for a BEC Potential

The Hamiltonian for a BEC in a harmonic trap is written in dimensionally scaled oscillator units and with the choice

$$\kappa(D) = D^2 \bar{a}_{\text{ho}}.$$

The result is a dimensionally-scaled potential term (in units where $\hbar = m = 1$)

$$\bar{V}_{\text{BEC}} = \sum_{i=1}^N \frac{1}{2} \bar{r}_i^2 + \sum_{i=1}^{N-1} \sum_{j=i+1}^N \bar{V}_{\text{int}}(\bar{r}_{ij}), \quad (\text{J.1})$$

where the interparticle interaction \bar{V}_{int} depends upon the model chosen. In Reference (82), McKinney *et al.* choose a particular form which limits to the hard-sphere contact potential in the limit $D \rightarrow 3$:

$$\bar{V}_{\text{int}}(\bar{r}_{ij}) = \frac{\bar{V}_o}{1 - 3\delta} \sum_{i=1}^{N-1} \sum_{j=i+1}^N (1 - \tanh \Theta_{i,j}), \quad (\text{J.2})$$

where $\delta = 1/D$ is the perturbation parameter and the interatomic separation is

$$\bar{r}_{ij} = \sqrt{\bar{r}_i^2 + \bar{r}_j^2 - 2\bar{r}_i \bar{r}_j \gamma_{ij}}. \quad (\text{J.3})$$

This potential has a number of adjustable parameters, V_0 and others contained in Θ_{ij} in Eq. 8.5.

$$\Theta_{i,j} = \frac{\bar{c}_o}{1 - 3\delta} \left(\frac{\bar{r}_{ij}}{\sqrt{2}} - \bar{\alpha} - 3\delta(\bar{a} - \bar{\alpha}) \right) \left(1 + (1 - 3\delta) \frac{\bar{c}_1 \bar{r}_{ij}^2}{2} \right)$$

In what follows, we define Θ_∞ as in Eq. 8.7, as well as Θ'_∞ , and Θ''_∞ :

$$\Theta_\infty = \Theta_{ij} \Big|_\infty = \bar{c}_0 \left(\sqrt{1 - \gamma_\infty} \bar{r}_\infty - \bar{\alpha} \right) \left(1 + (1 - \gamma_\infty) \bar{c}_1 \bar{r}_\infty^2 \right) \quad (\text{J.4})$$

$$\Theta'_\infty = \frac{\partial \Theta_{ij}}{\partial \bar{r}_{ij}} \Big|_\infty = \frac{\bar{c}_0}{\sqrt{2}} \left(\bar{c}_1 \left(-2\sqrt{1 - \gamma_\infty} \bar{\alpha} \bar{r}_\infty + 3(1 - \gamma_\infty) \bar{r}_\infty^2 \right) + 1 \right) \quad (\text{J.5})$$

$$\Theta''_\infty = \frac{\partial^2 \Theta_{ij}}{\partial \bar{r}_{ij}^2} \Big|_\infty = -\bar{c}_0 \bar{c}_1 \left(\bar{\alpha} - 3\sqrt{1 - \gamma_\infty} \bar{r}_\infty \right). \quad (\text{J.6})$$

J.1.1 Elements of the harmonic-order Hamiltonian

The elements of the harmonic-order effective potential for a BEC were calculated in Eqs. (120) of (81). Here, I report a general calculation of these elements. In this work I label elements by graph, and specify the perturbation order and matrix rank.

J.1.1.1 Derivatives with respect to δ : ${}^{(0)}_0F$

The DPT perturbation series is a Taylor series in $\delta^{1/2}$, and involves some derivatives of the effective potential with respect to δ . At the present (first anharmonic) order, only the first-order derivative with respect to δ is needed.

In the present notation, the harmonic-order term ${}^{(0)}_2F$ replaces ν_0 in Eq. (125) of Reference (81). This term consists of the first-order derivative (with respect to δ) of the centrifugal potential, the confining potential, and the interaction potential. The derivative of the centrifugal potential was calculated in Eq. (D.48). The derivative of the confining potential is zero,

$$\left. \frac{d\bar{V}_{\text{conf}}}{d\delta} \right|_{\infty} = 0. \quad (\text{J.7})$$

I take the derivative of V_{int} with respect to δ below. In order to simplify the expression, I set $\delta \rightarrow 0$ without invoking the large- D values of the internal coordinates:

$$\begin{aligned} \left. \frac{d\bar{V}_{\text{int}}}{d\delta} \right|_{\delta \rightarrow 0} &= 3\bar{V}_0 \sum_{i=1}^{N-1} \sum_{j=i+1}^N (1 - \tanh \Theta_{i,j}) - \bar{V}_0 \sum_{i=1}^{N-1} \sum_{j=i+1}^N \text{sech}^2 \Theta_{i,j} \frac{\partial \Theta_{i,j}}{\partial \delta} \\ &= 3\bar{V}_0 \sum_{i=1}^{N-1} \sum_{j=i+1}^N (1 - \tanh \Theta_{i,j} + \\ &\quad - \text{sech}^2 \Theta_{i,j} \left(\frac{\bar{r}_{i,j}}{\sqrt{2}} - \bar{a} + (\bar{\alpha} - \bar{a}) \bar{c}_1 \frac{\bar{r}_{i,j}^2}{2} \right)). \end{aligned} \quad (\text{J.8})$$

The above Eq. (J.8) can be used at first-anharmonic order, where an additional derivative with respect to an internal coordinate will be taken. Taking the full large- D limit, I obtain:

$$\left. \frac{d\bar{V}_{\text{int}}}{d\delta} \right|_{\infty} = \frac{3}{2} N(N-1) \bar{V}_0 \left(1 - \tanh \Theta_{\infty} - \bar{c}_0 \text{sech}^2 \Theta_{\infty} \left(\bar{r}_{\infty} \sqrt{1 - \gamma_{\infty}} - \bar{a} + (\bar{\alpha} - \bar{a}) \bar{c}_1 \bar{r}_{\infty}^2 (1 - \gamma_{\infty}) \right) \right). \quad (\text{J.9})$$

J.1.1.2 Derivatives with respect to internal coordinates: ${}^{(0)}_2F$

The derivatives with respect to internal coordinates are more straight-forward:

$$\begin{aligned} \left. \left(\frac{\partial^2 \bar{V}_{\text{conf}}}{\partial \bar{r}_i^2} \right) \right|_{\infty} &= 1 \\ \left. \left(\frac{\partial^2 \bar{V}_{\text{int}}}{\partial \bar{r}_i^2} \right) \right|_{\infty} &= \frac{1}{2} (N-1) \bar{V}_0 \text{sech}^2 \Theta_{\infty} \left(-\frac{(1 + \gamma_{\infty}) \Theta'_{\infty}}{\sqrt{2} \sqrt{1 - \gamma_{\infty}} \bar{r}_{\infty}} \right) \end{aligned} \quad (\text{J.10a})$$

$$+(1 - \gamma_\infty) \left(2 \tanh \Theta_\infty (\Theta'_\infty)^2 - \Theta''_\infty \right) \quad (\text{J.10b})$$

$$\left(\frac{\partial^2 \bar{V}_{\text{int}}}{\partial \bar{r}_i \partial \bar{r}_j} \right) \Big|_\infty = \frac{1}{2} \bar{V}_0 \text{sech}^2 \Theta_\infty \left(\frac{(1 + \gamma_\infty) \Theta'_\infty}{\sqrt{2} \sqrt{1 - \gamma_\infty} \bar{r}_\infty} + (1 - \gamma_\infty) (2 \tanh \Theta_\infty (\Theta'_\infty)^2 - \Theta''_\infty) \right) \quad (\text{J.10c})$$

$$\left(\frac{\partial^2 \bar{V}_{\text{int}}}{\partial \bar{r}_i \partial \gamma_{ij}} \right) \Big|_\infty = \frac{1}{2} \bar{V}_0 \text{sech}^2 \Theta_\infty \left(\frac{\Theta'_\infty}{\sqrt{2} \sqrt{1 - \gamma_\infty}} - \bar{r}_\infty (2 \tanh \Theta_\infty (\Theta'_\infty)^2 + \Theta''_\infty) \right) \quad (\text{J.10d})$$

$$\left(\frac{\partial^2 \bar{V}_{\text{int}}}{\partial \gamma_{ij}^2} \right) \Big|_\infty = \frac{1}{2} \bar{V}_0 \text{sech}^2 \Theta_\infty \left(\frac{\bar{r}_\infty \Theta'_\infty}{\sqrt{2} (1 - \gamma_\infty)^{3/2}} + \frac{2 \bar{r}_\infty^2 \tanh \Theta_\infty (\Theta'_\infty)^2 - \bar{r}_\infty \Theta''_\infty}{1 - \gamma_\infty} \right). \quad (\text{J.10e})$$

J.1.2 Elements of the first anharmonic-order Hamiltonian

J.1.2.1 Rank-one Hamiltonian Elements

The rank-one first anharmonic order Hamiltonian coefficients result from a derivative with respect to δ and with respect to an internal coordinate. The derivative with respect to δ was calculated in Eq. (J.8):

$$\left(\frac{\partial}{\partial \bar{r}_i} \frac{\partial \bar{V}_{\text{conf}}}{\partial \delta} \right) \Big|_\infty = \left(\frac{\partial}{\partial \gamma_{ij}} \frac{\partial \bar{V}_{\text{conf}}}{\partial \delta} \right) \Big|_\infty = 0 \quad (\text{J.11})$$

$$\begin{aligned} \left(\frac{\partial}{\partial \bar{r}_i} \frac{\partial \bar{V}_{\text{int}}}{\partial \delta} \right) \Big|_\infty &= \frac{3}{2} (N - 1) \bar{V}_0 \bar{c}_0 \text{sech}^2 (\Theta_\infty) \sqrt{1 - \gamma_\infty} \times \left(-\frac{\sqrt{2} \Theta'_\infty}{\bar{c}_0} - 1 \right. \\ &\quad \left. - 2\sqrt{2} \left(-(\bar{a} - \bar{\alpha}) (\gamma_\infty - 1) \bar{c}_1 r_\infty^2 - \sqrt{1 - \gamma_\infty} r_\infty + \bar{a} \right) \tanh (\Theta_\infty) \Theta'_\infty \right. \\ &\quad \left. + 2(\bar{a} - \bar{\alpha}) r_\infty \sqrt{1 - \gamma_\infty} \bar{c}_1 \right) \end{aligned} \quad (\text{J.12a})$$

$$\begin{aligned} \left(\frac{\partial}{\partial \gamma_{ij}} \frac{\partial \bar{V}_{\text{int}}}{\partial \delta} \right) \Big|_\infty &= \frac{3}{2} \bar{V}_0 \bar{c}_0 \text{sech}^2 (\Theta_\infty) \frac{r_\infty}{\sqrt{1 - \gamma_\infty}} \left(-1 + \frac{\sqrt{2} \Theta'_\infty}{\bar{c}_0} + \right. \\ &\quad \left. 2(\bar{a} - \bar{\alpha}) r_\infty \sqrt{1 - \gamma_\infty} \bar{c}_1 + \right. \\ &\quad \left. - 2\sqrt{2} \left(-(\bar{a} - \bar{\alpha}) (\gamma_\infty - 1) \bar{c}_1 r_\infty^2 - \sqrt{1 - \gamma_\infty} r_\infty + \bar{a} \right) \tanh (\Theta_\infty) \Theta'_\infty \right) \end{aligned} \quad (\text{J.12b})$$

J.1.2.2 Rank-three Hamiltonian Elements

$$\left(\frac{\partial^3 \bar{V}_{\text{conf}}}{\partial \bar{r}_i^3} \right) \Big|_\infty = 0 \quad (\text{J.13})$$

$$\begin{aligned}
\left. \left(\frac{\partial^3 \bar{V}_{\text{int}}}{\partial \bar{r}_i^3} \right) \right|_{\infty} &= (N-1) \bar{V}_0 \operatorname{sech}^2 \Theta_{\infty} \left[-\operatorname{sech}^2 \Theta_{\infty} \frac{(1-\gamma_{\infty})^{3/2} (-1+2\bar{r}_{\infty}^2) (\Theta'_{\infty})^3}{2\sqrt{2}\gamma_{\infty}\bar{r}_{\infty}^2} \right. \\
&\quad - \frac{3 \tanh \Theta_{\infty}}{4 \gamma_{\infty} \bar{r}_{\infty}^3} \times (-1+2\bar{r}_{\infty}^2) \Theta'_{\infty} \left((1+\gamma_{\infty}) \Theta'_{\infty} + \sqrt{2} (1-\gamma_{\infty})^{3/2} \bar{r}_{\infty} \Theta''_{\infty} \right) \\
&\quad + \frac{(1-2\bar{r}_{\infty}^2)}{16(1-\gamma_{\infty})\gamma_{\infty}\bar{r}_{\infty}^4} \left(\sqrt{2-2\gamma_{\infty}} \Theta'_{\infty} (3(1+\gamma_{\infty}) + 8(1-\gamma_{\infty})^2 \bar{r}_{\infty}^2 (\Theta'_{\infty})^2) \right. \\
&\quad \left. \left. + 2(-1+\gamma_{\infty})\bar{r}_{\infty} (3(1+\gamma_{\infty})\Theta''_{\infty} + \sqrt{2}(1-\gamma_{\infty})^{3/2} \bar{r}_{\infty} \Theta_{\infty}) \right) \right] \quad (\text{J.14a})
\end{aligned}$$

$$\begin{aligned}
\left. \left(\frac{\partial^3 \bar{V}_{\text{int}}}{\partial \bar{r}_i^2 \partial \bar{r}_j} \right) \right|_{\infty} &= \bar{V}_0 \operatorname{sech}^2 \Theta_{\infty} \left[-\frac{1}{\sqrt{2}} \operatorname{sech}^2 \Theta_{\infty} (1-\gamma_{\infty})^{3/2} (\Theta'_{\infty})^3 \right. \\
&\quad + \tanh \Theta_{\infty} \left(\frac{3(1-\gamma_{\infty})^{3/2} \Theta'_{\infty} \Theta''_{\infty}}{\sqrt{2}} - \frac{(1+\gamma_{\infty}) (\Theta'_{\infty})^2}{2\bar{r}_{\infty}} \right) \\
&\quad \left. - \frac{(1+\gamma_{\infty}) \Theta'_{\infty}}{4\sqrt{2}\sqrt{1-\gamma_{\infty}}\bar{r}_{\infty}^2} + \frac{(1-\gamma_{\infty})^{3/2} (4(\Theta'_{\infty})^3 - \Theta_{\infty}^3)}{2\sqrt{2}} + \frac{(1+\gamma_{\infty})\Theta''_{\infty}}{4\bar{r}_{\infty}} \right] \quad (\text{J.14b})
\end{aligned}$$

$$\left. \left(\frac{\partial^3 \bar{V}_{\text{int}}}{\partial \gamma_{ij} \partial^2 \bar{r}_i} \right) \right|_{\infty} = \bar{V}_0 \operatorname{sech}^2 \Theta_{\infty} \left(1 + \frac{\operatorname{sech}^2 \Theta_{\infty} \sqrt{1-\gamma_{\infty}} \bar{r}_{\infty} (\Theta'_{\infty})^3}{\sqrt{2}} \right) \quad (\text{J.14c})$$

$$\begin{aligned}
\left. \left(\frac{\partial^3 \bar{V}_{\text{int}}}{\partial \gamma_{ij} \partial \bar{r}_i \partial \bar{r}_j} \right) \right|_{\infty} &= \bar{V}_0 \operatorname{sech}^2 \Theta_{\infty} \left[\frac{\operatorname{sech}^2 \Theta_{\infty} \sqrt{1-\gamma_{\infty}} \bar{r}_{\infty} (\Theta'_{\infty})^3}{\sqrt{2}} + \right. \\
&\quad \tanh \Theta_{\infty} \left(\frac{(-1+3\gamma_{\infty}) (\Theta'_{\infty})^2}{2(1-\gamma_{\infty})} - \frac{3\sqrt{1-\gamma_{\infty}} \bar{r}_{\infty} \Theta'_{\infty} \Theta''_{\infty}}{\sqrt{2}} \right) - \left(\frac{\sqrt{2}(-3+\gamma_{\infty}) \Theta'_{\infty}}{8(1-\gamma_{\infty})^{3/2} \bar{r}_{\infty}} \right. \\
&\quad \left. \left. + \frac{(-1+3\gamma_{\infty}) \Theta''_{\infty}}{4(1-\gamma_{\infty})} + \frac{\sqrt{1-\gamma_{\infty}} \bar{r}_{\infty} (4(\Theta'_{\infty})^3 - \Theta_{\infty}^3)}{2\sqrt{2}} \right) \right] \quad (\text{J.14d})
\end{aligned}$$

$$\begin{aligned}
\left. \left(\frac{\partial^3 \bar{V}_{\text{int}}}{\partial \gamma_{ij}^2 \partial \bar{r}_i} \right) \right|_{\infty} &= \bar{V}_0 \operatorname{sech}^2 \Theta_{\infty} \left(-\frac{\operatorname{sech}^2 \Theta_{\infty} \bar{r}_{\infty}^2 (\Theta'_{\infty})^3}{\sqrt{2}\sqrt{1-\gamma_{\infty}}} \right. \\
&\quad + \tanh \Theta_{\infty} \left(\frac{\bar{r}_{\infty} (\Theta'_{\infty})^2}{2(1-\gamma_{\infty})} + \frac{3\bar{r}_{\infty}^2 \Theta'_{\infty} \Theta''_{\infty}}{\sqrt{2}\sqrt{1-\gamma_{\infty}}} \right) \\
&\quad \left. + \frac{\Theta'_{\infty}}{4\sqrt{2}(1-\gamma_{\infty})^{3/2}} - \frac{\bar{r}_{\infty} \Theta''_{\infty}}{4(1-\gamma_{\infty})} + \frac{\bar{r}_{\infty}^2 (4(\Theta'_{\infty})^3 - \Theta_{\infty})}{2\sqrt{2}\sqrt{1-\gamma_{\infty}}} \right) \quad (\text{J.14e})
\end{aligned}$$

$$\begin{aligned}
\left. \left(\frac{\partial^3 \bar{V}_{\text{int}}}{\partial \gamma_{ij}^3} \right) \right|_{\infty} &= \bar{V}_0 \operatorname{sech}^2 (\Theta_{\infty}) \left[\frac{\bar{r}_{\infty}^3 (\Theta'_{\infty})^3 \operatorname{sech}^2 (\Theta_{\infty})}{\sqrt{2}(1-\gamma_{\infty})^{3/2}} \right. \\
&\quad + \frac{\bar{r}_{\infty} (2\sqrt{2}(\gamma_{\infty}-1) (4(\Theta'_{\infty})^3 - \Theta''_{\infty}) \bar{r}_{\infty}^2 - 6\sqrt{1-\gamma_{\infty}} \Theta''_{\infty} \bar{r}_{\infty} + 3\sqrt{2} \Theta'_{\infty})}{8(1-\gamma_{\infty})^{5/2}} \\
&\quad \left. + \frac{3}{2} \bar{r}_{\infty}^2 \tanh (\Theta_{\infty}) \Theta'_{\infty} \left(\frac{\Theta'_{\infty}}{(\gamma_{\infty}-1)^2} - \frac{\sqrt{2} \bar{r}_{\infty} \Theta''_{\infty}}{(1-\gamma_{\infty})^{3/2}} \right) \right] \quad (\text{J.14f})
\end{aligned}$$

J.2 Optimization to benchmark data

J.2.1 Fitness function

In Reference (82), McKinney *et. al.* use a chi-square statistic (108) as the fitness function to minimize in order to optimize the parameters of the interparticle potential. The chi-square fitness function measures how close the analytic DPT energies are to the six exact low- N DMC energies (53). The optimal set of s parameters $\{\bar{V}_0, \bar{\alpha}\} \cup \{\bar{c}_n; \forall n : 0 \leq n \leq s - 3\}$ were determined by minimizing the chi-square as a function of those parameters.

$$\chi^2 = \sum_{i=1}^6 \left(\frac{\bar{E}_i^{(DMC)} - \bar{E}^{(DPT)}(N_i; \bar{V}_0, \bar{\alpha}, \{\bar{c}_n\})}{\sigma_i} \right)^2, \quad (\text{J.15})$$

where $\bar{E}_i^{(DMC)}$ is the DMC energy, and σ_i is the statistical uncertainty for a condensate with atom number N_i .¹

The Q -probability is used to avoid overfitting by introducing too many parameters:

$$Q \left(\frac{\nu}{2}, \frac{\chi^2}{2} \right) \equiv \frac{\Gamma(\frac{\nu}{2}, \frac{\chi^2}{2})}{\Gamma(\frac{\nu}{2})} \equiv \frac{1}{\Gamma(\frac{\nu}{2})} \int_{\chi^2/2}^{\infty} e^{-t} t^{\nu/2-1} dt \quad (\text{J.16})$$

The Q -probability for a particular χ^2 with ν degrees of freedom is the probability that a subsequent determination of χ^2 would be higher. A Q probability of 1 means that χ^2 cannot be lower (a perfect fit), and a Q probability of 0 means that one cannot help but find a lower χ^2 (and hence a better fit). We follow the lead of McKinney *et. al.* in choosing the minimum number of parameters s that affords a fit with Q greater than 0.5. This choice is made in order to extract the essential information from the DMC data without fitting to the noise.

J.2.2 Benchmark data

We optimize to six essentially exact, low- N diffusion Monte Carlo benchmark energies (53) for each scattering length (see column 1 of Tables J.2, and J.2.2)

¹The uncertainties in the DMC energies are an estimation of both of statistical and systematic uncertainties. The systematic uncertainties are thought to be small. (D. Blume, private communication)

N	DMC	DPT	GP	MGP
5	7.8356(15)	7.8356	7.8265	7.8340
10	16.426(6)	16.4261	16.383	16.426
20	35.475(15)	35.4746	35.297	35.497
50	103.99(3)	103.991	102.96	104.21
75	171.1(1)	171.096		
100	245.4(1)	245.4	241.85	246.24

Table J.1: Ground-state BEC energies (in units $\hbar\omega_{ho}$) for ^{87}Rb with $a = 1,000$ a.u. and $\omega_{ho} = 2\pi \times 77.87$ Hz, (which corresponds to $a = 0.0433a_{ho}$, in oscillator units). Column 2 contains DMC energies from Ref. (53) (with the statistical uncertainty in parenthesis). Column 3 contains our N -body DPT energies. Columns 4 and 5 contain the GP and MGP energies from Ref. (82).

Table J.2: Ground-state BEC energies (in units $\hbar\omega_{ho}$) for ^{87}Rb with $a = 10\,000$ a.u. and $\omega_{ho} = 2\pi \times 77.87$ Hz, (which corresponds to $a = 0.433a_{ho}$, in oscillator units). Column 2 contains DMC energies from Ref. (53) (with the statistical uncertainty in parenthesis). Column 3 contains our N -body DPT energies. Columns 4 and 5 contain the GP and MGP energies from Ref. (82).

N	DMC	DPT	GP	MGP
2	3.3831(7)	3.38331	3.3040	3.3950
3	5.553(3)	5.54945	5.329	5.611
5	10.577(2)	10.5773	9.901	10.772
10	26.22(8)	26.2651	23.61	26.84
20	66.9(4)	67.216	57.9	68.5
50	239.2(3)	239.121	196.12	243.45